UNIVERSITY OF SOUTHAMPTON
FACULTY OF PHYSICAL AND APPLIED SCIENCES
ELECTRONICS AND COMPUTER SCIENCE

Distributed Relay Selection Aided Cooperative Medium Access Control

by

Jiao Feng
BEng, MSc

A thesis submitted for the degree of Doctor of Philosophy
at the University of Southampton

January 2014

Supervisor: *Professor Lajos Hanzo*
Dipl Ing, MSc, PhD, DSc, FIET, FIEEE, FREng
Chair in Telecommunications, Head of Group

Supervisor: *Dr. Rong Zhang*
BEng, MEng, PhD
Communications, Signal Processing and Control Group
Electronics and Computer Science
University of Southampton
Southampton, SO17 1BJ
United Kingdom

Dedicated to my family and my fiance Peng.

UNIVERSITY OF SOUTHAMPTON

ABSTRACT

FACULTY OF PHYSICAL AND APPLIED SCIENCES
Electronics and Computer Science

Doctor of Philosophy

DISTRIBUTED RELAY SELECTION AIDED COOPERATIVE MEDIUM ACCESS CONTROL

by Jiao Feng

A variety of cooperative medium access control (MAC) schemes are designed for the sake of improving the achievable transmit rate and for reducing the transmit energy dissipation of cooperative communication systems relying on realistic greedy - rather than altruistic - relay nodes (RNs). Based on the system's objective functions (OF), novel distributed relay selection schemes are developed for selecting the best relay node (RN) set. In order to investigate the effect of the proposed MAC schemes on the performance of the cooperative communication systems considered, the system's stability is analysed with the aid of queueing theory.

Specifically, we first consider a cooperative spectrum leasing system (CSLS) supporting a licensed source node (SN) and a licensed destination node (DN) as well as multiple unlicensed greedy RNs, which require rewards for providing cooperative transmission assistance. A 'win-win' (WW) cooperative framework (WWCF) is formulated for sake of improving the achievable transmit rate and for simulanteously minimizing the energy dissipation of the cooperative spectrum leasing system considered. Based on the proposed WWCF, the licensed SN intends to lease part of its spectrum to the unlicensed RNs in exchange for cooperative support, leading to an improved transmit rate, while simultaneously reducing the transmit power. The unlicensed RNs also have an incentive to provide cooperative transmission assistance for the SN, since in exchange for relaying assistance they are allowed to access the licensed spectrum for transmitting their own data, and even to maintain their own target Quality of Service (QoS). Furthermore, a distributed WW cooperative MAC protocol is developed for implementing the proposed WWCF by designing a specific signalling procedure and the format of both the data frame control messages as well as a distributed relay selection scheme. More explicitly, a novel backoff algorithm is designed for distributively selecting the best RN in order to optimize the system's OF formulated by our WWCF. Our simulation results demonstrated that both substantial rate improvements and considerable

energy savings are achieved by implementing the proposed distributed WW cooperative MAC protocol.

However, encountering a low service rate at the MAC layer may excessively increase the length of queue in the buffer storing the incoming packet. Hence, the queueing system may become unstable due to the low service rate limited by an inferior MAC protocol design. Hence we conceived a queueing model for our cooperative spectrum leasing system relying on the proposed distributed WW cooperative MAC protocol. In order to simplify the stability analysis, some idealized simplifying assumptions are invoked and a non-Markovian analysis method is used for investigating the transmission probability of each node and for deriving the average departure rates at both the SN and the RNs operating under the control of the proposed distributed WW cooperative MAC protocol. Our simulation results confirmed that an increased stable throughput is provided by the proposed distributed WW cooperative MAC protocol for both the SN and RNs compared to the benchmark schemes.

As an improved extension of the proposed WWCF, a WW reciprocal-selection-based framework (WWRSF) is formulated for a cooperative spectrum leasing system hosting multiple licensed transmission pairs and multiple unlicensed transmission pairs. The SN of a licensed pair of nodes is referred as the primary transmitter (PT), while the SN of an unlicensed transmission pair is termed as the secondary transmitter (ST). Based on the proposed WWRSF, the PT intends to lease its spectral resources to an appropriate secondary transmitter (ST) in exchange for cooperative transmission assistance for the sake of minimizing its transmit power and simultaneously satisfying its transmit rate requirement. The ST has an incentive to collaborate with the best PT for the sake of minimizing the ST's transmit power under the constraint of its QoS requirement, whilst simultaneously winning a transmission opportunity for its own traffic. Based on the OFs of the proposed WWRSF, a distributed WW reciprocal-selection-based medium access scheme (DWWRS-MAS) is designed, which is capable of producing the best cooperative pairs set for the sake of reducing the transmit power of both the PT and of the ST in each cooperative pair, whilst simultaneously satisfying their transmit rate requirements. This is achieved with the aid of the proposed distributed reciprocal selection between the active PTs and STs, which have the capability of providing successful cooperative transmission assistance. Moreover, we analyse both the queueing stability and the algorithmic stability of our cooperative spectrum leasing system exploiting our DWWRS-MAS. In comparison to the benchmark schemes considered in the literature, the proposed DWWRS-MAS is capable of achieving a performance, which is comparable to that of the optimal schemes in terms of the system's transmit power and system's achievable transmit rate.

Declaration of Authorship

I, **Jiao Feng**, declare that the thesis entitled

Distributed Relay Selection Aided Cooperative Medium Access Control

and the work presented in it are my own and has been generated by me as the result of my own original research. I confirm that:

1. This work was done wholly or mainly while in candidature for a research degree at this University;
2. Where any part of this thesis has previously been submitted for a degree or any other qualification at this University or any other institution, this has been clearly stated;
3. Where I have consulted the published work of others, this is always clearly attributed;
4. Where I have quoted from the work of others, the source is always given. With the exception of such quotations, this thesis is entirely my own work;
5. I have acknowledged all main sources of help;
6. Where the thesis is based on work done by myself jointly with others, I have made clear exactly what was done by others and what I have contributed myself;
7. Parts of this work have been published, as seen in the list of publications.

Signed:

Date:

Acknowledgements

I would like to express my heartfelt gratitude to my first supervisor Professor Lajos Hanzo for his outstanding supervision. This thesis would not have been produced without his extremely generous and friendly support throughout my PhD career. His guidance, inspiration and encouragement have greatly benefited me not only in work but also in life. Especially, his diligence and endless energy deserve my sincere respect.

Meanwhile, I would like to express my greatest appreciation to my second supervisor Dr. Rong Zhang for his professional guidance, patient explanations and inspiring discussions throughout my research. I am grateful to him for his encouragement, teaching and invaluable friendship.

Moreover, I wish to thank Dr. Soon Xin Ng for his friendly support and patient guidance as well as the useful discussions.

Furthermore, I am also grateful to other academic staff of our group, especially to Professor Lie-Liang Yang, Professor Sheng Chen, Dr. Rob Maunder and Dr. Mohammed El-Hajjar. Many thanks to other colleagues within our group, Dr. Hong Chen, Dr. Jiayi Zhang, Dr. Wei Liu, Dr. Shinya Sugiura, Dr. Jing Zuo, Dr. Xinyi Xu, Dr. Dandan Liang, Dr. Li Li, Wei Liang, Xu Chao, Chen Dong, Shaoshi Yang, Yongkai Huo, Kent Cheung and Jie Hu, etc., for their help, discussions and friendship throughout my PhD study. Special thanks to Mr. and Mrs. Robson and to my lovely housemates who made my life in the UK full of fun and joy.

The financial support of the China-UK Scholarship Council is gratefully acknowledged.

Finally, I want to express my immense and never-ending gratitude to my admirable parents and my affection to Peng for their endless love and unconditional support and empathy.

List of Publications

Journal Papers:

1. **J. Feng and R. Zhang and L. Hanzo and S.X. Ng**, "Cooperative Medium Access Control Based on Spectrum Leasing", accepted by *IEEE Transactions on Vehicular Technology*, July 2013.

2. **W. Liang and J. Feng and S.X. Ng and L. Hanzo**, "Pragmatic Distributed Algorithm for Spectral Access in Cooperative Cognitive Radio Networks", submitted to *IEEE Transactions on Communications*, 2013.

3. **J. Feng and W. Liang and S.X. Ng and L. Hanzo**, "A Reciprocal-Selection-Based Spectrum Leasing Cooperative Medium Access Control and its Stability Analysis", prepared to be submitted to *IEEE Transactions on Vehicular Technology*, 2013.

4. **J. Feng and R. Zhang and L. Hanzo**, "A Survey on Win-Win Cooperative Medium Access Control", prepared to be submitted to *Communications Surveys and Tutorials*, 2013.

5. **J. Feng and R. Zhang and L. Hanzo**, "A Spectrum Leasing Cooperative Medium Access Protocol and its Stability Analysis", *IEEE Transactions on Vehicular Technology*, vol. 61, pp. 3718 - 3730, Oct. 2012.

Conference Papers:

1. **J. Feng and R. Zhang and S. X. Ng and L. Hanzo**, "Relay Selection for Energy-Efficient Cooperative Media Access Control", Wireless Communications and Networking Conference (WCNC), 2011 IEEE, Cancun, Mexico, March 2011, pp. 1-6.

2. **J. Feng and R. Zhang and L. Hanzo**, "Auction-Style Cooperative Medium Access Control", Vehicular Technology Conference (VTC), 2011 IEEE 74th, San Francisco, USA, September 2011, pp. 1-5.

List of Symbols

General notation

- The notation $\mathbb{E}\{\boldsymbol{x}\}$ indicates the average of $\boldsymbol{x}$.
- The notation $\mathbb{P}\{\boldsymbol{x}\}$ indicates the probability of $\boldsymbol{x}$.
- The notation $\mathbb{P}\{\boldsymbol{x},\boldsymbol{y}\}$ indicates the joint probability function of $\boldsymbol{x}$ and $\boldsymbol{y}$.
- The notation $\overline{\mathbb{P}\{\boldsymbol{x},\boldsymbol{y}\}}$ indicates the probability of $1-\mathbb{P}\{\boldsymbol{x},\boldsymbol{y}\}$.
- The notation $\mathbb{P}\{\boldsymbol{x}|\boldsymbol{y}\}$ indicates the conditional probability that event $\boldsymbol{x}$ will happen when event $\boldsymbol{y}$ has occurred, which is the conditional probability of $\boldsymbol{x}$ given $\boldsymbol{y}$.
- The subscripts $_{\mathcal{S}}$ and $_{\mathcal{R}_\jmath}$ are used to indicate the performance of the source node (SN) and relay node (RN) $\mathcal{R}_\jmath$, respectively.
- The subscripts $_{\mathcal{S},\mathcal{D}}$, $_{\mathcal{S},\mathcal{R}_\jmath}$ and $_{\mathcal{R}_\jmath,\mathcal{D}}$ are used to describe the SD link, SR link and RD link respectively.
- The subscripts $_{WW}$ and $_{noncoop}$ are used for indicating the performance of the system relying on the proposed distributed "win-win" (WW) cooperative medium access control (MAC) protocol and non-cooperative system respectively.
- The superscript ^{DWWRSMAS} and subscript $_{DWWRSMAS}$ are used to indicate the behaviour of the users and the achievable performance of the system relying on the proposed DWWRSMAS.
- The superscript ^{other} and subscript $_{other}$ are used to indicate the behaviour of the users relying on other stable matching algorithms.
- ^{unstable} and $_{unstable}$ are used to indicate the behaviour of the users relying on the unstable matching algorithms.
- The subscripts and superscripts $_{CCS1}$, $_{CCS2}$, $_{nCS-1}$ and $_{nCS-2}$ are used to indicate the parameters and the achievable performance in the first centralized cooperative system (CCS-1), the second centralized cooperative system (CCS-2), the first non-cooperative system (nCS-1) and the second non-cooperative system (nCS-2), respectively.

Special symbols

A the set of $(l-1)$ labels for the 'willing' RNs.

a represents a man.

$\mathbb{A}$ Packet arrival process of the queue at a node.

$A_{SU}^{(q)}(i,n,P_z)$ The event that PT_i has q candidate cooperative partners including ST_m, while ST_n also is the candidate cooperative partner of PT_i.

B The set of $(m-l)$ labels representing the 'unwilling' RNs.

b represents a woman.

$\mathbb{B}$ Service distribution of the queue at a node.

$B_{SU}^{(q)}(i,m,P_y)$ The event that PT_i has q candidate cooperative partners apart from ST_m when PT_i intends to transmit its data at transmit power P_y, but ST_m is the only candidate cooperative partner of PT_i when transmit power P_{y-1} is exploited by PT_i.

B_w Bandwidth.

$\mathbb{C}$ Number of the servers at a node.

$C_{\boldsymbol{A},\boldsymbol{B}}^{max}$ Maximum achievable transmit rate of the link between the transmitter $\boldsymbol{A}$ and receiver $\boldsymbol{B}$.

$\mathcal{C}_{PT}(i,P_{p_1})$ The candidate RN set of PT_i when PT_i broadcasts its data at transmit power P_{p_1}.

$C_{\mathcal{R}_i}^{\mathcal{R}}$ The achievable transmit rate of the RN's data.

$CWmin$ the minimum contention window duration.

CW_{now} contention window required for calculating the backoff time before retransmission.

$\mathbb{D}$,D Destination node.

$\mathcal{D}$ Buffer size of a node.

d The transmitter-to-receiver distance.

$Data_i$ Data frame with ordering index i.

D_Q Duration from a packet's arrival at the input of a queue Q until its transmission is complete under steady state conditions.

$\boldsymbol{E}$ The set of the specific STs, which may be the candidate cooperative partners of PT_i.

$E_{\boldsymbol{S}}$ The system's total transmission energy dissipation in the system $\boldsymbol{S}$.

E_{D_i} Transmit energy required for successfully conveying the data frame D_i.

E_{error} The system's total energy dissipation for the WW-CSLS, where the control message may be corrupted.

$E_{error-free}$ The system's total energy dissipation for the WW-CSLS, where error-free control messages are assumed.

$E_{non-CSLS3}$ The energy consumption of $\mathcal{S}$ in the non-CSLS 3 arrangement, which achieves the same transmit rate for $\mathcal{S}$ as that of our CSLS.

E_{ran} The system's total transmission energy dissipation in the Ran-CSLS, where the best RN is randomly selected.

$E_{\mathcal{R}_i}$ Transmit energy required for successfully forwarding the SN's data and for correctly conveying the data of RN $\mathcal{R}_i$.

$E_{\mathcal{S}}$ Transmit energy dissipated by SN for conveying its data with the aid of cooperative transmission.

$\mathbb{F}(x)$ A specific distribution function which approaches the value of unity, as the variable x tends to infinity.

F_{U1} The event that PT_i wins the cooperative transmission assistance provided by ST_m, while PT_j selects another ST ST_n as its coopertive partner.

F_{U2} The event that PT_i wins the cooperative transmission assistance provided by ST_m, while PT_j selects the new winner of the ST's contention as its cooperative partner by increasing its power.

$F_{\Phi 1}$ The event that PT_j and ST_m constitute a cooperative pair, when PT_j has multiple candidate cooperative partners and ST_m is the best candidate cooperative partner of both PT_i and PT_j, when they intend to transmit their data at power P_z.

$F_{\Phi 2}$ The event that PT_j and ST_m constitute a cooperative pair when PT_j wins the PTs' contention at a power of P_{z-1}, while ST_m is the winner of the STs' contention when PT_j intends to transmit its data at power P_{z-1}, but ST_m is not the winner of ST contention when PT_j increases its power to P_z.

F_{Ω_1} The event that PT_i and ST_m constitute a cooperative pair when PT_i fails to win the cooperative transmission assistance provided by its best cooperative partner ST_n, assuming that PT_i intends to transmit its data at transmit power P_z and ST_m is the second best candidate cooperative partner of PT_i when the PT's transmit power is P_z.

F_{Ω_2} The event that PT_i and ST_m constitute a cooperative pair, when PT_i fails to win the cooperative transmission assistance provided by its best cooperative partner ST_n, assuming that PT_i intends to transmit its data at transmit power P_{z-1} and ST_m wins the contention for transmission opportunity provided by PT_i when the PT's transmit power is P_z.

G General distribution.

$\boldsymbol{G}$ The set of the STs which cannot be the candidate cooperative partners of PT_i, excluding ST_m.

g The ordering index of RN.

$|h|$ The magnitude of the flat Rayleigh channel between the transmitter and receiver.

$H_{\boldsymbol{AB}}$ The channel gain of the link between node $\boldsymbol{A}$ and node $\boldsymbol{B}$, which is equal to $|h_{\boldsymbol{AB}}|^2$.

$H_{\mathcal{R}_i,max}$ The channel gain of the RD link between $\mathcal{R}_i$ and the destination node, when the maximum transmit power P_{max} is required for satisfying the transmit rate requirement of both the RN $\mathcal{R}_i$ and the source node.

$H^{(II)}_{\mathcal{SD},max}$ The channel gain of the SD link, when $\mathcal{S}$ retransmits its data to $\mathcal{D}$ at the maximum transmit power for the sake of satisfying its transmit rate requirement.

i The ordering index.

$\hat{i}$ The ordering index of the best RN.

$\mathcal{I}$ Number of primary transmission pairs.

$I^*(m)$ The ordering index of the cooperative partner of the secondary transmitter ST_m.

K Number of men in the marriage matching model.

V Number of women in the marriage matching model.

$\mathcal{K}$ The set of the q candidate cooperative partners of PT_i excluding ST_n.

$\mathbb{L}$ A very long duration.

L_{D_i},L_{data} The length of the data frame in bits.

M Poisson process.

$\mathcal{M}$ Number of secondary transmission pairs.

$M^*(i)$ The ordering index of the cooperative partner of the primary transmitter PT_i.

M_1^* The ordering index of the winner of the STs' contention.

M_2^* The ordering index of the second best ST.

$\widetilde{M}(i)$ The size of the candidate cooperative partner set of PT_i.

$\widehat{M}(i)$ The index of the ST, which wins the STs' contention for the transmission opportunities leased by PT_i.

N Total number of relay nodes.

N_{all} The total number of instances of our DWWRSMAS in the Monte Carlo simulation.

$\mathcal{N}_{control}$ Number of control messages exchanged between PTs and STs.

$N_{ST,all}^{coop}$ Total number of transmission opportunities granted to all the STs.

$N_{ST}^{coop}(m)$ Number of transmission opportunities granted to ST_m.

N_Q,$Q(t)$ Number of packets in the queue Q.

N_s Number of packets in service.

$OF_{\boldsymbol{A}}$ The objective function of node $\boldsymbol{A}$.

OF_{ST}^{sys} The objective function of the secondary network.

$\mathcal{O}(PT_i, ST_m)$ A cooperative pair, which consists of the primary transmitter PT_i and a secondary transmitter ST_m.

P_{D_i} Transmit power required for transmitting the data frame D_i.

P_{max} Maximum transmit power.

P_{max}^{PT},P_{max}^{ST} Maximum transmit power of the PTs and STs, respectively.

P_N Power of the Additive White Gaussian Noise.

$\mathbb{P}_{out,\boldsymbol{AB}}$ Outage probability of the transmission from node $\boldsymbol{A}$ to node $\boldsymbol{B}$.

P_{p_l} The l-th transmit power level of the primary transmitter.

$P_{PT}(i,m)$ Transmit power dissipated by PT_i for successfully conveying its data with the aid of the cooperative transmission provided by ST_m.

$P_{PT_i}^{nc}$ Transmit power required for successful direct transmission, when the primary transmitter PT_i cannot obtain cooperative transmission assistance.

$P_{PT}^{x}(i)$ Transmit power dissipated by PT_i, whilst relying on either the cooperative transmission or the direct transmission of its data to PR_i during the x-th instance of the Monte Carlo simulation

$P_{\mathcal{R}_i}$ Transmit power required for guaranteeing the transmit rate requirement of both SN and RN $\mathcal{R}_i$.

$P_{\mathcal{R}_i^{min}}$ The minimum transmit power required for guaranteeing the transmit rate requirement of both SN and RN $\mathcal{R}_i$.

$P_{\mathcal{R}_i}^{\mathcal{R}}$ Transmit power required for achieving the target transmit rate of RN $\mathcal{R}_i$.

$P_{\mathcal{R}_i^{min}}^{\mathcal{R}}$ The minimum transmit power required for achieving the target transmit rate of RN $\mathcal{R}_i$.

$P_{\mathcal{R}_i}^{\mathcal{S}}$ Transmit power required for satisfying the transmit rate requirement of SN.

$\mathbb{P}_{suc,\boldsymbol{AB}}$ The probability of successful transmission from node $\boldsymbol{A}$ to node $\boldsymbol{B}$.

$\mathbb{P}_{suc,PTS}(i,m,P_x)$ The probability of successful transmission from PT_i to ST_m when PT_i intends to transmit its data at transmit power P_x.

$\mathbb{P}_{suc,SPR}(i,m,P_x)$ The probability of successful cooperative transmission from ST_m to PR_i, when PT_i intends to transmit data at transmit power P_x.

$P_{\mathcal{S}}$ Transmit power dissipated by $\mathcal{S}$ for conveying its data with the aid of cooperative transmission.

$P_{\mathcal{S}-data}$ Transmit power exploited by the source node for broadcasting its data.

$P_{\mathcal{S}-data}^{(2)}$ Transmit power required for achieving the SN's target transmit rate by retransmitting its data on its own in non-CSLS 2.

$P_{\mathcal{S},\mathcal{D}}^{(II)}$ Transmit power required for achieving the SN's target transmit rate on its own in the CSLS exploiting the proposed distributed WW cooperative MAC protocol, when no RN provides cooperative transmission assistance.

$\mathbb{P}_{\mathcal{S},noncoop}$ The probability of the SN's transmission without cooperation.

$\mathbb{P}_{\mathcal{S},noncoop}^{R_{coop}}$ The probability of the SN's non-cooperative transmission, which is capable of satisfying its transmit rate requirement.

PR_i Primary receiver with ordering index i.

$P_{ST}(i,m)$ The total transmit power consumed by ST_m, while satisfying the transmit rate requirement of both PT_i and ST_m, when they constitute a best cooperative pair.

$P_{ST}^{P}(i,m)$ The transmit power required for achieving the target transmit rate of PT_i, which is the cooperative partner of ST_m.

$P_{ST}^{S}(i,m)$ The transmit power required for achieving the target rate of ST_m, when PT_i is selected as its cooperative partner.

$P_{ST}^{x}(m)$ Transmit power dissipated by ST_m, while successfully conveying the superposition-coded data during the x-th instance of the Monte Carlo simulation.

PT_i Primary transmitter with ordering index i.

$PT_{\hat{i}}$ The winner of the contention between PTs.

P_x The x-th transmit power level of the primary transmitter.

Q A queue.

$Q_{\mathcal{R}_i}$ The queue at the RN $\mathcal{R}_i$ set up for buffering its own data.

$Q_{PT_i}, Q_{\mathcal{S}}$ The queue at PT_i and the SN set up for buffering their data.

Q_{PT,ST_m} The queue at the secondary transmitter ST_m set up for buffering the data received from the primary transmitters.

$Q_{\mathcal{SR}_i}$ The queue at the RN $\mathcal{R}_i$ constructed for buffering the SN's data.

Q_{ST_m} The queue at the secondary transmitter ST_m constructed for buffering its own data.

R,r Achievable transmit rate.

$\mathcal{R}$ Relay node set.

$R_{\boldsymbol{AB}}$ The transmit rate of the transmission from node $\boldsymbol{A}$ to node $\boldsymbol{B}$.

$\mathcal{R}_c$ The RN set, which can correctly over-hear both the RTS and CTS messages.

$\mathcal{R}_{cc}$ The potential candidate RN set, the members of which decide to contend for the transmission opportunities.

R_{D_i} Achievable transmit rate associated with the data frame D_i.

$R_{DWWRSMAS}$,R_{NCS-1} The achievable total transmit rate of our DWWRSMAS system and NCS-1, respectively.

$\mathcal{R}_i$ The relay node with ordering index i.

$R_{PT}^{x}(i)$ Transmit rate achieved by either the cooperative transmission or the direct transmission of its data to PR_i during the x-th instance of the Monte Carlo simulation.

R_{PT_i} The transmit rate of PT_i achieved with the aid of cooperative transmission.

$R_{PT_i}^{nc}$ Transmit rate achieved by successful direct transmission, when the primary transmitter PT_i cannot obtain cooperative transmission assistance.

$R_{PT_i}^{req}$ Transmit rate requirement of the primary transmitter PT_i.

$R^x_{ST}(m)$ The achievable transmit rate of the ST, when the ST ST_m is granted a transmit opportunity during the x-th instance of the Monte Carlo simulation.

R^y_{ST} Transmit rate of the ST achieved, when the y-th transmission opportunity is granted to ST.

R_{ST_m} The achievable transmit rate of the ST's data, when ST_m is selected as the best cooperative partner.

$R^{req}_{ST_m}$ The transmit rate requirement of the secondary transmitter ST_m.

$\mathcal{S}$ Source node.

ST_m Secondary transmitter with ordering index m.

$ST_{\hat{m}}$ The winner of the contention between the STs.

SR_m Secondary receiver with ordering index m.

T Total time required for successfully transmitting the data frame.

t Time index.

$T_{Backoff}$ Backoff time of a user before transmitting its data.

T_{error} Throughput achieved by the WW-CSLS, where the control message may be corrupted.

$T_{error-free}$ Throughput achieved by the WW-CSLS, when the control messages are assumed to be correctly received.

$T_{\mathcal{R}_i}(r)$ The event that RN $\mathcal{R}_i$ is selected as the best RN.

$T_{\mathcal{R}_i,bo}$ Backoff duration of the RN $\mathcal{R}_i$.

$T^{coop}_{PT_i}$ The event when PT_i is capable of obtaining cooperative transmission assistance.

$T^{(II)}_{\mathcal{S}}(r)$ The event when the source node is capable of guaranteeing its target transmit rate on its own in isolation, regardless, whether the best RN was selected or not.

T_{ST_m} The event when ST_m is selected as the cooperative partner of a PT.

$T_{ST,bo}(i,m)$ Backoff duration of ST_m before contending for the transmission opportunity leased by PT_i.

$T^{(1)}_{ST_m}(i)$ The event that PT_i and ST_m constitute a cooperative pair, when only PT_i has data to send at the beginning of current time slot.

$T_{ST_m}^{(2)}$ The event that ST_m wins the specific cooperative transmission opportunity leased by its cooperative partner, when two PTs have data to send at the beginning of the current time slot.

T_w Contention window length.

$\mathbb{U}$ Utilization of the server of the queue.

u Number of nodes in the simulation scenario.

$U_{\mathcal{R}_i}^{(n)}$ The event when RN $\mathcal{R}_i$ was selected as the best RN, when n RNs are capable of providing cooperative transmission assistance for $\mathcal{S}$.

$V_{\mathcal{R}_g}(r)$ The event when the RN $\mathcal{R}_g$ is capable of providing cooperative transmission for SN.

$V_{\mathcal{R}_i}^{m,l}(r)$ The event when both RN $\mathcal{R}_i$ and $(l-1)$ other RNs are capable of providing successful cooperative transmission assistance for SN, whilst $(m-l)$ RNs cannot be the potential candidate RN.

$V_{su}(i,m,P_x)$ The event when ST_m is capable of providing cooperative transmission for PT_i, assuming that PT_i intends to transmit its data at P_x.

$\overline{V_{su}(i,m,P_x)}$ The event when ST_m cannot provide cooperative transmission for PT_i, when PT_i intends to transmit its data at P_x.

$\mathcal{W}$ The set of STs, which cannot be the candidate cooperative partner of PT_i.

$W_{SU}^{(q)}(j,m,P_x)$ The event that ST_m is the candidate partner of PT_j, when PT_j intends to transmit its data at power P_x, but ST_m is not the winner of the ST's contention.

X A marriage matching.

$X(a)$ Matching partner of a.

$\{X_t\}$ A stochastic process.

$X_{unstable}$ An unstable matching.

$X_{DWWRSMAS}$ The matching produced by the proposed DWWRSMAS.

$Y(x)$ An increasing function of the variable x, which is equal to $(1+\nu x)^{\alpha}$.

$Z(x)$ An increasing function of the variable x, which is equal to $(1+\nu x)^{\alpha}-\nu x$.

$Z_{SU}(i,m,P_x)$ the event that SU_m is capable of successfully forwarding data for PT_i, when PT_i intends to transmit data at the transmit power P_x, but SU_m cannot be the candidate cooperative partner of PT_i, assuming that PT_i relies on a power of P_{x-1}.

$\varphi_{backoff}$ A pseudo-random integer limited between 0 and the contention window (CW).

κ Retransmission counter.

$\boldsymbol{\lambda}$ The wave-length.

λ Average arrival rate at the input of a queue.

$\lambda_{\mathcal{R}_i}$ Average arrival rate at the input of the queue storing the data of RN $\mathcal{R}_i$.

λ_{PT_i} Average arrival rate at the input of PT_i.

λ_S,$\lambda_{\mathcal{S}}$ Average arrival rate at the input of the SN's buffer.

λ_{SR},$\lambda_{\mathcal{SR}_i}$ Average arrival rate at the input of the queue storing the source's data at the relay node.

λ_{ST_m} Average arrival rate at the input of the queue at ST_m, which stores its own data.

$\Lambda_{SU}(i, m, P_x)$ The event that PT_i has multiple candidate cooperative partners, when PT_i intends to transmit its data at transmit power P_x and ST_m is the winner of the ST's contention for the transmit opportunities leased by PT_i.

μ Average packet service/departure rate of a queue.

$\mu_{\mathcal{R}_i}$ Average packet departure rate at RN $\mathcal{R}_i$.

$\mu_{PT_i}^{max}, \mu_{\mathcal{S}}^{max}$ Maximum average packet departure rate at the PT_i and source node, respectively.

$\mu_{PT_i}^{coop}$,$\mu_{PT_i}^{noncoop}$ Average packet departure rate at PT_i both with and without the aid of cooperative transmission respectively.

μ_S,$\mathcal{S}$ Average packet departure rate at the source node.

μ_{SR},$\mu_{\mathcal{SR}_i}$ Average packet departure rate of the queue storing the source's data at the relay node.

$\mu_{\mathcal{S},coop}$ Average packet departure rate achieved at the source node with the aid of cooperation.

$\mu_{\mathcal{S},non}^{R_{coop}}$ Average packet departure rate at the source node achieved by non-cooperative transmission, which is capable of achieving the source's target transmit rate.

$\mu_{\mathcal{S},non}^{R_{non}}$ Average packet departure rate achieved at the source node achieved by non-cooperative transmission, when the source cannot satisfy its transmit rate requirement in isolation under the constraint of the maximum transmit power.

τ Time duration having an arbitrary length.

ρ The pathloss between the transmitter and the receiver.

η The pathloss exponent.

α The SN's 'factor of greediness'.

β The RN's 'factor of greediness'.

$\zeta_{\mathcal{S}}$ The ratio of the transmit power dissipated by the source node used for broadcasting its data to the maximum transmit power.

$\xi_{\mathcal{R}_i}$ Binary indicator flag, which indicates, whether RN $\mathcal{R}_i$ is selected as best RN.

$\xi_{ps}(i,m)$ Binary indicator flag, which indicates, whether the primary transmitter PT_i and the secondary transmitter ST_m constitute a best cooperative pair.

$\gamma_{ps}(i,P_{p_l})$ The target-QoS of PT_i, which has to be guaranteed by its best cooperative partner, when PT_i broadcasts its data at transmit power P_{p_l}.

$\gamma_{\mathcal{R}_i}^{\mathcal{S}}$ The receive SNR of the SN's data, which should be guaranteed by the best RN during the relying phase.

$\gamma_{\mathcal{R}_i,\mathcal{D}}^{\mathcal{S}}$ The receive SNR of the SN's data forwarded by the RN $\mathcal{R}_i$.

$\gamma_{\mathcal{S},\mathcal{D}}^{(1)}$ The receive SNR of the direct transmission during the broadcast phase.

$\Gamma_{SU}(j,n,P_x)$ The event that ST_n is the best candidate cooperative partner of PT_j.

$\varphi_{\mathcal{R}_i}$ Contention priority of RN $\mathcal{R}_i$.

$\varphi_{ST}(i,m)$ Contention priority of ST_m, when it intends to contend for the transmission opportunity leased by PT_i.

$\Omega_{\mathcal{S}\mathcal{R}_i}$ A variable defined as $1+\frac{\rho_{\mathcal{S},\mathcal{R}_i}H_{\mathcal{S},\mathcal{R}_i}P_{\mathcal{S}-data}}{P_N}$.

$\Omega_{\mathcal{R}_i\mathcal{D}}$ A variable defined as $1+\frac{\rho_{\mathcal{R}_i\mathcal{D}}H_{\mathcal{R}_i\mathcal{D}}P_{max}}{P_N}$.

$\Omega_{SU}(i,m,P_z)$ The event that PT_i and ST_m constitute a cooperative pair, when PT_i fails to win the cooperative transmission assistance provided by its best cooperative partner ST_n.

ν A variable defined as $\frac{\rho_{\mathcal{S},\mathcal{D}}P_{max}}{P_N}$.

$\Theta_{PTP}(PT,PR)$ The set of primary transmission pairs.

$\Theta_{PTP_i}(PT_i,PR_i)$ The primary transmission pair with ordering index i.

$\Theta_{STP}(ST, SR)$ The set of secondary transmission pairs.

$\Theta_{STP_m}(ST_m, SR_m)$ The secondary transmission pair with ordering index m.

Δ Step-size of the PT's transmit power.

$\Psi_{SU}(j, m, P_x)$ The event that ST_m cannot be the cooperative partner of PT_j, when PT_j has a candidate cooperative partner transmitting at the x-th power level.

$\Phi_{SU}(j, m, P_z)$ The event that PT_j and ST_m constitute a cooperative pair.

Functions and Variables in Appendices

$\mathcal{C}$ is equal to $\frac{L}{Bw}$.

$\mathcal{F}_{\mathcal{R}_i}(P_{\mathcal{R}_i})$ is equal to $\log_2(1+\Upsilon_{\mathcal{R}_i,\mathcal{D}}P_{\mathcal{R}_i}) - \dfrac{\Upsilon_{\mathcal{R}_i,\mathcal{D}}P_{\mathcal{R}_i}}{(1+\Upsilon_{\mathcal{R}_i,\mathcal{D}}P_{\mathcal{R}_i})\cdot\ln 2}$.

$F_X(x)$ The CDF of the random variable x.

$f_X(x)$ The PDF of the random variable x.

$G_{\mathcal{R}_i}$ is equal to $\rho_{\mathcal{R}_i,\mathcal{D}}|h_{\mathcal{R}_i,\mathcal{D}}|^2$.

$G_{\mathcal{S}}$ is equal to $\rho_{\mathcal{S},\mathcal{D}}|h_{\mathcal{S},\mathcal{D}}|^2$.

H_i is equal to $|h_{\mathcal{R}_i,\mathcal{D}}|^2$.

H_j is equal to $|h_{\mathcal{R}_j,\mathcal{D}}|^2$.

H_k is equal to $|h_{\mathcal{R}_k,\mathcal{D}}|^2$.

I is equal to $\rho_{\mathcal{R}_i,\mathcal{D}}$.

J is equal to $\rho_{\mathcal{R}_j,\mathcal{D}}$.

K is equal to $\rho_{\mathcal{R}_k,\mathcal{D}}$.

$\Upsilon_{\mathcal{R}_i,\mathcal{D}}$ is equal to $\frac{\rho_{\mathcal{R}_i,\mathcal{D}}|h_{\mathcal{R}_i,\mathcal{D}}|^2}{P_N}$.

ϕ is equal to $\gamma^{\mathcal{S}}_{\mathcal{R}_i}(r)+1$.

φ is equal to $P_{max}\frac{G_{\mathcal{R}_i}}{P_N}$.

Ψ is equal to $1+\varphi(1-\beta)-(1+\varphi)^{(1-\beta)}$.

Contents

Chapter 1

Introduction

1.1 Motivation

Wireless networks are expected to support an increased number of wireless terminals and for satisfying their demand at an increased Quality of Service (QoS). However, the throughput versus energy consumption relationship relies on a tradeoff [1, 2]. Cooperative communication constitutes an efficient technique of improving cell-edge performance by allowing relay nodes (RNs) to forward the data of the source node (SN) [3, 4]. More explicitly, the SN to destination node (DN) channnel may exhibit such a low quality that it may have to be considered as unavailable. Based on the broadcast nature of the wireless medium, the RNs may overhear the SN's transmission and may provide cooperative transmission assistance for the SN for the sake of improving unreliable wireless link spanning from the SN to DN. Hence the RN is capable of improving the achievable throughput [5], enlarging the network coverage [6] and reducing the energy consumption [7].

The concept of cooperative communications may be traced back to [8], which analysed the capacity of a relay channel. Based on the notion of cooperative communications, meritorious solutions have been proposed for example in [9–15] for improving on the performance of wireless communications. Most existing contributions on the subject of cooperative communications were developed in the information theory and signal processing domains [11,12,16,17], with a special emphasis on the physical layer.

However, the benefit of cooperative transmissions employed purely at the physical layer may be eroded by the conventional Medium Access Control (MAC) layer. For example, the RNs are required to buffer and forward the SN's data frames relying on the broadcast nature of the wireless network. However, the conventional MAC layer protocol always ignores the data which is not destined for itself. Furthermore, the conventional MAC protocols do not

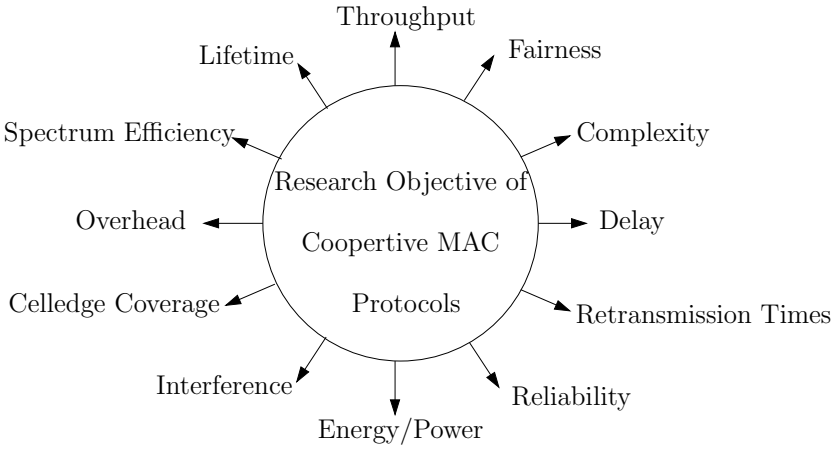

FIGURE 1.1: The diverse factors affecting the design of cooperative MAC protocols.

include the process of selecting best RNs and cannot support the coordination between the different users in a source-relay-destination model. Hence, the appropriate design of the MAC layer is important for supporting the cooperative transmissions, whilst relying on efficiently selecting the best RNs.

1.2 Overview - Cooperative Medium Access Control

In contrast to the legacy wireless MAC protocols, cooperative MAC protocols aim for cooperatively scheduling the medium access of all nodes. Many meritorious cooperative MAC protocols have been proposed for optimizing the system's objective functions. To the best of our knowledge, none of the existing cooperative MAC protocols are superior to the others, because they have both benefits and drawbacks. However, these existing contributions were developed by taking into account some common design features. In this section, we present an overview of the existing cooperative MAC protocols in terms of their fundamental design features, including their basic objective, system architecture, cooperative activation, relay selection decisions and the signalling procedure design.

1.2.1 Research Objective

Aiming for mitigating the deleterious effects of wireless propagation, the so-called user cooperation concept relying on a new form of diversity, namely antenna sharing and relaying was proposed in [18]. Recently, cooperative transmission schemes have been developed for diverse purposes [2]. According to the specific design objectives shown in Fig 1.1, the existing cooperative MAC protocols may be classified as follows.

- **Single-Objective Protocols.** Most existing cooperative MAC protocols were developed for optimizing a single research objective. Improving the attainable system throughput is one of the popular research objectives [19–29] considered in the contributions on cooperative MAC protocols. More explicitly, an increased throughput may be achieved with the aid of cooperative transmission by employing high-data-rate RNs to assist the low-data-rate SN, while increasing the entire system's throughput [24,30,31]. Furthermore, cooperative transmission allows the RNs to be distributed across the entire network. Hence, a beneficial energy/power reduction [32–39] may be achieved with the aid of an appropriate RN set, where the RNs benefit from a better channel spanning from themselves to the DN than the direct link. In a cooperative communication system, the specific RNs, which flawlessly receive the SN's data may provide cooperative transmission assistance for the SN. Hence, the transmission reliability may be improved with the aid of the RNs' transmissions [40–42]. Ultimately, improving the achievable fairness [43, 44], reducing the interference [45, 46] and extending the cell-edge coverage [47] were also considered as design objectives for the existing cooperative MAC protocols, as seen in Fig 1.1.

- **Multiple-Objective Protocols.** Although using a single optimization objective is capable of simplifying the design, striking an attractive trade-off amongst several potentially conflicting design objectives of Fig 1.1 typically results in more beneficial systems. Hence, multiple optimization objectives were considered in [48–51]. Striking an attractive tradeoff between the attainable system throughput and energy/power dissipation has led to meritorious cooperative MAC protocols [52–55]. Furthermore, some cooperative MAC protocols jointly optimized for example the attainable throughput and delay [56–60], the throughput and coverage quality [61,62], or the throughput and fairness [63–65] into joint objective function (OF).

1.2.2 Cooperative Communication System Architecture

A conventional cooperative communication system includes a SN, which intends to transmit its data to the DN, a DN receiving the data and a RN which both receives and forwards the SN's data [66]. Apart from the simple three-terminal system of Fig 1.2, more complex cooperative communication systems were also investigated in the existing literature [24, 34–36, 48, 52, 55, 67–70] which are summarized as follows:

- **Tow-hop single-relay-aided network:** Most existing cooperative MAC protocols [24,36,67,71] were developed for the tow-hop single-relay-aided network of Fig 1.2. The cooperative transmission regime of this system relies on two phases. In the fist phase, the SN conveys its data to the adjacent RN. Then the best RN forwards the

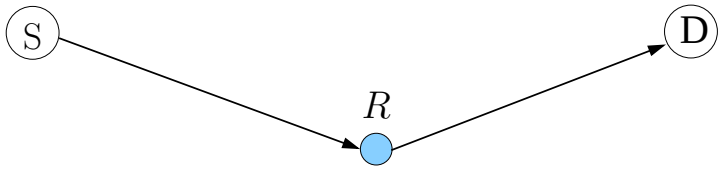

FIGURE 1.2: Topology of a two-hop, single-relay-aided network.

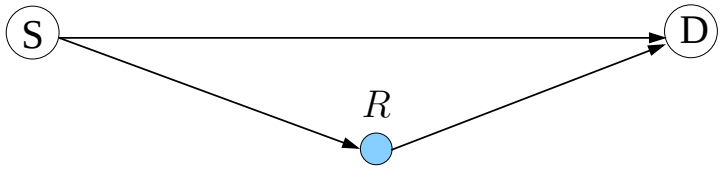

FIGURE 1.3: Topology of a single-hop, single-relay-aided network.

SN's data to the DN within the second phase. The tow-hop single-relay-aided network may host multiple candidate RNs. In order to optimize the system's OF, a single RN selection technique is required for selecting the best RN [24, 36, 67, 71].

- **Single-hop single-relay-aided network:** For the single-hop, single-relay-aided networks of Fig 1.3, the cooperative MAC protocol also contains two phases. However, in the first phase, both the DN and RN intend to store the data received from the SN. In the second phase, different actions may be exploited according to different cooperative MAC protocols. For example, the best RN may forward the SN's data to the DN, while the DN combines the direct transmission and collaborative transmission by invoking frame combining techniques [52, 55, 72]. Alternatively, when the DN fails to successfully receive the SN's data during the first phase, the DN discards the erroneous data and waites for the recovered and retransmitted data of the bets RN within the second phase [41, 73, 74]. Another option to consider, when the DN erroneously received the SN's data is to ensure that both the SN and the RN cooperatively transmit their data by invoking a space-time code during the second phase [75].

- **Multiple-source single-relay-aided network:** For a cooperative communication system, where the number of SNs is higher than that of the RNs, a RN may forward data for multiple SNs. With the goal of investigating the family of cooperative protocols in the context of these systems, the multiple-source single-relay-aided network of Fig 1.4 was considered in [34, 63]. After correctly receiving the SNs' data, the RN may jointly encode the data gleaned from different SNs with the aid of physical layer techniques, such as superposition coding [76, 77] and network coding [34, 63, 68, 78]. Some cooperative MAC protocols allow the RN to store the data received from different SNs in its buffer. Then the RN may forward the data from its buffer based on its near-instantaneous system state information [79, 80], such as the specific QoS requirement, the buffer-fullness or channel quality.

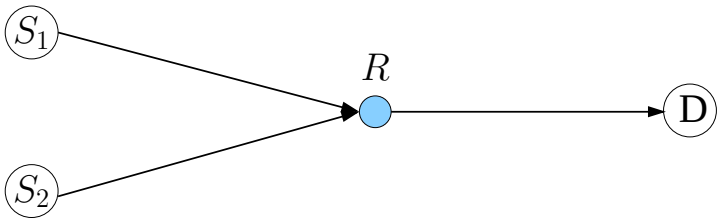

FIGURE 1.4: Topology of a multiple-source, single-relay-aided network.

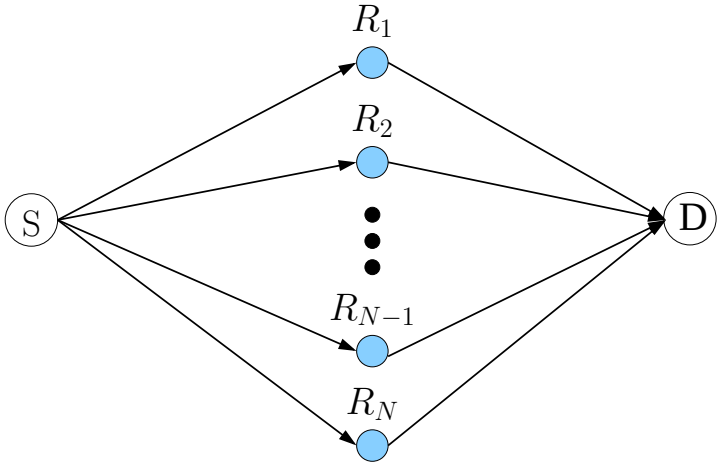

FIGURE 1.5: Topology of a two-hop, multiple-relay-aided network.

- **Two-hop multiple-relay-aided network:** For the two-hop multiple-relay-aided network shown in Fig 1.5, the SN first broadcasts its data to the adjacent RNs. Then the SN's data may be forwarded by the RNs with the aid of the appropriate physical layer techniques, such as diverse multiple-input-multiple-output (MIMO) schemes [19, 21, 45, 48, 58, 81, 82], including space-time coding [19, 21, 26, 83] and beamforming technology [20, 45, 82].

- **Multiple-hop multiple-relay-aided network:** Using two-hop cooperative transmission is not the only collaborative transmission solution between the SN and multiple RNs. Some cooperative MAC protocols were designed for the multiple-hop multiple-relay-aided networks portrayed in Fig 1.6. Based on the architecture of the RN set, the multiple-hop multiple-relay-aided networks may be further classified as follows:

  - **Serial multiple-hop multiple-relay-aided network:** For the serial multiple-hop multiple-relay-aided network shown in Fig 1.6(a), the SN broadcasts its data to the adjacent RNs. Then the specific RNs which successfully received the SN's data may relay the data to the next RN or directly to the DN [54, 69, 84]. The serial multiple-hop multiple-relay-aided network of Fig 1.6(a) is capable of further extending the coverage or shortening the length of each hop for the sake of saving the transmit energy, albeit at the cost of an extra delay.

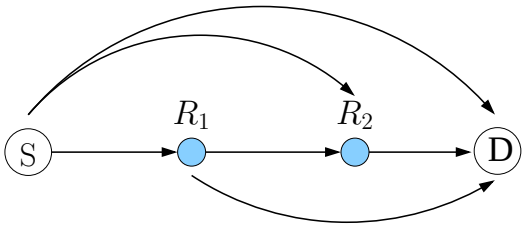

(a) Serial multiple−hop multiple−relay−aided network

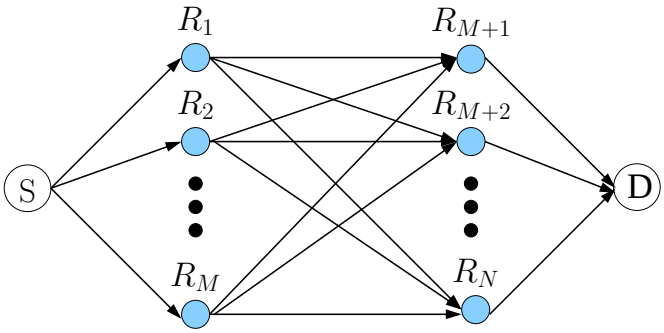

(b) Parallel multiple−hop multiple−relay−aided network

FIGURE 1.6: Topology of a multiple-hop multiple-relay-aided network.

– **Parallel multiple-hop multiple-relay-aided network:** In [70], a parallel multiple-hop multiple-relay-aided network was considered, which is shown in Fig 1.6(b). A cooperative protocol was developed [70] for selecting both the transmitter helper group and a receiver helper group for the sake of saving energy by shortening the range of the first and third hops. Furthermore, a parallel multiple-hop multiple-relay-aided network may be conceived for improving the system's throughput [85, 86]. However, the design of cooperative protocols may become significantly more complex due to the complex network architecture [70, 85–87].

Clearly, multiple-hop multiple-relay-aided cooperation is capable of providing additional diversity gain attained with the aid of several independently fading signal paths.

- **Multiple-source multiple-relay network:** In contrast to the cooperative networks of Fig 1.2-Fig 1.6, the multiple-source multiple-relay network of Fig 1.7 may be used for modelling multiple-user cooperative systems. The SNs invoked in a multiple-source multiple-relay network are assumed to rely on their unique, user-specific channel resource. In order to improve the system's performance, efficient cooperative partner selection may be exploited for supporting cooperative transmission in the context of multiple-source multiple-relay network of Fig 1.7. For example, each RN selectively provides cooperative assistance for some, but not for all of the SNs [35]. Furthermore, meritorious reciprocal selection schemes were investigated in [88, 89] for the sake of

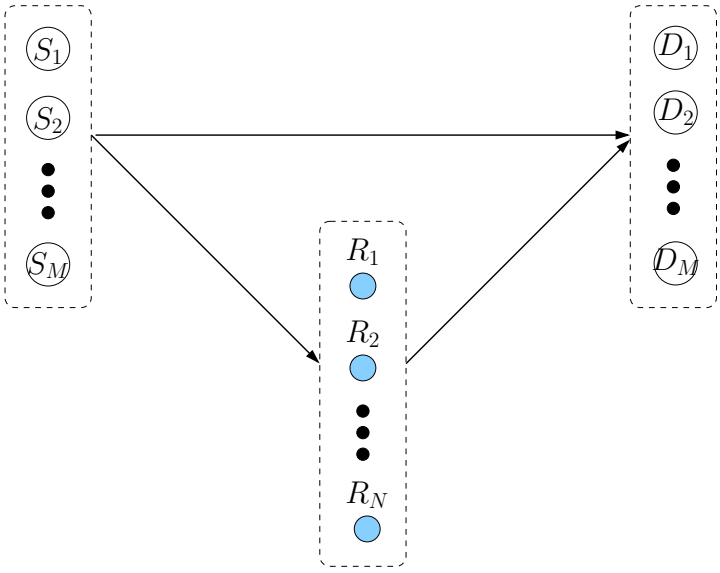

FIGURE 1.7: Topology of a multiple-source multiple-relay network.

allowing both the SN and the RN to select their best cooperative partner. Due to the rather involved negotiations between SNs and RNs, the design of a cooperative MAC protocol for a multiple-source multiple-relay network remains essentially open research area at the time of writing.

1.2.3 Cooperation Activation

A cooperative MAC protocol has to specify the cooperation activation rule invoked for informing the RNs about the specific instant of providing cooperative transmission assistance. According to the instant triggering collaborative transmission, the cooperation activation rule of existing cooperative MAC protocols may be classified as follows:

- **Proactive relay selection scheme.** According to proactive relay selection scheme of Fig 1.8(a), the best relay is selected before the source is notified whether its data was correctly received by the destination with the aid of an acknowledgement (ACK) message or by the negative-acknowledgement (NACK) message [19, 21, 24, 29, 30, 35, 54, 59, 67, 71, 78, 86, 90, 91]. Proactive relay selection scheme of Fig 1.8(a) is capable of substantially improving the system's performance by selecting the appropriate RN set. However, the cooperative MAC protocol may require fairly complex negotiations between the nodes for implementing relay selection as well as for exchanging the cooperative notifications necessitated. The important contributions on cooperative MAC protocol design relying on proactive relay selection scheme are shown in Table 1.1.

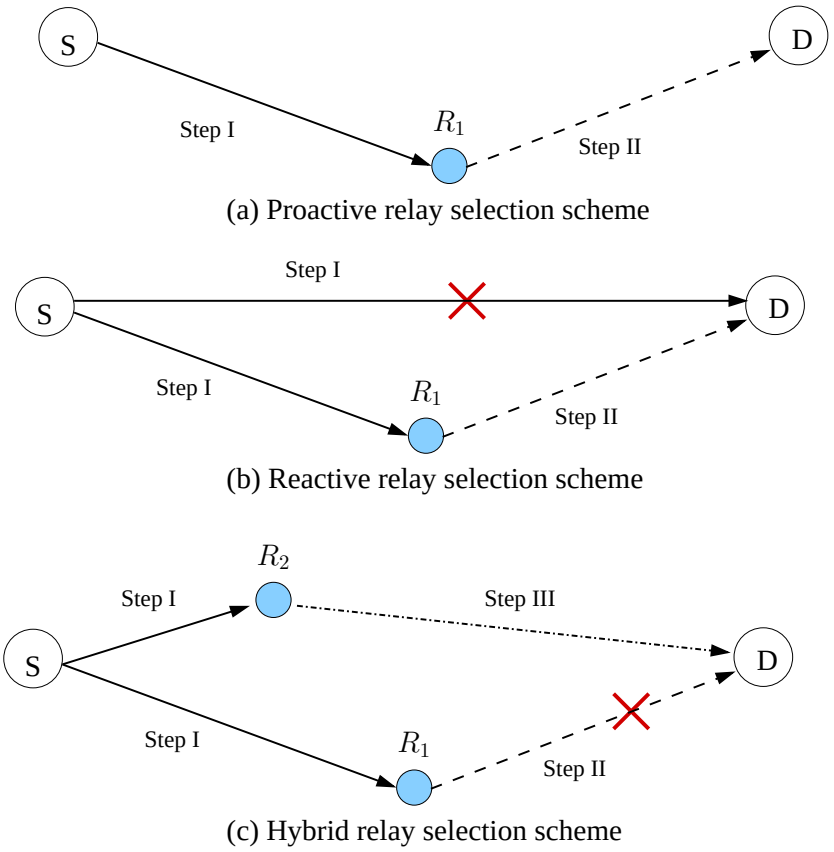

FIGURE 1.8: Examples of proactive and reactive as well as hybrid relay selection schemes.

- **Reactive relay selection scheme.** When invoking a reactive selection scheme of Fig 1.8(b), the cooperation is initialized only when the direct transmission has failed [92, 93]. Using an Automatic Repeat reQuest (ARQ) strategy is a common solution for implementing the reactive relay selection scheme of Fig 1.8(b) [28, 42, 44, 48, 60, 75, 94, 95]. More explicitly, the RN may forward the SN's data, when it receives a NACK, indicating that the DN failed to correctly receive the SN's data. Hence, the reactive relay selection scheme of Fig 1.8(b) allows the RN to recover the erroneous direct transmission for the sake of improving the transmission reliability, whilst simultaneously reducing the SN's retransmission time. Table 1.2 lists the important contributions on the subject of cooperative MAC protocol design relying on the reactive relay selection scheme of Fig 1.8(b).

- **Hybrid relay selection scheme.** In [84], a combination of the proactive and reactive relay selection scheme of Fig 1.8(a) and Fig 1.8(b) was conceived, which is shown in Fig 1.8(c). According to the proactive relay selection scheme of Fig 1.8(a), a best RN is selected for the sake of maximizing the throughput, while a second RN selected by the relay selection scheme provides potential backup for the erroneous transmission received via the first best RN - DN route, as seen in Fig 1.8(c). Although the hybrid

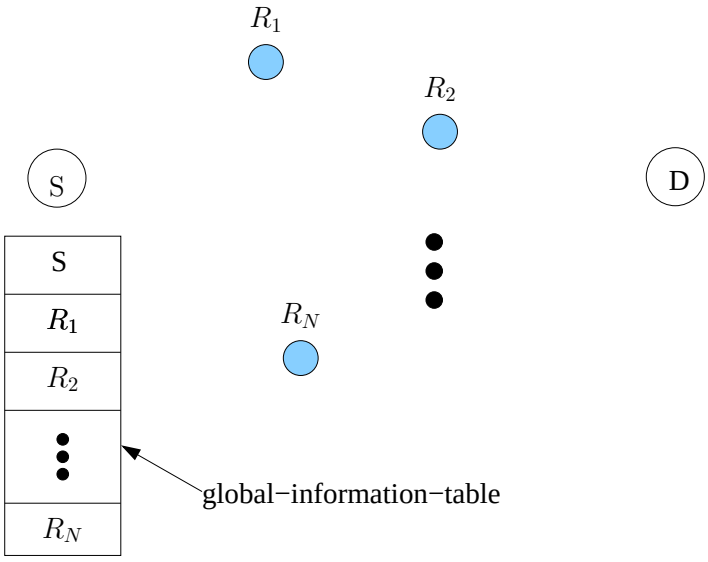

(a) Global−information−based protocol

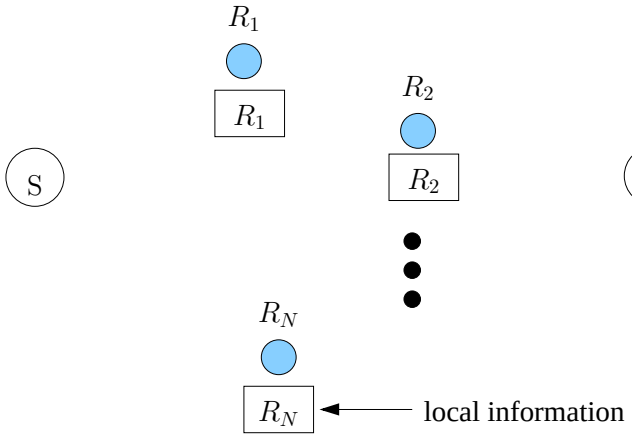

(b) Local−information−based protocol

FIGURE 1.9: Examples of global-information-based and local-information-based protocols.

relay selection scheme is capable of improving the system's performance, the MAC protocol design is complex.

1.2.4 Relay Selection Decisions

A cooperative MAC protocol may employ a single RN or in fact several of the pool of candidate RNs to provide cooperative transmission assistance. Hence, the best RN set has to be appropriately selected, depending on the near-instantaneous system state and the OF considered. Provided that this information related to all of the potential candidate RNs has been acquired, the system is capable of selecting the best RN set. Depending on the specific

information on the potential RNs, the existing cooperative MAC protocols may be classified as follows:

- **Global-information-based protocol:** When aiming for optimizing the system's objective function, the global information collected from all the potential candidate RNs may be invoked for selecting the optimal RN set for providing cooperative transmission assistance. The family of table-based cooperative MAC protocols [30,62,84,89,96] relies on prestored global information tables of Fig 1.9(a) for selecting the optimal RN set. The SN invoked in the system relying on table-based cooperative MAC protocols has to maintain and update a table recording the relevant information on the potential RNs, as shown in Fig 1.9(a). The SN selects the best RN set by comparing the information stored in its table. However, a long time-duration may be required for discovering the potentially most beneficial RNs and for constructing the information table. Furthermore, if the table is not updated in a timely manner, the SN may select a low-quality RN as the best RN based on the obsolete table. In order to avoid erroneous decision caused by an outdated table, typically a centralized controller is employed for collecting the near-instantaneous information of all potential candidate RNs and for selecting the best RN set by analysing the global information [21, 24, 35, 48, 67, 91, 97]. However, conveying global information may complicate the MAC protocol design and dissipate more energy, while exchanging the extra control messages. Moreover, global-information-based protocols may impose an excessive complexity at the centralized controller, while selecting the best RN set.

- **Local-information-based protocol:** In order to simplify the design of cooperative MAC protocols, simplified local-information-based relay selection scheme may be conceived, albeit they achieve a sub-optimal system performance. According to the local-information-based protocol of Fig 1.9(b), the candidate RNs are capable of making autonomous decisions concerning whether to provide cooperative transmission assistance, while the best RN set is distributively selected without collecting information of all the candidate RNs and without complex calculations and decisions at the centralized controller [52,54,55,68,71,75,82]. Hence, the local-information-based relay selection scheme of Fig 1.9(b) is capable of simplifying the control message exchange required by the cooperative MAC protocol. However, an appropriate strategy is required for supporting realistic distributed relay selection schemes. Furthermore, designing a local-information-based protocol, which is capable of omptimizing the system's performance remains essentially an open challenge.

1.2.5 Signalling Procedure Design

In order to practically implement the proposed cooperative transmission protocols, most existing work developed appropriate signalling procedures for the sake of conveying the control information between the nodes and for supporting cooperative transmissions. Compared to designing a new MAC protocol, developing a cooperative MAC protocol by extending the conventional MAC protocol is conceptually more appealing technique of practically implementing cooperative transmissions without introducing fundamental changes into the existing wireless communication network.

Both the proactive and reactive relay selection schemes of Fig 1.8(a) and Fig 1.8(b) may be implemented based on the Distributed Coordination Function (DCF) specified in the Institute of Electrical and Electronics Engineers (IEEE) 802.11 standards [21, 24, 30, 52, 54, 62, 67, 68, 71, 84]. More explicitly, the SN is capable of indicating its transmission intention and of inviting cooperative transmission assistance with the aid of its Request-to-Send (RTS) / Clear-to-Send (CTS) handshake, which is specified in the DCF scheme [21, 54, 62]. Extra control messages may be introduced into the conventional DCF scheme for the sake of supporting the prompt information exchange between the SN and RNs [24,52,71], such as the "Helper Ready To Send" (HTS) invoked in CoopMAC [30]. Furthermore, cooperative MAC protocols relying on the reactive relay selection scheme of Fig 1.8(b) may be implemented by invoking the ARQ strategy specified in the DCF scheme [48, 98, 99]. According to the cooperative system considered, some cooperative MAC protocols were developed relying on other conventional protocols, such as those of the IEEE 802.16 standards [19].

Based on the above signalling procedure designs, the cooperative communication systems exploiting the cooperative MAC protocols which are backward-compatible with the conventional protocols are capable of coexisting with traditional wireless communication systems.

1.3 Organisation of the Thesis

In order to simplify their investigations, early contribution [51, 54, 71] on cooperative communication assume that the RNs agree to altruistically forward the SN's data. However, this unconditional altruistic behaviour is unrealistic to expect from the mobile stations (MS), which may intend to acquire 'revenue' by providing cooperative transmission assistance. Considering this greedy nature of the RNs, the cooperative spectrum leasing scheme of [100–102] was proposed as a possible solution for supporting the cooperation between the SNs and the greedy RNs. More explicitly, based on the cooperative spectrum leasing philosophy, the licensed SNs lease part of their spectral resource, which was originally granted to

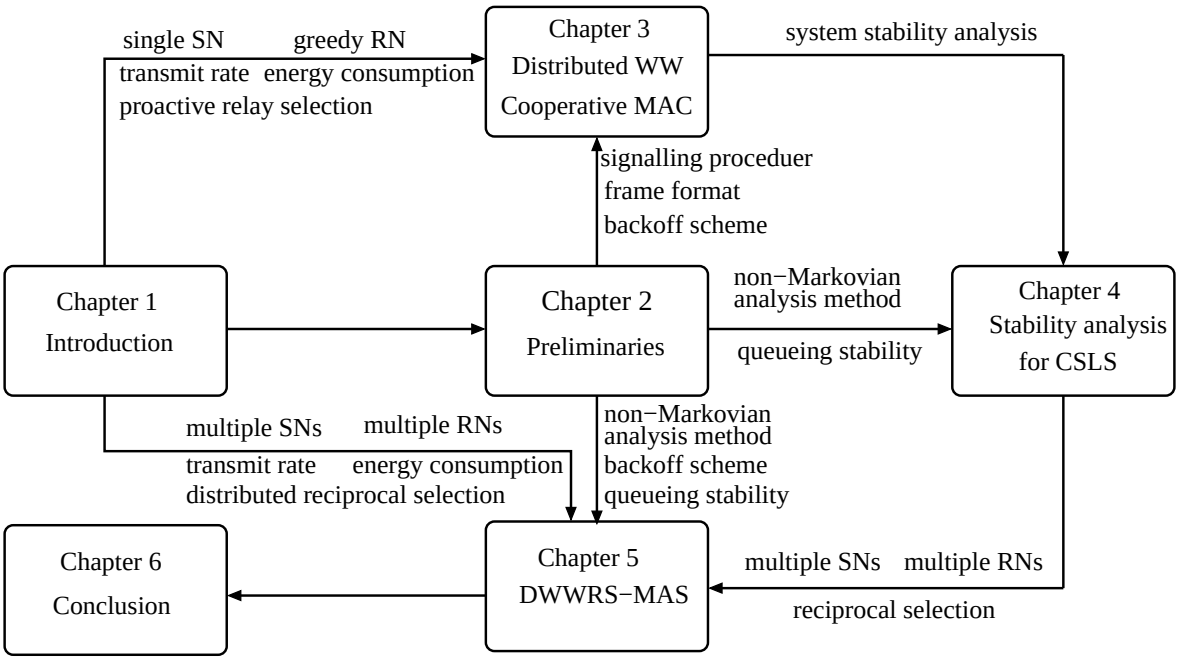

FIGURE 1.10: The structure of this thesis.

them by assigning a fraction of it to the unlicensed RNs in exchange for cooperative transmission assistance. The unlicensed RNs are granted the opportunity to access the licensed spectrum for the sake of transmitting their own traffic in exchange for providing cooperative transmission assistance for the licensed SNs. In this thesis, we consider cooperative spectrum leasing in Chapter 3, Chapter 4 and Chapter 5 for the sake of supporting the collaboration between the SN and greedy RNs.

In a cooperative spectrum leasing system, both the SNs and RNs may store their incoming data into a buffer, when either the current transmission is not completed or they cannot access the medium immediately. When the new packets keep arriving, while the corresponding service rate is insufficiently high for flushing the buffer, the size of the queue in the buffer would keep on increasing. Hence, these queues may become unstable. The service rate of both the SN's data and the RNs' data in a cooperative spectrum leasing system is intimately related to the cooperative MAC protocol, which specifies both the scheduling policies of the different users as well as the relay selection rules. It is plausible that a queueing network is globally stable, provided that all the users are capable of handling all the incoming teletraffic relying on a reasonable scheduling rule [103]. Hence, analysing the stability of the cooperative spectrum leasing system is a fundamental technique of investigating the impact of a cooperative MAC protocol on the system's performance. In order to characterize the performance of the proposed cooperative MAC protocols, in Chapter 4 and Chapter 5 we will analyse the stability of the cooperative spectrum leasing systems relying on the proposed cooperative MAC protocols.

Fig 1.10 illustrates the dependencies among all chapters based on the above-mentioned aspects. The outline and novel contributions of this thesis are summarised as follows:

- **Chapter 2:** In this chapter, the fundamental techniques relied upon in this thesis are introduced. In order to characterize the functions of the MAC layer, Section 2.2 introduces the classic layered network protocol architecture. Then in Section 2.3, we elaborate on the functions of the MAC layer and on the existing conventional wireless medium access schemes. Furthermore, the conventional MAC protocols specified in the IEEE 802.11 standards are detailed in Section 2.3.2. Section 2.4 commences with the fundamental characterization of queueing systems and outlines the corresponding important theorems as the preliminaries of our stability analysis. Then in Section 2.4.2, we formulate the definition of stability for the queueing system considered. Section 2.4.2 is concluded by discussing the method of analysing the stability of cooperative queueing system.

- **Chapter 3:** Based on our discussions in Chapter 1 and Chapter 2, a 'win-win' (WW) cooperative MAC protocol is proposed for striking a tradeoff between the achievable system rate improvement and energy dissipation. Our solution relies on granting transmission opportunities for the unlicensed RNs. Based on the cooperative spectrum leasing system considered, Section 3.2 formulates a WW cooperative framework (WWCF), where the licensed SN intends to lease part of its spectrum to the unlicensed RNs in exchange for its cooperative support for the sake of saving the SN's transmit power, whilst simultaneously improving the SN's transmit rate. As a benefit, the unlicensed RNs have an incentive to provide cooperative transmission assistance for the SN in exchange for accessing the licensed spectrum for transmitting their own data. Then in Section 3.3, a distributed WW cooperative MAC protocol is developed for implementing the proposed WWCF. In order to support cooperative transmission, we design a specific signalling procedure and detail the format of the data frame and control messages. Furthermore, a novel backoff algorithm is developed for selecting the best RN according to the OF of the proposed WWCF. Our simulation results provided in Section 3.4 demonstrate that both substantial rate improvements and considerable energy savings are achieved by implementing the proposed WW cooperative MAC protocol. Section 3.5 summarises this chapter.

  Contribution 1: *A WWCF is formulated for the sake of encouraging the SN to lease part of its spectral resources to the unlicensed RN for the sake of* ***improving the SN's transmit rate*** *and for simultaneously* ***reducing the SN's energy consumption****, while ensuring that the unlicensed RNs are capable of* ***securing a transmission opportunity for their own traffic*** *and for* ***satisfying their QoS****. Furthermore,*

the proposed WWCF selects the best RN for the sake of ***minimizing the system's energy consumption*** *[104].*

Contribution 2: *A distributed WW cooperative MAC protocol is developed for* ***practically implementing*** *the proposed WWCF by designing the required* ***signalling procedures*** *for implementing the negotiation between the SN and the greedy RN. Furthermore, the* ***frame structure*** *of both the data and control messages is also conceived for conveying all the required information [104].*

Contribution 3: *A* ***distributed RN selection scheme*** *is proposed relying on a novel backoff algorithm. Based on the proposed distributed WW cooperative MAC protocol, the RNs carry out autonomous decisions concerning whether to contend for a cooperative transmission opportunity based on the local information. Furthermore, the specific priority of the candidate RNs can be identified by the proposed backoff algorithm according to the results of local calculations carried out at each candidate RN. Based on the proposed backoff algorithm, the SN is capable of discovering its best RN without collecting and comparing the specific parameters promised by the individual candidate RNs [104].*

- **Chapter 4:** In this chapter, we analyse the stability of the cooperative spectrum leasing system relying the proposed distributed WW cooperative MAC protocol. According to the system model outlined in Section 4.2, in Section 4.3 we construct the queueing model and detail our assumptions stipulated for the sake of simplifying the analysis. Relying on the non-Markovian analysis method discussed in Chapter 2, we derive the stable throughput for both the SN and the RNs, which is limited by the proposed distributed WW cooperative MAC protocol. Section 4.4 quantifies the stable throughput of both SN and RNs in different scenarios. The results of our stability analysis are confirmed by our simulation results. Finally, Section 4.5 concludes this chapter and motivates the following chapters.

  Contribution 4: *The stability analysis of* ***a cooperative spectrum leasing system*** *is offered in this chapter. To the best of our knowledge, the queueing stability of the cooperative spectrum leasing system has not been investigated [52].*

  Contribution 5: *In this chapter, we analyse the stability of a cooperative queueing system having* ***multiple objectives****. More explicitly, the cooperative spectrum leasing system considered is capable of improving the SN's* ***transmit rate****, whilst simultaneously reducing the system's total* ***energy consumption*** *as well as satisfying the* ***QoS*** *of the RNs by exploiting the proposed distributed WW cooperative MAC protocol. Furthermore, the* ***probability expression of a RN winning a contention*** *for a cooperative transmission opportunity is derived. Additionally, we analyse the stability of a* ***unique*** *cooperative MAC protocol [52].*

- **Chapter 5:** Considering the proposed cooperative spectrum leasing system of Section 5.2.1, which has multiple licensed primary transmission pairs and multiple unlicensed secondary transmission pairs, a WW reciprocal-selection-based framework (WWRSF) is formulated in Section 5.2.2 for selecting the optimal cooperative pairs. This optimal pair consists of a primary transmitter (PT) and a secondary transmitter (ST), which relies on carefully matched cooperative pairs, specifically selected for striking a tradeoff between the achievable rate improvement and the transmit power. More explicitly, each PT selects an appropriate ST as its cooperative partner for the sake of minimizing its transmit power and for simultaneously improving its transmit rate. Furthermore, the ST intends to provide cooperative assistance for the best PT for the sake of minimizing the ST's transmit power, whilst simultaneously accessing the licensed spectrum for conveying its own traffic. Based on the OFs of the proposed WWRSF, in Section 5.3 a distributed WW reciprocal-selection-based medium access scheme (DWWRS-MAS) is designed for producing the best cooperative pairs. In order to further study the proposed DWWRS-MAS, in Section 5.4 we analyse both the queueing stability and the algorithmic stability of our cooperative spectrum leasing system relying on our DWWRS-MAS. In Section 5.5 the cooperative spectrum leasing system exploiting the proposed DWWRS-MAS is benchmarked against a pair of different optimal centralized systems and against two non-cooperative systems for the sake of benchmarking our system. Finally, Section 5.6 concludes this chapter.

  Contribution 6: *Considering a* ***cooperative spectrum leasing system*** *supporting* ***multiple*** *primary users (PUs) and secondary users (SUs), the proposed DWWRS-MAS produces the best cooperative pairs relying on our novel* ***distributed reciprocal selection*** *between the PUs and SUs for the sake of reducing* ***the transmit power dissipated by the PTs and STs*** *as well as for improving the* ***achievable transmit rate of PTs*** *and simultaneously satisfying the* ***ST's QoS requirement*** *[105].*

  Contribution 7: *The queueing stability analysis of a* ***cooperative spectrum leasing system*** *having* ***multiple transmission pairs*** *is offered. To the best of the authors' knowledge, the queueing stability of a cooperative spectrum leasing system hosting multiple transmission pairs has not been investigated at the time of writing [105].*

  Contribution 8: *In this chapter, we analyse the stability of a* ***unique*** *cooperative queueing system supporting both* ***multiple design objectives*** *and* ***multiple transmission pairs****. Furthermore,* ***the cooperative probability expression of both PT and ST*** *is derived based on our* ***distributed reciprocal selection scheme*** *[105].*

  Contribution 9: *The* ***algorithmic stability*** *analysis of the proposed DWWRS-MAS is offered. When using the proposed DWWRS-MAS, both the PT and the ST of the best cooperative pair achieve their best performance. Hence, neither of them can*

acquire an increased profit by selecting other cooperative partners. Moreover, at least one cooperative pair produced by the proposed DWWRS-MAS is capable of acquiring more benefit in terms of a reduced transmit power and increased transmit rate than the cooperative pairs produced by other matching algorithms [105].

- **Chapter 6:** In this final chapter, the conclusions of our investigations are presented, followed by a variety of suggestions for future research.

TABLE 1.1: Major contributions on cooperative MAC protocols exploiting proactive relay selection

Years	Authors	Contributions
2007	Liu *et al.* [30]	designed a table-based cooperative MAC protocol referred to as CoopMAC for improving the total network throughput.
2008	Zhou *et al.* [90]	proposed a selective single-relay cooperative scheme relying on physical layer power control for improving the energy efficiency.
2009	Hua *et al.* [91]	designed a cooperation-aware MAC protocol relying on proactive relay selection for improving the system's throughput.
	Yang *et al.* [29]	proposed a cooperative multi-group service priority based MAC protocol for improving the system throughput.
2010	Argyriou [78]	conceived a cooperative MAC protocol for maximizing the system's throughput by combining network coding and cross-layer adaptation.
	Verde *et al.* [59]	designed a rate-adaptive cross-layer operation aided MAC protocol relying on multiple RNs for minimizing the overall transmission duration.
	Zhou *et al.* [86]	proposed a cooperative cross-layer MAC protocol for improving both the system's throughput and energy efficiency by combining space-time coding and adaptive modulation at the physical layer as well as by exploiting automatic repeat request (ARQ) at the MAC layer.
2011	Oh *et al.* [24]	developed an active relay-based cooperative MAC protocol for improving the system's throughput and for providing a transmission opportunity for the RNs to convey their own traffic.
	Shan *et al.* [71]	designed a cooperative cross-layer aided MAC protocol, which can identify the beneficial cooperative rate allocations relying on identifying the most beneficial cooperation region for increasing the system throughput.
	Zhou *et al.* [54]	proposed a link-utility-based cooperative MAC protocol for improving both the achievable transmission rate and the energy efficiency by distributively selecting the best RN based on the link utility of the candidate RNs.
2012	Liu *et al.* [21]	proposed a cooperative MAC protocol referred to as STiCMAC for improving the system's achievable rate by supporting the concurrent transmission of multiple RNs with the aid of randomized distributed space-time coding (DSTC).
	Fang *et al.* [35]	proposed a cooperative cross-layer MAC protocol, which is capable of minimizing the transmit power under certain QoS requirements, whilst relying on a distributed RN selection scheme and optimal power allocation strategy.
	Liang *et al.* [67]	developed a double-loop cooperative MAC protocol for increasing the transmit rate by exploiting both the available spatial and temporal diversity gain.
2013	Nie *et al.* [19]	designed a cooperative MAC for the Worldwide Interoperability for Microwave Access (WiMAX) system in order to improve the system's throughput by exploiting randomized DSTC.

TABLE 1.2: Major contributions on cooperative MAC protocols exploiting reactive relay selection

Years	Authors	Contributions
2009	Guo *et al.* [42]	designed a differentiated cooperative MAC protocol to satisfy the QOS requirements of different services with aid of cooperative retransmission assistance provided by the RN.
	Zhang *et al.* [28]	proposed a cooperative vehicular MAC protocol for improving the throughput of gateway-downloading services in vehicular networks by selecting the optimal collision-free relay set.
2010	Yang *et al.* [94]	proposed a cooperative time division multiple access (TDMA) MAC protocol for improving the system's throughput by relying on retransmission from RNs during the free time slots.
	Kong *et al.* [44]	designed a cooperative retransmission MAC protocol for improving the system's throughput and the node fairness.
	Lu *et al.* [95]	proposed a hybrid spatial/temporal retransmission protocol, which improves the throughput of wireless video streaming applications and satisfies the timing constraints with the aid of a time-based adaptive retransmission strategy at the MAC layer.
2011	Aguilar [75]	proposed a cross-layer framework, which consists of two cross-layer designs, namely a network-MAC design for next hop selection and a MAC-physical design for relay selection.
2012	Wang *et al.* [60]	designed a network coding aware cooperative MAC protocol for improving the system's throughput and for reducing its delay.
2013	Chu *et al.* [48]	designed a MIMO-based cooperative MAC protocol for improving the transmission reliability and throughput with the aid of retransmissions from the RN for recovering the erroneous direct transmission packets.

Chapter 2

Preliminaries

2.1 Introduction

This thesis focuses on developing and analysing cooperative medium access control (MAC) schemes for supporting cooperative communications. Hence, before delving into the novel contributions of the thesis, we briefly review the history of wireless medium access control schemes, with an emphasis on the stability analysis of queueing systems.

The layered Open Systems Interconnection (OSI) network protocol architecture will be briefly introduced in Section 2.2. We will also highlight the function of each protocol layer specified in the Transport Control Protocol (TCP)/Internet Protocol (IP) (TCP/IP) model.

Based on the OSI model, Section 2.3 first highlights the conventional wireless medium access schemes. Then the MAC protocols specified in the Institute of Electrical and Electronics Engineers (IEEE) 802.11 standards are addressed in Section 2.3.2. Since most existing cooperative MAC schemes are developed on the basis of the so-called distributed coordination function (DCF) [21,30,52], we will elaborate on the handshake procedure and on the formats of both the data frame and control messages specified by the DCF scheme. Moreover, Section 2.3 will also highlight the other MAC schemes specified by the IEEE 802.11 standards, such as the point coordination function (PCF) scheme [106].

More explicitly, in Section 2.4 we will investigate the stability of the queue procedure buffering the packets, which are waiting for the service provided by the MAC protocol. Based on the definition of the stability of the queueing system addressed in Section 2.4.1, Section 2.4.2 will discuss the most popular methods of analysing the stability of a queueing system.

Finally, we will summarise this chapter in Section 2.5.

2.2 Network Protocol Architecture

Data exchange between the terminals supported either by the same system or by different systems are complex procedures. A range of procedures have to be established for successfully transmitting data from the source node (SN) to the destination node (DN) [107]:

- A data path between a SN and DN has to be discovered by the network, which relies on the identification of the terminals.
- The SN has to be informed, when the DN is capable of receiving the SN's data.
- The format of messages exchanged between the communication nodes should be identical. If different data formats are used in the communication systems, format translation has to be performed.
- Both error protection and file management should be implemented for the sake of guaranteeing that the data is successfully received.
- Appropriate resource allocation schemes have to be conceived for supporting multiple transmission pairs.

Hence, a high degree of coordination is required between the communication systems supporting the SN and DN. Since integrating the communication procedures is a complex task, the OSI architecture and the TCP/IP architecture were developed for the sake of simplifying the communication protocols by breaking the communication procedures into several less complex functions [107]. More explicitly, the network protocols are organized into layers of the OSI architecture of Fig 2.1, where each layer implements its own functions relying on the 'services' provided by the lower layer right below it. Furthermore, each layer has to offer a service for the layers above it and has to conceal the details of its own function.

2.2.1 OSI Model

The OSI model was designed by the International Organization for Standardization (ISO) as a framework conceived for the sake of developing the network protocol standards. The OSI model consists of seven layers [107], namely the application layer, presentation layer, session layer, transport layer, network layer, data link layer and physical layer, as seen in Fig 2.1. The functions of each layer are described as follows [107, 108]:

- **Layer 7**: *Application Layer*. The application layer is capable of directly providing services to the users. Numerous widely used services are supported at the application layer, such as file downloading and email services [107, 108].

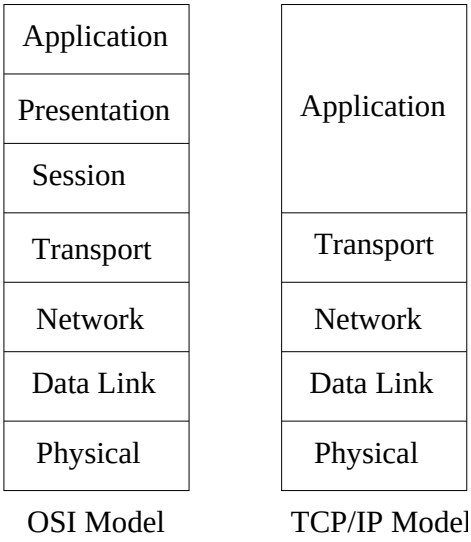

FIGURE 2.1: Comparison of the layered OSI architecture of [107, 108] and of the TCP/IP model [107, 109].

- **Layer 6**: *Presentation Layer*. The presentation layer is capable of transforming the different data formats of all applications into a standard format, which can then be understood by the lower layer. Furthermore, at the presentation layer, the network's data format has to be translated into the specific formats that can be accepted by the application layer. Hence, the presentation layer provides the common interface for the different services at the application layer [107, 108].

- **Layer 5**: *Session Layer*. The function of session layer is that of managing the connections (sessions) between two application processes invoked from different terminals, including session establishment, session maintenance and session termination [107, 108].

- **Layer 4**: *Transport Layer*. The transport layer provides reliable end-to-end transmission of the messages destined for the higher layers, whilst relying on the flow control [107, 108], segmentation and error control procedures.

- **Layer 3**: *Network Layer*. The main function of network layer is to discover the set of legitimate transmission paths between the SN and DN, which are located in different networks and then routing the data through the networks, whilst taking into account the prevalent network conditions, service priority, the Quality of Service (QoS) requirements and other factors [108]. A pair of adjacent nodes exchange their data with the aid of the peer protocol at their network layer and the lower layers. However, they may be intermediate nodes selected by the routing protocol, because the SN and DN may be separated by many intermediate networks [107].

- **Layer 2**: *Data Link Layer*. The data link layer is responsible for providing reliable transmission over the physical layer, while relying on the medium access management,

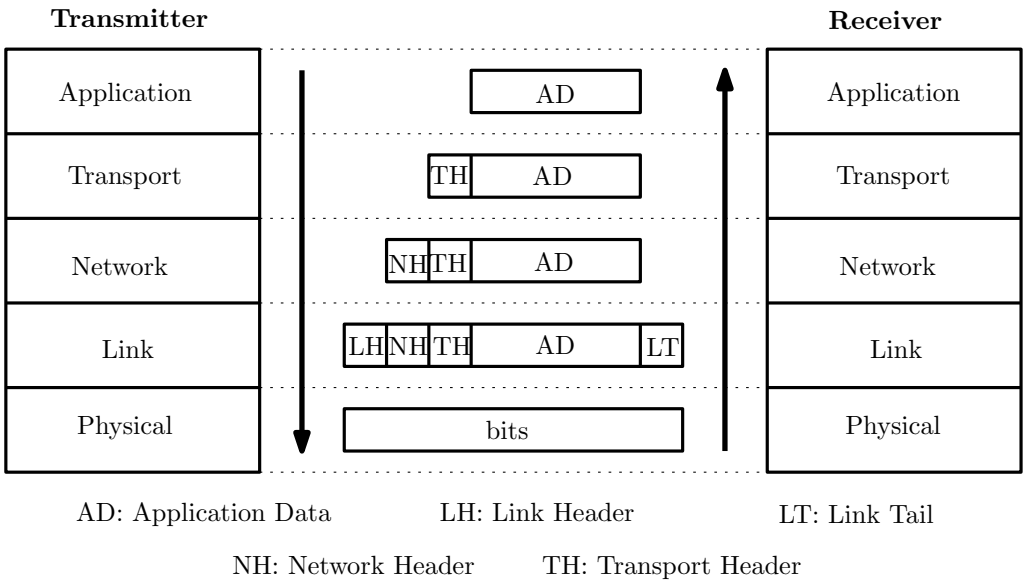

FIGURE 2.2: The procedure of data encapsulation and data decapsulation at each layer in the TCP/IP model [107, 109].

frame error checking and recovering, frame delimiting and sequencing as well as link establishment and termination [107, 108]. More explicitly, the protocols at the data link layer have to appropriately allocate the shared spectral resources to the users supported by the same network. Furthermore, the integrity of the received frame will be checked at the link layer and the erroneous data frames might be retransmitted.

- **Layer 1**: *Physical Layer*. As the lowest layer of the OSI model of Fig 2.1, the physical layer carries the signals of the above layers over the physical transmission medium and controls both the transmission as well as the reception of the bit stream over the physical medium [107, 108]. The typical techniques used at the physical layer are channel coding, modulation, channel estimation, equalization, etc.

2.2.2 TCP/IP Model

Compared to the OSI model, the TCP/IP model has a simplified protocol architecture, which consists of five layers: the application, transport, network, link and physical layers [107, 109], as shown in Fig 2.1. Here, the main functions of each layer from the top to the bottom are listed as follows.

- **Layer 5**: *Application Layer*. The functions of the application layer, presentation layer and session layer in the OSI model are integrated into the application layer of the TCP/IP model, which provides useful network services to the users [109]. The application layer encapsulates a number of protocols, such as the Hypertext Transfer

Protocol (HTTP) [110] supporting Web browsing, File Transfer Protocol (FTP) [111] supporting file down-loading and the Simple Mail Transfer Protocol (SMTP) [112] conceived for E-mail systems, etc.

- **Layer 4**: *Transport Layer.* The transport layer specified by the TCP/IP model performs the same functions as those of the OSI model, hence assisting in the support of end-to-end transmissions of messages passed to it from the application layer. Both the TCP and the User Datagram Protocol (UDP) are part of the transport layer of the TCP/IP model [107,109]. The TCP protocol provides reliable connection-oriented transmissions between two hosts with the aid of error control, flow control and congestion control. However, the UDP provides a connectionless service, which cannot guarantee that all the data successfully reaches the destination [107, 109].

- **Layer 3**: *Network Layer.* The network layer of the TCP/IP model is responsible for addressing the hosts and for routing packets through the networks. The IP protocol belongs to this layer, which specifies the IP addresses of all Internet components. The IP protocol is implemented by both the terminals and the routers. Two different networks are connected by a router, which is responsible for forwarding data from one network to another [107, 109]. Furthermore, the data stream may be fragmented into smaller packets at the network layer, if it is longer than the maximum transmission unit (MTU). The appropriately partitioned data stream will be then reassembled at the destination [107, 109].

- **Layer 2**: *Link Layer.* The link layer of the TCP/IP model corresponds to the second layer of the OSI model, namely the data link layer. According to the Medium Access Control (MAC) addresses, this layer is responsible for conveying packets along the point-to-point link between two adjacent hosts within the same network [107]. The operation of the link layer protocols depends on the quality of the physical medium encountered [107, 109]. For example, the Institute of Electrical and Electronics Engineers (IEEE) specifies the link layer protocol, namely the 802.3 for MAC in the Ethernet and the 802.11 MAC for Wireless Local Areas Networks (WLANs). Based on the layered protocol structure, the layers above the link layer do not have to be concerned with the specifics of the physical medium [107, 109].

- **Layer 1**: *Physical Layer.* Similar to the physical layer of the OSI model, the physical layer in the TCP/IP model controls the transmissions of data over the physical medium, which is often termed as the PHY layer. This layer is concerned with specifying the characteristics of the physical medium, the nature of the signals, the data rate and other related features [107, 109]. Different propagation media may require specific PHY protocols. The above-mentioned IEEE 802.3, IEEE 802.11 specifications also define the contents of the PHY layer [107, 109].

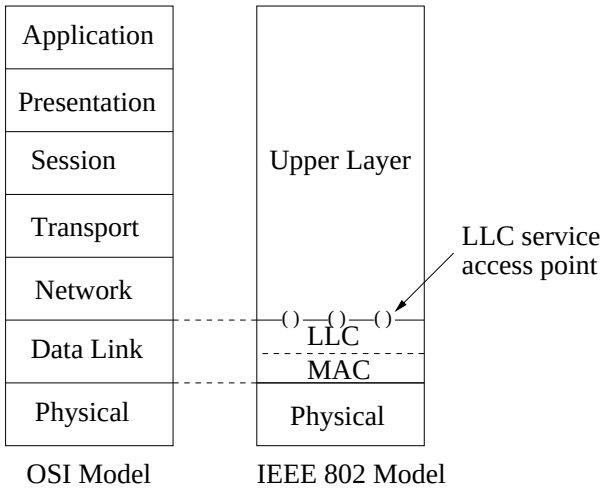

FIGURE 2.3: The data link layer specified in the IEEE 802 reference model [106, 107].

When a SN intends to send its data to the DN, the application layer's data has to be encapsulated by the protocols in each layer, before it is forwarded to the next lower layer [109]. More explicitly, assuming that the TCP protocol is used at the transport layer for ensuring reliable end-to-end transmissions, the control information required by the TCP protocol is appended to the application layer's data as the TCP header, as seen in Fig 2.2. The data units formed by the TCP protocol are referred to as TCP segments. TCP sends each segment to the IP protocol, which belongs to the network layer [109]. When aiming for routing the data across one or more networks, the IP appends a control information header to each segment for informing the IP datagram which is the data unit formed by the IP protocol, as seen in Fig 2.2. Then each IP datagram is passed to the link layer, which encapsulates the datagram as a frame by appending both a header and a tail for the sake of carrying the control information required for reliable transmission across the first network along the route of this data [107], as seen in Fig 2.2. The data exchanged at any protocol level is referred to as a protocol data unit (PDU). When a protocol layer receives a PDU from a lower layer, it removes the control information, namely the header and tailer appended by the peer protocol in the corresponding layer of the transmitter and sends the remainder to the next higher layer [107, 109].

2.3 Medium Access Control in Wireless Network

2.3.1 Wireless Medium Access Control Schemes

According to our discussions in Section 2.2, the higher-layer protocols, namely those that are above the data link layer in the OSI model are independent of the network's architecture. However, compared to the wired network, wireless networks are less reliable due to the time-

varying and error-prone nature of the wireless channel. Hence, the IEEE 802 Standards Committee created and maintained a set of standards for wireless communications [106] by regulating the behaviour of the lower layer of the OSI model, namely of the data link layer and of the physical layer. Figure 2.3 relates the LAN protocols to the OSI architecture. This architecture was developed by the IEEE 802 committee and has been adopted by numerous organizations working on the specification of LAN standards. It is generally referred to as the IEEE 802 reference model [106,107]. Observe in Figure 2.3 that the data link layer is further split into two sublayers, namely the Logical Link Control (LLC) and the Medium Access Control (MAC). The LLC sublayer is the upper sublayer of the data link layer, while MAC sublayer is located below the LLC sublayer. As the interface between the MAC sublayer and the network layer, the LLC sublayer constitutes a standardized interface between the higher layer protocols and the different MAC layer protocols, such as the IEEE 802.3 MAC for Ethernet [113], the IEEE 802.5 MAC for Token Ring [114] and the IEEE 802.11 MAC for WLANs [106].

The MAC sublayer is responsible for efficiently managing the access of different users to the communications medium with the aid of providing frame error checking and recovery. Some of the protocols in the MAC layer focus on assigning the different users to different channels [115]. The most popular multiple access methods conceived for dividing the spectrum are frequency division multiple access (FDMA), time division multiple access (TDMA), code division multiple access (CDMA) and hybrid methods [115], which are capable of supporting multiple users. When aiming for improving the attainable system performance, these channelization-based MAC protocols [115–121] assign appropriate sub-channels to the users without imposing contention or collisions.

However, when the transmissions of the source nodes are bursty, the assignment of dedicated channels becomes inefficient. For these types of sources random access schemes have been developed for efficiently providing medium access control for the network, where the users generate bursty traffic [52, 115, 124–127]. Hence in the context of random access schemes multiple users contend for accessing the channel, whenever they have data to send [115]. The Aloha protocol is a conventional random access scheme in the open literature [122]. Fig 2.4 shows the signalling procedure of the Aloha protocol, where the users transmit their data without checking the channel's state [123]. An acknowledgement packet is transmitted to the source, if the data frame is correctly received. Otherwise, the source node has to wait for a random duration, before retransmitting its data for the sake of avoiding collision with other users [122, 123], as seen in Fig 2.4. The slotted Aloha protocol constitutes an improvement of the original Aloha protocol. More explicitly, the slotted Aloha protocol requires that each user having a packet in its buffer has to transmit his/her data at the

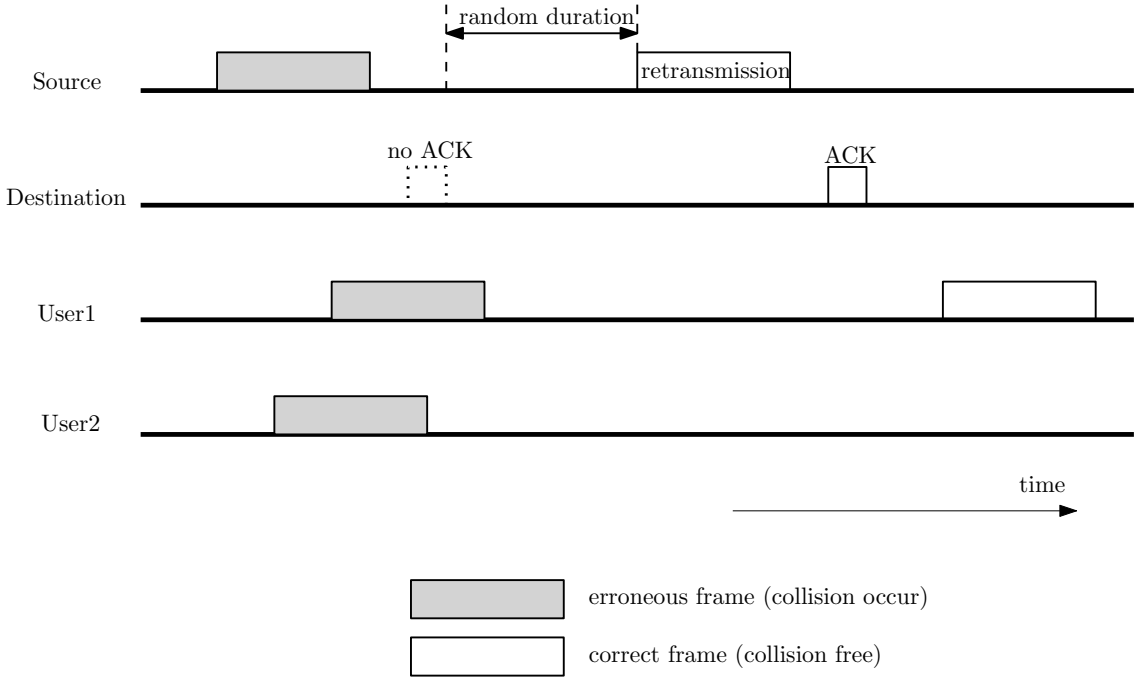

FIGURE 2.4: The procedure of the Aloha protocol [122, 123].

beginning of a timeslot [1] [128], as shown in Fig 2.5. Compared to the Aloha protocol, the slotted Aloha protocol is capable of reducing the probability of collisions, hence improving the maximum attainable throughput by relying on the provision of discrete timeslots [128]. As a further advance, the IEEE 802 Standards Committee specified three random access schemes as MAC protocol standards [129], which are detailed in the next section.

2.3.2 IEEE 802.11 Medium Access Control Protocol

As mentioned above, the IEEE 802.11 working group specified three different random access mechanisms for WLANs, namely the distributed coordination function (DCF), the point coordination function (PCF) and the hybrid coordination function (HCF) [106, 107]. More specifically, the DCF is a primary access scheme, which should be supported by all stations, regardless whether they operate in ad hoc or infrastructure aided network configurations. By contrast, PCF is a collision-free scheme, which is optional for all stations. Finally, the HCF arrangement becomes capable of guaranteeing that the QOS requirements of diverse applications may be met. Since the cooperative MAC protocols proposed in this thesis are developed on the basis of the DCF scheme, this section continues by introducing the intricacies of the DCF scheme. The features of the PCF scheme are outlined after the introduction of the DCF scheme.

[1] For example, observe in Fig 2.5 that user 3 has a packet to send within the first time slot, but it has to start its transmission at the beginning of the following timeslot, namely the second timeslot according to the slotted Aloha protocol.

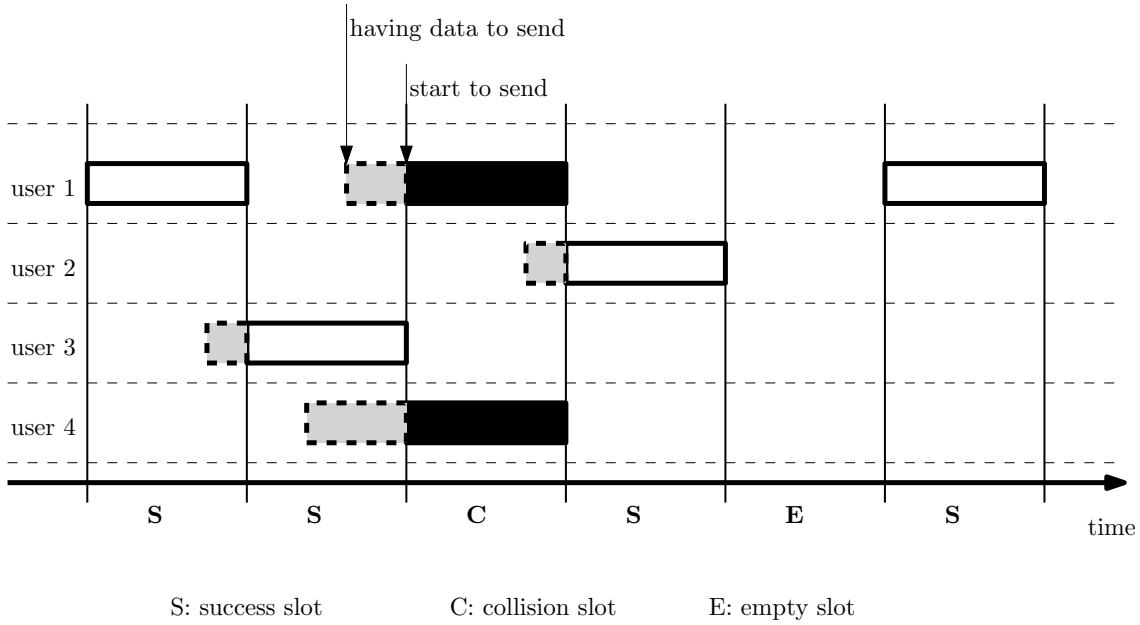

FIGURE 2.5: The procedure of the slotted Aloha protocol [128] which may be contrasted to the standard Aloha of Fig 2.4.

2.3.2.1 Distributed Coordination Function

In the IEEE 802.11 standards, the DCF is defined as the basic medium access method, which facilitates for the stations to share the channel and to reduce the probability of collisions by exploiting the so-called carrier sense multiple access with collision avoidance (CSMA/CA) technique. This is also combined with the so-called binary exponential backoff algorithm which aims for minimizing the probability of repeated collisions of nodes by doubling their contention delays after each collision. The standards [106] specified two methods of performing carrier sensing, namely a physical carrier-sense and a virtual carrier-sense mechanism [106, 130].

Physical Carrier-Sense Mechanism

The physical carrier-sense mechanism constitutes a fundamental strategy, which specifies that each transmitter has to sense the channel's quality before conveying a frame, as seen in Fig 2.6. According to the rate of the transmission medium, the transmitter may opt for the following actions:

- When the medium is deemed to be idle by the carrier-sense mechanism, i.e. sufficiently 'quiet', the transmitter will send the frame following the elapse of a DCF Interframe Space (DIFS) duration, provided that the medium is not be accessed during this waiting interval, as indicated by the behaviour of user 1 in Fig 2.6.

- If the medium is busy, the transmitter has to defer its transmission until it becomes

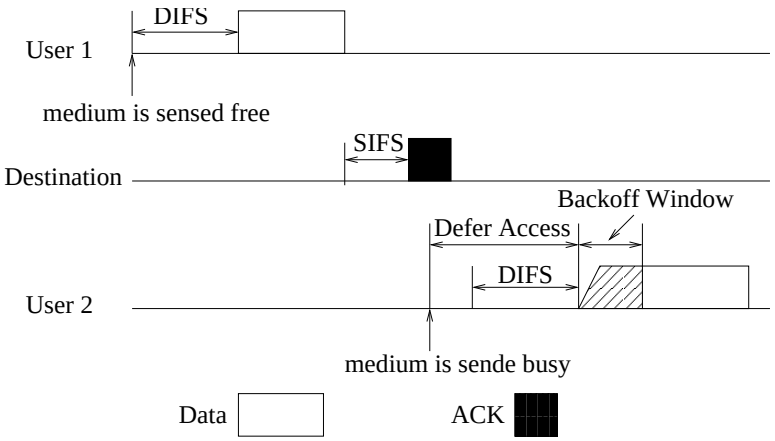

FIGURE 2.6: Physical carrier-sense mechanism used in the DCF scheme [106, 130]. DIFS: DCF Interframe Space [106]; SIFS: Short Interframe Space [106].

free [130]. When the medium is sensed to be free during a DIFS interval, the transmitter will send its pending frame after a random backoff time duration, which is necessary for the sake of avoiding the collisions with other users, as exemplified by the behaviour of user 2 in Fig 2.6.

The backoff time can be formulated as [106]:

$$T_{Backoff} = \varphi_{backoff} \cdot aSlotTime, \qquad \varphi_{backoff} \in [0, CW], \tag{2.1}$$

where $\varphi_{backoff}$ is a pseudo-random integer between 0 and the contention window (CW) parameter [130]. Furthermore, aSlotTime is defined in [106] as a slot-duration specified by the IEEE 802.11 standards, which is given by the sum of the time required to physically sense the channel quality and to declare the channel to be "clear", plus the MAC processing delay, the propagation delay, and the "receiver/transmitter turn-around time", namely the time required for the physical layer to switch from its receive to its transmit mode at the start of the first bit [106, 130]. When a station determines the backoff time $T_{Backoff}$ for the first time, it will set CW to the minimum contention window (CWmin) parameter and randomly selects the value of $\varphi_{backoff}$ from a uniform distribution within the interval between 0 and CWmin.

If the destination receives the frame correctly, it will send a positive acknowledgement (ACK) message to the transmitter after a short interframe space (SIFS) duration, as seen in Fig 2.6. Since SIFS interval is shorter than the DIFS interval, the ACK frame can be protected from the collision caused by the frame transmission of other users. After sending a data frame, the transmitter sets a timer for waiting to receive an ACK message. If the transmitter has not received an ACK frame until the prescribed timeout interval expires, it will retransmit the previous frame. The retransmissions will not cease until an ACK message is received at

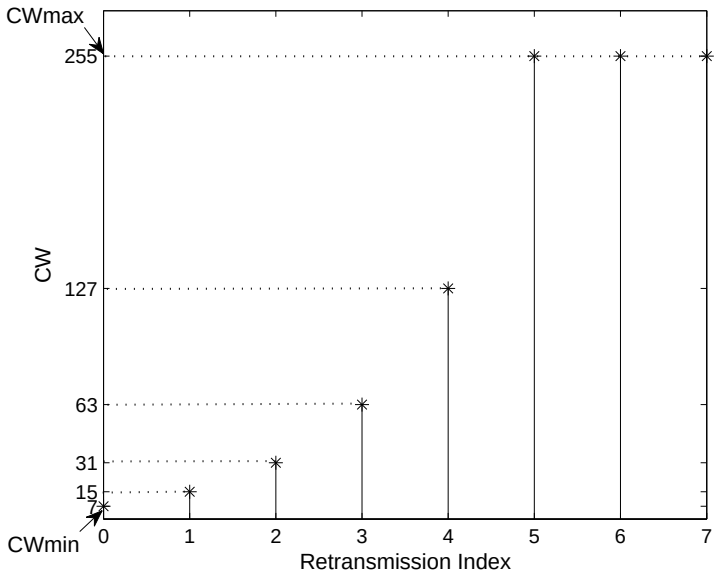

FIGURE 2.7: An example of the exponential increase of the CW in the physical carrier-sense mechanism of Fig 2.6 [106].

the transmitter node or the maximum retransmission index is reached.

If a retransmission is required, the transmitter has to wait for the duration of the extended interframe space (EIFS) and the subsequent backoff time [106] to elapse, before retransmitting its frame. The CW duration required for accounting also for the backoff time before a retransmission is activated is determined by the binary exponential backoff algorithm, which may be written as [106] $CW_{now} = 2^{\kappa}(CWmin + 1) - 1$, where κ is the retransmission index. When CW reaches the maximum of contention window (CWmax) parameter value, the successive retransmission will rely on the parameter value of CWmax for calculating the backoff time. An example of the exponential increase of CW is shown in Fig 2.7. In this example, $CW = 7$ is set, which is the value of CWmin. For the first retransmission, CW is increased to 15. When it reaches $CWmax = 255$, it remains fixed to 255 for the rest of the retransmissions [106]. By contrast, if the frame is transmitted successfully, the transmitter will set CW to CWmin again.

Virtual Carrier-Sense Mechanism

As seen in Fig 2.8, station S_1 and station S_2 are outside of each other's carrier sensing range and hence they cannot overhear each other's transmissions, although they rely on the CSMA/CA scheme. Hence, when S_1 and S_2 transmit their data to the station S_3 of Fig 2.8 at the same time, a collision occurs, which is referred to as the "hidden terminal" problem [106]. The virtual carrier-sense mechanism substantially reduces the probability of collisions caused by the "hidden terminal" problem by introducing two short control messages, namely the Request-To-Send (RTS) and Clear-To-Send (CTS) messages, as seen

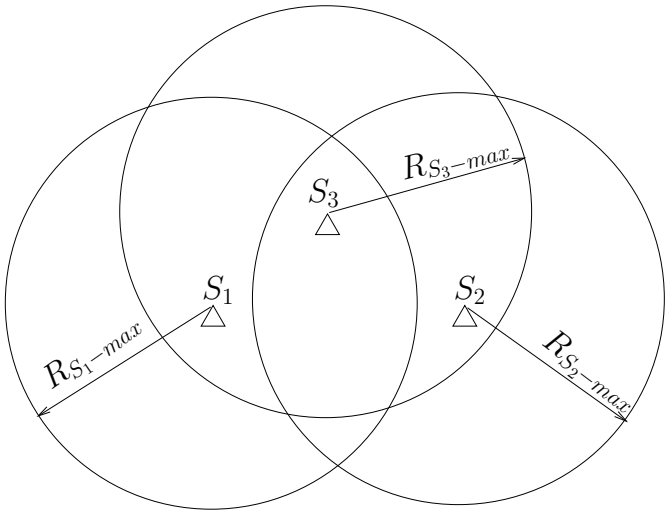

FIGURE 2.8: The hidden node problem [106].

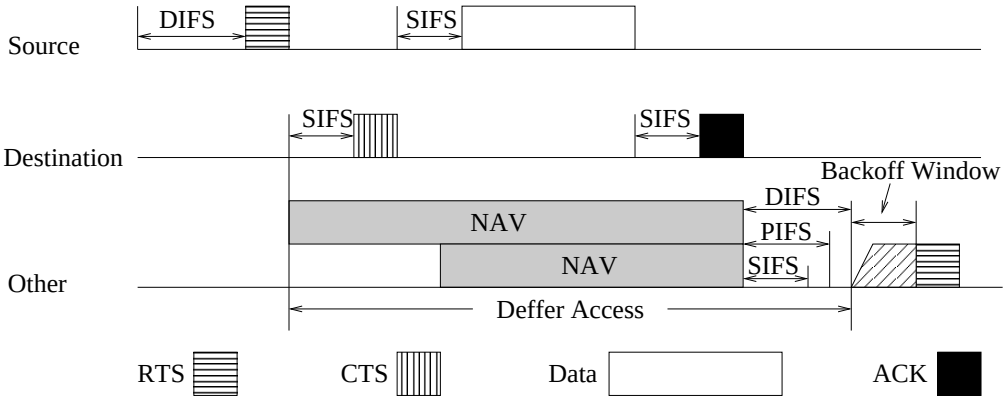

FIGURE 2.9: RTS/CTS exchange procedure of virtual carrier-sense mechanism used in the DCF scheme [106]. RTS: Request-To-Send; CTS: Clear-To-Send; ACK: Acknowledgement; DIFS: DCF Interframe Space; SIFS: Short Interframe Space; PIFS: PCF Interframe Space [106].

in Fig 2.9.

Fig 2.9 describes the RTS/CTS exchange procedure. Observe in Fig 2.9 that if the transmitter has a data frame to send, it first transmits a RTS frame, which includes the transmitter's address, the receiver's address and the transmission duration of its pending data frame after waiting for a DIFS interval, provided that the channel is deemed to be free. When the destination correctly receives this RTS message, after a SIFS duration it replies with a CTS message, which includes the data transmission duration, as seen in Fig 2.9. All the neighbours which are in the carrier sensing ranges of the source and destination are capable of overhearing either the RTS message or the CTS message and hence they become aware of the duration of the current transmission, which is again indicated by the RTS and CTS messages. These neighbours will remain silent within the duration of the current transmission, although they sense that the medium is free [130].

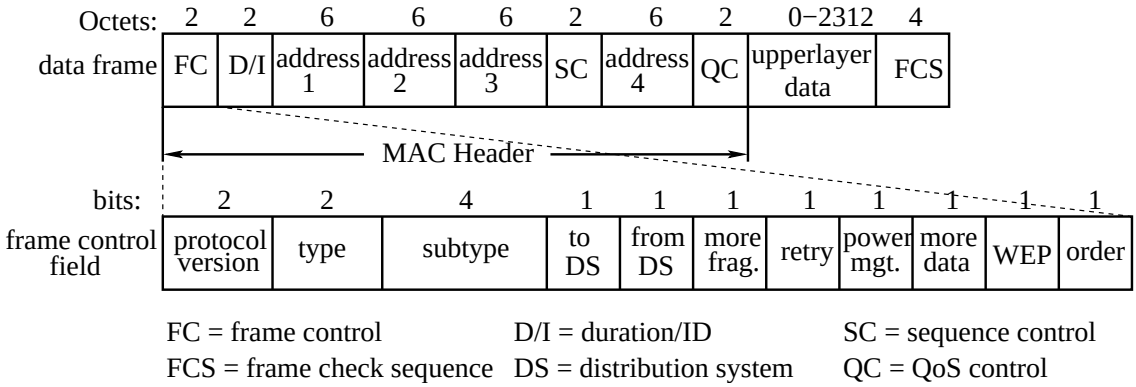

FIGURE 2.10: The format of the MAC data frame in the DCF scheme of Fig 2.6 and Fig 2.9 [106].

When the source node receives the CTS message from the destination, it conveys its data frame after the elapse of another SIFS duration. If the data frame is successfully received, the destination waits for a SIFS interval and replies with an ACK message, as seen in Fig 2.9. Hence again, the virtual carrier-sense mechanism is capable of efficiently handling the "hidden terminal" problem and "exposed terminal" with the aid of the RTS/CTS procedure of Fig 2.9.

MAC Frames

Observe in Fig 2.6 and Fig 2.9 that different frames are introduced by the DCF scheme in the MAC layer. The format of both the control frames and of the data frame are detailed in this section.

Data Frame Format The MAC data frame specified in the IEEE 802.11 standards consists of a MAC header and the upper layer packet body as well as a frame check sequence (FCS), as shown in Fig 2.10.

MAC Header: According to the IEEE 802.11 standard [106], the maximum size of MAC header is 32 bytes, which consists of eight fields, namely the Frame Control (FC) field, Duration/ID (D/I) field, Sequence Control (SC) field, QoS Control (QC) field and four address fields. The function of each field is described as follows:

- Frame Control Field: as shown in Fig 2.10, the frame control field contains control information, which identifies the specific type of 802.11 MAC frame and provides information required for the receiver to process the MAC data frame. The description of each field in the frame control field is summarized in Table 2.1.
- Duration/ID Field: this field indicates the duration of the current transmission.

- Address Fields: as shown in Fig 2.10, the MAC header has four address fields. According to the values of "To DS" and "From DS" fields in the frame control field as shown in Table 2.1, the four address fields are capable of carrying different combinations of the following address types:
  - *The Source Address (SA)* indicates the MAC address of the original source, which initially created and transmitted the frame.
  - *The Destination Address (DA)* indicates the MAC address of the final destination of this frame.
  - *The Transmitter address (TA)* specifies the MAC address of the transmitter, which transmitted the current frame over the wireless medium.
  - *The Receiver Address (RA)* represents the MAC address of the specific receiver, which should receive from that particular transmitter, whose MAC address is carried by the TA field.
  - *The Basic Service Set ID (BSSID)* uniquely identifies each Basic Service Set (BSS), which is the basic building block of an IEEE 802.11 WLAN [106, 130], as seen in Fig 2.11. When the frame is transmitted from a user in an infrastructure aided BSS, the BSSID is the MAC address of the AP. When the frame is originated from a user in an Independent Basic Service Set (IBSS), where all the stations are mobile stations with no connection with other BSSs, the BSSID is generated randomly.
- Sequence Control Field: the sequence control field of Fig 2.10 consists of a 4-bit fragment number and a 12-bit sequence number. The fragment number indicates the index of each sub-frame of a fragmented frame. The initial value is set to 0 and then incremented by one for each subsequent frame. The sequence number indicates the index of each frame. The specific sub-frames which belong to the same fragmented frame have the same sequence number.
- QoS Control Field: the QoS control field of Fig 2.10 identifies the different QoS levels in terms of the traffic categories and QoS-related information [106].

Frame Body: The frame body contains the upper layer packet, which consists of the upper layer header and the data body.

Frame Check Sequence: The transmitter exploits a cyclic redundancy check (CRC) protecting all the fields of the MAC header of Fig 2.10 and the frame body field for calculating the value of the frame check sequence (FCS). When a node receives this frame, it calculates its FCS to verify, whether any errors encountered during the transmission by comparing its own FCS to that included in the frame.

TABLE 2.1: The function of each fields in the frame control field of Fig 2.10 [106].

Field	Bits	Description
Protocol Version	2	Indicates the current version of the 802.11 protocol used
Type	2	Identifies the function of the frame. There are three different frame type fields: control, data and management.
Subtype	4	Identifies the function of the frame. There are multiple subtype fields for each frame type, which determine the specific function to be performed by associated frame type.
To DS	1	"1": represents that the frame is transmitted to the Distribution System (DS), which is the architectural component used to interconnect multiple Basic Service Sets (BSSs)[1], as seen in Fig 2.11.
From DS	1	"1": represents that the frame is exiting from the distribution system (DS).
More Fragments	1	"1": more fragments will arrive; "0": this is the last fragment or an unfragmented frame.
Retry	1	"1": it is a retransmitted frame.
Power Management	1	"1": the transmitter is in a power save mode; "0": the transmitter is in an active mode.
More Data	1	informs a user, which is in the power-save mode that the AP has more frames to send. It is also used for APs to indicate that additional broadcast/multicast frames are to follow.
WEP	1	"1": the encryption and authentication are used in the frame.
Order	1	"1": frames must be strictly ordered.

[1] A basic service set (BSS) constitutes a fundamental building block of an IEEE 802.11 LAN. It consists of some stations executing the same MAC protocol and competing for access to the same shared wireless medium [106, 130].

Control Frame Format Control frames are introduced for the sake of improving the reliability of the data transmissions over the MAC layer and for providing administrator access to the wireless medium. The control messages seen in Fig 2.12 are significantly shorter than the data frame. As seen in Fig 2.9, the virtual carrier-sense scheme relies on the RTS, CTS and the ACK messages for the sake of reducing the collision probability and for providing reliable transmission. The format of these three message are described in the following paragraphs.

RTS Message: The RTS frame of Fig 2.12 is used for reserving the medium for the following data transmission. As shown in Fig 2.12, the RTS message includes two address fields, namely the Transmitter Address (TA) and Receiver Address (RA), while the other fields of the RTS message have the same structure and function as those of the MAC data frame seen in Fig 2.10.

CTS message: When the destination correctly received the RTS message, a CTS frames is

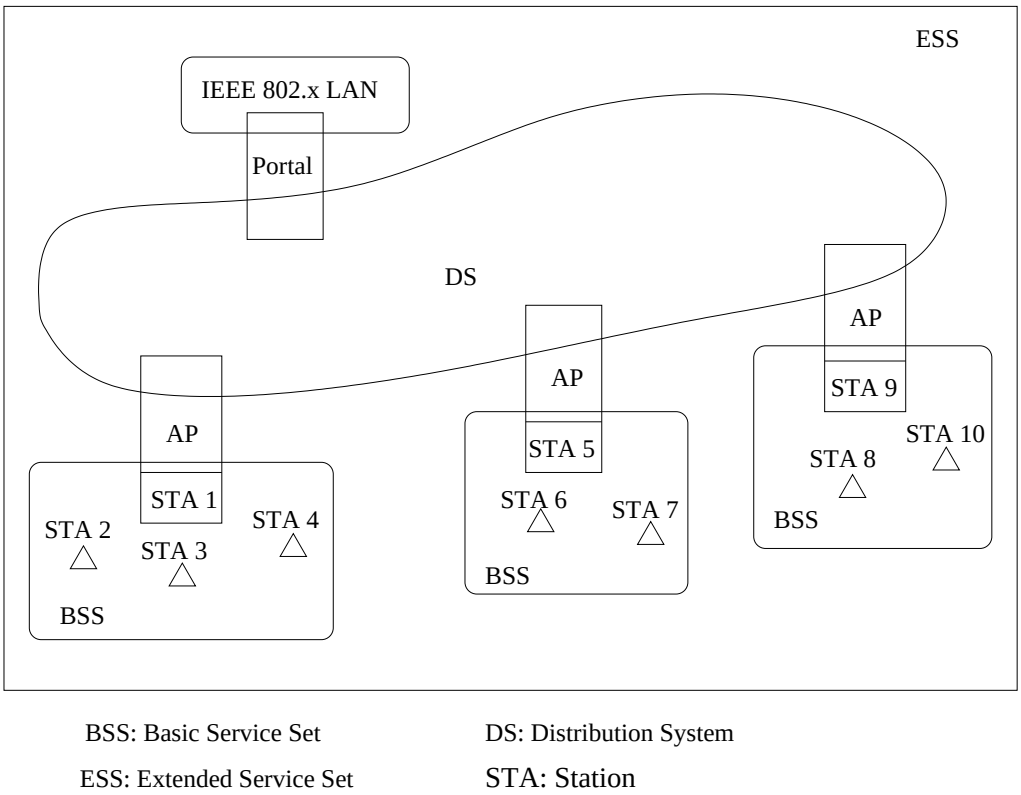

FIGURE 2.11: IEEE 802.11 architecture [106, 107].

sent to the source. As seen in Fig 2.12, the CTS message contains 14 Bytes, including a frame control field, a duration field, a receiver address field and a FCS field. In response to the corresponding RTS message, it is not necessary for the CTS message to carry the transmitter's address.

ACK Message: When a node correctly receives a data frame, it will send an ACK message to the transmitter for informing it about the successful reception. As seen in Fig 2.12, the ACK message also has only a single address fields, namely the receiver address field, for the sake of reducing the MAC overhead introduced by the control message. The other fields have the same format and function as the corresponding fields in the MAC data frame of Fig 2.10.

2.3.2.2 Point Coordination Function

Based on the DCF scheme, extra delay may be imposed, when a retransmission is required for recovering the erroneous frame caused by a collision. When supporting time-sensitive interactive services, the IEEE 802.11 standard [106] specifies the Point Coordination Function (PCF) to provide collision-free medium access by exploiting a token-based medium

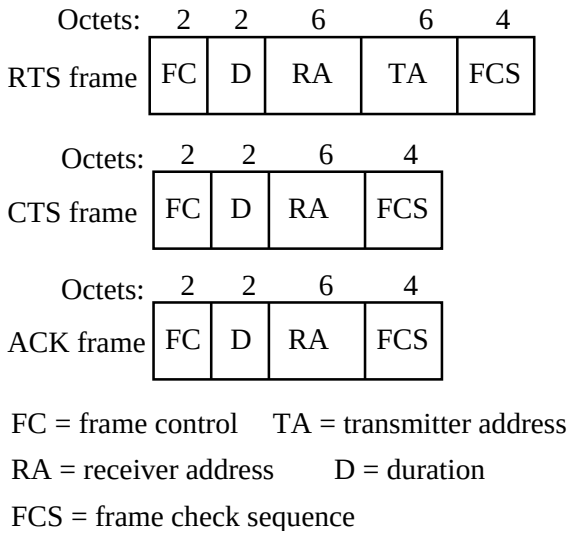

FIGURE 2.12: The format of MAC control message in the DCF scheme of Fig 2.6 and Fig 2.9 [106] [106], which may be contrasted to the MAC data frame of Fig 2.10.

access control scheme. Hence, the PCF of Fig 2.13 and Fig 2.14 is employed in infrastructure based network configurations, which have an access point (AP) behaving as the point coordinator (PC) for reserving the shared channel and for managing the access among the PCF-assisted users [106, 107]. As a polling master, the PC will reserve the shared channel, when the channel is sensed to be free for a PCF Interframe Space (PIFS) interval. The PIFS of Fig 2.14 is shorter than the DIFS, which implies that the PCF has a higher priority than the DCF of Fig 2.6 and PC is capable of accessing the channel before the stations which operate under the DCF scheme of Fig 2.6 and Fig 2.9. However, the high priority of the PCF of Fig 2.13 and Fig 2.14 forces all other asynchronous traffics to lose the transmission opportunity. When aiming for supporting the coexistence of PCF traffic and DCF traffic, a repetition interval is specified by the IEEE 802.11 standard [106], where the PCF controls frame transfers during a Contention Free Period (CFP), which is then followed by a Contention Period (CP), during which the DCF takes over the frame transfers [106].

As shown in Fig 2.13, alternating periods of contention-free and contention-based service intervals repeat at regular instants. The PC is responsible for providing contention-free services within the CFP of Fig 2.13 and for controlling the length of a CFP, while no centralized controller determines the length of a CP. Hence, the CFP may not start at the expected time-instant, because the medium is occupied by the transmission taking place during the CP, as seen in Fig 2.13. The IEEE 802.11 standards [106] specify that the CFP has to be shortened by the appropriate amount of the delay without interrupting the current transmission, if the contention-based service runs past the expected beginning of the following CFP, as seen in Fig 2.13. However, the length of CFP must not exceed the maximum duration of the CFP, namely CFPMaxDuration.

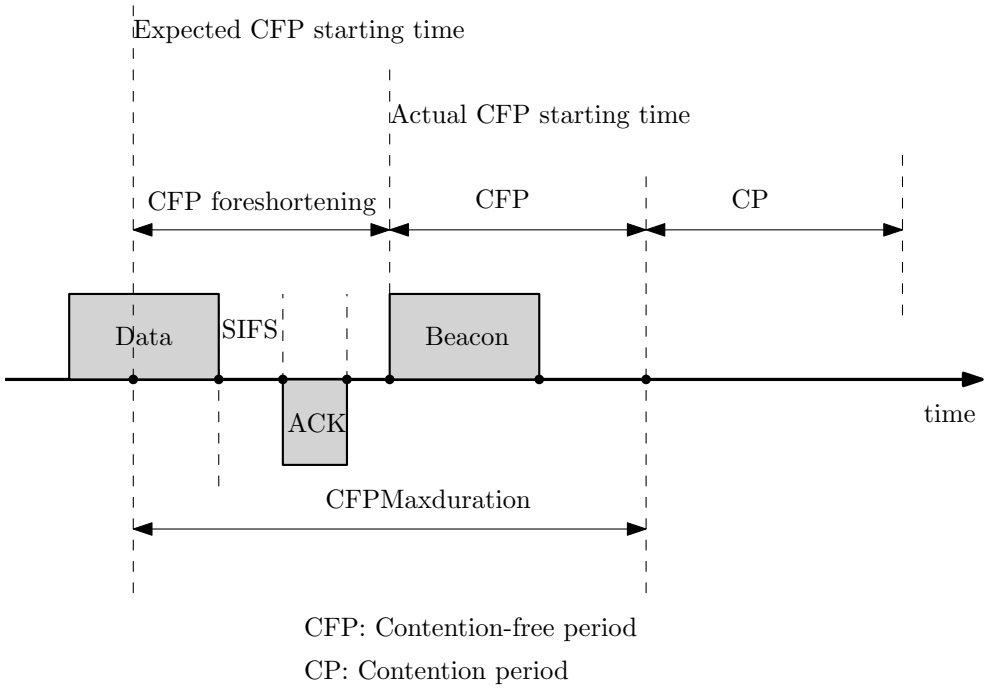

FIGURE 2.13: Timing diagram of the contention-free and contention based period. [106] SIFS: Short Interframe Space; ACK: Acknowledgement [106].

During the contention-free period, the CF-pollable users may transmit if and only if the PC grants a transmission opportunity for it with the aid of a polling frame. Fig 2.14 shows an example of the frame exchange procedure based on the PCF scheme. As seen in Fig 2.14, when the PC occupies the transmission medium, it issues a beacon message for the sake of informing the PCF-enabled users about the start of the CFP and of the value of CFPMaxDuration [106]. Then PC initiates the transmission of a Contention-Free-Poll (CF-Poll) frame to a polled user after the expiry of a SIFS duration. When a PCF-enabled user receives a CF-Poll frame, it becomes capable of conveying its suspended data after waiting for a SIFS interval [106], as exemplified by the behaviour of user 1 in Fig 2.14. However, if the polled station has nothing to send, it has to transmit either a null frame as its response to the PC or a Contention-Free-Acknowledgement (CF-ACK) message for the sake of acknowledging the previous reception [106], as seen for user 3 in Fig 2.14. After receiving the response of the polled station, the PC issues another CF-Poll message for the next station after waiting for a SIFS duration. If no response is received from the polled station, such as user 2 in Fig 2.14, the PC will pass the transmission opportunity to the next station after waiting for a PISF interval [106]. At the end of the CFP, the PC sends a Contention-Free-End (CF-End) frame for the sake of completing this polling period. Following the CFP of Fig 2.14, all the stations enter CP. The following frame types may be issued after the PC transmits its beacon message, but before the PC ends the CFP by sending the CF-End message [106].

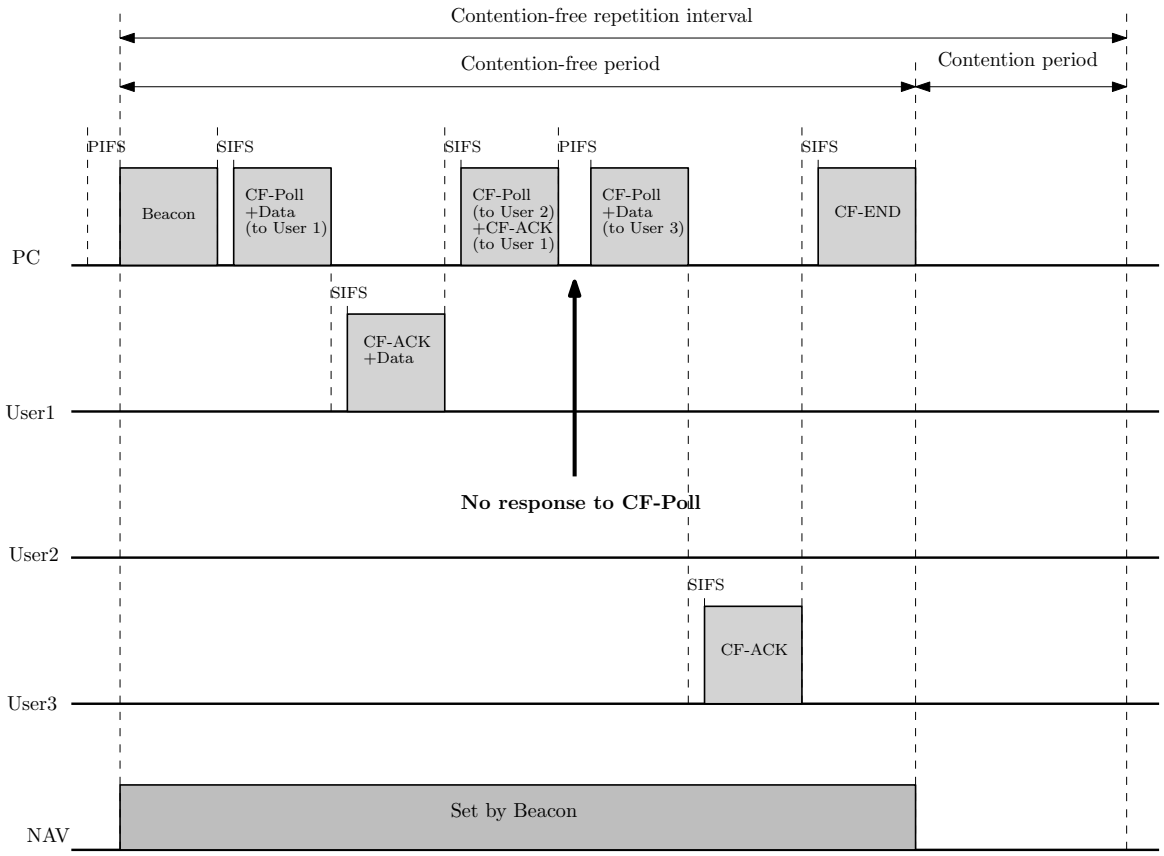

FIGURE 2.14: Example of the PCF signalling procedure [106]. PIFS: PCF Interframe Space; SIFS: Short Interframe Space; CF-Poll: Contention-Free-Poll; CF-ACK: Contention-Free-Acknowledgement; CF-End: Contention-Free-End [106].

- *CF-Poll*: The CF-Poll frames of Fig 2.14 are issued by the PC to a CF-pollable user who is capable of transmitting a single buffered frame after the expiry of a SIFS interval, when the PC has no data to send to this user and simultaneously the PC has no previous frame to acknowledge.

- *Data*: The Data frames of Fig 2.14 are transmitted, when the PC has data for transmission to the specific user, who is not the next polled user, provided that the PC does not have to simultaneously acknowledge a previous transmission. The format of the data frame transmitted during the contention-free period is identical to that used during the contention-based periods.

- *CF-ACK*: The CF-ACK message seen in Fig 2.14 may be sent either by the PC or a CF-pollable user for informing the transmitter of the successful reception of the previous data transmission. For example, user 3 in Fig 2.14 sends the CF-ACK message for acknowledging the reception of the frame from the PC.

- *CF-Poll+Data*: The PC may send this message frame to a CF-pollable user, while simultaneously granting transmission opportunities for this user, when the PC has no

previous frame to acknowledge, as portrayed in Fig 2.14.

- *CF-Ack+Data*: This frame combines the data transmission from the transmitter to the receiver and the acknowledgement message representing the success/failure of the previous reception at the transmitter for this "CF-Ack+Data" frame, as exemplified by the behaviour of user 1 in Fig 2.14.

- *CF-Poll+CF-ACK*: This frame combines the functions of both the CF-Poll and of the CF-ACK messages. The PC may issue this frame, when it intends to grant the opportunity of transmitting to a CF-pollable user, who is capable of transmitting a single buffered frame after the expiry of a SIFS interval, but the PC has no data to send to this CF-pollable user, provided taht simultaneously the PC has a previous received frame to acknowledge.

- *CF-Poll+CF-ACK+Data*: The PC may send this frame, when it has data for transmission to the next user, which is granted the opportunity to occupy the medium and the PC has to acknowledge the previous reception.

Compared to the DCF of Fig 2.6 and Fig 2.9, the PCF is more suitable for delay-sensitive traffic, because it is capable of avoiding the collision between the stations, hence reducing the delay imposed by the retransmissions due to such collisions. However, the null frame introduced by the PCF will waste both the bandwidth and the energy of the stations. Furthermore, the frame exchange procedures of the PCF scheme seen in Fig 2.14 are more complicated than those of DCF scheme portrayed in Fig 2.6 and Fig 2.9. As an optional scheme ratified by the IEEE 802.11 standards [106], the PCF of Fig 2.13 and Fig 2.14 has not been widely implemented. Hence, this thesis develops cooperative MAC protocol based on the DCF scheme.

2.4 Stability Analysis of Queueing Systems

2.4.1 Queueing System

If the arrival rate of the packets received from the network layers is higher than the departure rate of the data frames at the MAC layer, the new packets have to be stored in a buffer. Hence, these new packets form a queue. When the current data frame is successfully transmitted to the destination node or the retransmission index achieves its maximum affordable value, the MAC protocol would transmit a new packet stored in the queue until the queue becomes empty.

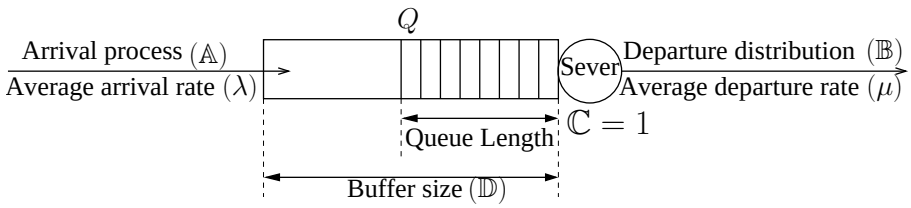

FIGURE 2.15: Queuing model parameters used in the analysis of the queueing system in Section 2.4.2 [103, 131].

2.4.1.1 Queueing Model

According to Kendall's notation [131], a single queueing node is characterized as $\mathbb{A}/\mathbb{B}/\mathbb{C}/\mathbb{D}$, where $\mathbb{A}$ describes the packet arrival process, while $\mathbb{B}$ represents the packet departure distribution. Furthermore, $\mathbb{C}$ is the number of servers at the node and $\mathbb{D}$ denotes the buffer size [132], as shown in Fig 2.15. Kendall's notation describes both the packet arrival process and the service distribution characterizing the packet departure distribution by using the following variables [103, 131]:

- D denotes a deterministic process, where D may be used for replacing $\mathbb{A}$ or $\mathbb{B}$ in the general notation of $\mathbb{A}/\mathbb{B}/\mathbb{C}/\mathbb{D}$.
- M denotes the Poisson packet arrival process, when we have $\mathbb{A} = M$. By contrast, $\mathbb{B} = M$ implies that the instants of packet departure have an exponential distribution in the context of the generic notation of $\mathbb{A}/\mathbb{B}/\mathbb{C}/\mathbb{D}$.
- G denotes the general distribution.

When an infinite buffer is assumed, the effect of $\mathbb{D}$ is usually ignored. For example, the notation M/M/1 denotes a single-server queue obeying a Poisson packet arrival process and exponential service time as well as having an infinite buffer. Furthermore, G/G/1 represents a single-server queue associated with an arbitrary arrival process and an arbitrary service time distribution, when an infinite buffer is assumed.

2.4.1.2 Utilization

The efficient exploitation of the available resources is an important issue, when evaluating the performance of queueing systems, which may be characterized by that specific proportion of time, when a server is busy [103]. This may be quantified in terms of the the so-called utilization [103]. Let λ denote the average arrival rate of packets at the input of a G/G/1 queue, while μ represent the average service rate, which is also referred to as the departure rate, as shown in Fig 2.15. Provided that the average service rate is higher than the arrival

rate, namely we have $\mu > \lambda$, the queue length will not increase on average even if the server is busy at certain instants and the queue will eventually become empty. The average number of packets arriving at the queue within a sufficiently long duration $\mathbb{L}$ may be written as $\lambda\mathbb{L}$. The average number of packets departing from the queue is equal to $\mu \cdot \mathbb{U} \cdot \mathbb{L}$, where $\mathbb{U}$ denotes the utilization of the server in the G/G/1 queue [103]. Since the queue may become empty after a long duration of $\mathbb{L}$, the packet which arrives at the input of the queue will be immediately served. Hence, the average number of packets departing from the queue is equal to the average number of the packets arriving at the input of the queue, namely $\lambda\mathbb{L} = \mu \cdot \mathbb{U} \cdot \mathbb{L}$. Based on the above discussions, the utilization of the server may be formulated as [103]:

$$\mathbb{U} = \frac{\lambda}{\mu}. \tag{2.2}$$

The utilization of a multi-server queueing system is defined as the overall average utilization of the individual servers. More explicitly, each server will have its own utilization defined by the proportion of time during which it is busy, whilst the utilization of the entire multi-server system will be found as the average of the individual server utilization.

2.4.1.3 Little's Theorem

Little's theorem is a fundamental law of queueing systems. It states that in the steady state condition the average number of packets in a queue is equal to the average arrival rate of the packets multiplied by the average time that a packet spends in the queue [103, 133], which may be formulated as:

$$\mathbb{E}\{N_Q\} = \lambda \cdot \mathbb{E}\{D_Q\}, \tag{2.3}$$

where $\mathbb{E}\{N_Q\}$ denotes the average number of packets in the queue Q, when the system reaches its steady state, including the packets that are being served at this instant. Furthermore, $\mathbb{E}\{D_Q\}$ represents the average time duration spanning from a packet's arrival at the input of the queue Q until its delivery to the destination is complete under steady state conditions.

Assuming that the average arrival rate at the input of the queue Q is lower than the average departure rate, a G/G/1 queue Q may be empty in the steady state condition, which implies that the packets arriving at the input of the queue Q will be immediately served in the steady state condition. Hence, the time that a packet is in the queue Q is the service time, when

the queue is in the steady state [103]. Based on above discussions, we have:

$$\mathbb{E}\{D_Q\} = \frac{1}{\mu} \quad \text{and} \quad \mathbb{E}\{N_Q\} = \mathbb{E}\{N_s\}, \tag{2.4}$$

where $\mathbb{E}\{N_s\}$ denotes the average number of packets that are being transmitted by the server at the current instant. When a G/G/1 queue Q is in its steady state, the number of packets at the server of a G/G/1 queue Q may be either 0 or 1, which implies that the server is either busy due to transmitting a packet or it is free. Hence, when the queue Q is in its steady state, $\mathbb{E}\{N_s\}$ may be formulated as:

$$\begin{aligned}\mathbb{E}\{N_s\} &= 0 \cdot \mathbb{P}\{N_s = 0\} + 1 \cdot \mathbb{P}\{N_s = 1\} \\ &= 0 \cdot \mathbb{P}\{N_s = 0\} + 1 \cdot \Big(1 - \mathbb{P}\{N_s = 0\}\Big) \\ &= 1 - \mathbb{P}\{N_s = 0\},\end{aligned} \tag{2.5}$$

where $\mathbb{P}\{N_s = 0\}$ denotes the probability that the server of queue Q is not busy for scheduling the transmission for a packet. Let $\mathbb{P}\{N_Q = 0\}$ represent the probability that the queue Q is empty. According to Little's theorem and Eq (2.4) as well as Eq (2.5), we have:

$$1 - \mathbb{P}\{N_Q = 0\} = \frac{\lambda}{\mu} \quad \Rightarrow \quad \mathbb{P}\{N_Q = 0\} = 1 - \frac{\lambda}{\mu}. \tag{2.6}$$

Hence, the probability that a queue is empty when the system reaches its steady state may be calculated by Eq (2.6), which is derived according to Little's theorem.

2.4.2 Stability Analysis

2.4.2.1 Definition of Stability in Queueing Systems

Stability constitutes a fundamental state of a queueing system. When all the queues in the queueing system are stable, this system is stable [103]. Generally speaking, a queue is stable if the queue length remains finite, when the time tends to infinity. Definition 2.1 formulates a more rigorous definition of the stability for a queue [134, 135].

Definition 2.1: A queue is said to be stable, provided that distribution of the queue length $Q(t)$ converges to a specific distribution function $\mathbb{F}(x)$, which approaches the value of unity, as the variable x tends to infinity, which is formulated as:

$$\lim_{t\to\infty} \mathbb{P}(Q(t) < x) = \mathbb{F}(x), \text{and} \lim_{x\to\infty} \mathbb{F}(x) = 1, \tag{2.7}$$

where $Q(t)$ denotes the length of the queue Q at time instant t.

When aiming for investigating the stability of a queueing system, it is necessary to find the conditions of stability for all the queues in the queueing system which are predetermined by whether the given queues are stable or not for the specific tele-traffic source considered. Hence, the conditions under which the system retains its stability characterizes the entire system. The widely-used Loynes' theorem [134] specifies the conditions of stability for the queue fed by a stationary arrival process and supporting a stationary service process [2]. More explicitly, Loynes' theorem specifies that if the arrival process and service process of a queue Q are stationary, the following holds [134]:

- If the average arrival rate λ is lower than the average departure rate of μ, namely we have $\lambda < \mu$, then the queue Q is stable.
- If the average arrival rate λ is higher than the average departure rate of μ, namely when we have $\lambda > \mu$, then the queue Q is unstable.
- If $\lambda = \mu$, the the queue Q may either be stable or unstable.

2.4.2.2 Stability Analysis Methods

According to Loynes' theorem [134], only some specific arrival rates are capable of ensuring that the system retains stable. Hence, most existing work focused on the investigation of a set of average arrival rates which satisfies the conditions to be obeyed by a stable system [25, 136–138]. This set of average arrival rates is referred to as the stability region. If the offered tele-traffic input-load remains within the stability region, the system or its queues under consideration are stable; otherwise, they are unstable. When a queue is stable, the average departure rate is defined as the achievable stable throughput of this queue [52, 139–142].

In order to investigate the stability region of systems and their stable throughput, the classic Markov chain based technique is invoked for modelling the stochastic process of the queueing system by analysing the queues' state under the specific of the Quality of Service (QoS) constraint considered, as detailed in [82, 143–148]. A Markov chain is capable of efficiently describing the different states of a dynamic queue. However, the Markovian

[2] A stochastic process $\{X_t\}$ is a stationary process, if the joint probability function $\mathbb{P}_X\{X_{t_1}, X_{t_2}, \cdots, X_{t_k}\}$ of any subset $\{X_{t_1}, X_{t_2}, \cdots, X_{t_k}\}$ remains unaffected by a shift of the time-axis, namely when we have $\mathbb{P}_X\{X_{t_1}, X_{t_2}, \cdots, X_{t_k}\} = \mathbb{P}_X\{X_{t_1+\tau}, X_{t_2+\tau}, \cdots, X_{t_k+\tau}\}$ [103]. In other words, $\mathbb{P}_X\{X_{t_1}, X_{t_2}, \cdots, X_{t_k}\}$ is independent of τ.

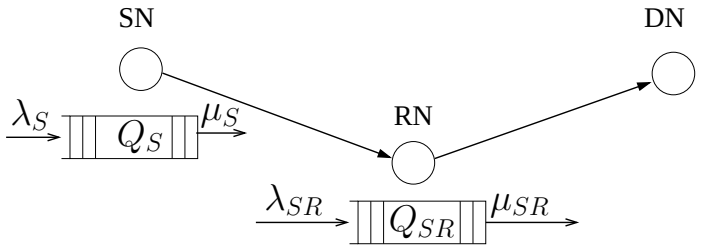

FIGURE 2.16: An example of the cooperative queueing system of Fig 1.2 discussed in Section 1.2.2 [52, 139]

stability analysis methods typically impose a high computational complexity. Hence, non-Markovian methods have also been developed for analysing the stability of systems which impose a lower complexity [25,137,139,141]. Let us hence discuss some of the non-Markovian methods of analysing the stability of cooperative communication system.

Non-Markovian Analysis Methods

Non-Markovian analysis method has been widely employed for the sake of investigating the stability of queues in cooperative communication systems [25, 52, 137, 139–142]. Given a cooperative queueing system, the medium access control scheme determines the departure rate of queues at both the source nodes and the relay nodes as well as the arrival rate of the queue storing the source's data at the relay nodes, which are denoted by μ_S, μ_{SR} and λ_{SR} in Fig 2.16. Hence, the first step of non-Markovian analysis methods is constituted by deriving the average departure rate μ_S of the queues at the source nodes, as seen in Fig 2.16. Then both the average arrival rate and average departure rate of the queues storing the source's data at the relay nodes, namely λ_{SR} and μ_{SR} of Fig 2.16 may be formulated based on the proposed cooperative medium access control scheme. Finally, the stability regions and the stable throughput of both the sources' queues and relays' queues may be derived by checking the stability of all the constituent queues according to Loynes' theorem and Little's theorem.

2.5 Chapter Summary

This chapter introduced the fundamental concepts of this thesis. These covered the layered OSI network protocol architecture, the legacy wireless medium access control schemes and the stability analysis of queueing systems.

As seen in Figure 2.3, the MAC protocol is an inherent part of the layered network architecture. In order to investigate the rudiments of conventional wireless MAC protocols, Section 2.2 briefly introduced the layered network protocol architecture. The OSI and TCP/IP

models of Fig 2.1 constitute widely-used layered protocols. We provided a rudiments of description of the function of each protocol layer in Section 2.2. Both of the OSI and TCP/IP models rely on the link layer, which is responsible for supporting reliable transmissions along point-to-point links between two adjacent hosts.

Based on the OSI model, Section 2.3 further detailed the function of the MAC layer and the existing conventional wireless medium access schemes. As an inherent sublayer of the data link layer, the MAC layer is responsible for the efficient medium access management of multiple users as well as for frame error checking and recovery. Since the cooperative MAC scheme developed in this thesis is based on the DCF scheme specified by the IEEE 802.11 standards, Section 2.3.2 elaborated on the handshaking procedure of the DCF scheme and on the formats of both the data frame and control messages introduced by the DCF scheme, which were portrayed in Fig 2.6, Fig 2.9,Fig 2.10 and Fig 2.12. Moreover, Section 2.3 detailed the PCF scheme which is specified by the IEEE 802.11 standards for the family of time-sensitive services.

Section 2.4 investigates the stability of the queue buffering the packets which are waiting for the services to be provided by the MAC protocol. A basic description of the queueing system and of the relevant theorems was provided in Section 2.4.1 with the aid of Fig 2.15. Generally speaking, a queue may be described by four parameters: the average arrival rate of the packets, the average departure rate, the number of servers and the size of the buffer. Moreover, Section 2.4.1 introduced the fundamental laws characterizing a queueing system, namely Little's theorem, which outlines the relationship between the average queue size and the average arrival rate of the packets as well as the average delay under the steady-state conditions. The probability that a queue is empty when the system reaches its steady state was elaborated on Section 2.4.1. Based on the fundamental concepts of queueing systems, Section 2.4.2 provided the definition of a stable queueing system. Generally speaking, a queue is said to be stable, if the queue length remains finite, as the time tends to infinity. When all the queues in the queueing system are stable, this system is stable [103] According to the definition of a stable queue, Loynes' theorem was developed for characterizing the stability of a queueing system. Furthermore, Section 2.4.2 briefly highlighted one of the popular methods routinely invoked for analysing the stability of a cooperative queueing system, namely a non-Markovian stability analysis method, which will be exploited in Chapter 4 and Chapter 5 of this thesis for analysing the stability of the proposed cooperative communication system. The first step of the non-Markovian stability analysis method is to derive the average arrival rate and average departure rate for each queues in the system. Then the stability region and stable throughput of a system were defined according to the stability conditions specified by Loynes' theorem.

Based on the above fundamental concepts, let us now embark on developing a "win-win"

cooperative MAC protocol for supporting cooperative communications based on the classic RTS/CTS scheme in the following chapter.

Chapter 3

Distributed "Win-Win" Cooperative Medium Access Control

3.1 Introduction

As alluded to in Chapter 1, cooperative communications techniques have recently attracted substantial research attention [3,4] as a benefit of their significant throughput improvements, energy savings and cellular coverage enhancements. However, these benefits may be eroded by the conventional Medium Access Control (MAC) protocol, which was designed for classic non-cooperative systems, as detailed in Chapter 2. In contrast to the legacy wireless MAC protocols, cooperative MAC protocols aim for cooperatively scheduling the medium access of all nodes, whilst selecting the best relay nodes (RNs) to buffer and forward the others' data frames by exploiting the broadcast nature of the wireless network, instead of ignoring these data frames. Hence, it is important to design appropriate MAC protocols for supporting cooperative physical layer techniques and for optimizing the most appropriate objective function (OF) of cooperative communication systems.

There are numerous contributions in the literature on designing cooperative MAC protocols, most of which aim for maximizing the throughput [59, 78, 149–154], including the widely recognized CoopMAC of [30]. A potential impediment of above-mentioned cooperative MAC protocols is that its energy efficiency was traded-off against the throughput benefits claimed. Therefore, the authors of [36, 90, 155–158] aimed for minimizing the energy consumption by developing energy-efficient cooperative MAC protocols. However, these solutions often remained oblivious of the associated throughput reduction. In order to jointly consider these

conflicting design objectives, the authors of [51,159,160] designed meritorious algorithms for improving the achievable throughput and for simultaneously enhancing the energy efficiency achieved.

However, the above-mentioned cooperative MAC protocols were developed on the basis of the common assumption that the relay nodes (RNs) agree to altruistically forward the data of the source node (SN). This unconditional altruistic behaviour is unrealistic to expect for the mobile stations (MS). In fact, a greedy RN behaviour is likely to be the norm in spectrum leasing system [100], where the licensed users intend to lease part of its spectral resources to the unlicensed relay node (RN) for appropriate 'remuneration', while the unlicensed users have an incentive to provide the corresponding 'remuneration' to the licensed users in exchange for a transmission opportunity. The cooperative spectrum leasing system's philosophy [41, 100, 161, 162] allows the licensed SN to acquire cooperative transmission assistance as its 'remuneration', while the unlicensed RN is granted transmission opportunity on the licensed spectrum for its traffic by forwarding data for the the licensed SN. This cooperative strategy allows both the SN and RN to satisfy their individual requirements. Based on this cooperative spectrum leasing system (CSLS), some early ***theoretical*** studies have been conducted in [41, 161–165]. Bearing in mind the greedy behaviour of the mobile RNs, meritorious game theoretic frameworks were proposed in [41, 161, 163, 164] for maximizing the SN's *transmit rate*, while simultaneously satisfying the requirements of the RNs. Furthermore, the authors of [162, 165] aimed for miminizing the *energy consumption* of cooperative spectrum leasing systems by designing beneficial game-aided strategies. However, the joint optimization of the transmit rate and of the energy consumption has not been considered in these existing works. Furthermore, the design of an appropriate cooperative MAC protocol for practically implementing the theoretical framework was not discussed in [41, 161–165].

Against the above background, the contributions of this chapter are as follows:

1. We first formulates a 'Win-Win' (WW) Cooperative Framework (WWCF) for encouraging the SN to lease part of its spectral resources to the unlicensed RN **for the sake of improving the SN's *transmit rate* and for simultaneously reducing the SN's *energy consumption***, while ensuring that the unlicensed RNs are capable of securing a transmission opportunity for their own traffic and for satisfying their Quality-of-Service (QoS). Furthermore, the proposed WWCF selects the best RN for the sake of ***minimizing the system's energy consumption***.

2. Secondly, **a distributed WW cooperative MAC protocol is developed for *practically implementing* our WWCF in a cooperative spectrum leasing system** by designing the required *signalling procedures* for implementing the negoti-

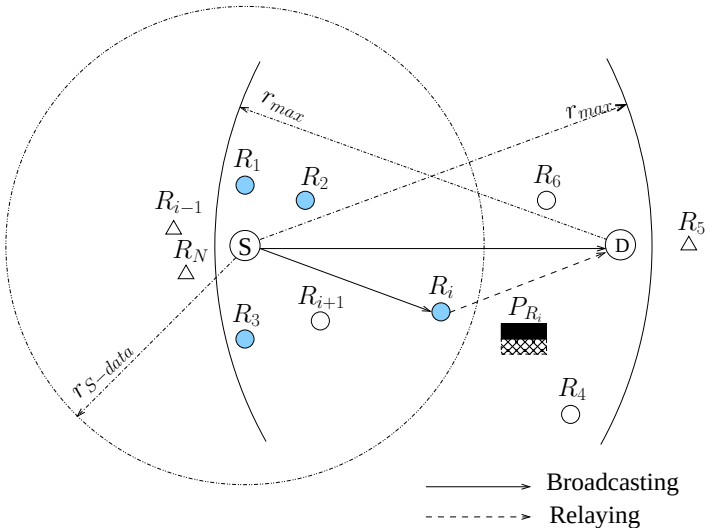

FIGURE 3.1: The cooperative topology consists of a single source $\mathcal{S}$, a single destination $\mathcal{D}$ and a total of N relays $\mathcal{R} = \{\mathcal{R}_1, \ldots, \mathcal{R}_N\}$.

ation between the SN and the greedy RN. Similarly, the *frame structure* of both the data and control messages is also conceived for conveying all the required information. In order to simplify the signalling procedures at the MAC layer, the proposed distributed WW cooperative MAC protocol relies on both a distributed RN selection scheme and on the classic Request-To-Send (RTS) / Clear-To-Send (CTS) handshake of the IEEE 802.11 standards [106].

3. Additionally, in contrast to the RN's time / frequency slot reservation strategy of [41], superposition coding is invoked at the RN for jointly encoding both the SN's and RN's data. Fortunately, the resultant interference can be eliminated at the DN using Successive Interference Cancellation (SIC) for separating the SN's and RN's data, whilst beneficially amalgamating both the direct and relayed components using frame combining.

This section is organized as follows. The network construction and the proposed DWWCF are introduced in Section 3.2. Section 3.3 describes the details of the proposed Distributed WW cooperative MAC protocol. In Section 3.4, the attainable performance of our scheme is quantified. Finally, we conclude in Section 3.5.

3.2 'Win-Win' Cooperative Framework

3.2.1 System Model

As seen in Fig 3.1, we consider a cooperative network having a single SN $\mathcal{S}$ and a total of N RNs in the set $\mathcal{R} = \{\mathcal{R}_1, \ldots, \mathcal{R}_N\}$, as well as a common DN $\mathcal{D}$, where $\mathcal{D}$ may be a Base Station (BS) or an ad hoc cluster head. Both $\mathcal{S}$ and $\mathcal{D}$ are granted access to the licensed spectrum, while the N RNs are not licensees. As a dynamic spectrum access strategy, we allow the licensees ($\mathcal{S}$) to trade their spectrum with the RNs. In order to simplify our investigations, we made the following assumptions:

1. All the channels involved are assumed to undergo quasi-static Rayleigh fading, hence the complex-valued fading envelope remains constant during a transmission burst [1], while it is faded independently between the consecutive transmission bursts. Within a given transmission burst, the duplex bi-directional channels between a pair of actively communicating nodes are assumed to be identical, while the channels of any of the remaining links are independent.

2. We consider the effects of free-space pathloss that is modelled by $\rho = \boldsymbol{\lambda}^2/16\pi^2 d^\eta$ [115], where $\boldsymbol{\lambda}$ represents the wave-length, d is the transmitter-to-receiver distance and η denotes the pathloss exponent, which is set to $\eta = 2$. All nodes are assumed to be limited by the same maximum transmit power P_{max}.

3. The DN is assumed to be located within the maximum transmit range of $\mathcal{S}$ [2]. However, $\mathcal{S}$ may intend to acquire cooperative transmission assistance by leasing its spectral resources for the sake of reducing the energy consumption and for improving its transmission rate.

4. In this chapter, we assume having an infinite supply of buffer-content for both the SN and the RNs.

3.2.2 WW Cooperative Framework

SN's Behaviour Rather than relying on monetary remuneration, $\mathcal{S}$ in our WWCF intends to lease part of its spectrum to the RNs in exchange for cooperatively supporting the source's transmission for the sake of saving the SN's transmit power and for satisfying the SN's transmit rate requirement. More explicitly, based on the RN's assistance, $\mathcal{S}$ is capable of

[1] We define a transmission burst as a single transmission attempt, excluding any subsequent retransmission attempts.

[2] This assumption has been exploited in e.g. [90]

successfully conveying its data at a *reduced* transmit power of $P_{\mathcal{S}-data} = \zeta_{\mathcal{S}} \cdot P_{max}$ ($0 < \zeta_{\mathcal{S}} < 1$) and an *increased* transmit rate of $\alpha C^{max}_{\mathcal{S},\mathcal{D}}$ ($\alpha \geq 1$), which is the SN's target transmit rate. In more detail, α is the ratio of the desired and affordable throughput termed as the SN's 'factor of greediness', while $C^{max}_{\mathcal{S},\mathcal{D}}$ is the maximum achievable rate of the Source-to-Destination (SD) link, which can be formulated as $C^{max}_{\mathcal{S},\mathcal{D}} = \log_2(1 + \frac{\rho_{\mathcal{S},\mathcal{D}}|h_{\mathcal{S},\mathcal{D}}|^2 P_{max}}{P_N})$, where P_N is the power of the Additive White Gaussian Noise (AWGN), while $|h_{\mathcal{S},\mathcal{D}}|$ denotes the magnitude of the flat Rayleigh channel between $\mathcal{S}$ and $\mathcal{D}$. Furthermore, $\rho_{\mathcal{S},\mathcal{D}}$ is the free-space pathloss gain between $\mathcal{S}$ and $\mathcal{D}$. If $\mathcal{S}$ cannot acquire any cooperative transmission assistance, it directly transmits its data to $\mathcal{D}$ at a higher transmit power $P^{(II)}_{\mathcal{S},\mathcal{D}}$ for guaranteeing its target transmit rate of $\alpha C^{max}_{\mathcal{S},\mathcal{D}}$ or failing that, it resorts to using the maximum affordable transmit power of P_{max}.

RN's Behaviour Considering the greedy nature of RNs discussed in Section 3.1, the RNs also have an incentive to forward data for $\mathcal{S}$ in our WWCF for the sake of accessing the SN's spectrum to convey their own traffic. Based on the proposed WWCF, the greedy RN $\mathcal{R}_i$ reserves a certain fraction of $\beta C^{max}_{\mathcal{R}_i,\mathcal{D}}$ ($0 < \beta < 1$) of the Relay-to-Destination (RD) channel's capacity for conveying its own traffic, where β is the RN's 'factor of greediness' and $C^{max}_{\mathcal{R}_i,\mathcal{D}}$ is given by: $C^{max}_{\mathcal{R}_i,\mathcal{D}} = \log_2(1 + \frac{\rho_{\mathcal{R}_i,\mathcal{D}}|h_{\mathcal{R}_i,\mathcal{D}}|^2 P_{max}}{P_N})$, while $|h_{\mathcal{R}_i,\mathcal{D}}|$ denotes the magnitude of the flat Rayleigh channel between $\mathcal{R}_i$ as well as $\mathcal{D}$, and $\rho_{\mathcal{R}_i,\mathcal{D}}$ is the free-space pathloss gain between $\mathcal{R}_i$ and $\mathcal{D}$. When the RN provides cooperative transmission assistance, extra energy is dissipated for relaying data for $\mathcal{S}$. Hence, the RNs also intend to reduce this extra energy consumption.

System Objective Function According to the behaviour of both the SN and of the RNs in the proposed WWCF, the system's objective function (OF) used for our WWCF may be formulated as:

$$OF = \min \sum_{i=1}^{N} \left\{ E_{\mathcal{S}} + \xi_{\mathcal{R}_i} \cdot E_{\mathcal{R}_i} \right\} \tag{3.1}$$

subject to

$$R_{\mathcal{S}} = \alpha C_{\mathcal{S},\mathcal{D}}^{max}, \qquad \alpha > 1, \tag{3.2}$$

$$P_{\mathcal{S}} = \zeta_{\mathcal{S}} \cdot P_{max}, \qquad 0 < \zeta_{\mathcal{S}} < 1, \tag{3.3}$$

$$R_{\mathcal{R}_i} = \beta C_{\mathcal{R}_i,\mathcal{D}}^{max}, \qquad 0 < \beta < 1, \quad \forall i \in \{1, \ldots, N\}, \tag{3.4}$$

$$P_{\mathcal{R}_i} \leq P_{max}, \qquad \forall i \in \{1, \ldots, N\}, \tag{3.5}$$

$$\sum_{i=1}^{N} \xi_{\mathcal{R}_i} \leq 1, \qquad \forall i \in \{1, \ldots, N\}, \tag{3.6}$$

$$\xi_{\mathcal{R}_i} \in \{0, 1\}, \qquad \forall i \in \{1, \ldots, N\}, \tag{3.7}$$

where $E_{\mathcal{S}}$ denotes the transmit energy consumed by $\mathcal{S}$ for conveying its data with the aid of cooperative transmission, while $E_{\mathcal{R}_i}$ represents the transmit energy required for successfully forwarding the SN's data and for correctly conveying the data of the RN $\mathcal{R}_i$. Moreover, $P_{\mathcal{S}}$ denotes the transmit power dissipated by $\mathcal{S}$ while conveying its data with the aid of cooperative transmission. Furthermore, N denotes the total number of unlicensed RNs. When $\mathcal{R}_i$ is selected as the best RN, $\xi_{\mathcal{R}_i}$ is equal to 1. Otherwise, $\xi_{\mathcal{R}_i}$ is set to 0. Eq (3.2) and Eq (3.3) characterize the transmit rate requirement and the target transmit power of $\mathcal{S}$. Based on Eq (3.2) and Eq (3.3), an increased transmit rate can be achieved and additionally, a fraction of $(1-\zeta_{\mathcal{S}}) \cdot P_{max}$ power may be saved with the aid of the cooperative transmission assistance provided by $\mathcal{R}_i$. Eq (3.4) formulates the transmit rate requirement of $\mathcal{R}_i$, while Eq (3.5) portrays the maximum transmit power constraint at $\mathcal{R}_i$. Furthermore, single relay selection is exploited in the proposed WWCF. Hence, Eq (3.6) is introduced for ensuring that only one RN provides cooperative transmission assistance for $\mathcal{S}$. According to the OF formulated by Eq (3.1), the specific RN, which is capable of minimizing the system's total transmit energy consumption (EC) [3], while simultaneously satisfying the QoS requirement of both $\mathcal{S}$ and itself may be selected as the best RN in the proposed WWCF.

Based on above discussions, we designed a distributed WW Cooperative MAC Protocol for implementing our WWCF in the next section.

3.3 Distributed WW Cooperative MAC Protocol

Based on the Request-To-Send (RTS) / Clear-To-Send (CTS) signalling of the legacy IEEE 802.11 protocol, a distributed WW cooperative MAC protocol is developed for practically implementing the proposed WWCF, which is introduced in Section 3.2.2. The proposed signalling procedure is detailed in Fig 3.2, which includes three phases, as detailed below.

[3] Minimizing the system's total transmit energy consumption has been frequently exploited as the objective function for designing energy efficient protocols for wireless network [166–168].

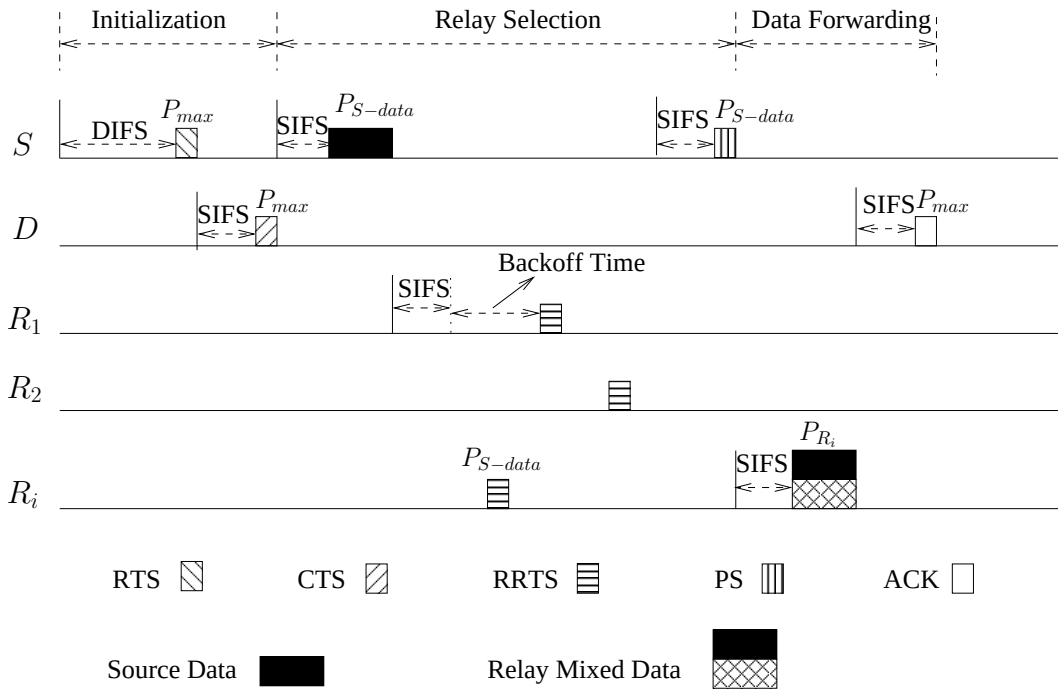

FIGURE 3.2: The overall signalling procedure of the proposed distributed WW cooperative MAC protocol used in the cooperative network topology of Fig 3.1. RTS: Request-To-Send; CTS: Clear-To-Send; RRTS: Relay-Request-To-Send; PS: Please-Send; ACK: Acknowledgment; DIFS: Distributed Interframe Space; SIFS: Short Interframe Space.

3.3.1 Phase I: Initialization

Before $\mathcal{S}$ transmits any data frame, it issues a RTS message to $\mathcal{D}$ at the maximum transmission power P_{max} for reserving the shared channel, similar to the legacy IEEE 802.11 protocol, as shown in Fig 3.2. When $\mathcal{D}$ correctly receives the RTS message, it replies with a CTS message employing the same transmission power P_{max}. Any RNs in the set $\mathcal{R}$, which can correctly over-hear both the RTS and CTS messages will be aware of the imminently forthcoming transmission. These RNs - which are denoted by filled or hollow circles in Fig 3.1 - form a potential cooperative RN set $\mathcal{R}_c \subset \mathcal{R}$.

3.3.2 Phase II: Relay Selection

Following the initialization phase, the RN selection procedure is constituted by a data transmission and two beacon message exchanges, as detailed below.

Step I: Invitation for Cooperation

If $\mathcal{S}$ does not receive a CTS message from $\mathcal{D}$, it would retransmit the RTS message as specified in the legacy IEEE 802.11 protocol [106]. By contrast, if $\mathcal{S}$ receives a CTS message

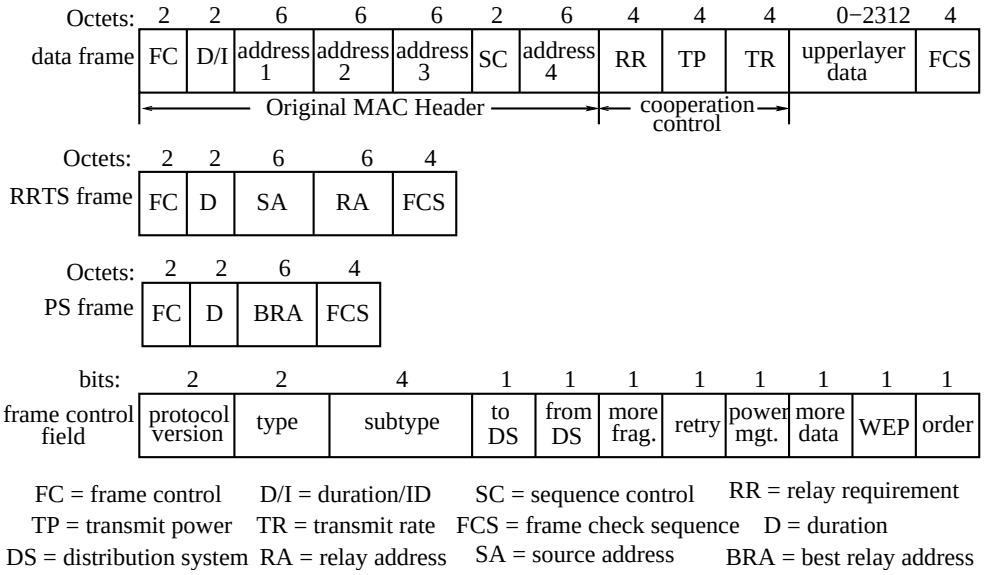

FIGURE 3.3: The formats of data frame, of the RRTS message as well as of the PS message of the proposed distributed WW cooperative MAC protocol of Fig 3.2 which is designed for the cooperative network topology of Fig 3.1.

from $\mathcal{D}$, it calculates the maximum achievable transmit rate of $C^{max}_{\mathcal{S},\mathcal{D}}$ according to the Signal-to-Noise-Ratio (SNR) of the receiver during the reception of the CTS message, while bearing in mind the assumptions detailed in Section 3.2.1. Then $\mathcal{S}$ broadcasts its data frame after a Short Interframe Space (SIFS) [106] interval at an *increased* target transmit rate of $\alpha C^{max}_{\mathcal{S},\mathcal{D}}$ ($\alpha \geq 1$) and at a *reduced* power of $P_{\mathcal{S}-data} = \zeta_{\mathcal{S}} \cdot P_{max}$ ($0 < \zeta_{\mathcal{S}} < 1$), as seen in Fig 3.2. This action is taken for the sake of satisfying its transmit rate requirement and for saving its target transmit power, as formulated in Eq (3.2) and Eq (3.3), respectively.

As a result, both the DN $\mathcal{D}$ as well as the RNs in the set $\mathcal{R}_c$ may hear this broadcast. The factor α is exploited by $\mathcal{S}$ for achieving further rate improvements, which may in fact result in exceeding $C^{max}_{\mathcal{S},\mathcal{D}}$ that would normally only be achievable in the absence of relaying. When α is higher than unity, the SN's data cannot be successfully transmitted to $\mathcal{D}$ in its entirety. However, $\mathcal{D}$ will store this data frame and exploits the classic Chase combining scheme [169] for combining it with the duplicated data frame, which was transmitted independently by the potential candidate relays, in order to achieve throughput improvements. Therefore, the SN's aggregated rate achieved by using Chase combining may be expressed by [170]

$$\alpha C^{max}_{\mathcal{S},\mathcal{D}} = \log_2(1 + \gamma^{(1)}_{\mathcal{S},\mathcal{D}} + \gamma^{\mathcal{S}}_{\mathcal{R}_i}) \qquad \alpha \geq 1, \tag{3.8}$$

where $\gamma^{(1)}_{\mathcal{S},\mathcal{D}}$ denotes the receive SNR of the direct transmission during the broadcast phase. Furthermore, $\gamma^{\mathcal{S}}_{\mathcal{R}_i}$ represents the receive SNR of the SN's data frame, which is transmitted during the relaying phase to be introduced.

Based on the receive SNR during the CTS message, $\mathcal{S}$ calculates the receive SNR of $\gamma^{\mathcal{S}}_{\mathcal{R}_i}$,

TABLE 3.1: The procedure of the relay's operation during the Phase II of the signalling procedure of Fig 3.2 in the cooperative network of Fig 3.1.

```
0:  if erroneously receive data frame Data_i from S
1:      drop data frame Data_i
2:  else
3:      read the relay requirement γ^S_{R_i}
4:      calculate the values of P^S_{R_i}, P^R_{R_i} and P_{R_i}
5:      if P_{R_i} ≤ P_max
6:          calculate its backoff time T_{R_i,bo}
7:          backoff for T_{R_i,bo} interval
8:          if T_{R_i,bo} timeout
9:              send RRTS to S
10:             wait for PS message
11:         else
12:             keep backoff
13:     else
14:         drop data frame Data_i
```

which must be guaranteed by the best RN and includes the value of $\gamma^{\mathcal{S}}_{\mathcal{R}_i}$ into its data frame for implicitly informing the RNs of the SN's transmit requirement $\alpha C^{max}_{\mathcal{S},\mathcal{D}}$. The RNs in the vicinity, which correctly receive the SN's data frame are capable of inferring the value of $\gamma^{\mathcal{S}}_{\mathcal{R}_i}$ by reading the relay requirement (RR) field of the appropriately designed cooperative MAC data frame, as shown in Fig 3.3. For the specific data frame, which was relayed by the best RN or was retransmitted by $\mathcal{S}$, the contents of the relay requirement field should be zero.

Step II: Submit for Cooperation

For clarity, we break the discussion of this step into several subtopics, namely the cooperation decision, backoff algorithm and contention message derivation. We also include the specifically designed flow-chart of Fig 3.4 for describing the RN's behaviour, which will be frequently referred to.

Cooperation Decision: If a particular RN $\mathcal{R}_i \in \mathcal{R}_c$ erroneously receives the data frame from $\mathcal{S}$, $\mathcal{R}_i$ would drop this data frame and would keep on sensing the channel, as seen in Table 3.1 and in Fig 3.4. On the other hand, if a cooperative RN $\mathcal{R}_i \in \mathcal{R}_c$ correctly receives a data frame from $\mathcal{S}$, it calculates the maximum achievable transmit rate $C^{max}_{\mathcal{R}_i,\mathcal{D}}$ of RD link based on the receive SNR of CTS message which is issued by $\mathcal{D}$ within the initialization phase. Then $\mathcal{R}_i$ calculates both the transmit power $P^{\mathcal{R}}_{\mathcal{R}_i}$ required for achieving its target transmit rate of $\beta C^{max}_{\mathcal{R}_i,\mathcal{D}}$ and the transmit power $P^{\mathcal{S}}_{\mathcal{R}_i}$ necessitated for satisfying the SN-rate requirement.

As seen in Fig 3.4 and Table 3.1, if the sum of transmit powers $P_{\mathcal{R}_i} = P^{\mathcal{S}}_{\mathcal{R}_i} + P^{\mathcal{R}}_{\mathcal{R}_i}$ is higher

than P_{max}, $\mathcal{R}_i$ has to give up contending for the cooperative opportunity and drop this SN's data frame. On the other hand, if $P_{\mathcal{R}_i}$ does not exceed the maximum transmit power P_{max}, $\mathcal{R}_i$ would send a Relay-Request-To-Send (RRTS) message to $\mathcal{S}$ at the transmit power and transmit rate specified in the transmit power (TP) and transmit rate (TR) fields after waiting for a SIFS interval plus its backoff time, which is calculated based on the proposed backoff algorithm [4] for the sake of contending for a transmission opportunity, as seen both in Fig 3.2 and in Table 3.1. The RRTS message of Fig 3.2 informs $\mathcal{S}$ about the RN's correct reception and its intention to cooperate. As seen in Fig 3.3, the RRTS frame includes both a transmitter address field and a receiver address field for the sake of enabling the $\mathcal{S}$ to uniquely recognize the different RNs. It is noted that the value of $P_{\mathcal{R}_i}$ is not included in the RRTS message of Fig 3.3, since the proposed backoff algorithm can identify the different values of $P_{\mathcal{R}_i}$ promised by the contending RNs. Hence, the specific RNs, which decide to contend for the shared channel form a smaller contending set of $\mathcal{R}_{cc} \subset \mathcal{R}_c$. These RNs are represented by the filled circles in Fig 3.1.

Backoff Algorithm: In order to minimize the total transmit EC, which is formulated by Eq (3.1), we design a backoff algorithm for selecting the best RN. As seen in Fig 3.2, before issuing the RRTS message, the RN $\mathcal{R}_i \in \mathcal{R}_{cc}$ has to wait for a SIFS interval plus for a subsequent backoff duration of $T_{\mathcal{R}_i,bo}$, which is defined as:

$$T_{\mathcal{R}_i,bo} = \varphi_{\mathcal{R}_i} T_w, \tag{3.9}$$

where $T_w = CWmin \cdot aSlotTime$ is the contention window length [5], where $CWmin$ is the minimum contention window (CW) duration specified in the IEEE 802.11 standards [106]. The coefficient $\varphi_{\mathcal{R}_i}$ denotes the contention priority of $\mathcal{R}_i$. Let us now derive the expression of $\varphi_{\mathcal{R}_i}$.

The transmit energy dissipated while conveying a data frame D_i may be formulated as $E_{D_i} = \frac{P_{D_i} \cdot L_{D_i}}{B_w \cdot R_{D_i}}$, where P_{D_i} denotes the transmit power required for transmitting the data frame D_i, while R_{D_i} is the achievable transmit rate of the data frame D_i. Furthermore, L_{D_i} denotes the length of the data frame in bits and B_w is the bandwidth. Given the length of the data frame and the bandwidth, the transmit energy $E_{\mathcal{S}}$ consumed by $\mathcal{S}$ for successfully conveying its data with the aid of cooperative transmission is a function of $R_{\mathcal{S}}$ and $P_{\mathcal{S}}$, which are formulated by Eq (3.2) and Eq (3.3). Hence, given the value of α and $\zeta_{\mathcal{S}}$, the energy dissipation of $E_{\mathcal{S}}$ retains the same value, regardless which candidate RN forwards

[4] The proposed backoff algorithm is designed for selecting the best RN. The details of the proposed backoff algorithm will be described in the next subtopic of this section.

[5] In the IEEE 802.11 standard, an aSlotTime consists of the time required to physically sense the medium and to declare the channel as "clear", plus the MAC processing delay, the propagation delay, and the "receiver/transmitter turn-around time" which is the time required for the physical layer to change from receiving to transmitting at the start of the first bit [106].

its data. Based on the above discussions, Eq (3.1) may be rewritten as:

$$\hat{i} = \arg\min_{i} \sum_{i=1}^{N} \left\{ \xi_{\mathcal{R}_i} \cdot E_{\mathcal{R}_i} \right\}, \tag{3.10}$$

subject to Eq (3.2), Eq (3.3), Eq (3.4), Eq (3.5), Eq (3.6) and Eq (3.7), where $\hat{i}$ denotes the index of the best RN, which is capable of minimizing the system's total energy consumption.

To elaborate on $\varphi_{\mathcal{R}_i}$ a little further, we formulate the following proposition.

Proposition 3.1: The transmit energy $E_{\mathcal{R}_i}$ dissipated, while successfully delivering the data of both $\mathcal{S}$ and $\mathcal{R}_i$ is a monotonically increasing function of the corresponding transmit power $P_{\mathcal{R}_i}$, when perfect capacity-achieving coding operating exactly at the capacity is exploited at RN $\mathcal{R}_i$. See AppendixA.1 for the proof.

Based on the Proposition 3.1, Eq (3.10) may be rewritten as:

$$\hat{i} = \arg\min_{i} \sum_{i=1}^{N} \left\{ \xi_{\mathcal{R}_i} \cdot P_{\mathcal{R}_i} \right\}, \tag{3.11}$$

subject to Eq (3.2), Eq (3.3), Eq (3.4), Eq (3.5), Eq (3.6) and Eq (3.7). Eq (3.11) implies that the specific RN $\mathcal{R}_{\hat{i}}$, which requires the lowest transmit power for conveying both the SN's and its own data should be selected as the best RN for the sake of minimizing the system's total transmit energy dissipation relying on our WWCF. Hence, the contention priority of $\mathcal{R}_i$ is formulated as:

$$\varphi_{\mathcal{R}_i} = \frac{P_{\mathcal{R}_i^{min}}}{P_{max}}. \tag{3.12}$$

According to Eq (3.12), the specific candidate RN, which promises to dissipate the lowest transmit power may transmit its RRTS message first as an explicit benefit of its shortest backoff time.

In each RN selection phase, $\mathcal{S}$ has to wait for a fixed period of time ($T_w + aSlotTime$) to collect the responses of the potential candidate RNs. If $\mathcal{S}$ correctly receives the RRTS message during its fixed waiting duration times out, it selects the transmitter of the specific RRTS which was the first one to be received correctly as the best RN, without considering the RRTS messages arriving later and without comparing the specific transmit power promised by the individual candidate RNs. Hence, based on the proposed backoff algorithm formulated by Eq (3.9) and Eq (3.12), the specific candidate RN, which promises to dissipate the lowest transmit power may be selected as the best RN, which is an explicit benefit of

its shortest backoff time. It is worth noting that the best RN is selected in a distributed manner, i.e. without any information exchange between the candidate RNs and without requiring a centralized controller, which would be required to collect and compare the rate information of all the candidate RNs. Since the value of $P_{\mathcal{R}_i}$ promised by the candidate RN $\mathcal{R}_i$ is always lower than P_{max}, the back-off time allocated to $\mathcal{R}_i$ will not exceed the SN's fixed waiting duration ($T_w + aSlotTime$). Hence, all the candidate RNs may issue their RRTS messages before $\mathcal{S}$ stops waiting for the responses.

Contention Message Derivation: Considering the selfish nature of the RNs, the greedy RN may exploit an increased transmit rate, which is higher than its rate requirement of $\beta C^{max}_{\mathcal{R}_i,\mathcal{D}}$ for improving the QOS of its data. However, the particular RN which promises the lowest transmit power may be granted the transmission opportunity by $\mathcal{S}$ relying on the proposed backoff algorithm. Hence, the greedy RN has to minimize its transmit power by 'just' satisfying its rate requirement of $\beta C^{max}_{\mathcal{R}_i,\mathcal{D}}$ in order to wait for a shorter backoff time, which is calculated based on the proposed backoff algorithm. Therefore, we have:

$$P_{\mathcal{R}_i^{min}}(P^{\mathcal{S}}_{\mathcal{R}_i}, P^{\mathcal{R}}_{\mathcal{R}_i^{min}} \mid \alpha, \beta) = P^{\mathcal{S}}_{\mathcal{R}_i} + P^{\mathcal{R}}_{\mathcal{R}_i^{min}}, \tag{3.13}$$

subject to the condition of:

$$C^{\mathcal{R}}_{\mathcal{R}_i} = \beta C^{max}_{\mathcal{R}_i,\mathcal{D}}, \qquad \forall 0 < \beta < 1, \tag{3.14}$$

$$\gamma^{\mathcal{S}}_{\mathcal{R}_i,\mathcal{D}} = \gamma^{\mathcal{S}}_{\mathcal{R}_i}, \tag{3.15}$$

where $\gamma^{\mathcal{S}}_{\mathcal{R}_i,\mathcal{D}}$ denotes the destination's received SNR for SN's data forwarded by the RN $\mathcal{R}_i$. Naturally, the transmit rate requirement of $\mathcal{S}$ determines the minimum SNR that has to be guaranteed by the relayed transmission, as mentioned in Section 3.3.2.

Let us now consider how to find $P^{\mathcal{S}}_{\mathcal{R}_i}$ and $P^{\mathcal{R}}_{\mathcal{R}_i^{min}}$ of Eq (3.13). In our design, the RN employs superposition coding (SPC) [171, 172] for jointly encoding both the SN's and its own data. The $\mathcal{D}$ then extracts the SN's data from the SPC relayed composite signal with the aid of SIC. Finally, the extracted relayed and the direct component are combined.

Assuming $\mathcal{D}$ treats the RN's data frame as interference [6], the receive SNR $\gamma^{\mathcal{S}}_{\mathcal{R}_i}$ of the SN's data frame relayed by the RN is given by:

$$\gamma^{\mathcal{S}}_{\mathcal{R}_i} = \frac{\rho_{\mathcal{R}_i,\mathcal{D}}|h_{\mathcal{R}_i,\mathcal{D}}|^2 P^{\mathcal{S}}_{\mathcal{R}_i}}{P_N + \rho_{\mathcal{R}_i,\mathcal{D}}|h_{\mathcal{R}_i,\mathcal{D}}|^2 P^{\mathcal{R}}_{\mathcal{R}_i}}. \tag{3.16}$$

[6] In general, SPC detected with the aid of SIC achieves the same sum-rate for the different possible superposition decoding orders [171, 172]. Hence, the total transmit power $P_{\mathcal{R}_i^{min}}$ necessitated for satisfying the transmit rate requirements of both $\mathcal{S}$ and $\mathcal{R}_i$ remains the same for different possible superposition decoding orders based on the system model considered in Section 3.2.1. This implies that the superposition decoding order does not influence the result of the relay selection in our distributed WW cooperative MAC.

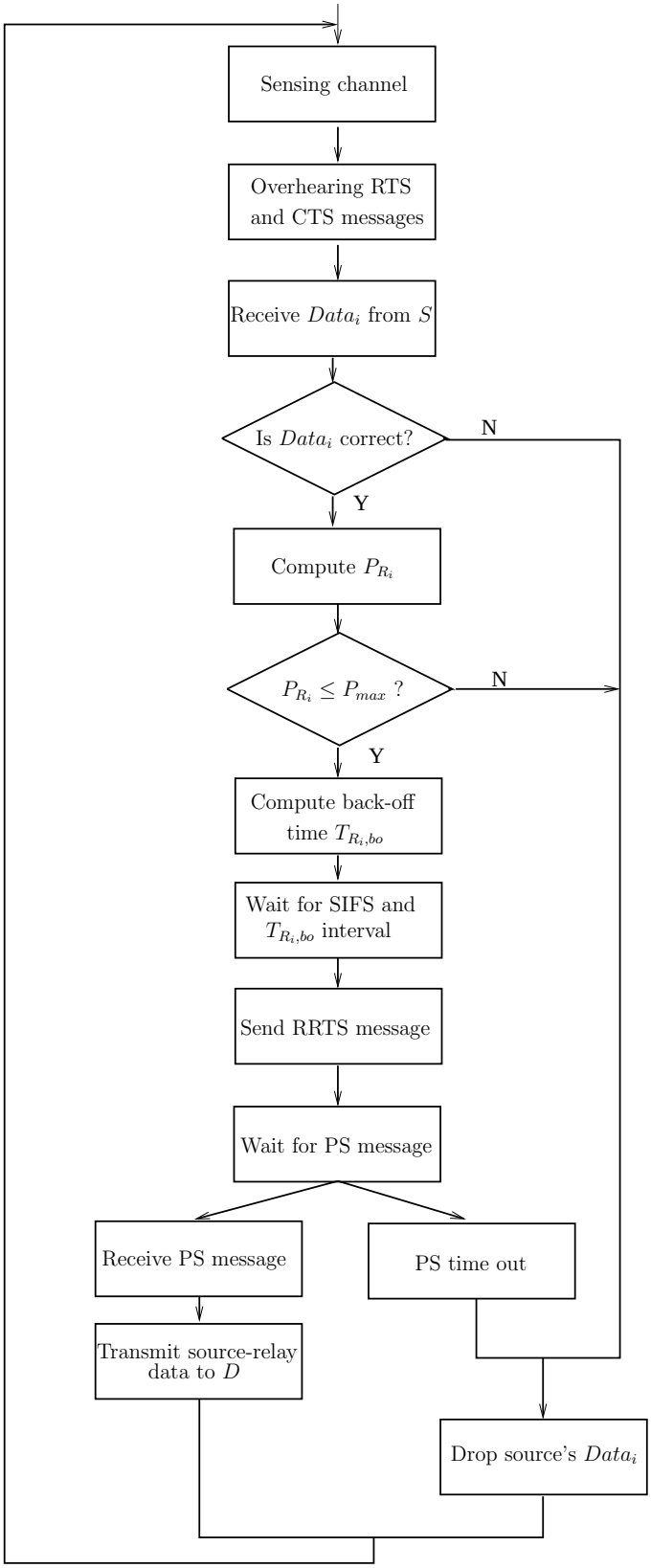

FIGURE 3.4: The flow chart of the relay operations relying on the proposed distributed WW cooperativ MAC protocol of Fig 3.2 in a cooperative network of Fig 3.1, when using the data format of Fig 3.3.

After successfully retrieving the SN's data frame, $\mathcal{D}$ becomes capable of decoding the RN's data frame by removing the SN's interference with the aid of a SIC scheme [173]. Hence, the achievable rate of the RN may be formulated as $C^{\mathcal{R}}_{\mathcal{R}_i} = \log_2(1 + \frac{\rho_{\mathcal{R}_i,\mathcal{D}}|h_{\mathcal{R}_i,\mathcal{D}}|^2 P^{\mathcal{R}}_{\mathcal{R}_i}}{P_N})$. According to the relaying strategy employed, the RN calculates the minimum power required for the rate $C^{\mathcal{R}}_{\mathcal{R}_i}$ to reach $\beta C^{max}_{\mathcal{R}_i,\mathcal{D}}$. Thus, the value of $P^{\mathcal{R}}_{\mathcal{R}^{min}_i}$ is explicitly given as:

$$P^{\mathcal{R}}_{\mathcal{R}^{min}_i} = \frac{(2^{\beta C^{max}_{\mathcal{R}_i,\mathcal{D}}} - 1)P_N}{\rho_{\mathcal{R}_i,\mathcal{D}}|h_{\mathcal{R}_i,\mathcal{D}}|^2} \qquad 0 < \beta < 1. \tag{3.17}$$

Likewise, based on Eq (3.16) and Eq (3.17), the RN is capable of calculating the transmit power $P^{\mathcal{S}}_{\mathcal{R}_i}$ required for satisfying SN's transmit rate requirement of $\alpha C^{max}_{\mathcal{S},\mathcal{D}}$, which is given by:

$$\begin{aligned} P^{\mathcal{S}}_{\mathcal{R}_i} &= \gamma^{\mathcal{S}}_{\mathcal{R}_i}\left(\frac{P_N}{\rho_{\mathcal{R}_i,\mathcal{D}}|h_{\mathcal{R}_i,\mathcal{D}}|^2} + P^{\mathcal{R}}_{\mathcal{R}^{min}_i}\right) \\ &= (2^{\alpha C^{max}_{\mathcal{S},\mathcal{D}}} - \gamma^{(1)}_{\mathcal{S},\mathcal{D}} - 1)\cdot \quad \left[\frac{P_N}{\rho_{\mathcal{R}_i,\mathcal{D}}|h_{\mathcal{R}_i,\mathcal{D}}|^2} + \frac{(2^{\beta C^{max}_{\mathcal{R}_i,\mathcal{D}}} - 1)P_N}{\rho_{\mathcal{R}_i,\mathcal{D}}|h_{\mathcal{R}_i,\mathcal{D}}|^2}\right], \qquad \alpha > 1 \qquad 0 < \beta < 1, \end{aligned} \tag{3.18}$$

where $\gamma^{\mathcal{S}}_{\mathcal{R}_i}$ has been given in Step I. Based on the above derivation, $\mathcal{R}_i$ calculates the value of $P^{min}_{\mathcal{R}_i}$ as the sum of $P^{\mathcal{S}}_{\mathcal{R}_i}$ and $P^{\mathcal{R}}_{\mathcal{R}^{min}_i}$.

Step III: Accept for Cooperation

After waiting for the fixed duration of $(T_w + aSlotTime)$ specified by the proposed backoff algorithm and for a subsequent SIFS interval, $\mathcal{S}$ replies to the best RN $\mathcal{R}_{\hat{i}}$ associated with the first RRTS message that was correctly received by sending a Please-Send (PS) message, provided that $\mathcal{S}$ correctly received the RRTS message during its fixed waiting period of $(T_w + aSlotTime)$, as shown in both Fig 3.2 and Fig 3.5. The format of the PS frame is characterized in Fig 3.3. Since the SN sends its data frame and PS message at the same transmission power of $P_{\mathcal{S}-data}$, all the RNs, which have correctly received the data frame from the SN will overhear the PS message. This guarantees that only the best RN forwards its data frame to $\mathcal{D}$ during the data relaying phase.

3.3.3 Phase III: Cooperative Transmission

In this phase, the best RN $\mathcal{R}_{\hat{i}}$ forwards the superposition-coded data to $\mathcal{D}$, if $\mathcal{S}$ successfully selects the best RN. Otherwise, $\mathcal{S}$ retransmits its data frame to $\mathcal{D}$, as seen in Fig 3.2 and Fig 3.5.

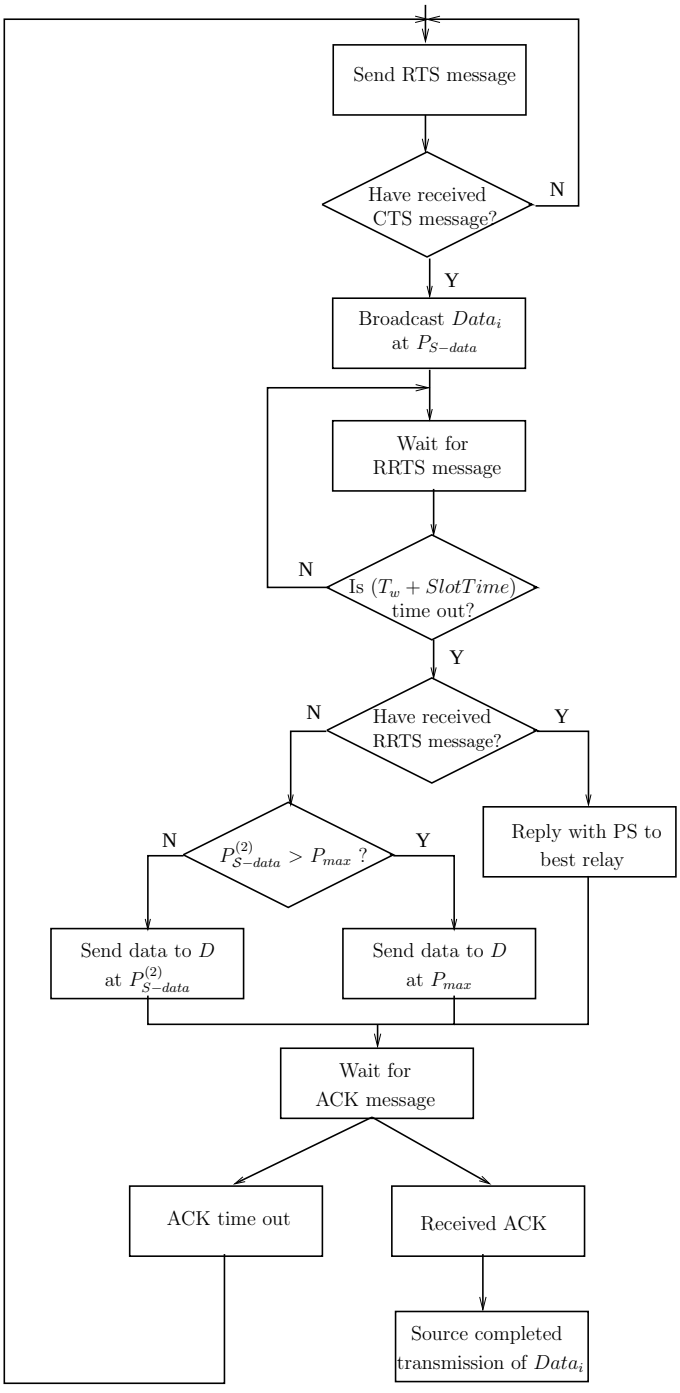

FIGURE 3.5: The flow chart of the source operations in the cooperative network of Fig 3.1 relying on the proposed distributed WW cooperative MAC protocol of Fig 3.2 and the data format of Fig 3.3. This may be contrasted to the RN's flow char in Fig 3.4 as discussed in Section 3.3.

Data Forwarding

If RN $\mathcal{R}_i \in \mathcal{R}_{cc}$ found that the receiver of the received PS message is not itself, it would drop the SN's data and would keep on sensing the medium, as shown in Fig 3.4. On the other hand, if the RN $\mathcal{R}_i \in \mathcal{R}_{cc}$ received a PS message which is destined for itself, it will encode both the SN's and its data with the aid of SPC and will forward the superposition-coded data frame to $\mathcal{D}$ at its pre-calculated transmission power of $P_{\mathcal{R}_i^{min}}$ after a SIFS period, acting as the best RN, as seen in Fig 3.2. Finally, at the DN, the classic Automatic Repeat reQuest (ARQ) procedure will be initiated, when receiving the forwarded data and successfully decoding as well as combing it with the most recent direct transmission during Step-I of Phase-II.

Source Retransmission

Fig 3.2 shows the signalling procedure when the source's data is transmitted with the aid of cooperative transmission assistance from the best RN. By contrast, if none of the RNs competes for a transmission opportunity or multiple RRTS messages collided at the SN, $\mathcal{S}$ directly sends its data to $\mathcal{D}$ as a replica without relaying, as shown in Fig 3.6. This transmission takes place either at the specific transmit power of $P_{\mathcal{S},\mathcal{D}}^{(II)}$, which is capable of guaranteeing the expected rate of $\alpha C_{\mathcal{S},\mathcal{D}}^{max}$ or failing that, it resorts to using the maximum affordable transmit power of P_{max}, as seen in Fig 3.5.

If $\mathcal{D}$ receives this data frame, it replies with an ACK message to $\mathcal{S}$ after successfully decoding and combining the frame with the most recent erroneous data frame broadcast by $\mathcal{S}$. If $\mathcal{S}$ does not receive an ACK message from $\mathcal{D}$, it will repeat the above three phases for retransmitting its data. The procedure of SN retransmission is characterized in Fig 3.5, which includes both the RN selection procedure and the SN's direct transmission.

Remarks: The proposed distributed WW cooperative MAC protocol is capable of improving the SN's transmit rate and minimizing the system transmit energy consumption. This is an explicit benefit of the cooperative regime and the proposed relay selection scheme. More importantly, the RNs compete for the right to cooperate with $\mathcal{S}$ in a *unilateral* fashion, where the RNs do not have to exchange any detailed information with the other RNs, since each RN executes its decisions autonomously. Furthermore, the $\mathcal{S}$ selects the transmitter of the RRTS message, which is first correctly received as the best RN without considering the responses from the other candidate RNs. Hence, our RN selection scheme does not require any centralized control for collecting and comparing the state information of all the candidate RNs.

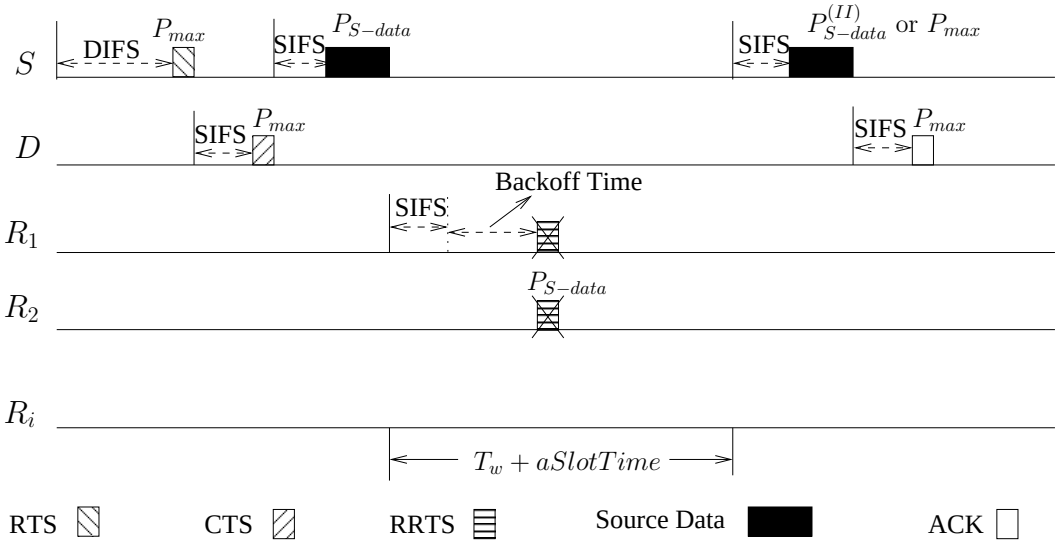

FIGURE 3.6: The overall signalling procedure of the proposed distributed WW cooperative MAC protocol for the scenario where the source cannot select best RN to forward its data in the network topology of Fig 3.1 relying on the data format of Fig 3.3. This may be contrasted to the signalling procedure of Fig 3.2. RTS: Request-To-Send; CTS: Clear-To-Send; RRTS: Relay-Request-To-Send; ACK: Acknowledgement; DIFS: Distributed Interframe Space; SIFS: Short Interframe Space.

TABLE 3.2: Simulation parameters used by the cooperative network of Fig 3.1 relying on the proposed distributed WW cooperative MAC protocol of Fig 3.2 and Fig 3.6 as well as on the data format of Fig 3.3.

$\zeta_{\mathcal{S}}$	$\frac{1}{4}, \frac{1}{2}, \frac{3}{4}$
α	1,1.5,2,2.5,3
β	0,0.4,0.8
P_{max}	2 mW
Data Length	1024 $Bytes$
CWmin	7
aSlotTime	20 μs
SIFS	10 μs
RRTS Length	20 $Bytes$
PS Length	14 $Bytes$
RTS Length	20 $Bytes$
CTS Length	14 $Bytes$
ACK Length	14 $Bytes$

3.4 Simulation Results

3.4.1 Simulation Scenarios

In order to evaluate the achievable performance of the proposed scheme, we present our simulation results based on Omnet++. We consider two scenarios for investigating both the achievable rate and EC improvement, as well as for analyzing the RN's behaviour.

- In the first scenario, all the RNs are randomly distributed across the entire network

area, while $\mathcal{S}$ and $\mathcal{D}$ have fixed positions. The network size considered ranges from $u = 5$ nodes to $u = 30$ nodes for the sake of evaluating the influence of the networks-size on the achievable transmit rate and EC.

- In the other scenario we consider a small network supporting $u = 5$ nodes, i.e. the $\mathcal{S}$, $\mathcal{D}$ plus three RNs, where all the nodes have fixed positions. One of the three RNs is allocated at the position of $d = 1/4$ along the SD link. Another RN is in the middle of SD link at $d = 1/2$, while the third RN is at the point $d = 3/4$ of the SD link.

Two non-cooperative systems are introduced as the benchmarkers of our comparisons.

- We compare the system's achievable total transmit rate (TTR) constituted by the sum of the SN's and RN's transmit rate to that of the non-cooperative system 1 (NCS-1), which consumes the same total transmission energy as the WW cooperative spectrum leasing system (WW-CSLS) relying on the proposed distributed WW cooperative protocol.
- We compare the total transmission EC to that of the non-cooperative system 2 (NCS-2), which is capable of achieving the same TTR as our WW-CSLS.

Since the SN's data is transmitted twice by itself and additionally by the best RN, if the cooperative transmission is successful, two direct transmission phases are exploited in both NCS-1 and NCS-2.

In Section 3.4.2, we compare the performance of our WW-CSLS to that of a random CSLS (Ran-CSLS), where the best RN is randomly selected. Additionally, all the assumptions mentioned in Section 3.2 are exploited by both NCS-1 and NCS-2 as well as by the Ran-CSLS. In order to evaluate their performance, we adopt the idealized simplifying assumption that the control messages are received without errors in our WW-CSLS and in all benchmark systems. In Section 3.4.6, we investigated a more practical network, where we consider the non-zero control message error probability in our WW-CSLS. Furthermore, we evaluate the jointly achievable improvements attained either by the SPC and the SIC or by our frame combining technique based on the second scenario hosting $u = 5$ nodes in Section 3.4.8. The length of the data frame generated at the application layer is 1024 *Bytes*. The greedy factors α and β are pre-determined for each simulation. We adjust their values to estimate the performance of different scenarios. The main simulation parameters are listed in Table 3.2.

3.4.2 Effect of Relay Selection

Let us now consider the first scenario and investigate the effect of the RN selection scheme proposed in Section 3.3.2 by evaluating the achievable performance of our WW-CSLS and

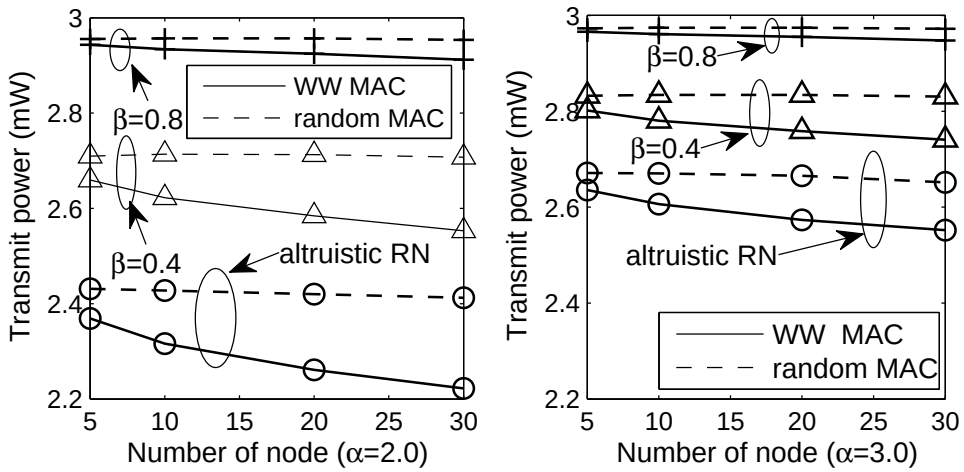

FIGURE 3.7: The system's data transmit power dedicated purely to the data in the cooperative network of Fig 3.1 relying on the signalling procedure of Fig 3.2 and Fig 3.6 as well as the data format of Fig 3.3.

Ran-CSLS, where the best RN is randomly selected.

3.4.2.1 Transmit Power

According to the distributed WW cooperative MAC protocol proposed in Section 3.3, the specific RN, which promises the lowest transmit power $P_{\mathcal{R}_i}$ required for successfully conveying the superposition-coded data is selected as the best RN. However, the best RN is randomly selected in the Ran-CSLS of Section 3.4.1 without considering any system parameters, such as the transmit power $P_{\mathcal{R}_i}$. Hence, the RN's transmit power $P_{\mathcal{R}_i}$ is the crucial parameter for investigating the effect of the proposed RN selection scheme. Fig 3.7 quantifies the system's total data transmit power (TDTP) for our WW-CSLS and that consumed in Ran-CSLS. The system's TDTP is defined as the sum of the SN's transmit power required for conveying its data plus the RN's transmit power necessitated for delivering the superposition-coded data [7].

Based on the backoff algorithm proposed in the Section 3.3.2, the system's TDTP consumed in our WW-CSLS is lower than that of Ran-CSLS, as seen in Fig 3.7. When the SN or RN becomes greedier, less RNs can afford the increased transmit power required for providing successful cooperative transmission assistance. This phenomenon increases the probability that the same RN is selected as the best RN in both WW-CSLS and Ran-CSLS. Hence, the difference between the TDTP of our WW-CSLS and that of Ran-CSLS is reduced, when either α or β is increased, as seen in Fig 3.7. Moreover, the TDTP of both our WW-CSLS and of the Ran-CSLS is reduced, when the network hosts more RNs due to the increased

[7]The transmit power dissipated for exchanging control messages is not quantified in Fig 3.7

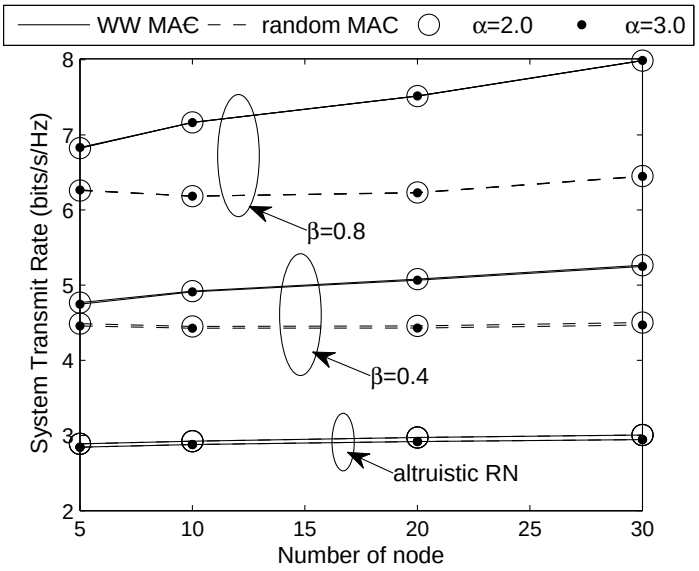

FIGURE 3.8: The system's total achievable rate improvement in the cooperative network of Fig 3.1 relying on the signalling procedure of Fig 3.2 and Fig 3.6 as well as the data format of Fig 3.3.

probability of having RNs, which promise to reduce the transmit power in comparison to a smaller network. However, the probability of the event that a low-quality RN - namely one which requires a higher transmit power than other RNs - is selected as the best RN in the Ran-CSLS is increased, when the network becomes larger. Hence, compared to our WW-CSLS, an increased TDTP is conserved by Ran-CSLS, when the network's size is increased.

3.4.2.2 Achievable Transmit Rate

Fig 3.8 compares the system's TTR, namely the sum of both the SN's rate and the RN's rate achieved by our WW-CSLS to that achieved by the Ran-CSLS of Section 3.4.1. As shown in Fig 3.8, the system's achievable TTR relying on our WW-CSLS is 8 $bit/s/Hz$ for $\beta = 0.8$ and $u = 30$, whilst a lower TTR of 6.5 $bit/s/Hz$ is achieved by Ran-CSLS, given β and the network size. Compared to Ran-CSLS, the system's TTR can be improved by our WW-CSLS even for lower β values and for smaller networks, such as for example for $\beta = 0.4$ and $u = 5$, as seen in Fig 3.8. Based on our WW-CSLS, the specific RN which promises a lower transmit power of $P_{\mathcal{R}_i}$ may achieve a higher transmit rate of $\beta C^{max}_{\mathcal{R}_i,\mathcal{D}}$ as a benefit of having an improved RD link. Hence, compared to Ran-CSLS, a higher TTR is achieved by our WW-CSLS relying on selecting the specific RN, which promises the lowest transmit power $P_{\mathcal{R}_i}$.

Observe in Fig 3.8 that the proposed WW cooperative MAC protocol is capable of providing a higher TTR improvement than Ran-CSLS, when β is increased. When a RN becomes greedier, its target transmit rate is increased. This phenomenon increases the difference

between the RN's transmit rate achieved by our WW-CSLS and that achieved by Ran-CSLS, when a RN suffering from a low-quality RD link is selected by Ran-CSLS. Hence, the difference between the TTR of our WW-CSLS and that of Ran-CSLS is increased, when the RN becomes greedier. Considering the CSLS, where the RN altruistically forwards data for $\mathcal{S}$, the system's TTR is equal to the SN's rate. Hence, the system's TTR remains the same, regardless of which particular candidate RN is selected as the best RN, when the RNs are altruistic, as seen in Fig 3.8.

As shown in Fig 3.8, the system's TTR achieved by our WW-CSLS is increased, when the network becomes larger. However, the effect of the network's size on the TTR achieved by Ran-CSLS is not as obvious as that on our WW-CSLS. When the network hosts more RNs, the number of candidate RNs may be increased. This phenomenon increases the probability that a low-quality RN having a lower transmit rate is selected as the best RN in Ran-CSLS. However, these low-quality RNs cannot win the cooperative transmission opportunity in our WW-CSLS, if the specific RN promising a reduced transmit power also contends for the transmission opportunity. Hence, a higher TTR improvement is provided by the proposed WW cooperative MAC protocol, as the network becomes larger, as seen in Fig 3.8. The above investigations imply that the proposed WW cooperative MAC protocol is capable of saving a substantial amount of transmit power, while simultaneously providing significant TTR improvements compared to Ran-CSLS.

3.4.3 Effect of Cooperative Transmission

Let us now investigate the system's EC and achievable total rate both in our WW-CSLS and in NCS-1 as well as in NCS-2.

3.4.3.1 Energy Consumption

Fig 3.9 and Fig 3.10 show the achievable energy consumption ratio (ECR) of $\frac{E_{noncoop}}{E_{WW}}$, where E_{WW} denotes the system's total transmission EC for our distributed WW cooperative MAC protocol and $E_{noncoop}$ represents that of NCS-2, which is capable of achieving the same TTR as our CSLS.

As seen in Fig 3.9, compared to NCS-2, more than two third of the system's total energy may be saved by exploiting the proposed distributed WW cooperative MAC protocol, given $\beta = 0.8$. In the network hosting $u = 30$ nodes, an ECR of $\frac{E_{noncoop}}{E_{WW}} = 9$ may be achievable for $\alpha = 2.0$ and $\beta = 0.8$. The system's total energy is the sum of the energy of all the data frames and control messages transmitted by $\mathcal{S}$ and $\mathcal{D}$, as well as by the RNs. Given the same β and network size, the probability of successful cooperative transmission is reduced,

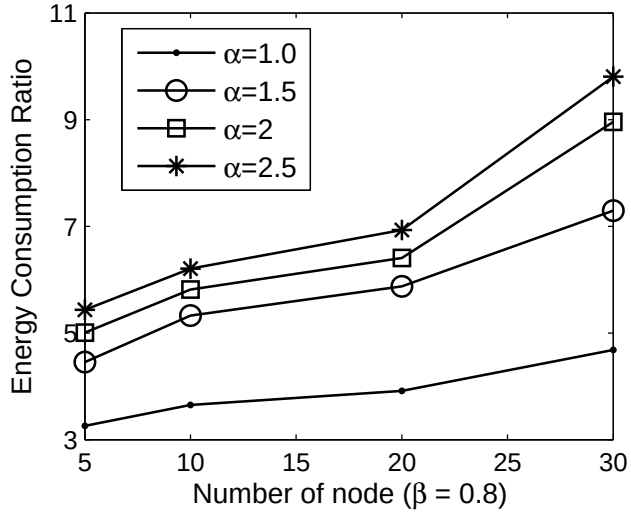

FIGURE 3.9: Energy consumption ratio of $\frac{E_{noncoop}}{E_{WW}}$ in the cooperative network of Fig 3.1 relying on the signalling procedure of Fig 3.2 and Fig 3.6 as well as the data format of Fig 3.3.

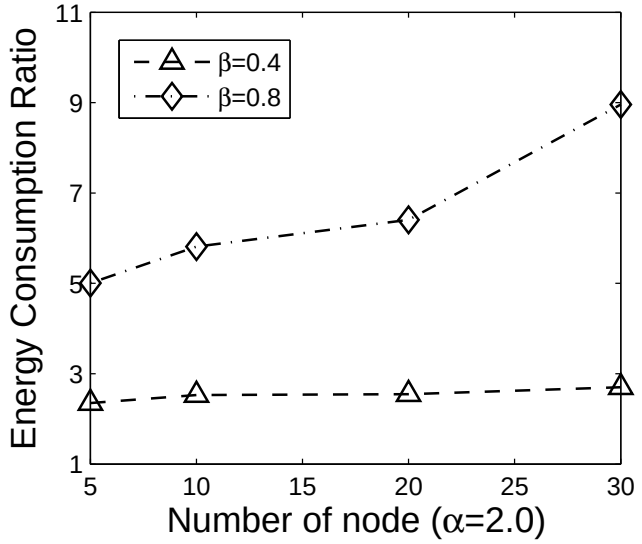

FIGURE 3.10: Energy consumption ratio of $\frac{E_{noncoop}}{E_{WW}}$ in the cooperative network of Fig 3.1 relying on the signalling procedure of Fig 3.2 and Fig 3.6 as well as the data format of Fig 3.3.

as α is increased. Hence, $\mathcal{S}$ requires more transmission energy for satisfying its rate requirement. However, the RNs' EC is reduced due to the decreased transmission probability, when the SN's greediness factor is increased. Therefore, the EC E_{WW} of our WW-CSLS is reduced when $\mathcal{S}$ becomes greedier. By contrast, the EC $E_{noncoop}$ of NCS-2 is increased, when $\mathcal{S}$ becomes greedier due to the increased system rate of WW-CSLS. Hence, the ECR is increased, when $\mathcal{S}$ becomes greedier, as shown in Fig 3.9.

Given $\alpha = 2.0$, more than half of the system's energy is conserved by our distributed WW

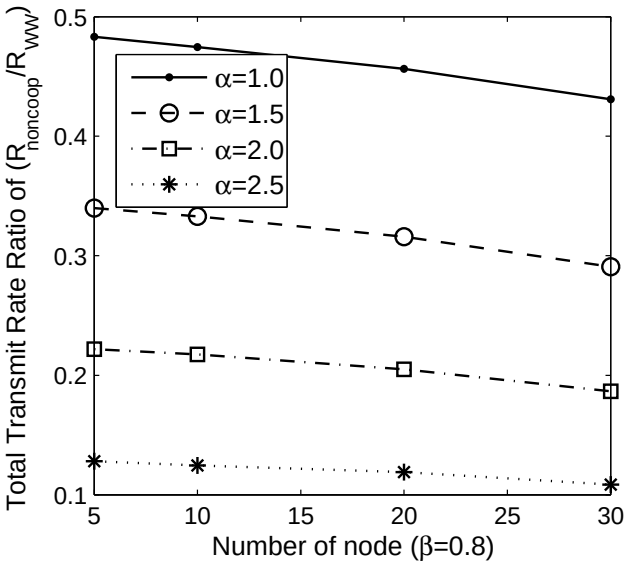

FIGURE 3.11: The total transmit rate ratio of $\frac{R_{noncoop}}{R_{WW}}$ in the cooperative network of Fig 3.1 relying on the signalling procedure of Fig 3.2 and Fig 3.6 as well as the data format of Fig 3.3.

cooperative MAC protocol for $\beta = 0.4$, as seen in Fig 3.10. As β is increased, the system's ECR is increased from 2.5 to 5 for $\alpha = 2.0$ and $u = 5$, as shown in Fig 3.10. When the RNs become greedier, less RNs can afford the increased power required for successfully forwarding the superposition-coded data. However, the transmit rate achieved by the best RN is considerably increased. Hence, an increased total energy is required by NCS-2 for the sake of achieving the same system rate as our WW-CSLS. Therefore, the system's ECR of $\frac{E_{noncoop}}{E_{WW}}$ is increased, when the RN becomes greedier.

An increased total EC is required by NCS-2 for achieving the increased total system rate of our CSLS, when the number of nodes increases from $u = 5$ to $u = 30$. Hence, the ECR is increased when the network hosts more RNs, as seen in Fig 3.9 and Fig 3.10. Based on the above discussions, the proposed WW cooperative MAC protocol is capable of offering a satisfactory energy efficiency compared to non-cooperative system.

3.4.3.2 Achievable Transmit Rate

Fig 3.11 and Fig 3.12 compare the system's total transmit rate ratio (TTRR) of $\frac{R_{noncoop}}{R_{WW}}$, where R_{WW} denotes the sum of both the SN's rate and the RN's rate achieved by WW-CSLS relying on the proposed distributed WW cooperative MAC protocol and $R_{noncoop}$ represents that of NCS-1 when $\zeta_{\mathcal{S}} = \frac{1}{2}$[8]. Observe in Fig 3.11 that as expected, the system's achievable TTR relying on our WW-CSLS is more than twice as high as that achieved by NCS-1, which consumes the same total transmission energy, given the same values of α and

[8]The effect of different values of $\zeta_{\mathcal{S}}$ is investigated in Section 3.4.7

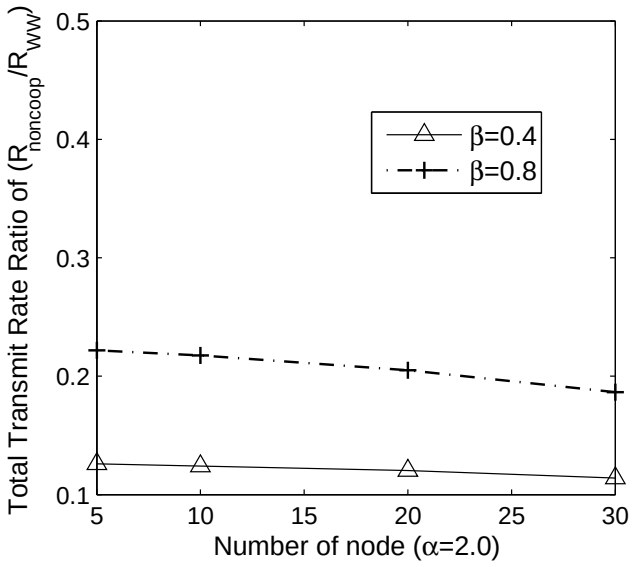

FIGURE 3.12: The total transmit rate ratio in the cooperative network of Fig 3.1 relying on the signalling procedure of Fig 3.2 and Fig 3.6 as well as the data format of Fig 3.3.

β. For $\alpha = 2.5$ and $\beta = 0.8$, the system's TTR may be improved by a factor of nine with the aid of our WW protocol compared to that achieved by NCS-1 in a network hosting $u = 30$ nodes. Observe in Fig 3.12 that the TTRR of $\frac{R_{noncoop}}{R_{WW}}$ is less than 0.25 for $\beta = 0.4$ and $\alpha = 2.0$. Hence, the proposed WW cooperative MAC protocol is capable of providing a considerable TTR improvement.

As shown in Fig 3.11, the TTRR of $\frac{R_{noncoop}}{R_{WW}}$ is reduced, when $\mathcal{S}$ becomes greedier, because an increased system's TTR is achieved by our WW-CSLS, when the SN's transmit rate requirement is increased. Furthermore, as discussed in Section 3.4.3.1, the system's total energy is the sum of the energy of all the data frames and control messages transmitted by $\mathcal{S}$ and $\mathcal{D}$, as well as by the RNs. Given the same β and network size, the probability of successful cooperative transmission is reduced, as α is increased. Hence, $\mathcal{S}$ requires more transmission energy for satisfying its rate requirement. However, the RNs' EC is reduced due to the decreased transmission probability, when the SN's greediness factor is increased. Hence, a reduced TTR has to be tolerated by NCS-1, when $\mathcal{S}$ becomes greedier due to the reduced system's EC, when invoking the WW-CSLS. Hence, the TTRR of $\frac{R_{noncoop}}{R_{WW}}$ is decreased, when $\mathcal{S}$ becomes greedier, as seen in Fig 3.11. Additionally, when the RN's factor of greediness (β) is increased, the best RN will be rewarded by a considerably higher rate for its own traffic, provided that the cooperation is successful, due to the RN's increased transmit rate requirement. However, an increased transmit power $P_{\mathcal{R}_i}$ is required for achieving the higher target transmit rate of the RN, when the RN becomes greedier. This phenomenon increases the transmit energy dissipated by the RNs. Therefore, an increased TTR is achieved by NCS-1, when RN becomes greedier due to the increased system's EC, when invoking the WW-CSLS. Hence, the TTRR of $\frac{R_{noncoop}}{R_{WW}}$ is increased, when the RN becomes greedier, as

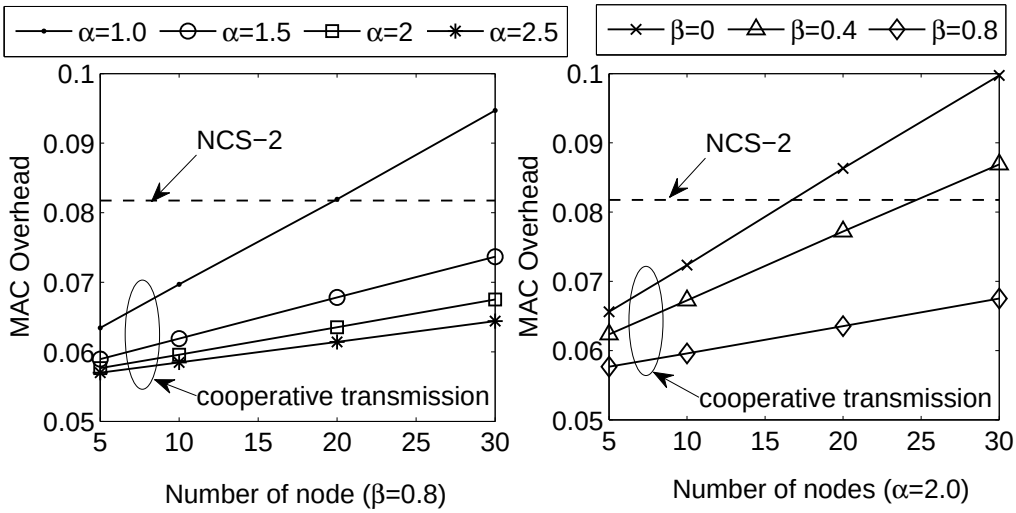

FIGURE 3.13: MAC overhead for $\beta = 0.8$ or $\alpha = 2.0$ in the cooperative network of Fig 3.1 relying on the proposed distributed WW cooperative MAC protocol of Fig 3.2 and Fig 3.6 as well as the data format of Fig 3.3.

shown in Fig 3.12.

Moreover, the TTRR of $\frac{R_{noncoop}}{R_{WW}}$ is reduced, when the network becomes larger, as seen in Fig 3.11 and Fig 3.12. This is due to the increased probability of beneficial RN candidates which are capable of increasing the cooperative transmission probability and reducing the EC. Hence, when the network becomes larger, the achievable TTR of our WW-CSLS is increased and that of NCS-1 is reduced. Therefore, the TTRR of $\frac{R_{noncoop}}{R_{WW}}$ is reduced, when the network becomes larger, as seen in Fig 3.11 and Fig 3.12.

The above investigations imply that the proposed distributed WW cooperative MAC protocol is capable of achieving a considerable system rate improvement, while offering a satisfactory energy efficiency.

3.4.4 MAC Overhead

Fig 3.13 compares the MAC overhead of the proposed distributed WW cooperative MAC protocol to that of NCS-2, which is based on the RTS/CTS signalling regime of IEEE 802.11 standards [106]. The MAC overhead is defined as the ratio of $\frac{\mathcal{N}_{mac-c}+\mathcal{N}_{mac-h}+\mathcal{N}_{mac-t}}{\mathcal{N}_{mac-d}}$, where $\mathcal{N}_{mac-c}$ denotes the number of bits of all MAC control messages, while $\mathcal{N}_{mac-h}$ and $\mathcal{N}_{mac-t}$ represent the number of header and tailing bits of the MAC data frame, respectively. Furthermore, $\mathcal{N}_{mac-d}$ denotes the number of bits in the payload data packet, including the headers introduced by the higher layers.

Observe in Fig 3.13 that the MAC overhead of the proposed distributed WW cooperative MAC protocol is decreased, when either α or β is increased, because the number of candidate

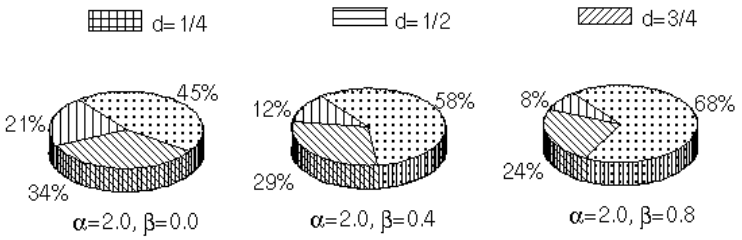

FIGURE 3.14: The RN's transmission probability in a network hosting $u = 5$ nodes, namely $\mathcal{S}$, $\mathcal{D}$ and three RNs relying on the proposed distributed WW cooperative MAC protocol of Fig 3.2 and Fig 3.6 as well as the data format of Fig 3.3.

RNs is reduced, while the SN or the RN becomes greedier. Compared to the traditional RTS/CTS scheme specified in the IEEE 802.11 standards [106], the RRTS message and PS message are introduced into our WW-CSLS for assisting in RN selection, if cooperation can be exploited. Hence, an increased MAC overhead is generated, when more cooperative transmission sessions are initiated. However, compared to NCS-2, the RN's data can also be transmitted with the aid of cooperation in our WW-CSLS, although extra control messages are introduced. Since the length of RN's data frames is higher than that of the extra control messages, the MAC overhead introduced by our distributed WW protocol is lower than that of the NCS-2, when the network size is smaller than $u = 20$. When the network hosts more than $u = 20$ nodes, the overhead of our CSLS becomes higher than that of NCS-2, because more RRTS messages are generated, when the number of potential RNs increases. However, the MAC overhead introduced by our WW protocol remains always lower than 0.1 for $\beta = 0.8$ or $\alpha = 2.0$.

3.4.5 Relay Behaviour

In order to investigate the behaviour of the relays, we analyze both the transmission probability of each RN and the Cumulative Distribution Function (CDF) of the relays' transmit power for the configuration of $\alpha = 2.0$ in the network hosting $u = 5$ nodes, as shown in Fig 3.14 and Fig 3.15. Observe in Fig 3.14 that the RN at "$d = 3/4$" always benefits from the highest transmission probability, while the RN at "$d = 1/4$" has the lowest probability of cooperative opportunities, because the RN at "$d = 1/4$" may suffer a lower quality of RD link when free-space pathloss is considered. Furthermore, when the RN becomes greedier, an increased transmit power is required for satisfying the transmit rate requirement of both SN and RN. Hence, under the constraint of the maximum transmit power, the transmission probability of the RNs at "$d = 1/4$" and "$d = 1/2$" is reduced when the RN becomes greedier. However, as a benefit of having a better channel for the RD link, the transmission probability of the RN at "$d = 3/4$" is increased upon increasing β, as shown in Fig 3.14 .

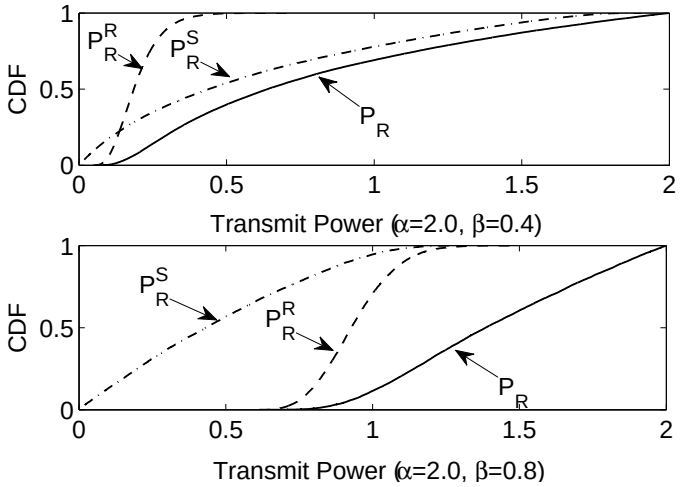

FIGURE 3.15: The CDF of the average RN transmit power $P_{\mathcal{R}}^{\mathcal{S}}$ required for conveying the SN's data, average RN transmit power $P_{\mathcal{R}}^{\mathcal{R}}$ assigned to its own data and the average total RN transmit power $P_{\mathcal{R}}$ in a network hosting $u = 5$ nodes namely $\mathcal{S}$, $\mathcal{D}$ and three RNs relying on the proposed distributed WW cooperative MAC protocol of Fig 3.2 and Fig 3.6 as well as the data format of Fig 3.3.

Fig 3.15 illustrates the CDF of the average RN transmit power $P_{\mathcal{R}}^{\mathcal{S}} = \mathbb{E}[P_{\mathcal{R}_i}^{\mathcal{S}}], \forall R_i$ required for conveying the SN's data and that required for its own data transmission, namely $P_{\mathcal{R}}^{\mathcal{R}} = \mathbb{E}[P_{\mathcal{R}_i}^{\mathcal{R}}], \forall R_i$, as well as that of the average RN transmit power of $P_{\mathcal{R}} = P_{\mathcal{R}}^{\mathcal{S}} + P_{\mathcal{R}}^{\mathcal{R}}$ for the configuration of $\alpha = 2.0$ in the network hosting $u = 5$ nodes. When $\beta = 0.4$, the RN assigns more transmit power for relaying the SN's data frame. However, as expected, the transmit power $P_{\mathcal{R}}^{\mathcal{R}}$ assigned for transmitting the RN's data increases, when the RN becomes greedier. Indeed, $P_{\mathcal{R}}^{\mathcal{R}}$ becomes even higher than $P_{\mathcal{R}}^{\mathcal{S}}$, when $\beta = 0.8$.

3.4.6 Effect of Erroneous Control Messages

In our previous discussion the control messages were assumed to be correctly received. However, the control messages may be corrupted in practical networks. Hence in this section, we investigate the detrimental effects of erroneous control messages on the performance of the proposed distributed WW cooperative MAC protocol by considering two specific scenarios. According to the proposed distributed WW cooperative MAC protocol, $\mathcal{S}$ and $\mathcal{D}$ issue RTS and CTS messages for reserving the shared channel. Hence, the adjacent nodes of both $\mathcal{S}$ and $\mathcal{D}$ may postpone their transmissions for the sake of avoiding the multi-flow collisions. However, the RTS message issued by $\mathcal{S}$ may be corrupted either when $\mathcal{S}$ and the other SNs concurrently send their RTS message. Hence, let us consider the RTS error probability for modelling the RTS collision events in the first scenario, where multiple transmission pairs and potentially erroneous control messages are assumed [174]. Furthermore, any of the control messages introduced by the proposed distributed WW cooperative MAC protocol may be corrupted by the transmissions of the other SNs, which cannot overhear either the

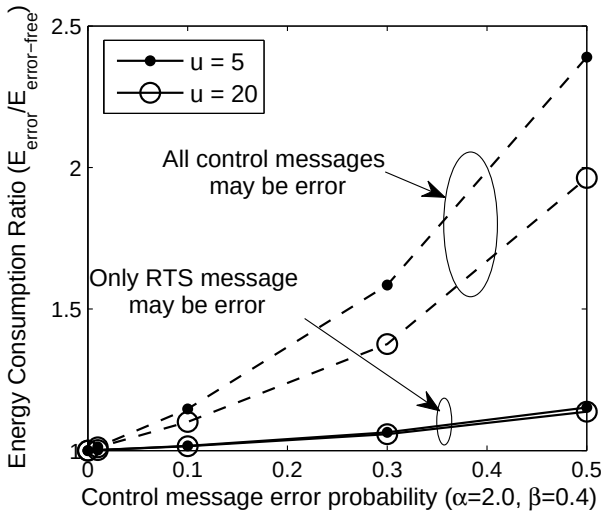

FIGURE 3.16: The system's energy consumption ratio of $\frac{E_{error}}{E_{error-free}}$ parameterized with different control message error probabilities in the cooperative network of Fig 3.1 relying on the signalling procedure of Fig 3.2 and Fig 3.6 as well as the data format of Fig 3.3.

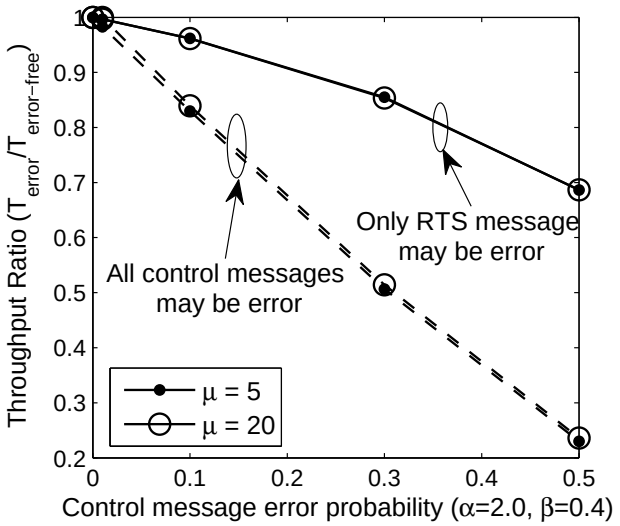

FIGURE 3.17: The system's throughput parameterized with different control message error probabilities in the cooperative network of Fig 3.1 relying on the signalling procedure of Fig 3.2 and Fig 3.6 as well as the data format of Fig 3.3.

RTS message of $\mathcal{S}$ or the CTS message of $\mathcal{D}$. Hence, all the control messages are assumed to be corrupted according to the given error probability in the second scenario, where multiple transmission pairs and hidden nodes are assumed [174].

Fig 3.16 and Fig 3.17 illustrate the system's ECR of $\frac{E_{error}}{E_{error-free}}$ and throughput ratio of $\frac{T_{error}}{T_{error-free}}$ respectively, which are achieved by our distributed WW cooperative MAC protocol, parametrised with different control message error probabilities. The variable E_{error} denotes the system's total EC for our WW-CSLS, where the control message may be corrupted. Furthermore, $E_{error-free}$ is the system's total EC for our WW-CSLS, where error-

free control messages are assumed. In this chapter, the throughput is assumed to be a parameter of the MAC layer, given by the number of bits successfully transmitted per second. Hence, the throughput may be formulated as $\frac{L_{data}}{T}$, where T is the total time required for successfully transmitting the data frame, which consists of the handshaking time of the signalling procedure and the waiting time of each node specified in our distributed WW cooperative protocol as well as the transmission time of both the data and control messages. Hence, the total time interval T is capable of characterizing the delay introduced both by the signalling procedure and by the retransmission regime. The variable T_{error} denotes the throughput achieved by our WW-CSLS, where the control message may be corrupted. Moreover, $T_{error-free}$ represents the throughput achieved by the WW-CSLS, when the control messages are assumed to be correctly received.

Observe in Fig 3.16 that as expected, when the control message error probability is increased, an increased total system energy is dissipated by our WW-CSLS in both the "RTS-error" scenario and in the "all-control-error" scenario, because having more potentially erroneous control messages reduces the probability of successful transmission, while the extra retransmissions of both control messages and of the data frame consume extra energy. Additionally, the system's throughput is also decreased, when more control messages are corrupted, which is due to the extra delay introduced by the increased number of both control message retransmissions and data retransmissions, as seen in Fig 3.17. In the "RTS-error" scenario, only the RTS message is retransmitted, when $\mathcal{S}$ does not receive a CTS response from $\mathcal{D}$. However, both the data and control messages may be retransmitted in the "all-control-error" scenario, if other control messages are corrupted, as seen in Fig 3.4 and Fig 3.5. Hence, compared to the "RTS-error" scenario, an increased EC is encountered in the "all-control-error" scenario, as shown in Fig 3.16. Furthermore, the throughput achieved in the "all-control-error" scenario is lower than that of the "RTS-error" scenario due to the increased delay introduced by data retransmission, as seen in Fig 3.17. It is worth noting that the event of only the RTS message being occurred more often than the event of all control messages being corrupted, because the RTS and CTS messages are capable of protecting all other control messages by informing the adjacent nodes concerning the other nodes' transmission intentions [174]. Based on our above discussion, the number of candidate RNs may be increased, when the network hosts more RNs. Hence, the detrimental effect of erroneous RRTS messages misinforming $\mathcal{S}$ about the RN's intention to cooperate is reduced in a larger network. This phenomenon reduces the system's EC and additionally, achieves a higher throughput improvement in the "all-control-error" scenario having $u = 20$ nodes. Since only RTS retransmissions occur in the "RTS-error" scenario, the effect of the network size on both the system's EC and throughput remains negligible, when only the RTS message may be corrupted.

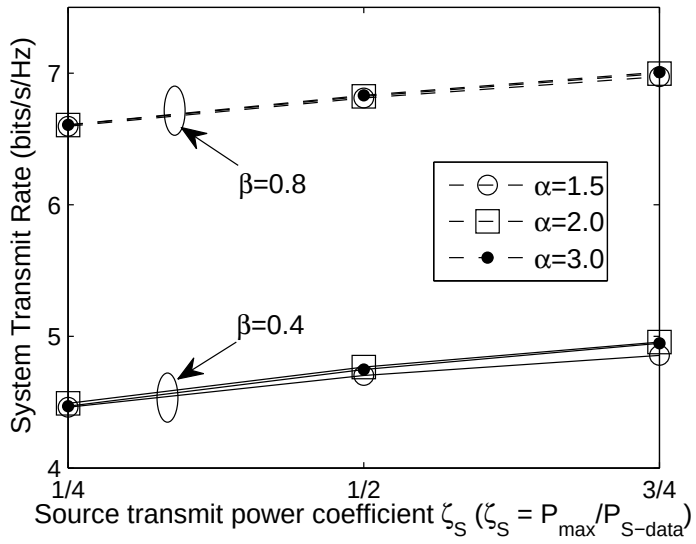

FIGURE 3.18: The system's achievable transmit rate with different SN transmit power $P_{\mathcal{S}-data}$ in the cooperative network of Fig 3.1 relying on the signalling procedure of Fig 3.2 and Fig 3.6 as well as the data format of Fig 3.3.

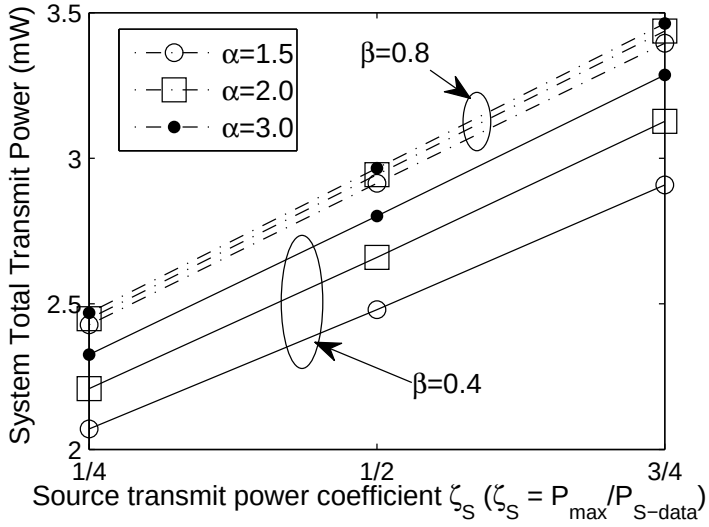

FIGURE 3.19: The system's data transmit power with different SN transmit power $P_{\mathcal{S}-data}$ in the cooperative network of Fig 3.1 relying on the signalling procedure of Fig 3.2 and Fig 3.6 as well as the data format of Fig 3.3.

3.4.7 Effect of the SN's Transmit Power $P_{\mathcal{S}-data}$

In the above discussions, $\mathcal{S}$ is assumed to broadcast its data at a transmit power of $P_{\mathcal{S}-data} = \frac{1}{2}P_{max}$, which is associated with $\zeta_{\mathcal{S}} = \frac{1}{2}$ for the sake of inviting the RNs to provide cooperative transmission assistance. Let us now investigate the effect of different SN transmit powers $P_{\mathcal{S}-data}$. Fig 3.18, Fig 3.19 and Fig 3.20 characterize the system's TTR, TDTP and ECR of $\frac{E_\zeta}{E_{(\frac{1}{4})}}$ respectively, when the SN's transmit power coefficient $\zeta_{\mathcal{S}}$ ranges from $\frac{1}{4}$ to $\frac{3}{4}$ and the network's size is $u = 5$, where E_ζ denotes the system's EC, when $\mathcal{S}$ broadcasts its

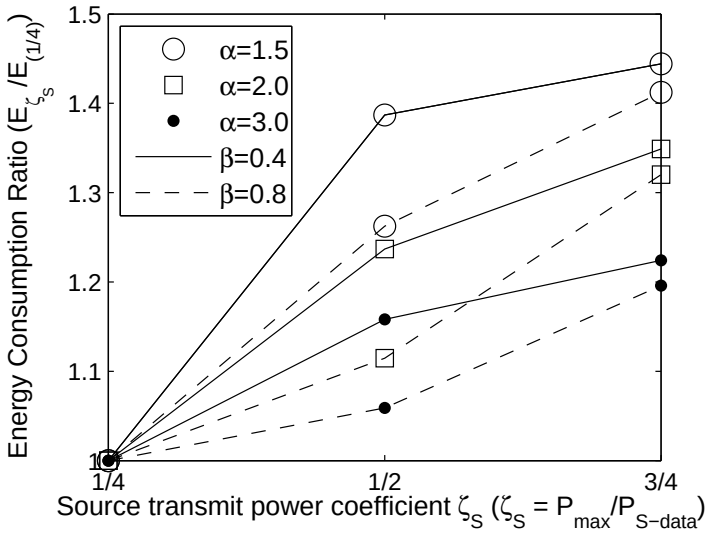

FIGURE 3.20: The system's energy consumption ratio of $\frac{E_\zeta}{E_{(\frac{1}{4})}}$ with different SN transmit power $P_{\mathcal{S}-data}$ in the cooperative network of Fig 3.1 relying on the signalling procedure of Fig 3.2 and Fig 3.6 as well as the data format of Fig 3.3.

data at a transmit power of $P_{\mathcal{S}-data} = \zeta_{\mathcal{S}} P_{max}$, while $E_{(\frac{1}{4})}$ represents the system's EC for $\zeta_{\mathcal{S}} = \frac{1}{4}$.

When $\mathcal{S}$ relies on a higher transmit power for broadcasting its data, more RNs are capable of correctly receiving the SN's data. Furthermore, the transmit power $P^{\mathcal{S}}_{\mathcal{R}_i}$ required for satisfying the SN's transmit rate requirement is reduced, when the SN's transmit power $P_{\mathcal{S}-data}$ is increased. This increases the cooperative transmission probability. Hence, a higher TTR can be achieved, when $\mathcal{S}$ broadcasts its data at a higher transmit power. However, both the system's TDTP and the system's EC are increased for a higher SN transmit power coefficient ζ owing to the increased SN transmit power $P_{\mathcal{S}-data}$. Based on the above discussion, the transmit energy dissipated, while exchanging control messages is increased, when more RNs contend for transmission opportunities. Furthermore, a higher transmit energy is consumed as the cooperation probability is increased, because more RNs are granted transmission opportunities. Hence, the increase of the system's EC in the scenario, where $\beta = 0.8$ is higher than that in the scenario, where we have $\beta = 0.4$ and when $\zeta_{\mathcal{S}}$ is increased from $\frac{1}{2}$ to $\frac{3}{4}$, due to the higher improvement of the cooperation probability for $\beta = 0.8$. Based on the above discussions, increasing the SN's transmit power $P^{\mathcal{S}}_{\mathcal{R}_i}$ is capable of improving the system's TTR at the cost of consuming more energy. Hence, the tradeoff between the system's TTR and the system's EC may be balanced by appropriately designing the value of $P^{\mathcal{S}}_{\mathcal{R}_i}$, which may be developed in our future research.

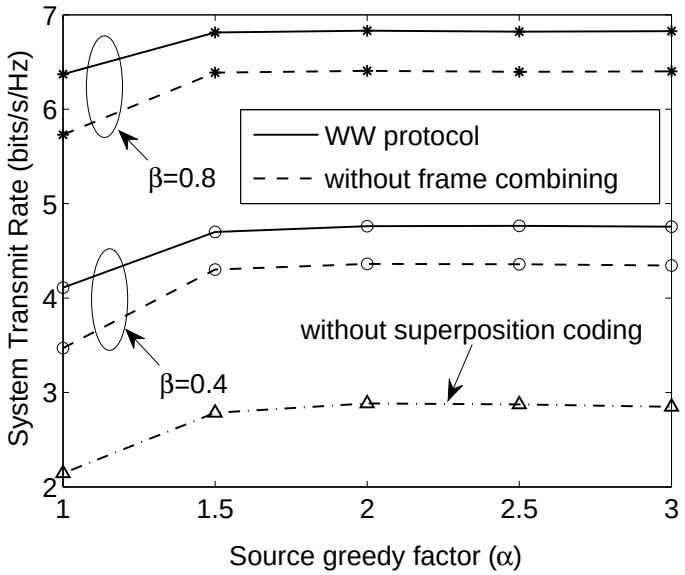

FIGURE 3.21: The system's total achievable transmit rate versus the SN's greedy factor both with and without superposition coding and SIC as well as frame combining in the cooperative network of Fig 3.1 relying on the signalling procedure of Fig 3.2 and Fig 3.6 as well as the data format of Fig 3.3.

3.4.8 Effect of either Superposition Coding or Frame Combining

According to the proposed distributed WW cooperative MAC protocol, the best RN jointly encodes both the SN's and its own data with the aid of SPC for simultaneously transmitting them when a transmission opportunity was granted. After correctly receiving the SPC data, $\mathcal{D}$ invokes SIC for separating the SN's and RN's data. In order to evaluate the achievable TTR improvement jointly attained by SPC and SIC, we compare the system's TTR achieved by our WW-CSLS to that of the CSLS operating without exploiting these techniques, as shown in Fig 3.21. Since there are only two data transmissions during a successful cooperation according to our distributed WW cooperative MAC protocol, the best RN, which does not exploit SPC is assumed to forward only the SN's data instead of the SPC data. As seen in Fig 3.21, the system's TTR may be increased from $2.9bits/s/Hz$ to $6.9bits/s/Hz$ for $\alpha = 2.0$ and $\beta = 0.8$ by jointly exploiting the SPC and SIC. Hence, these techniques are capable of significantly improving the system's transmit rate.

In order to improve the SN's transmit rate, $\mathcal{D}$ invokes frame combining for amalgamating both the direct and relayed SN data after successfully separating the SN's and RN's data. Fig 3.21 shows the system's TTR improvement achieved by exploiting frame combining.

3.5 Chapter Summary

Based on our discussions in Chapter 1 and Chapter 2, we first formulated a WWCF for striking a tradeoff between the achievable rate improvement and the energy consumption, while granting transmission opportunities for the unlicensed RNs in Section 3.2. More explicitly, $\mathcal{S}$ in the proposed WWCF intends to lease part of its spectrum to the unlicensed RNs in exchange for cooperatively supporting the source's transmissions for the sake of saving the SN's transmit power and for improving the SN's transmit rate. Furthermore, the unlicensed RNs have an incentive to provide cooperative transmission assistance for $\mathcal{S}$ in our WWCF for the sake of accessing the SN's spectrum to convey their own traffic. Based on the behaviour of both the $\mathcal{S}$ and RN described in Section 3.2.2, minimizing the system's total transmit energy dissipation, whilst simultaneously satisfying the transmit rate requirements of both the $\mathcal{S}$ and the RN is based on conceiving a beneficial OF, as formulated in Eq (3.1)-Eq 3.7.

In Section 3.3, a distributed WW cooperative MAC protocol was developed for implementing our WWCF, which was characterized in Fig 3.2-Fig 3.6 and Table 3.1. Based on the RTS/CTS signalling regime of the legacy IEEE 802.11 protocol, $\mathcal{S}$ first issues an RTS message to $\mathcal{D}$ for reserving the channel and for declaring its transmission intention. As seen in Fig 3.2 and Fig 3.5, upon receiving the CTS message from $\mathcal{D}$, $\mathcal{S}$ broadcasts its data at its increased transmit rate and reduced the transmit power. During the relay selection phase of Fig 3.2, the specific RNs, which correctly receive the SN's data and are capable of affording the transmit power required for successfully conveying the superposition-coded data under the constraint of the maximum transmit power constitute a candidate RN set, as characterized in Table 3.1 and in Fig 3.4 as well as in Fig 3.1. According to the proposed relay selection scheme detailed in Section 3.3.2, the specific RN, which promises to require the lowest transmit power may be selected as the best RN for the sake of minimizing the system's transmit energy consumption. As detailed in Section 3.3.3, the best RN will then jointly encode both the SN's and its own data with the aid of SPC and will forward the superposition-coded data frame to $\mathcal{D}$ within Phase III of the proposed signalling procedure detailed in Fig 3.2. Finally, $\mathcal{D}$ employs SIC for decoding the superposition-coded source-relay data received from the relay and subsequently retrieves the source data by appropriately combining the direct and the relayed cooperative transmission, as detailed in Section 3.3.3.

Section 3.4 evaluates the achievable performance of the proposed distributed WW cooperative MAC protocol by introducing two non-cooperative systems and a Ran-CSLS as the benchmarker used in our comparisons. Section 3.4.2 compares the system's TDTP and TTR for our WW-CSLS to the corresponding performance of Ran-CSLS, where the best RN is randomly selected. Explicitly, observe in Fig 3.7 and Fig 3.8 that compared to the Ran-CSLS

benchmarker, the proposed WW cooperative MAC protocol is capable of achieving a considerable sum-rate improvement, while simultaneously achieving a beneficial transmit power reduction. When compared to NCS-2 of Section 3.4.1 which is capable of achieving the same TTR as our WW-CSLS, the proposed distributed WW cooperative MAC protocol is capable of offering a satisfactory energy efficiency, as quantified in Fig 3.9 and Fig 3.10. Furthermore, compared to the non-cooperative system NCS-1 of Section 3.4.1, which consumes the same energy as the WW-CSLS, considerable TRR improvements may be achieved by relying on the proposed distributed WW cooperative MAC protocol as demonstrated by Fig 3.11 and Fig 3.12. Based on the classic RTS/CTS scheme of Fig 3.2, as specified in the IEEE 802.11 standards, extra control messages are introduced by the proposed distributed WW cooperative MAC protocol of Section 3.3 for the sake of supporting cooperative transmissions and RN selection. Hence, we quantified the associated MAC overhead in Section 3.4.4. Observe in Fig 3.13 that although the MAC overhead of our WW-CSLS is increased as the network becomes larger, the MAC overhead of our WW-CSLS remains lower than that of the NCS-2, when the network size is smaller than $u = 20$. Furthermore, the MAC overhead introduced by our WW protocol is seen in Fig 3.13 to be always lower than 0.1, even for $u = 30$. Based on our investigations of the RN's behaviour in Section 3.4.5, the specific RN, which is close to $\mathcal{D}$ maintains a higher transmission probability than the other RNs, because we have the highest probability that the RN at "$d = 3/4$" is selected as the best RN. Since the above discussions is based on the idealized simplifying assumption of having error-free control messages, we further investigated the effects of erroneous control messages in Section 3.4.6. The erroneous transmission of control messages dissipates extra energy required for retransmitting both the data frame and the erroneous control messages, whilst reducing the throughput owing to the increased delay introduced by the retransmissions, when all the control messages may be corrupted, as seen in Fig 3.16 and Fig 3.17. However, as discussed in Section 3.4.6, these detrimental effects are significantly reduced, when only the RTS message may be corrupted, and this event may occur more often than the event of all control messages being corrupted, because the RTS and CTS messages are capable of protecting all other control messages by informing the adjacent nodes concerning the other nodes' transmission intentions [174]. Section 3.4.7 investigated the effect of different SN transmit powers $P_{\mathcal{S}-data}$. Observe in Fig 3.18 that the system's TTR can be considerably improved upon increasing the SN's transmit power $P^{\mathcal{S}}_{\mathcal{R}_i}$ due to the increased number of candidate RNs. However, as seen in Fig 3.19 an increased transmit power has to be dissipated for the sake of achieving a TTR improvement. Hence, appropriately designing the value of $P^{\mathcal{S}}_{\mathcal{R}_i}$ may further balance the tradeoff between the system's TTR and the system's EC. Finally, we investigated the benefits provided by either superposition coding or frame combining in Section 3.4.8. As evidenced by Fig 3.21 a significant TTR improvement can be achieved with the aid of joint SPC employed at the RN for both the SN's and RN's data

as well as by combining the SD and RD signals at $\mathcal{D}$.

In the next chapter we will introduce the queueing model of our WW-CSLS and analyse its stability based on the queueing theory.

Chapter 4

Stability Analysis of "Win-Win" Cooperative Spectrum Leasing System

4.1 Introduction

In Chapter 1, we introduced the cooperative communications techniques [3, 4] which has recently attracted substantial attention, since it has shown a great potential in terms of mitigating the deleterious effects of wireless propagation. As detailed in Chapter 1, in a cooperative communication system, the source node (SN) relies on Relay Nodes (RNs) [175], which are capable of providing cooperative transmission assistance by forwarding the source's data to the destination node (DN) for the sake of improving the throughput, reducing the energy consumption as well as providing a diversity gain for the SN [52].

In order to improve the exploitation of the available spectrum bands, the concept of Cognitive Radio (CR) technology [176–180] has been conceived for supporting both licensed and unlicensed users relying on shared spectral resources. The existing cognitive radio techniques may be classified into two categories, namely the common model [181] and the spectrum leasing model [181, 182].

- According to the common model, the licensed users can access the spectrum any time and are oblivious of the presence of unlicensed users. The unlicensed users are allowed to sense and to exploit the spectrum holes for conveying their data on condition, if they do not substantially interfere with the transmissions of licensed users [181].

- Under the spectrum leasing model, the licensed users are aware of the presence of unlicensed users and intend to lease part of their spectral resources to these unlicensed users in exchange for appropriate 'remuneration' [181, 182].

As a further advance, the combination of CR and cooperative communications techniques is capable of enhancing the attainable bandwidth efficiency, hence improving the performance of both the licensed users as well as of the unlicensed users [153,162,181,183–185], regardless, which CR model is used. However, these benefits may be eroded by the conventional non-cooperative higher-layer protocols, which were designed for classic non-cooperative systems as detailed in Chapter 2. Hence, it is important to design appropriate higher layer protocols for supporting cooperative cognitive communications.

Based on the spectrum leasing model, a 'win-win' (WW) cooperative Medium Access Control (MAC) protocol is designed in Chapter 3 for the sake of minimizing the total energy consumption and for improving the source's throughput, while simultaneously conveying the relay's own traffic. More explicitly, the SN - which is typically considered to be the Primary User (PU) - leases part of its spectral resource to the unlicensed user (UN) in exchange for cooperative transmission. The UN is also termed as the Secondary User (SU). The UNs who act as RNs carry out autonomous decisions concerning whether to contend for a transmission opportunity for the sake of conveying their own traffic in the light of their individual energy and throughput requirements. More explicitly, superposition coding [172, 186] may be invoked at the relay node (RN) for jointly encoding both the source's as well as the relay's data, where the final DN may rely on Successive Interference Cancellation (SIC) for separating the source's and relay's data. Furthermore, the DN is typically capable of beneficially amalgamating both the direct and the relayed components using frame combining.

Some of the work on cooperative CR systems assumes that the PU always has data in its transmit buffer, whenever a transmission opportunity arises [82, 187–191]. Considering the bursty nature of transmissions in practical networks, queueing theory has found application at the higher OSI layers for the sake of characterizing the stability region of queueing systems [25, 137, 192], as detailed in Chapter 2. In [138], Sadek *et al.* designed a cognitive cooperative multiple access protocol and analyzed both its maximum stable throughput region and its delay. More explicitly, the protocol proposed in [138] allowed the unlicensed user to detect and utilize the unused time slots for retransmitting the failed packets of SN. However, Sadek *et al.* assumed that the unlicensed users, who act as RNs, do not have their own traffic. Moreover, El-Sherif *et al.* [143] designed and analyzed two relay arrangements for a cognitive multiple access network, which consists of SNs and cognitive RNs as well as unlicensed nodes (UN). Both the cognitive RNs and the UNs are allowed to access the spectrum during silence periods. However, the cognitive RNs of [143] are still assumed to *altruistically* forward the data for supporting the SNs. Furthermore, Liu *et*

TABLE 4.1: Major contributions on stability analysis for cooperative CR system.

Author(s)	CR Model	RN Nature	RN Behaviour
Sadek *et al.* [138]	common model	altruistic RN	altruistically forward SN's data
El-Sherif *et al.* [143]	common model	altruistic RN	altruistically forward SN's data
Liu *et al.* [193]	common model	altruistic RN	altruistically forward SN's data
Simeone *et al.* [139]	common model	selfish RN	process either SN's or its packet during a silence period
Bao *et al.* [194]	common model	selfish RN	process either SN's or its packet during a silence period
Krikides *et al.* [195]	common model	selfish RN	jointly encoding SN's and its data by using dirty-paper coding
Krikides *et al.* [77]	common model	selfish RN	jointly encoding SN's and its data by using superposition coding

al. [193], designed and analyzed a basic cooperative beaMforming and Automatic repeat request aided oppoRtunistic speCtrum scHeduling (MARCH) scheme for a cooperative CR system for supporting a PU with the aid of *altruistic* cognitive RNs as well as UNs. On the other hand, Simeone *et al.* [139] analyzed the stable throughput of a four-node cognitive cooperative system based on the common model [181], where the RN was assumed to be *greedy*. As a further advance, Bao *et al.* [194] proposed a MAC protocol for a cooperative CR system, which supports multiple PUs and one SU which acts as a RN. However, the RN relies upon in both [139] and [194] is assumed to be capable of processing only a *single packet* during a silence period, namely either that of the SN or that of the RN. By contrast, Krikides *et al.* employed both dirty-paper coding [195] and superposition coding [77] for designing protocols for multi-user cognitive cooperative systems. Furthermore, they analyzed the stability of their systems using queueing theory in [195] and [77], respectively. These two coding schemes facilitate for the RN to *simultaneously* convey both the SN's and its own data packets.

As seen in Table 4.1, the main features of the above state-of-the-art solutions may be summarized as follows:

- all the above contributions [77,138,139,143,193–195] relied on the *common model* [181].
- The *energy consumption* has not been considered in [77, 138, 139, 143, 193–195], where the unlicensed users were designed to forward data for the licensed users at the maximum transmit power for the sake of improving the system throughput.
- The authors of [77, 138, 139, 193, 195] have ignored the beneficial design option, when the system has the choice of multiple candidate RNs.

Based on above discussions, we developed the following investigation in this chapter:

- We analyze the queueing stability of a ***cooperative spectrum leasing system*** (CSLS), which supports a single primary transmission pair and exploits our previously proposed distributed WW cooperative MAC protocol of Section 3.3 [55]. To the best of the our knowledge, the queueing stability of the cognitive cooperative systems relying on ***spectrum leasing*** has not been investigated in the open literature.
- More specifically, in Section 4.3 we analyze both the queueing stability as well as the steady-state throughput of the RNs and SN which exploits the proposed ***power control scheme*** of our distributed WW cooperative MAC protocol.
- We mathematically derive the probability expression for a specific UN to be selected as the best RN in Section 4.3.3 in terms of the ***RN selection scheme*** of our distributed WW cooperative protocol proposed in Section 3.3.

This chapter is organised as follows. Our system model is introduced in Section 4.2, while Section 4.3 describes the queueing model of our CSLS and analyzes the queueing stability of both the SN and RN. In Section 4.4, the attainable performance of our scheme is quantified. Finally, we conclude in Section 4.5.

4.2 System Model

Let us first introduce the network topology and the physical layer model considered as well as the WW cooperative protocol exploited at the MAC layer.

4.2.1 Network Construction

As seen in Fig 4.1, we consider a cooperative network having a single SN $\mathcal{S}$ and a total of N RNs in the set $\mathcal{R} = \{\mathcal{R}_1, \ldots, \mathcal{R}_N\}$, as well as a common DN $\mathcal{D}$ [1].

Both $\mathcal{S}$ and $\mathcal{D}$ are granted access to the licensed spectrum, while the N RNs are not licensees. Based on the spectrum leasing strategy we improve both the throughput and energy efficiency attained by the system, where $\mathcal{S}$ invites the best RN candidate to cooperate in a manner that they both have an opportunity to transmit their buffer-content at a low total energy consumption and at their target transmit rate. In turn, all the RNs that have data in their buffer would compete for a transmission opportunity on the licensed spectrum with the proposed relay selection scheme. Finally $\mathcal{D}$ combines both the direct transmission

[1] A viable scenario would be for example one access network consuming large amount of data as the primary, while those infrequent and relatively small demanding access networks such as sensors as the secondary. Both these two access networks can have the same "hub" for connecting with the core network, but they belong to different traffic.

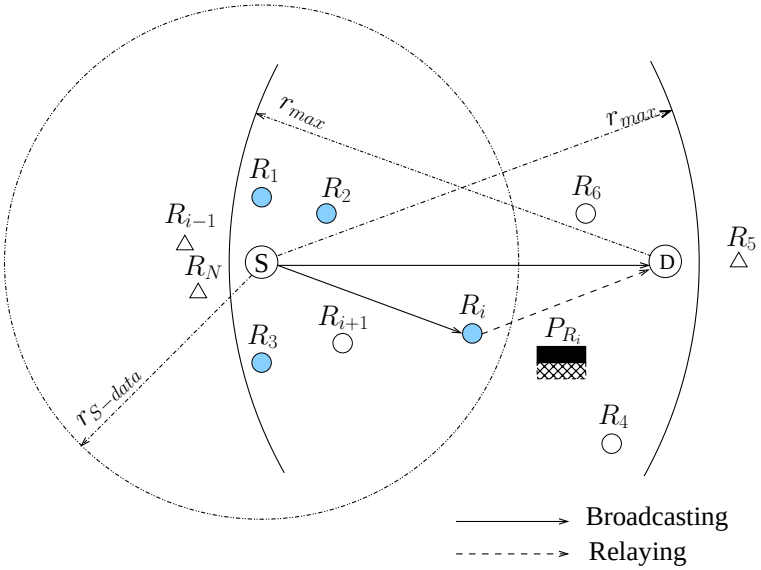

FIGURE 4.1: The cooperative topology consists of one source $\mathcal{S}$, one destination $\mathcal{D}$ and a total of N relays $\mathcal{R} = \{\mathcal{R}_1, \ldots, \mathcal{R}_N\}$.

from $\mathcal{S}$ and the superposition-coded relayed transmission from the best RN for the sake of achieving the higher integrate transmit rate of SN's data.

4.2.2 Physical Layer Model

► ***Channel Model***: all the channels involved are assumed to undergo quasi-static Rayleigh fading, hence the complex-valued fading envelope remains constant during a transmission burst, while it is faded independently between the consecutive transmission bursts. Here we define a transmission burst as a single transmission attempt which begins with a new Request-To-Send (RTS)/Clear-To-Send (CTS) signalling exchange, excluding any subsequent non-cooperative retransmission attempts [2]. Furthermore, the duplex bi-directional channels between a pair of actively communicating nodes are assumed to be identical within a given transmission burst, while the channels of any of the remaining links are independent.

► ***Wireless Environment***: we consider the effects of the free-space pathloss that is modelled by $\rho = \boldsymbol{\lambda}^2/16\pi^2 d^\eta$ [115], where $\boldsymbol{\lambda}$ represents the wave-length, d is the transmitter-to-receiver distance and η denotes the pathloss exponent, which is set to $\eta = 2$. The noise at all the receivers is assumed to be Additive White Gaussian Noise (AWGN) with zero mean and unit variance.

► ***Information Knowledge***: we assume perfect channel estimation for all nodes concerning their own channels, but no knowledge is assumed concerning the remaining links.

[2]The retransmissions, which begin with a new RTS/CTS message exchange, are referred to as non-cooperative transmission.

Furthermore, the nodes' own position information is assumed to be perfectly known at each node. Moreover, the control messages are assumed to be correctly received.

► ***Power Constraint***: all nodes are assumed to be limited to the same maximum transmit power P_{max}.

► ***RN's Behaviour***: the RN which is selected as the best RN for providing cooperative transmission assistance for $\mathcal{S}$ jointly encodes both the source's as well as its own data by using superposition coding and forwards this superposition-coded data to $\mathcal{D}$.

► ***DN's Behaviour***: after receiving the superposition-coded data, $\mathcal{D}$ relies on SIC [173] for separating the source's and the relay's data and then proceeds by retrieving the source data by appropriately combining the direct and the relayed components.

► ***Outage Probability***: when user i transmits data to user j at transmit power P_t, an outage occurs if the transmit rate $R_{i,j}$ is higher than the instantaneous capacity of the channel between these two users. Hence, the outage probability of link $i \rightarrow j$ may be characterized by [115]:

$$\begin{aligned}\mathbb{P}_{out,ij} &= \mathbb{P}\{\log_2(1+\frac{\rho_{i,j}|h_{i,j}|^2 P_t}{P_N}) < R_{i,j}\} \\ &= 1-\exp[-\frac{(2^{R_{i,j}}-1)P_N}{\rho_{i,j}P_t}],\end{aligned} \tag{4.1}$$

where $|h_{i,j}|$ denotes the magnitude of the flat Rayleigh channel between node i and node j, while P_N is the power of the AWGN, while $\rho_{i,j}$ is the free-space pathloss between node i and node j. Likewise, $\overline{\mathbb{P}_{out,ij}}$ denotes the probability of successful transmission between node i and node j.

4.2.3 The 'Win-Win' Cooperative MAC Protocol

Let us now briefly describe our previously proposed three-phase WW cooperative MAC protocol [55] of Section 3.3, which distributively selects the best RN from N RN candidates.

4.2.3.1 Phase I: Initialization

Before $\mathcal{S}$ transmits any data frame, it issues a Request-To-Send (RTS) message to $\mathcal{D}$ at the maximum transmission power P_{max}, as shown in Fig 4.2. Provided that $\mathcal{D}$ receives the RTS message correctly, it replies with a Clear-To-Send (CTS) message employing the same transmission power P_{max}. The instantaneous transmission ranges of SNs are illustrated in Fig 4.1. Any RNs in the set $\mathcal{R}$, which can over-hear both the RTS and CTS messages will be

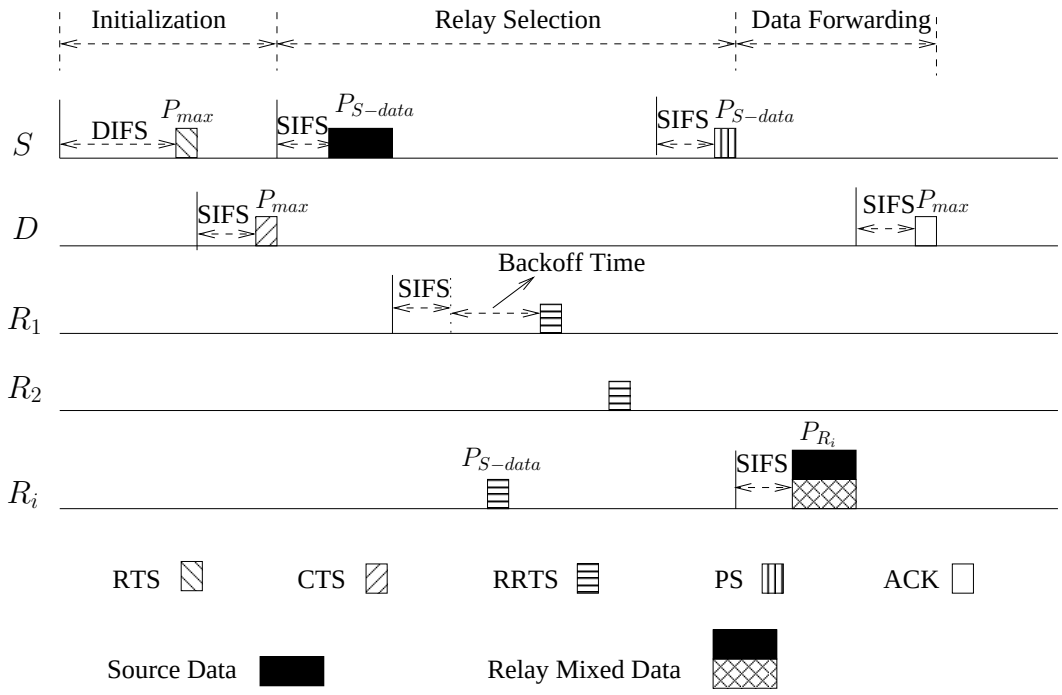

FIGURE 4.2: The overall signalling procedure for the cooperative network topology of Fig 4.1. RTS: Request-To-Send; CTS: Clear-To-Send; RRTS: Relay-Request-To-Send; PS: Please-Send; ACK: Acknowledgement; DIFS: Distributed Interframe Space; SIFS: Short Interframe Space.

aware of the imminently forthcoming transmission. Hence, these RNs - which are denoted by filled or hollow circles in Fig 4.1 - form a potential cooperative RN set $\mathcal{R}_c \subset \mathcal{R}$.

4.2.3.2 Phase II: Relay Selection

Following the initialisation phase, the RN selection procedure is constituted by a data transmission and two beacon message exchanges, as detailed below.

4.2.3.2.1 Step I: Invitation for Cooperation Following a successful RTS/CTS signalling exchange, $\mathcal{S}$ broadcasts its data frame at a *reduced* power of $P_{\mathcal{S}-data}$, simultaneously indicating its transmit rate requirement of $\alpha C_{\mathcal{S},\mathcal{D}}^{max}(\alpha > 1)$ that the potential relays should help to achieve, as seen in Fig 4.2. To elaborate a little further, α is the ratio of the desired and affordable transmit rate termed as the 'factor of greediness' of the source, while $C_{\mathcal{S},\mathcal{D}}^{max}$ is the maximum achievable rate of the Source-to-Destination (SD) link, which can be formulated as $C_{\mathcal{S},\mathcal{D}}^{max} = \log_2(1 + \frac{\rho_{\mathcal{S},\mathcal{D}}|h_{\mathcal{S},\mathcal{D}}|^2 P_{max}}{P_N})$. When α is higher than unity, the source data cannot be successfully transmitted to $\mathcal{D}$. However, $\mathcal{D}$ will store this data frame and combines it with the next data frame to achieve an increased aggregated throughput.

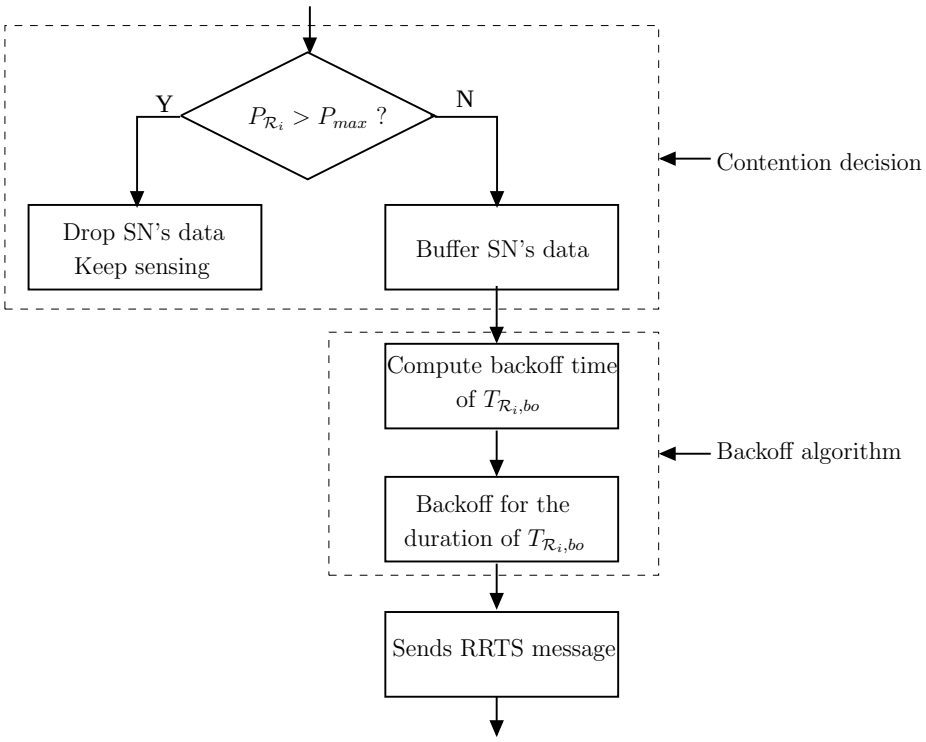

FIGURE 4.3: The flow chart of the "Contention Decision" and "Backoff Algorithm" operated by the RNs during the relay selection phase of the proposed signalling procedure of Fig 4.2 in the cooperative network topology of Fig 4.1.

4.2.3.2.2 Step II: Contend for Cooperation If an unlicensed RN $\mathcal{R}_i \in \mathcal{R}_c$ receives a data frame from $\mathcal{S}$ correctly, it calculates the transmit power $P^{\mathcal{S}}_{\mathcal{R}_i}$ required for satisfying the transmit rate requirement of SN, namely $\alpha C^{max}_{\mathcal{S},\mathcal{D}}$. Being naturally selfish, $\mathcal{R}_i$ also reserves a certain fraction of $\beta C^{max}_{\mathcal{R}_i,\mathcal{D}}(0 < \beta < 1)$ of the Relay-to-Destination (RD) channel capacity for conveying its own traffic, where β is the relay's factor of greediness and $C^{max}_{\mathcal{R}_i,\mathcal{D}}$ is given by: $C^{max}_{\mathcal{R}_i,\mathcal{D}} = \log_2(1 + \frac{\rho_{\mathcal{R}_i,\mathcal{D}}|h_{\mathcal{R}_i,\mathcal{D}}|^2 P_{max}}{P_N})$. Hence, $\mathcal{R}_i$ also has to determine the specific transmit power $P^{\mathcal{R}}_{\mathcal{R}_i}$ required for guaranteeing a throughput of $\beta C^{max}_{\mathcal{R}_i,\mathcal{D}}$.

Contention Decision: As shown in Fig 4.3, if the total transmit power $P_{\mathcal{R}_i} = P^{\mathcal{S}}_{\mathcal{R}_i} + P^{\mathcal{R}}_{\mathcal{R}_i}$ is higher than P_{max}, $\mathcal{R}_i$ has to give up contending for the cooperative opportunity and drop this source's data frame. Then it keeps on sensing the channel. On the other hand, if $P_{\mathcal{R}_i}$ required for successfully sending the the superposition-coded data to $\mathcal{D}$ does not exceed the maximum transmit power P_{max}, $\mathcal{R}_i$ would send Relay-Request-To-Send (RRTS) message to $\mathcal{S}$ after waiting its backoff time for the sake of contending for the cooperation opportunity, as seen in Fig 4.3.

Backoff Algorithm: As seen in Fig 4.2 and Fig 4.3, before issuing the RRTS message, the RN $\mathcal{R}_i$ has to wait for a SIFS interval and for a subsequent back-off time duration of $T_{\mathcal{R}_i,bo}$,

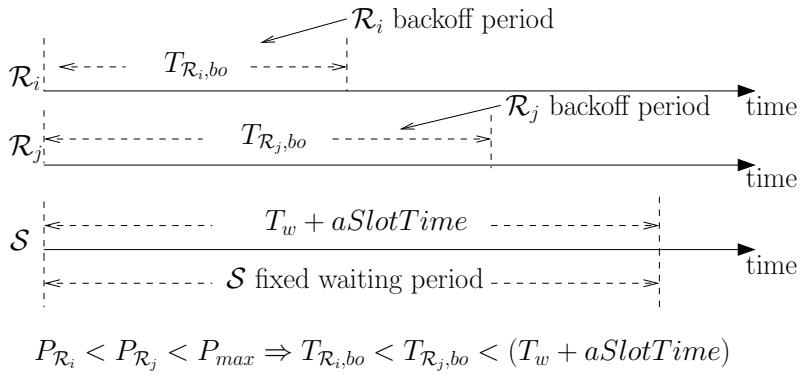

FIGURE 4.4: The backoff time of each RN and the fixed waiting period of $\mathcal{S}$ calculated in term of the backoff algorithm of Fig 4.3 during the relay selection phase of Fig 4.2 in the cooperative network topology of Fig 4.1.

which is defined as:

$$T_{\mathcal{R}_i,bo} = \varphi_{\mathcal{R}_i} T_w, \tag{4.2}$$

where $T_w = CWmin \cdot aSlotTime$ [3], where $CWmin$ is the minimum contention window (CW) duration specified in the IEEE802.11 standards [106]. The coefficient $\varphi_{\mathcal{R}_i}$ is defined as $\varphi_{\mathcal{R}_i} = P_{\mathcal{R}_i}/P_{max}$. In each RN selection phase, $\mathcal{S}$ has to wait for a fixed period of $(T_w + aSlotTime)$ duration to collect the RRTS messages of the potential candidate RNs. Fig 4.4 shows the length of both the backoff duration of different RNs and the fixed waiting period of $\mathcal{S}$. Since the value of $P_{\mathcal{R}_i}$ promised by the candidate RN $\mathcal{R}_i$ is always lower than P_{max}, the back-off time allocated to $\mathcal{R}_i$ will not exceed the source's fixed waiting duration of $(T_w + aSlotTime)$. Hence, $\mathcal{S}$ is not required to identify the most recent RRTS message, after which it should stop waiting and should commence transmitting its response to the best RN, because all the candidate RNs may issue their RRTS messages before $\mathcal{S}$ stops waiting for the responses. According to the proposed backoff scheme, the specific candidate RN, which is capable of promising a reduced transmit power may wait for a shorter backoff time. Hence, the particular candidate RN promising the lowest transmit power can first send its RRTS message to $\mathcal{S}$. Bearing in mind that some of the RNs cannot overhear the RRTS messages received from other candidate relays, we arranged for all the candidate RNs to send RRTS messages to $\mathcal{S}$, which allows $\mathcal{S}$ to select the best RN according to the responses received from them.

4.2.3.2.3 Step III: Accept for Cooperation As shown in both Fig 4.2 and Table 4.2, after waiting for a fixed duration of $(T_w + aSlotTime)$, $\mathcal{S}$ selects the transmitter of that

[3] In the IEEE 802.11 standard [106], aSlotTime consists of the time required to physically sense the medium and to declare the channel as "clear", plus the MAC processing delay, the propagation delay, and the "receiver/transmitter turn-around time" which is the time required for the physical layer to change from receiving to transmitting at the start of the first bit.

particular RRTS message, which was first received correctly and declares it to be the best relay without any further processing of other RRTS messages, if $\mathcal{S}$ receives RRTS messages from the candidate RNs. In turn, $\mathcal{S}$ responds to the best relay $\mathcal{R}_i$ by sending a Please-Send (PS) message, as shown in both Fig 4.2 and Table 4.2.

TABLE 4.2: The procedure of source during phase III of the proposed signalling procedure of Fig 4.2 which is designed for the cooperative network topology of Fig 4.1.

```
0:  if fixed waiting duration of T_w + aSlotTime times out
1:      if receive RRTS messages from the candidate RNs
2:          sends PS message to the transmitter associated with
            the first correctly received RRTS message
3:      else
4:          calculates the transmit power P^(II)_{S,D} for guaranteeing
            source's expected transmit rate of αC^max_{S,D}
5:          if P^(II)_{S,D} > P_max
6:              opts for P_max to directly sends its data to the destination without relaying
7:          else
8:              opts for P^(II)_{S,D} to directly sends its data to the destination without relaying
9:  else
10:     waiting for RRTS message
```

4.2.3.3 Phase III: Data Forwarding

In this phase, if $\mathcal{S}$ successfully selects RN $\mathcal{R}_i$ as the best RN, $\mathcal{R}_i$ encodes both the source's and its own data with the aid of superposition coding and will forward the superimposed SR data frame to $\mathcal{D}$ at its pre-calculated transmission power of $P_{\mathcal{R}_i}$ after a SIFS period, as seen in Fig 4.2. Finally, at the DN, the classic Automatic Repeat reQuest (ARQ) procedure will be initiated, when successfully extracting the SN's data from the superposition-coded relayed composite signal with the aid of SIC as well as combining the SN's relayed replica with its most recent direct transmission.

If none of the RNs compete for a transmission opportunity, $\mathcal{S}$ directly sends its data to $\mathcal{D}$ without any relaying [4] using either the specific transmit power of $P^{(II)}_{\mathcal{S},\mathcal{D}}$, which is capable of guaranteeing the expected transmit rate of $\alpha C^{max}_{\mathcal{S},\mathcal{D}}$ or failing that, it opts for using the maximum transmit power of P_{max}, which may achieve a lower aggregate transmit rate, as seen in Table 4.2.

[4]We called this retransmission as "cooperative retransmission". The channel fading envelop remains constant during the previous source's broadcasting and this cooperative retransmission. However, the "non-cooperative retransmission" which starts with a new RTS/CTS signalling exchange is considered as independent transmission burst, as mentioned in Section 4.2.

4.3 Stability of the Queues

Before analyzing the stability of the queues in the above system, we describe the queueing model of the cooperative spectrum leasing system, which supports a licensed single transmission pair and exploits our WW protocol.

4.3.1 Queueing Model

Based on our distributed WW cooperative MAC protocol, we consider a cooperative queueing system, where the unlicensed RNs have two queues, namely one for storing the SN's and one for its own data packet, as shown in Fig 4.5. In order to simplify the analysis of system stability, we made the following assumptions:

- We assume that all the nodes have infinite-capacity buffers for storing their incoming packets and all the control messages are error-free short frames.
- Each SN's data packet is transmitted within a specific time-slot (TS). Each TS begins with a new RTS/CTS signalling exchange and covers all three phases of our distributed WW cooperative protocol, namely the initialisation phase, the relay selection phase as well as the data forwarding phase, as seen in Fig 4.2. $\mathcal{S}$ has to transmit a RTS message at the beginning of each TS if it has data to send. Hence, we assume a network-wide synchronisation. According to the proposed distributed WW cooperative protocol, $\mathcal{S}$ first uses a specific segment of a TS to broadcast its data. Then the SN leases the rest of the TS to the best RN, whilst aiming for achieving its own target transmit rate. If no RNs offer cooperation for $\mathcal{S}$, the SN will use the rest of the TS to retransmit its own original data.
- The packet arrival processes at each node are assumed to be independent and stationary with a mean of $\lambda_{\mathcal{S}}$ packets per slot for $\mathcal{S}$ and $\lambda_{\mathcal{R}_i}$ packets per slot for RN $\mathcal{R}_i$.

The stability of a communication network is one of its fundamental performance measures. A network can be considered to be stable with a certain arrival rate vector, if all the queues are stable, which implies that the length of all the queues remains finite. According to Loynes' theorem [134], if the arrival and departure processes of a queueing system are stationary, the i_{th} queue is stable, when the average arrival rate λ_i is less than the average departure rate μ_i ($\lambda_i < \mu_i$). Based on our assumptions, the stability of the queues may be verified with the aid of Loynes' theorem.

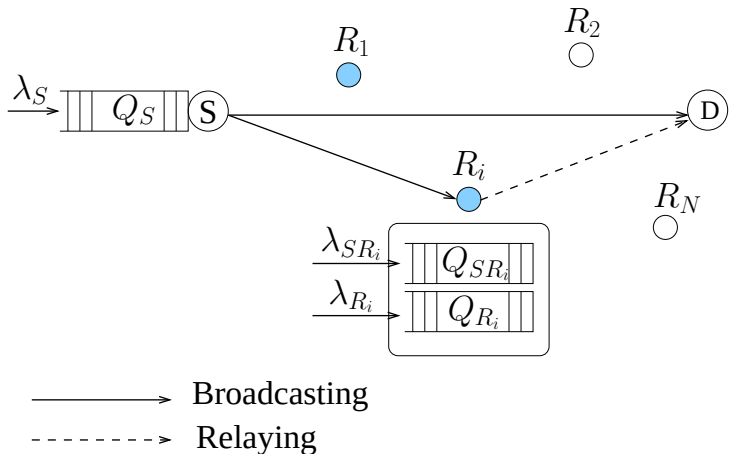

FIGURE 4.5: The queueing model of the cooperative spectrum leasing system relying on our 'win-win' cooperative MAC protocol of Fig 4.2-Fig 4.4 and Table 4.2.

4.3.2 Stability of the Source Node's Queue

As seen in Table 4.2, during the data forwarding phase, the source's data may be successfully delivered to the DN destination by the best RN or the SN in three different scenarios:

- When $\mathcal{S}$ correctly receives the RRTS message, its data is forwarded to $\mathcal{D}$ by the best RN. The aggregate transmit rate of $\mathcal{S}$ is capable of achieving the source's target transmit rate in this scenario.
- When $\mathcal{S}$ does not receive any RRTS messages, it may directly retransmit its data to $\mathcal{D}$ at the power of $P_{\mathcal{S},\mathcal{D}}^{(II)}$, namely at the power required by $\mathcal{S}$ for guaranteeing its target transmit rate on its own in isolation, if $P_{\mathcal{S},\mathcal{D}}^{(II)}$ does not exceed the maximum transmit power of P_{max}. The aggregate transmit rate of the source is also equal to the source's target rate in this scenario.
- When $\mathcal{S}$ does not receive any RRTS messages and it can not afford the transmit power $P_{\mathcal{S},\mathcal{D}}^{(II)}$ required for achieving its target transmit rate, namely $P_{\mathcal{S},\mathcal{D}}^{(II)} > P_{max}$, $\mathcal{S}$ may directly retransmit its data to $\mathcal{D}$ at the power of P_{max} without relaying. However, the aggregate transmit rate of the source is lower than the source's target rate, because P_{max} is lower than $P_{\mathcal{S},\mathcal{D}}^{(II)}$.

Based on the above discussions, the maximum departure rate at $\mathcal{S}$ consists of three components:

- the departure rate $\mu_{\mathcal{S},coop}$ achieved at $\mathcal{S}$ with the aid of cooperation;
- the departure rate $\mu_{\mathcal{S},non}^{R_{coop}}$ at $\mathcal{S}$, which was achieved by non-cooperative transmission, where $\mathcal{S}$ directly retransmits its data at the transmit power of $P_{\mathcal{S},\mathcal{D}}^{(II)}$ for achieving its target transmit rate, when $P_{\mathcal{S},\mathcal{D}}^{(II)} \leq P_{max}$;

- the departure rate $\mu_{\mathcal{S},non}^{R_{non}}$ achieved at $\mathcal{S}$ with the aid of non-cooperative transmissions from $\mathcal{S}$ to $\mathcal{D}$ at a power of P_{max}, when $\mathcal{S}$ cannot satisfy its transmit rate requirement in isolation under the constraint of the maximum transmit power, namely under $P_{\mathcal{S},\mathcal{D}}^{(II)} > P_{max}$.

More explicitly, the maximum departure rate at $\mathcal{S}$ is formulated as:

$$\mu_{\mathcal{S}}^{max} = \mu_{\mathcal{S},coop} + \mu_{\mathcal{S},non}^{R_{coop}} + \mu_{\mathcal{S},non}^{R_{non}}. \tag{4.3}$$

Let us now consider each term in detail.

4.3.2.1 Departure Rate of $\mu_{\mathcal{S},coop}$

According to our distributed WW cooperative MAC protocol, $\mathcal{S}$ may successfully select the best RN if and only if at least one of the RNs is capable of both correctly receiving the SN's data frame and of successfully forwarding the superposition-coded data to $\mathcal{D}$ under the power constraint of P_{max}. Hence, the average cooperative departure rate at $\mathcal{S}$ may be written as:

$$\mu_{\mathcal{S},coop} = \mathbb{E}\{\mu_{\mathcal{S},coop}(r)\} = \mathbb{E}\left\{1 - \prod_{i=1}^{N}\left[1 - \overline{\mathbb{P}_{out,\mathcal{SR}_i}(r)} \cdot \mathbb{P}_{suc,\mathcal{R}_i\mathcal{D}}(r)\right]\right\}, \tag{4.4}$$

where $\mu_{\mathcal{S},coop}(r)$ denotes the average departure rate at $\mathcal{S}$ achieved by the cooperation, when the SN's target transmit rate equals r. The average departure rate of $\mu_{\mathcal{S},coop}$ at $\mathcal{S}$ may be expressed by taking the expectation of $\mu_{\mathcal{S},coop}(r)$ for the source's target transmit rate r. Let us denote the probability of successful transmission from $\mathcal{S}$ to RN $\mathcal{R}_i$ by $\overline{\mathbb{P}_{out,\mathcal{SR}_i}(r)}$ when the source's target transmit rate is r. $\mathbb{P}_{suc,\mathcal{R}_i\mathcal{D}}(r)$ represents the probability that the RN $\mathcal{R}_i$ is capable of successfully relaying the superposition-coded data to $\mathcal{D}$ at the transmit power $P_{\mathcal{R}_i}(r)$, under the power constraint of P_{max}. Explicitly, the transmit power $P_{\mathcal{R}_i}(r)$ does not exceed P_{max}, when the SN's target transmit rate is equal to r. Let us denote furthermore the number of unlicensed RNs by N. As discussed above, if at least one of the RNs can correctly receive the source's data and additionally it successfully relays the superposition-coded data, then the source's data will be successfully delivered with the aid of cooperative transmission.

Probability of $\mathbb{P}_{out,\mathcal{SR}_i}(r)$***:*** Given the channel gain $|h_{\mathcal{S},\mathcal{D}}|^2$ of the SD link, the SN's target transmit rate of r may be written as $r = \alpha C_{\mathcal{S},\mathcal{D}}^{max}$. Hence, according to Eq (4.1), the outage probability between $\mathcal{S}$ and $\mathcal{R}_i$ is given by:

$$\mathbb{P}_{out,\mathcal{SR}_i}(r) = \mathbb{P}\{r > C_{\mathcal{SR}_i}\} = 1 - \exp\left[-\frac{(2^r - 1) \cdot P_N}{\rho_{\mathcal{S},\mathcal{R}_i} \cdot P_{\mathcal{S}-data}}\right], \tag{4.5}$$

where $C_{\mathcal{SR}_i} = \log_2(1 + \frac{\rho_{\mathcal{S},\mathcal{R}_i}|h_{\mathcal{S},\mathcal{R}_i}|^2 P_{\mathcal{S}-data}}{P_N})$ denotes the channel capacity of the $\mathcal{S}$ and $\mathcal{R}_i$ link.

Probability of $\mathbb{P}_{suc,\mathcal{R}_i\mathcal{D}}(r)$***:*** Based on the maximum transmit power constraint, RN $\mathcal{R}_i$ is capable of successfully forwarding the superposition-coded data to $\mathcal{D}$ if and only if the required transmit power of $P_{\mathcal{R}_i}$ does not exceeds P_{max}. Hence, when the source's target transmit rate is r, the probability of successful transmission from $\mathcal{R}_i(r)$ to $\mathcal{D}$ may be written as:

$$\mathbb{P}_{suc,\mathcal{R}_i\mathcal{D}}(r) = \mathbb{P}\{P_{\mathcal{R}_i}(r) < P_{max}\}. \tag{4.6}$$

According to our distributed WW cooperative MAC protocol, when superposition coding is used at the RN, while SIC and frame combining are employed at $\mathcal{D}$, the transmit power $P_{\mathcal{R}_i}$ required for successfully delivering the superposition-coded composite data is given by [36]

$$P_{\mathcal{R}_i}(r) = \gamma^{\mathcal{S}}_{\mathcal{R}_i}(r)\left[\frac{P_N}{\rho_{\mathcal{R}_i,\mathcal{D}}|h_{\mathcal{R}_i,\mathcal{D}}|^2} + \frac{(2^{\beta C^{max}_{\mathcal{R}_i\mathcal{D}}} - 1)P_N}{\rho_{\mathcal{R}_i,\mathcal{D}}|h_{\mathcal{R}_i,\mathcal{D}}|^2}\right] + \frac{(2^{\beta C^{max}_{\mathcal{R}_i\mathcal{D}}} - 1)P_N}{\rho_{\mathcal{R}_i,\mathcal{D}}|h_{\mathcal{R}_i,\mathcal{D}}|^2}, \tag{4.7}$$

where $\gamma^{\mathcal{S}}_{\mathcal{R}_i}(r)$ represents the Signal-to-Noise-Ratio (SNR) of the SN's data frame at $\mathcal{D}$, which is the minimum to be guaranteed by the RN during the data forwarding phase for the sake of satisfying the source's transmit rate requirement. The value of $\gamma^{\mathcal{S}}_{\mathcal{R}_i}(r)$ is broadcast along with the source's data, when the source invites the secondary users to cooperate.

Proposition 3.1: Given the Channel Sate Information (CSI) and the free-space pathloss $(h_{\mathcal{S},\mathcal{D}}, \rho_{\mathcal{S},\mathcal{D}})$ of the SD link, as well as the nodes' factor of greediness (α, β), which are subject to the condition of $\alpha \in (1, +\infty)$ and $\beta \in (0, 1)$, the transmit power $P_{\mathcal{R}_i}(r)$ of $\mathcal{R}_i$ required for successfully delivering the superposition-coded composite data is a decreasing function of $\rho_{\mathcal{R}_i,\mathcal{D}}|h_{\mathcal{R}_i,\mathcal{D}}|^2$ for different RNs. For RN $\mathcal{R}_i$, $P_{\mathcal{R}_i}(r)$ is a decreasing function of $|h_{\mathcal{R}_i,\mathcal{D}}|^2$. See Appendix B.1 for the proof.

Based on Proposition 3.1, $\mathbb{P}_{suc,\mathcal{R}_i\mathcal{D}}(r)$ may be expanded as:

$$\begin{aligned}\mathbb{P}_{suc,\mathcal{R}_i\mathcal{D}}(r) &= \mathbb{P}\{P_{\mathcal{R}_i}(r) < P_{max}\} \\ &= \mathbb{P}\{|h_{\mathcal{R}_i\mathcal{D}}|^2 > H_{\mathcal{R}_i,max}(r)\} \\ &= \exp\{-H_{\mathcal{R}_i,max}(r)\},\end{aligned} \tag{4.8}$$

where $H_{\mathcal{R}_i,max}(r)$ denotes the channel gain of the RD link between $\mathcal{R}_i$ and $\mathcal{D}$, when the transmit power $P_{\mathcal{R}_i}(r)$ required for successfully conveying the superposition-coded data reaches its maximum power of P_{max} and the SN's target transmit rate is r. Based on our

analysis above, we can calculate the departure rate at $\mathcal{S}$, which relies on cooperation.

4.3.2.2 Departure Rate of $\mu_{\mathcal{S},non}^{R_{coop}}$

As seen in Table 4.2, if $\mathcal{S}$ does not receive any RRTS message from the candidate RNs, it may retransmit its data to $\mathcal{D}$ at the transmit power of $P_{\mathcal{S},\mathcal{D}}^{(II)}$ for the sake of achieving the target transmit rate, provided that $P_{\mathcal{S},\mathcal{D}}^{(II)}$ does not exceed the maximum transmit power P_{max}. Hence, the departure rate of $\mathcal{S}$ in this scenario may be expressed as:

$$\mu_{\mathcal{S},non}^{R_{coop}} = \mathbb{E}\left\{\mathbb{P}\{T_{\mathcal{S}}^{(II)}(r)\} - \sum_{i=1}^{N}\mathbb{P}\{T_{\mathcal{R}_i}(r), T_{\mathcal{S}}^{(II)}(r)\}\right\}, \tag{4.9}$$

where $\mathbb{P}\{T_{\mathcal{S}}^{(II)}(r)\}$ denotes the probability of the event that $\mathcal{S}$ is capable of guaranteeing its target transmit rate r on its own in isolation, regardless, whether a best RN was selected or not. Hence, the probability $\mathbb{P}\{T_{\mathcal{S}}^{(II)}(r)\}$ consists of two components:

1. when the best RN was selected for relaying the SN's data, $\mathcal{S}$ also becomes capable of satisfying its transmit rate requirement on its own in isolation;
2. when no RN is capable of providing cooperative transmission assistance for $\mathcal{S}$, $\mathcal{S}$ is capable of guaranteeing its target transmit rate r by directly retransmitting its data at a power of $P_{\mathcal{S},\mathcal{D}}^{(II)}$ under the constraint of the maximum transmit power P_{max}.

Still considering Eq (4.9), $T_{\mathcal{R}_i}(r)$ represents the event that RN $\mathcal{R}_i$ is selected as the best RN, when the SN's target transmit rate is r. Hence, the probability of $\mathbb{P}\{T_{\mathcal{R}_i}(r), T_{\mathcal{S}}^{(II)}(r)\}$ represents the joint probability of the event that $\mathcal{S}$ is capable of guaranteeing its target transmit rate r by directly retransmitting its data to $\mathcal{D}$ and simultaneously $\mathcal{R}_i$ is granted the transmission opportunity to forward the superposition-coded data to $\mathcal{D}$. As observed in Fig 4.6, the left circle represents the probability of $P_{\mathcal{S},\mathcal{D}}^{(II)}$, while the right circle denotes the probability of $\mathbb{P}\{T_{\mathcal{R}_i}(r)\}$. The overlap region, which is filled with the horizontal lines in Fig 4.6 is the probability of $\mathbb{P}\{T_{\mathcal{R}_i}(r), T_{\mathcal{S}}^{(II)}(r)\}$, which can be written as [196, 197]:

$$\mathbb{P}\{T_{\mathcal{R}_i}(r), T_{\mathcal{S}}^{(II)}(r)\} = \mathbb{P}\{T_{\mathcal{R}_i}(r)\} \cdot \mathbb{P}\{T_{\mathcal{S}}^{(II)}(r)|T_{\mathcal{R}_i}(r)\}. \tag{4.10}$$

Hence, as seen in Fig 4.6 the probability of the event that $\mathcal{S}$ is capable of guaranteeing its target rate r on its own in isolation, when no best RN was selected may be expressed by subtracting the probability that both $\mathcal{S}$ and the best RN can guarantee the target rate r from the probability of $\mathbb{P}\{T_{\mathcal{S}}^{(II)}(r)\}$, as shown in Eq (4.9). Let us postpone our discussion on the probability of $\mathbb{P}\{T_{\mathcal{R}_i}(r)\}$ until the following section and proceed with the derivation of the rest of the probabilities as follows.

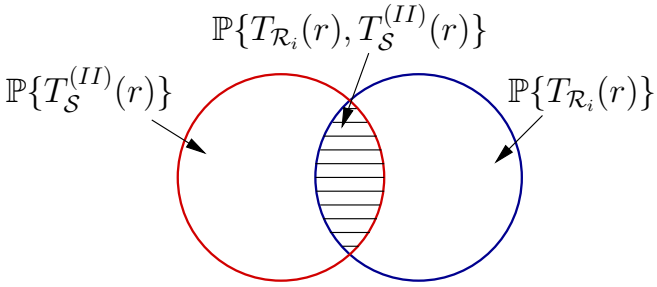

FIGURE 4.6: The relationship of $\mathbb{P}\{T_{\mathcal{S}}^{(II)}(r)\}$ and $\mathbb{P}\{T_{\mathcal{R}_i}(r)\}$ as well as $\mathbb{P}\{T_{\mathcal{R}_i}(r), T_{\mathcal{S}}^{(II)}(r)\}$ in Eq (4.9) and Eq (4.10) for charaterizing the source's operation when its rate requirement can be satisfied during the phase III of the proposed MAC protocol of Fig 4.2.

Probability of $\mathbb{P}\{T_{\mathcal{S}}^{(II)}(r)\}$***:*** Based on the power constraint of P_{max} and perfect CSI, $\mathcal{S}$ is capable of guaranteeing its target transmit rate r by directly retransmitting its data to $\mathcal{D}$ at the power of $P_{\mathcal{S},\mathcal{D}}^{(II)}(r)$ if and only if the retransmission power $P_{\mathcal{S},\mathcal{D}}^{(II)}(r)$ does not exceed the maximum transmit power P_{max}, as seen in Table 4.2. Hence, the probability of $\mathbb{P}\{T_{\mathcal{S}}^{(II)}(r)\}$ may be formulated as:

$$\mathbb{P}\{T_{\mathcal{S}}^{(II)}(r)\} = \mathbb{P}\{P_{\mathcal{S},\mathcal{D}}^{(II)}(r) < P_{max}\}. \tag{4.11}$$

Based on the perfect CSI and on our frame combining technique, the retransmission power of $P_{\mathcal{S},\mathcal{D}}^{(II)}(r)$ required for guaranteeing the source's target transmit rate r may be formulated by $P_{\mathcal{S},\mathcal{D}}^{(II)}(r) = \frac{(2^r-1)P_N}{\rho_{\mathcal{S},\mathcal{D}}|h_{\mathcal{S},\mathcal{D}}|^2} - P_{\mathcal{S}-data}$ [36].

Proposition 3.2: Given the CSI and the free-space pathloss $(h_{\mathcal{S},\mathcal{D}}, \rho_{\mathcal{S},\mathcal{D}})$ of the SD link, as well as the nodes' factor of greediness (α, β), which are subject to the condition of $\alpha \in (1, +\infty)$ and $\beta \in (0, 1)$, the transmit power $P_{\mathcal{S},\mathcal{D}}^{(II)}(r)$ required for successfully delivering the SN's data frame is an increasing function of $|h_{\mathcal{SD}}|^2$. See Appendix B.2 for the proof.

Based on Proposition 3.2, the probability that $\mathcal{S}$ is capable of guaranteeing its target transmit rate r on its own in isolation by retransmitting its data to $\mathcal{D}$ is given by

$$\mathbb{P}\{T_{\mathcal{S}}^{(II)}(r)\} = \mathbb{P}\{|h_{\mathcal{S},\mathcal{D}}|^2 < H_{\mathcal{SD},max}^{(II)}(r)\} = 1 - \exp\{-H_{\mathcal{SD},max}^{(II)}(r)\}, \tag{4.12}$$

where $H_{\mathcal{SD},max}^{(II)}(r)$ denotes the channel gain of the SD link, when $\mathcal{S}$ retransmits its data to $\mathcal{D}$ at the maximum transmit power P_{max} for the sake of achieving its target transmit rate r.

Probability of $\mathbb{P}\{T_{\mathcal{S}}^{(II)}(r)|T_{\mathcal{R}_i}(r)\}$***:*** To elaborate on $\mathbb{P}\{T_{\mathcal{S}}^{(II)}(r)|T_{\mathcal{R}_i}(r)\}$ a little further, we fomulate the following proposition.

Proposition 3.3: Given the nodes' factors of greediness (α, β), which are subject to the

condition of $\alpha \in (1, +\infty)$ and $\beta \in (0, 1)$, when RN $\mathcal{R}_i$ is selected as the best RN, the channel gain $H_{\mathcal{SD}}$ of the SD link has to be subject to the following two conditions:

$$(i) \qquad Y(H_{\mathcal{SD}}) < \Omega_{\mathcal{SR}_i}, \tag{4.13}$$

$$(ii) \qquad Z(H_{\mathcal{SD}}) < \Omega_{\mathcal{R}_i\mathcal{D}}^{(1-\beta)}, \tag{4.14}$$

where we have:

$$\begin{aligned}
Y(x) &= (1+\nu x)^{\alpha}, \\
Z(x) &= (1+\nu x)^{\alpha} - \nu x, \\
\Omega_{\mathcal{SR}_i} &= 1 + \frac{\rho_{\mathcal{S},\mathcal{R}_i} H_{\mathcal{S},\mathcal{R}_i} P_{\mathcal{S}-data}}{P_N} \\
\Omega_{\mathcal{R}_i\mathcal{D}} &= 1 + \frac{\rho_{\mathcal{R}_i\mathcal{D}} H_{\mathcal{R}_i\mathcal{D}} P_{max}}{P_N}, \\
\nu &= \frac{\rho_{\mathcal{S},\mathcal{D}} P_{max}}{P_N}, \\
H_{\mathcal{S},\mathcal{D}} &= |h_{\mathcal{S},\mathcal{D}}|^2, \\
H_{\mathcal{S},\mathcal{R}_i} &= |h_{\mathcal{S},\mathcal{R}_i}|^2, \\
H_{\mathcal{R}_i,\mathcal{D}} &= |h_{\mathcal{R}_i,\mathcal{D}}|^2.
\end{aligned}$$

Both $Y(x)$ and $Z(x)$ are monotonically increasing functions of x. See Appendix B.3 for the proof.

Based on Proposition 3.3 and Eq (4.12), the conditional probability of $\mathbb{P}\{T_{\mathcal{S}}^{(II)}(r)|T_{\mathcal{R}_i}\}$ introduced in Eq (4.9) may be formulated as:

$$\mathbb{P}\{T_{\mathcal{S}}^{(II)}|T_{\mathcal{R}_i}(r)\} = \mathbb{P}\{H_{\mathcal{S},\mathcal{D}} < H_{\mathcal{SD},max}^{(II)} | Y(H_{\mathcal{SD}}) < \Omega_{\mathcal{SR}_i}, Z(H_{\mathcal{SD}}) < \Omega_{\mathcal{R}_i\mathcal{D}}^{(1-\beta)}\}. \tag{4.15}$$

Since both $Y(x)$ and $Z(x)$ are increasing functions of x, $H_{\mathcal{S},\mathcal{D}}$ of the SD link must be lower than $H_{\mathcal{SD},max}^{(II)}$, if either $Y(H_{\mathcal{SD},max}^{(II)})$ is higher than $\Omega_{\mathcal{SR}_i}$ or $Z(H_{\mathcal{SD},max}^{(II)})$ is higher than $\Omega_{\mathcal{R}_i\mathcal{D}}^{(1-\beta)}$. However, if $Y(H_{\mathcal{SD},max}^{(II)})$ is lower than $\Omega_{\mathcal{SR}_i}$ and $Z(H_{\mathcal{SD},max}^{(II)})$ is lower than $\Omega_{\mathcal{R}_i\mathcal{D}}^{(1-\beta)}$, only the probability of $\mathbb{P}\{H_{\mathcal{S},\mathcal{D}} < H_{\mathcal{SD},max}^{(II)}\}$ should be counted. Hence, the probability of $\mathbb{P}\{T_{\mathcal{S}}^{(II)}(r)|T_{\mathcal{R}_i}\}$ may be written as:

$$\mathbb{P}\{T_{\mathcal{S}}^{(II)}|T_{\mathcal{R}_i}(r)\} = \mathbb{P}\{H_{\mathcal{S},\mathcal{D}} < H_{\mathcal{SD},max}^{(II)}\} \cdot \mathbb{P}\{M_{\mathcal{R}_i}^{H_{\mathcal{SD},max}^{(II)}}\} + (1 - \mathbb{P}\{M_{\mathcal{R}_i}^{H_{\mathcal{SD},max}^{(II)}}\}), \tag{4.16}$$

where we have

$$\mathbb{P}\{M_{\mathcal{R}_i}^{H_{\mathcal{SD},max}^{(II)}}\} = \mathbb{P}\{Y(H_{\mathcal{SD},max}^{(II)}) < \Omega_{\mathcal{SR}_i}\} \cdot \mathbb{P}\{Z(H_{\mathcal{SD},max}^{(II)}) < \Omega_{\mathcal{R}_i\mathcal{D}}^{(1-\beta)}\}. \tag{4.17}$$

4.3.2.3 Departure Rate of $\mu_{\mathcal{S},non}^{R_{non}}$

When considering the maximum transmit power constraint P_{max}, $\mathcal{S}$ may not be capable of affording the transmit power of $P_{\mathcal{S},\mathcal{D}}^{(II)}$ for retransmitting its data to $\mathcal{D}$ for the sake of guaranteeing the target transmit rate. Then $\mathcal{S}$ will directly retransmit its data to $\mathcal{D}$ at P_{max}. In this case, the non-cooperative departure rate at $\mathcal{S}$ may be formulated as:

$$\mu_{\mathcal{S},non}^{R_{non}} = \mathbb{P}_{\mathcal{S},noncoop} - \mathbb{P}_{\mathcal{S},noncoop}^{R_{coop}}, \tag{4.18}$$

where $\mathbb{P}_{\mathcal{S},noncoop}$ denotes the probability of the SN's transmission without cooperation, which is given by:

$$\mathbb{P}_{\mathcal{S},noncoop} = \mathbb{E}\left\{\prod_{i=1}^{N}\left[1 - \overline{\mathbb{P}_{out,\mathcal{SR}_i}(r)} \cdot .\mathbb{P}_{suc,\mathcal{R}_i\mathcal{D}}(r)\right]\right\}. \tag{4.19}$$

The second term of Eq (4.18), namely $\mathbb{P}_{\mathcal{S},noncoop}^{R_{coop}}$, denotes the probability of the SN's non-cooperative transmission, which is capable of satisfying its transmit rate requirement. Then we have:

$$\mathbb{P}_{\mathcal{S},noncoop}^{R_{coop}} = \mathbb{E}\left\{\mathbb{P}\{T_{\mathcal{S}}^{(II)}(r)\} - \sum_{i=1}^{N}\mathbb{P}\{T_{\mathcal{R}_i}(r), T_{\mathcal{S}}^{(II)}(r)\}\right\}. \tag{4.20}$$

Recall from Eq (4.3) that the total departure rate at $\mathcal{S}$ in our system is characterized by the sum of Eq (4.4), Eq (4.9) and Eq (4.18). Hence, the queue of the SN is stable, as long as we satisfy $\lambda_{\mathcal{S}} < \mu_{\mathcal{S}}^{max}$.

4.3.3 Stability of the Relay Nodes' Queue

4.3.3.1 Stability of $Q_{\mathcal{SR}_i}$

In order to support cooperative transmissions, the RN $\mathcal{R}_i$ is assumed to rely on the pair of queues $Q_{\mathcal{R}_i}$ and $Q_{\mathcal{SR}_i}$ for buffering both its own data and the SN's data, respectively, as shown in Fig 4.5. Under the power constraint of P_{max}, $\mathcal{R}_i$ will store the SN's data in $Q_{\mathcal{SR}_i}$, when the following two conditions are satisfied:

1. $\mathcal{S}$ had data to transmit at the beginning of this TS;

2. RN $\mathcal{R}_i$ was granted a transmission opportunity for conveying the superposition-coded content to $\mathcal{D}$.

Hence, the arrival rate of the SN's data at RN $\mathcal{R}_i$ is given by

$$\lambda_{\mathcal{S}\mathcal{R}_i} = \mathbb{E}\{\lambda_{\mathcal{S}\mathcal{R}_i}(r)\} = \mathbb{E}\left\{\mathbb{P}\{Q_{\mathcal{S}} \neq 0\} \cdot \mathbb{P}\{T_{\mathcal{R}_i}(r)\}\right\}, \tag{4.21}$$

where $\lambda_{\mathcal{S}\mathcal{R}_i}(r)$ denotes the arrival rate of the SN's data at RN $\mathcal{R}_i$, when the SN's target transmit rate equals r. $Q_{\mathcal{S}}$ denotes the queue of $\mathcal{S}$. Then, according to Little's theorem [198] the probability that the SN's queue is not empty ($\mathbb{P}\{Q_{\mathcal{S}} \neq 0\}$) is given by

$$\mathbb{P}\{Q_{\mathcal{S}} \neq 0\} = \lambda_{\mathcal{S}}/\mu_{\mathcal{S}}^{max}. \tag{4.22}$$

Furthermore, $\mathbb{P}\{T_{\mathcal{R}_i}(r)\}$ denotes the probability that RN $\mathcal{R}_i$ is granted the transmission opportunity to deliver the superposition-coded data, when $\mathcal{S}$ requires its transmission rate to be r. Let us now elaborate on $\mathbb{P}\{T_{\mathcal{R}_i}(r)\}$.

• *Twin-RN Scenario*: When more than one RN is capable of successfully forwarding the superposition-coded data to $\mathcal{D}$, RN $\mathcal{R}_i$ may be granted the transmission opportunity, provided that the transmit power $P_{\mathcal{R}_i}$ promised by RN $\mathcal{R}_i$ is lower than those promised by the other RNs. However, if only RN $\mathcal{R}_i$ is capable of providing successful cooperation, it will be selected as the best relay. Hence, considering a network, which consists of two RNs, $\mathbb{P}\{T_{\mathcal{R}_i}(r)\}$ may be characterized by:

$$\mathbb{P}\{T_{\mathcal{R}_i}(r)\} = \mathbb{P}\{U_{\mathcal{R}_i}^{(2)}(r)\} + \mathbb{P}\{U_{\mathcal{R}_i}^{(1)}(r)\}, \tag{4.23}$$

where $U_{\mathcal{R}_i}^{(n)}(r)$ represents the event that RN $\mathcal{R}_i$ was granted a transmission opportunity to forward its superposition-coded data, when n RNs are capable of providing cooperative transmission assistance for $\mathcal{S}$ and the target transmit rate of $\mathcal{S}$ is r. Firstly, the probability of $\mathbb{P}\{U_{\mathcal{R}_i}^{(1)}(r)\}$ is given by:

$$\mathbb{P}\{U_{\mathcal{R}_i}^{(1)}(r)\} = \mathbb{P}\{V_{\mathcal{R}_i}(r)\} \prod_{g=1, g\neq i}^{2} \left(1 - \mathbb{P}\{V_{\mathcal{R}_g}(r)\}\right). \tag{4.24}$$

Secondly, the probability of $\mathbb{P}\{U_{\mathcal{R}_i}^{(2)}(r)\}$ is given by:

$$\mathbb{P}\{U_{\mathcal{R}_i}^{(2)}(r)\} = \mathbb{P}\{P_{\mathcal{R}_i} = \min(P_{\mathcal{R}_g}|_{g=1}^{2})\} \cdot \prod_{g=1}^{2} \mathbb{P}\{V_{\mathcal{R}_g}(r)\}, \tag{4.25}$$

where $\mathbb{P}\{V_{\mathcal{R}_g}(r)\}$ denotes the probability of the event that the RN $\mathcal{R}_g$ is capable of providing cooperative transmission for $\mathcal{S}$, when the target transmit rate of $\mathcal{S}$ is r, which is given by:

$$\mathbb{P}\{V_{\mathcal{R}_g}(r)\} = \overline{\mathbb{P}_{out,\mathcal{S}\mathcal{R}_g}(r)} \cdot \mathbb{P}_{suc,\mathcal{R}_g\mathcal{D}}(r). \tag{4.26}$$

Moreover, $\mathbb{P}\{P_{\mathcal{R}_i} = \min(P_{\mathcal{R}_g}|_{g=1}^{N})\}$ is the probability of the event that $\mathcal{R}_i$ promises to request the minimum transmit power amongst all the relays for delivering the superposition-coded signal. According to Proposition 3.1, $\mathbb{P}\{P_{\mathcal{R}_i} = \min(P_{\mathcal{R}_g}|_{g=1}^{2})\}$ may be expressed as:

$$\begin{aligned}
&\mathbb{P}\{P_{\mathcal{R}_i} = \min(P_{\mathcal{R}_g}|_{g=1}^{2})\} \\
&= \mathbb{P}\{\rho_{\mathcal{R}_i,\mathcal{D}}|h_{\mathcal{R}_i,\mathcal{D}}|^2 > \rho_{\mathcal{R}_j,\mathcal{D}}|h_{\mathcal{R}_j,\mathcal{D}}|^2|_{j\neq i}\} \\
&= \frac{\rho_{\mathcal{R}_i,\mathcal{D}}}{\rho_{\mathcal{R}_i,\mathcal{D}} + \rho_{\mathcal{R}_j,\mathcal{D}}},
\end{aligned} \tag{4.27}$$

where the details of deriving Eq (4.27) are provided in Appendix B.4 [5].

• *Triple-RN Scenario*: Considering a network having three RNs, the probability $\mathbb{P}\{T_{\mathcal{R}_i}(r)\}$ of the event that RN $\mathcal{R}_i$ is selected as the best RN can be formulated as:

$$\mathbb{P}\{T_{\mathcal{R}_i}(r)\} = \mathbb{P}\{U_{\mathcal{R}_i}^{(3)}(r)\} + \mathbb{P}\{U_{\mathcal{R}_i}^{(2)}(r)\} + \mathbb{P}\{U_{\mathcal{R}_i}^{(1)}(r)\}, \tag{4.28}$$

where we have:
$$\mathbb{P}\{U_{\mathcal{R}_i}^{(n)}(r)\} = \begin{cases} \mathbb{P}\{P_{\mathcal{R}_i} = \min(P_{\mathcal{R}_g}|_{g=1}^{3})\} \cdot \prod_{g=1}^{3} \mathbb{P}\{V_{\mathcal{R}_g}(r)\} & n = 3 \\ \mathbb{P}\{P_{\mathcal{R}_i} = \min(P_{\mathcal{R}_g}|_{g=1}^{3})\} \cdot \mathbb{P}\{V_{\mathcal{R}_i}^{3,2}(r)\} & n = 2 \\ \mathbb{P}\{V_{\mathcal{R}_i}(r)\} \prod_{g=1,g\neq i}^{3} \left(1 - \mathbb{P}\{V_{\mathcal{R}_g}(r)\}\right) & n = 1. \end{cases}$$

In the above expressions, $U_{\mathcal{R}_i}^{(n)}(r)$ represents the event that RN $\mathcal{R}_i$ was granted a transmission opportunity to forward its superposition-coded data, when n RNs are capable of providing cooperative transmission assistance for $\mathcal{S}$ and the target transmit rate of $\mathcal{S}$ is r. Furthermore, $\mathbb{P}\{V_{\mathcal{R}_g}(r)\}$ denotes the probability of the event that the RN $\mathcal{R}_g$ is capable of providing cooperative transmission for $\mathcal{S}$, when the target transmit rate of $\mathcal{S}$ is r, which is characterized as Eq (4.26). $V_{\mathcal{R}_i}^{3,2}(r)$ represents the event that both RN $\mathcal{R}_i$ and another RN are capable of relaying the superposition-coded data, whilst the third RN cannot provide successful cooperation, when the target transmit rate of $\mathcal{S}$ is r. Hence, the probability of $\mathbb{P}\{V_{\mathcal{R}_i}^{3,2}(r)\}$

[5] According to our backoff scheme, collisions may occur if all the following three conditions are satisfied:(i) the SNs data was correctly received by multiple secondary users; (ii) under the constraint of P_{max}, the specific RNs, which correctly received the SN's data are capable of affording the transmit power required for successfully relaying the superposition-coded data; (iii) these candidate RNs have the same backoff time before sending the RRTS message, which implies that they promised to maintain the same transmit power, while relaying the superposition-coded data. The calculation of the collision probability in the relay selection phase is thus by no means straight-forward. However, it was confirmed by Monte Carlo simulations that this collision probability is vanishingly low. Hence, we ignored the collisions caused by simultaneous transmissions of multiple RRTS messages.

$$
\begin{aligned}
&\mathbb{P}\{P_{\mathcal{R}_i} = \min(P_{\mathcal{R}_g}|_{g=1}^{3})\} \\
=&\mathbb{P}\{P_{\mathcal{R}_j} < P_{\mathcal{R}_k}\}\mathbb{P}\{P_{\mathcal{R}_i} < P_{\mathcal{R}_j}|P_{\mathcal{R}_j} < P_{\mathcal{R}_k}\} + \mathbb{P}\{P_{\mathcal{R}_k} < P_{\mathcal{R}_j}\}\mathbb{P}\{P_{\mathcal{R}_i} < P_{\mathcal{R}_k}|P_{\mathcal{R}_k} < P_{\mathcal{R}_j}\} \\
=&\mathbb{P}\{\rho_{\mathcal{R}_i,\mathcal{D}}|h_{\mathcal{R}_i,\mathcal{D}}|^2 > \rho_{\mathcal{R}_j,\mathcal{D}}|h_{\mathcal{R}_j,\mathcal{D}}|^2 > \rho_{\mathcal{R}_k,\mathcal{D}}|h_{\mathcal{R}_k,\mathcal{D}}|^2\} \\
&+ \mathbb{P}\{\rho_{\mathcal{R}_i,\mathcal{D}}|h_{\mathcal{R}_i,\mathcal{D}}|^2 > \rho_{\mathcal{R}_k,\mathcal{D}}|h_{\mathcal{R}_k,\mathcal{D}}|^2 > \rho_{\mathcal{R}_j,\mathcal{D}}|h_{\mathcal{R}_j,\mathcal{D}}|^2\} \\
=&\frac{\rho_{\mathcal{R}_i,\mathcal{D}}}{\rho_{\mathcal{R}_i,\mathcal{D}} + \rho_{\mathcal{R}_j,\mathcal{D}}} + \frac{\rho_{\mathcal{R}_i,\mathcal{D}}}{\rho_{\mathcal{R}_i,\mathcal{D}} + \rho_{\mathcal{R}_k,\mathcal{D}}} - \frac{\rho_{\mathcal{R}_i,\mathcal{D}}\rho_{\mathcal{R}_k,\mathcal{D}} + \rho_{\mathcal{R}_i,\mathcal{D}}\rho_{\mathcal{R}_j,\mathcal{D}}}{\rho_{\mathcal{R}_i,\mathcal{D}}\rho_{\mathcal{R}_j,\mathcal{D}} + \rho_{\mathcal{R}_j,\mathcal{D}}\rho_{\mathcal{R}_k,\mathcal{D}} + \rho_{\mathcal{R}_i,\mathcal{D}}\rho_{\mathcal{R}_k,\mathcal{D}}} \qquad i \neq j \neq k.
\end{aligned} \tag{4.30}
$$

may be characterized as:

$$
\mathbb{P}\{V_{\mathcal{R}_i}^{3,2}(r)\} = \mathbb{P}\{V_{\mathcal{R}_i}(r)\}\sum_{j=1}^{3}\sum_{k=1}^{3}\mathbb{P}\{V_{\mathcal{R}_j}(r)\}(1 - \mathbb{P}\{V_{\mathcal{R}_k}(r)\}), \tag{4.29}
$$

subject to $i \neq j \neq k$. The probability expression of $\mathbb{P}\{P_{\mathcal{R}_i} = \min(P_{\mathcal{R}_g}|_{g=1}^{3})\}$ is formulated in Eq (4.30), where the detailed derivation of the probability $\mathbb{P}\{\rho_{\mathcal{R}_i,\mathcal{D}}|h_{\mathcal{R}_i,\mathcal{D}}|^2 > \rho_{\mathcal{R}_j,\mathcal{D}}|h_{\mathcal{R}_j,\mathcal{D}}|^2 > \rho_{\mathcal{R}_k,\mathcal{D}}|h_{\mathcal{R}_k,\mathcal{D}}|^2|_{i\neq j\neq k}\}$ is given in Appendix B.5.

• *General Case*: When the number of RNs is more than three, the probability $\mathbb{P}\{T_{\mathcal{R}_i}(r)\}$ of the event that the RN $\mathcal{R}_i$ is selected as the best RN is characterized by:

$$
\mathbb{P}\{T_{\mathcal{R}_i}(r)\} = \mathbb{P}\{U_{\mathcal{R}_i}^{(m)}(r)\} + \mathbb{P}\{U_{\mathcal{R}_i}^{(m-1)}(r)\} + \cdots + \mathbb{P}\{U_{\mathcal{R}_i}^{(1)}(r)\}, \tag{4.31}
$$

$$
\text{where:} \qquad \mathbb{P}\{U_{\mathcal{R}_i}^{(l)}(r)\} = \begin{cases} \mathbb{P}\{P_{\mathcal{R}_i} = \min(P_{\mathcal{R}_g}|_{g=1}^{m})\} \cdot \prod_{g=1}^{m}\mathbb{P}\{V_{\mathcal{R}_g}(r)\} & l = m \\ \mathbb{P}\{V_{\mathcal{R}_i}(r)\}\prod_{g=1,g\neq i}^{m}\left(1 - \mathbb{P}\{V_{\mathcal{R}_g}(r)\}\right) & l = 1 \\ \mathbb{P}\{P_{\mathcal{R}_i} = \min(P_{\mathcal{R}_g}|_{g=1}^{m})\} \cdot \mathbb{P}\{V_{\mathcal{R}_i}^{m,l}(r)\} & 1 < l < m, \end{cases}
$$

where $V_{\mathcal{R}_i}^{m,l}(r)$ represents the event that both RN $\mathcal{R}_i$ and $(l-1)$ other RNs are capable of providing cooperative transmission assistance for $\mathcal{S}$, whilst $(m-l)$ RNs cannot successfully forward the superposition-coded data to $\mathcal{D}$. The probability of $\mathbb{P}\{V_{\mathcal{R}_i}^{m,l}(r)\}$ is given by

$$
\mathbb{P}\{V_{\mathcal{R}_i}^{m,l}(r)\} = \prod_{j\in A}\mathbb{P}\{V_{\mathcal{R}_j}(r)\} \cdot \prod_{k\in B}\left(1 - \mathbb{P}\{V_{\mathcal{R}_k}(r)\}\right), \tag{4.32}
$$

where the variable A is the set of $(l-1)$ labels for the 'willing' RNs, while B denotes the set of $(m-l)$ labels representing the 'unwilling' RNs. Hence, $j \in A$ indicates that RN $\mathcal{R}_j$ is capable of successfully relaying the superposition-coded data, while $k \in B$ means that RN $\mathcal{R}_k$ will not be a potential relay candidate. According to Appendix B.5, the probability of $\mathbb{P}\{P_{\mathcal{R}_i} = \min(P_{\mathcal{R}_g}|_{g\in A})\}$ may be formulated by extending Eq (4.30).

When RN $\mathcal{R}_i$ is selected as the best RN, it provides a data output for both the relaying queue $Q_{\mathcal{SR}_i}$ and for the data queue $Q_{\mathcal{R}_i}$ by exploiting superposition coding. In order to decouple the interaction between these two queues, we assume that if the relay's data queue $Q_{\mathcal{R}_i}$ is empty, but $Q_{\mathcal{SR}_i}$ has packets in its buffer, then RN $\mathcal{R}_i$ will superimpose the SN's data on a "dummy" packet. Therefore, the departure rate of the relaying queue $Q_{\mathcal{SR}_i}$ may be expressed as:

$$\mu_{\mathcal{SR}_i} = \mathbb{E}\{\mu_{\mathcal{SR}_i}(r)\}, \tag{4.33}$$

where $\mu_{\mathcal{SR}_i}(r)$ denotes the departure rate of the relaying queue $Q_{\mathcal{SR}_i}$, when the SN's target transmit rate is r. According to our WW cooperative protocol, RN $\mathcal{R}_i$ may be granted a transmission opportunity for conveying the superposition-coded data, provided that both of the following two conditions are satisfied:

1. $\mathcal{S}$ has data to send with the aid of cooperation;
2. RN $\mathcal{R}_i$ is seclected as the best RN.

Hence, $\mu_{\mathcal{SR}_i}(r)$ is formulated as

$$\mu_{\mathcal{SR}_i}(r) = \mathbb{P}\{Q_{\mathcal{S}} \neq 0\} \cdot \mathbb{P}\{T_{\mathcal{R}_i}(r)\} \tag{4.34}$$

where $\mathbb{P}\{T_{\mathcal{R}_i}(r)\}$ is given by Eq (4.31). According to the metrics of $\lambda_{\mathcal{SR}_i}$ and $\mu_{\mathcal{SR}_i}$, we have:

$$\lambda_{\mathcal{SR}_i} = \mu_{\mathcal{SR}_i} \tag{4.35}$$

Eq (4.35) can also be confirmed by the description of the proposed WW cooperative MAC protocol, namely each arriving data transmission request will always be satisfied immediately in the relaying queue $Q_{\mathcal{SR}_i}$. Hence, the relaying queue $Q_{\mathcal{SR}_i}$ always remains empty.

4.3.3.2 Stability of $Q_{\mathcal{R}_i}$

Based on our WW cooperative MAC protocol, the RN $\mathcal{R}_i$ jointly encodes one of its data in the data queue $Q_{\mathcal{R}_i}$ and of the SN's data in the relaying queue $Q_{\mathcal{SR}_i}$ by superposition coding, when it is deemed to be the best RN. Hence, $Q_{\mathcal{SR}_i}$ and $Q_{\mathcal{R}_i}$ have the same average departure rate, namely:

$$\mu_{\mathcal{R}_i} = \mu_{\mathcal{SR}_i} = \mathbb{E}\left\{\mathbb{P}\{Q_{\mathcal{S}} \neq 0\} \cdot \mathbb{P}\{T_{\mathcal{R}_i}(r)\}\right\}. \tag{4.36}$$

Therefore, the stability of the relay's data queue requires $\lambda_{\mathcal{R}_i} < \mu_{\mathcal{R}_i}$.

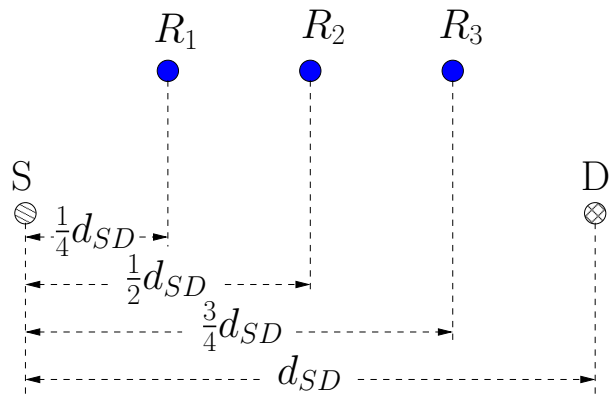

FIGURE 4.7: The network topology of the simulation scenario relying on the proposed WW cooperative MAC propocol of Fig 4.2 and the queueing model of Fig 4.5.

4.4 Simulation Results

4.4.1 Simulation Configuration

In order to evaluate the stability of the cooperative spectrum leasing system exploiting our WW cooperative MAC protocol of Fig 4.2, we consider a small cognitive network supporting $u = 5$ nodes, namely the $\mathcal{S}$, $\mathcal{D}$ plus $N = 3$ RNs, where all the nodes have fixed positions, as seen in Fig 4.7. Both $\mathcal{S}$ and $\mathcal{D}$ are licensed users, while the three RNs are unlicensed users located at the normalized position of [$d = 1/4$, $d = 1/2$ and $d = 3/4$] along the SD link, as seen in Fig 4.7. Based on this network topology, we investigate the stable throughput and stable transmit rate [6] of both $\mathcal{S}$ and of the RNs in the CSLS which exploits our WW cooperative protocol of Fig 4.2. Additionally, we consider two non-cooperative spectrum leasing systems (non-CSLS) as benchmarkers for our comparisons.

- In non-CSLS 1, $\mathcal{S}$ exploits the entire transmission duration for conveying its own data to $\mathcal{D}$ without power control, whilst maintaining the same maximum power constraint of P_{max}. More explicitly, $\mathcal{S}$ will transmit twice for the sake of achieving its target transmission rate of $\alpha C_{\mathcal{SD}}^{max}$, because the entire transmission duration is divided into two subslots in our CSLS. The SN first transmits its own data at the maximum transmit power of P_{max} and its target transmission rate of $\alpha C_{\mathcal{SD}}^{max}$. Then $\mathcal{S}$ retransmits its data at $P_{\mathcal{S},2}$ and $\alpha C_{\mathcal{SD}}^{max}$ for the sake of satisfying its transmit rate requirement, provided that $P_{\mathcal{S},2}$ is lower than P_{max}. Otherwise $\mathcal{S}$ retransmits its data at P_{max}.

- In non-CSLS 2, unlike in the non-CSLS 1 scheme, $\mathcal{S}$ exploits the *same* power control scheme and the same maximum power constraint of P_{max} as those of our CSLS. Hence,

[6] In this paper, the 'stable throughput' is introduced as a parameter of the MAC layer, which denotes the number of packets transmitted per slot, when the queue is stable. By contrast, the 'stable transmit rate' is a parameter of the physical layer in a stable queueing system, which is expressed in bits per second per Hz.

TABLE 4.3: The main simulation parameters of the simulation scenario of Fig 4.7 relying on the proposed WW cooperative MAC protocol of Fig 4.2, Fig 4.3 and Table 4.2 as well as the queueing model of Fig 4.5.

Position of $\mathcal{S}$	(0,0)
Position of $\mathcal{D}$	(1,0)
Position of $\mathcal{R}_1$	$(\frac{1}{4},\frac{1}{4})$
Position of $\mathcal{R}_2$	$(\frac{1}{2},\frac{1}{4})$
Position of $\mathcal{R}_3$	$(\frac{3}{4},\frac{1}{4})$
P_{max}	2 mW
$P_{\mathcal{S}-data}$	1 mW
α	[1.2,3.0]
β	[0.1,0.9]
$\lambda_{\mathcal{S}}$	[0.0,1.0]

$\mathcal{S}$ first transmits its data at its target rate of $\alpha C_{\mathcal{SD}}^{max}$ and at a *reduced* transmit power of $P_{\mathcal{S}-data}$. Then $\mathcal{S}$ retransmits its data at $P_{\mathcal{S}-data}^{(2)}$ and at the same target transmit rate of $\alpha C_{\mathcal{SD}}^{max}$, provided that $P_{\mathcal{S}-data}^{(2)}$ satisfies the power constraint, namely $P_{\mathcal{S}-data}^{(2)} < P_{max}$. Otherwise, $\mathcal{S}$ retransmits its data at P_{max}.

In the above two non-CSLS schemes, the duration of a transmission slot and the value of P_{max} are the same, as those in our CSLS. The greedy factors α and β are pre-determined. We appropriately adjust their values for estimating the performance of different scenarios.The main simulation parameters are listed in Table 5.5[7].

4.4.2 Stable Throughput of Each Node

4.4.2.1 Stable Throughput of $\mathcal{S}$

Fig 4.8 shows the maximum stable throughput $\mu_{\mathcal{S}}^{max}$ of $\mathcal{S}$ and the comparison of the source's stable throughput $(\mu_{\mathcal{S},coop} + \mu_{\mathcal{S},non}^{R_{coop}})$ achieved by both the cooperative and non-cooperative transmission, which can satisfy the source's rate requirement of $\alpha C_{\mathcal{S},\mathcal{D}}^{max}$ in our CSLS, non-CSLS 1 and non-CSLS 2 regimes. As seen in Fig 4.8, the maximum stable throughput $\mu_{\mathcal{S}}^{max}$ of $\mathcal{S}$ formulated by Eq (4.3) is one packet per slot, provided that $\mathcal{S}$ has at least one packet in its buffer at the beginning of the slot. However, the achievable transmit rates of some transmissions, namely $(\mu_{\mathcal{S},coop} + \mu_{\mathcal{S},non}^{R_{coop}})$ may match the SNs target rate of $\alpha C_{\mathcal{S},\mathcal{D}}^{max}$, while the transmit rates of the other transmissions are lower than $\alpha C_{\mathcal{S},\mathcal{D}}^{max}$, as seen in Table 4.2. Hence, we also quantify the stable throughput $(\mu_{\mathcal{S},coop} + \mu_{\mathcal{S},non}^{R_{coop}})$ of $\mathcal{S}$ formulated by Eq (4.4) and Eq (4.9), when its transmit rate requirement of $\alpha C_{\mathcal{S},\mathcal{D}}^{max}$ is satisfied, as shown in Fig 4.8.

[7]Given the value of α and β, we characterized the relay's stable throughput and stable transmit rate by simulating different scenarios associated with different values of the source's average arrival rate $\lambda_{\mathcal{S}}$. However, $\lambda_{\mathcal{S}}$ is fixed in each scenario.

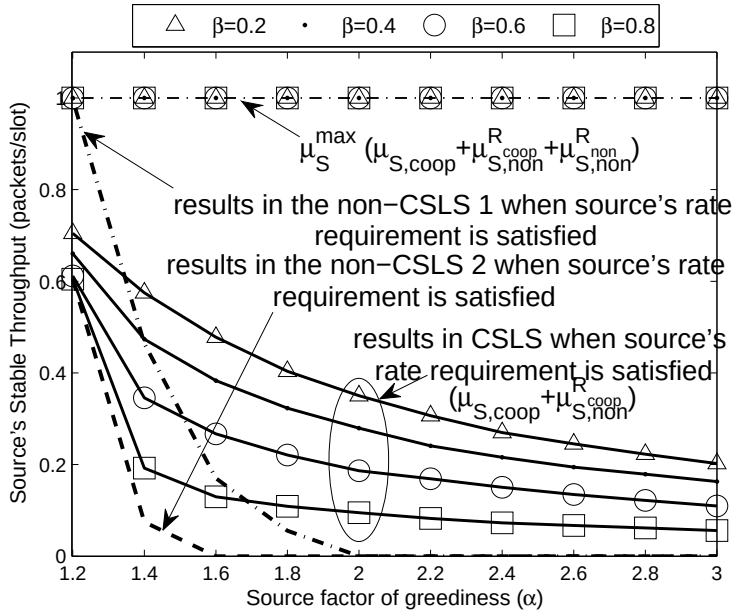

FIGURE 4.8: The source's stable throughput evaluated from Eq (4.3), Eq (4.4), Eq (4.9) and Eq (4.18) in the simulation scenario of Fig 4.7 relying on the WW cooperative MAC protocol of Fig 4.2 using the parameters of Table 4.3.

Effect of α: as mentioned in Section 5.4.1.2, the source's target rate of $\alpha C_{\mathcal{S},\mathcal{D}}^{max}$ can be achieved with the aid of cooperative transmissions whose stable throughput is $\mu_{\mathcal{S},coop}$, or with the aid of retransmissions from $\mathcal{S}$ when $P_{\mathcal{S},\mathcal{D}}^{(II)} < P_{max}$, whose stable throughput is $\mu_{\mathcal{S},non}^{R_{coop}}$. As observed in Fig 4.8, when the source's factor of greediness (α) is increased, the SN's stable throughput of $(\mu_{\mathcal{S},coop} + \mu_{\mathcal{S},non}^{R_{coop}})$ is reduced, because the probability of transmissions, which can indeed satisfy the SN's transmit rate requirement is reduced. More explicitly, when $\mathcal{S}$ becomes greedier, the SNR $\gamma_{\mathcal{R}_i}^{\mathcal{S}}$ which has to be guaranteed by the best RN with the cooperative transmission or by $\mathcal{S}$ during the retransmission is increased. Hence, the transmit power required for achieving the source's target rate is increased. However, the probability that either the RNs or $\mathcal{S}$ can afford the increased transmit power under the maximum power constraint is reduced, as $\mathcal{S}$ becomes greedier based on the discussions related to the probability of $\mathbb{P}_{suc,\mathcal{R}_i\mathcal{D}}(r)$ and $\mathbb{P}\{T_{\mathcal{S}}^{(II)}\}(r)$ in Section 4.3.2.1 and Section 4.3.2.2. Hence, the SN's stable throughput of $(\mu_{\mathcal{S},coop} + \mu_{\mathcal{S},non}^{R_{coop}})$ is decreased when α is increased as shown in Fig 4.8. Furthermore, observe in Fig 4.8 that $\mathcal{S}$ fails to satisfy its transmit rate requirement, namely $\mu_{\mathcal{S},non}^{R_{coop}} = 0$, when α exceeds 1.6 - indeed we have a throughput of zero for $\mathcal{S}$ in non-CSLS 2 which exploits the same power control scheme. Hence, observe in Fig 4.8 that if α is increased, the value of $(\mu_{\mathcal{S},coop} + \mu_{\mathcal{S},non}^{R_{coop}})$ is dramatically reduced, especially in the range of $\alpha < 1.6$, while it decreases more gradually for $\alpha \geq 1.6$.

Effect of β: additionally, observe in Fig 4.8 that the source's stable throughput of $(\mu_{\mathcal{S},coop} + \mu_{\mathcal{S},non}^{R_{coop}})$ is reduced, when the relay becomes greedier. When β is increased, a RN has to assign a higher transmit power of $P_{\mathcal{R}_i}^{\mathcal{R}}$ for the sake of achieving its target transmit rate

of $\beta C^{max}_{\mathcal{R}_i,\mathcal{D}}$. However, according the expression of the power $P_{\mathcal{R}_i}$ in Eq (4.7) less RNs can afford the increased transmit power required for satisfying the transmit rate $P_{\mathcal{R}_i}$ required for satisfying its increased transmit rate requirement, whilst simultaneously guaranteeing sources target rate under the constraint of P_{max}. This phenomenon reduces the probability of successful cooperative transmissions formulated by Eq (4.4)-Eq (4.8) and hence makes the influence of the source's transmissions more obvious, when $\mathcal{S}$ does indeed achieve its target rate without the relays' assistance as seen in Fig 4.8. For example, the curve of $(\mu_{\mathcal{S},coop} + \mu^{R_{coop}}_{\mathcal{S},non})$ dramatically decays in Fig 4.8 for $\beta = 0.8$ and $\alpha < 1.6$, because the value of $\mu^{R_{coop}}_{\mathcal{S},non}$ is noticeably reduced for $\alpha < 1.6$ in Fig 4.8. However, the stable throughput of $(\mu_{\mathcal{S},coop} + \mu^{R_{coop}}_{\mathcal{S},non})$ is gradually decreased for $\beta = 0.2$ and $\alpha < 1.6$ although $\mu^{R_{coop}}_{\mathcal{S},non}$ is significantly reduced, because the effect of $\mu_{\mathcal{S},coop}$ is more obvious than that of $\mu^{R_{coop}}_{\mathcal{S},non}$ for $\beta = 0.2$, as seen in Fig 4.8.

Comparison between CSLS and non-CSLS 1 as well as non-CSLS 2: compared to the non-CSLS 1 scheme introduced in Section 4.4.1, CSLS using our WW protocol is capable of achieving an increased stable throughput for $\mathcal{S}$ in conjunction with most of the "α" values investigated, as seen in Fig 4.8. However, these improvements are not universally applied. For example, when $\beta = 0.4$, the non-CSLS 1 scheme becomes capable of outperforming the CSLS scheme in Fig 4.8 for $\alpha < 1.4$, because a higher transmit power is used by $\mathcal{S}$ for its first transmission in the non-CSLS 1 scheme. More explicitly, $\mathcal{S}$ exploits the maximum power P_{max} for its first transmission in the non-CSLS 1 scheme, as described in Section 4.4.1. However, in our CSLS scheme, $\mathcal{S}$ broadcasts its data at a reduced power of $P_{\mathcal{S}-data}$ - which is lower than P_{max} - for the sake of reducing its energy dissipation, as seen in Fig 4.2 and Table 4.2. Hence, $\mathcal{S}$ has to afford a higher power for retransmitting its data in our CSLS scheme for the sake of satisfying its transmission rate requirement without cooperation. As observed in Fig 4.8, under the constraint of P_{max}, the probability of successful transmission, when $\mathcal{S}$ can achieve its target rate without relaying becomes higher in non-CSLS 1, which is a benefit of its higher transmit power. Therefore, the probability of successful cooperation in the CSLS scheme is eroded both by the selfish nature of RNs and the reduced transmit power of $P_{\mathcal{S}-data}$. Hence, observe in Fig 4.8 that the source's stable throughput guaranteeing its target rate of the non-CSLS 1 may be higher than that of the CSLS for $\alpha < 1.8$. In the absence of power control it also transpires from Fig 4.8 that the SN's transmit requirement cannot be satisfied by the non-CSLS 1 scheme for $\alpha \geq 2.0$. Additionally, the throughput curve of non-CSLS 2 which employs the same power control scheme as in CSLS also shows that $\mathcal{S}$ fails to achieve its target rate of $\alpha C^{max}_{\mathcal{S},\mathcal{D}}(t)$ for $\alpha \geq 1.6$, as seen in Fig 4.8. However, observe in Fig 4.8 that the SN's transmit requirement can still be satisfied for $\alpha > 1.6$ with the aid of cooperation. As observed in Fig 4.8, upon using our WW cooperative protocol, over 35% of the packets can be delivered at the source's target rate by the CSLS scheme, when $\alpha = 0.2$ and $\beta = 0.2$. Hence, the SN's stable throughput may be improved, when its

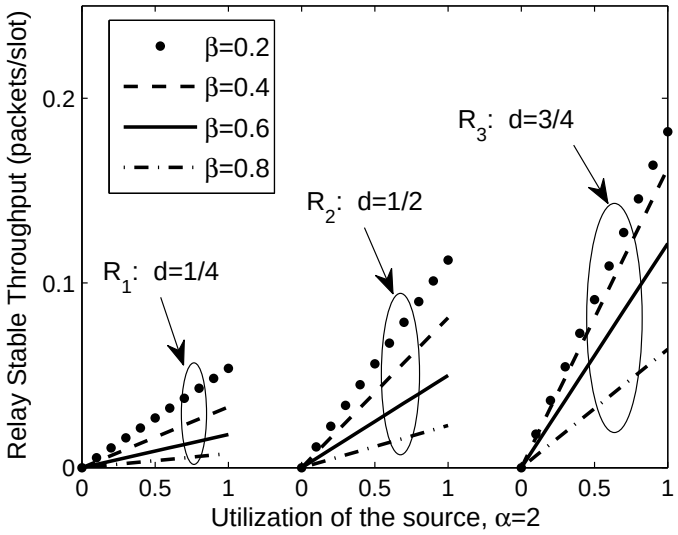

FIGURE 4.9: The relay's stable throughput evaluated from Eq (4.22), Eq (4.28) and Eq (4.36) in the simulation scenario of Fig 4.7 relying on the WW cooperative MAC protocol of Fig 4.2, when the source's factor of greediness is equal to 2 ($\alpha = 2$) and the other parameters are those seen in Table 4.3.

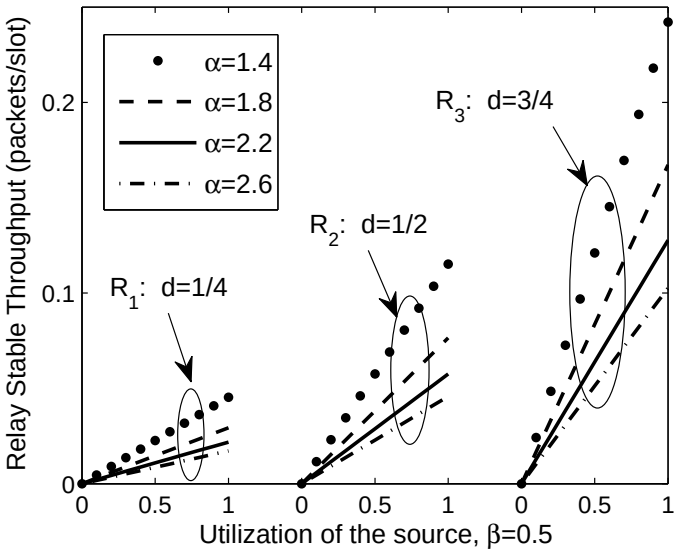

FIGURE 4.10: The relay's stable throughput evaluated from Eq (4.22), Eq (4.28) and Eq (4.36) in the simulation scenario of Fig 4.7 relying on the WW cooperative MAC protocol of Fig 4.2, when the relay's factor of greediness is equal to 0.5 ($\beta = 0.5$) and the other parameters are specified in Table 4.3.

target transmit rate is guaranteed by collaborating with the RNs.

4.4.2.2 Stable Throughput of the RN

Effect of utilization of $\mathcal{S}$: Fig 4.9 and Fig 4.10 show the relay's stable throughput expressed in terms of the number of packets/slot versus 'utilization' of $\mathcal{S}$ for different values of α and β, where 'utilization' of $\mathcal{S}$ is defined as the average proportion of time that $\mathcal{S}$ is busy [132]. According to Little's theorem [133, 198], the 'utilization'of $\mathcal{S}$ may be expressed as $\frac{\lambda_{\mathcal{S}}}{\mu_{\mathcal{S}}^{max}}$. As shown in Fig 4.9 and Fig 4.10, the relay's stable throughput is increased, as $\mathcal{S}$ becomes busier. However, the corresponding performance of the conventional CR protocol operating in the common model [139] has the opposite tendency, when the unlicensed users are capable of exploiting spectrum holes created by the primary users for transmitting their data. Hence, the available spectral resources exploited by the unlicensed users are reduced, when $\mathcal{S}$ becomes busier in the common model [139]. As a benefit of our CSLS relying on the proposed WW cooperative MAC protocol of Fig 4.2, the RNs may be granted a transmission opportunity only when $\mathcal{S}$ has data to send, which implies that the RNs may be granted more frequent transmission opportunities, when $\mathcal{S}$ has more packets to send, as evidenced by Eq (4.36). Hence, the relay's stable throughput seen in Fig 4.9 and Fig 4.10 is increased, as $\mathcal{S}$ becomes busier. In contrast to CSLS, the unlicensed users are unable to convey their data by the non-CSLS scheme, where $\mathcal{S}$ does not lease its spectral resources. Hence, the RNs are capable of attaining their stable throughput in our CSLS, when $\mathcal{S}$ intends to lease part of its spectral resources in exchange for the RNs' willingness to cooperate.

Effect of α and β: as seen in Fig 4.9, the relay's stable throughput is reduced, when the relay's factor of greediness, namely β is increased. When the RNs become greedier, a higher transmit power of $P_{\mathcal{R}_i}^{\mathcal{R}}$ is required for achieving their increased target transmit rate. Hence the total transmit power of $P_{\mathcal{R}_i}$ required for successfully forwarding the superposition-coded data is increased. Under the constraint of the maximum transmit power P_{max}, the probability of the event that a RN can afford an increased power of $P_{\mathcal{R}_i}$ for the sake of successful cooperation is decreased, when β is increased. Given the relay's factor of greediness, based on Eq (4.36) the relay's stable throughput is reduced, as the source's factor of greediness (α) is increased, as evidenced by Fig 4.10. When $\mathcal{S}$ becomes greedier, the outage probability of the SR link is increased, as seen in Eq (4.5). Hence less RNs are capable of successfully receiving the source's data. Additionally, as discussed above, in the context of Fig 4.8 the transmit power of $P_{\mathcal{R}_i}^{\mathcal{S}}$ required for guaranteeing the source's target rate is increased. Hence, when $\mathcal{S}$ becomes greedier, less RNs can afford the increased transmit power required for successfully forwarding the superposition-coded data to $\mathcal{D}$. Both of the above phenomena reduce the probability of successful cooperation between $\mathcal{S}$ and the RNs, as observed in Eq (4.4). Hence, the probability of the RN's transmission opportunities is reduced, when α is increased, as seen in Fig 4.10.

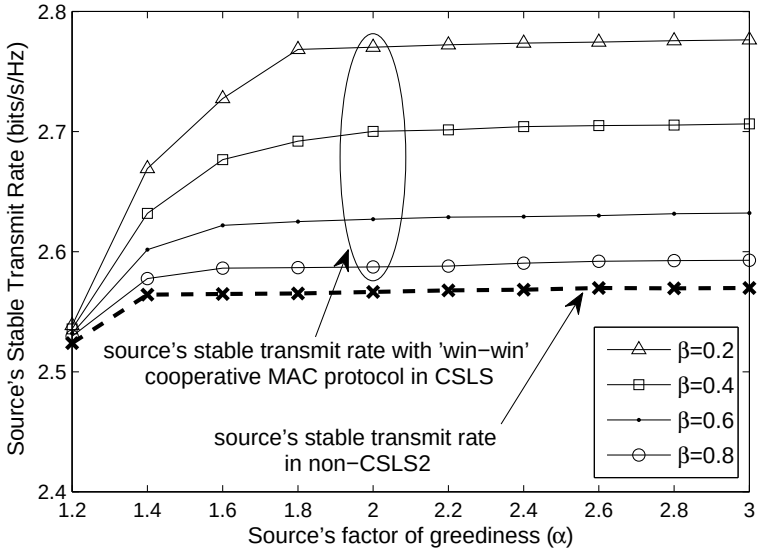

FIGURE 4.11: The source's stable transmit rate in the simulation scenario of Fig 4.7 relying on the WW cooperative MAC protocol of Fig 4.2 and using the parameters of Table 4.3.

Behaviour of each RN: observe both in Fig 4.9 and Fig 4.10 that the RN at '$d = 3/4$' - which is close to $\mathcal{D}$ - always achieves the highest stable throughput, while the RN at '$d = 1/4$' - which is close to the $\mathcal{S}$ - has the lowest stable throughput. Due to the pathloss encountered, the RN at '$d = 3/4$' suffers from the lowest outage probability for the RD link. Hence, the RN at '$d = 3/4$' in Fig 4.7 may exploit the lowest transmit power of $P^{\mathcal{S}}_{\mathcal{R}_i}$ required for guaranteeing source's target transmit power. Therefore, given the constraint of P_{max}, the probability of the event that the RN at '$d = 3/4$' promises to request the lowest power for conveying the superposition-coded data is higher than that for the other RNs in Fig 4.7. Therefore, observe both in Fig 4.9 and Fig 4.10 that the RN at '$d = 3/4$' achieves the highest stable throughput as a benefit of having the highest probability that it is selected as the best RN to provide cooperation for $\mathcal{S}$ and hence to win transmission opportunities for itself.

4.4.3 Stable Transmit Rate of Each Node

4.4.3.1 Stable Transmit Rate of $\mathcal{S}$

Because the transmit rates of both $\mathcal{S}$ and of the RNs vary all the time, it is necessary to evaluate the stable transmit rate. Fig 4.11 shows the stable transmit rate of $\mathcal{S}$ for different values of α and β. As seen in Fig 4.11, when the relay's factor of greediness (β) is increased, the source's stable transmit rate is reduced, because less RNs can afford the increased transmit power for satisfying the source's increased transmit rate requirement and simultaneously achieving their target transmit rate in the context of Fig 4.8. Hence, the probability of the cooperative transmission is reduced, namely the source's stable throughput

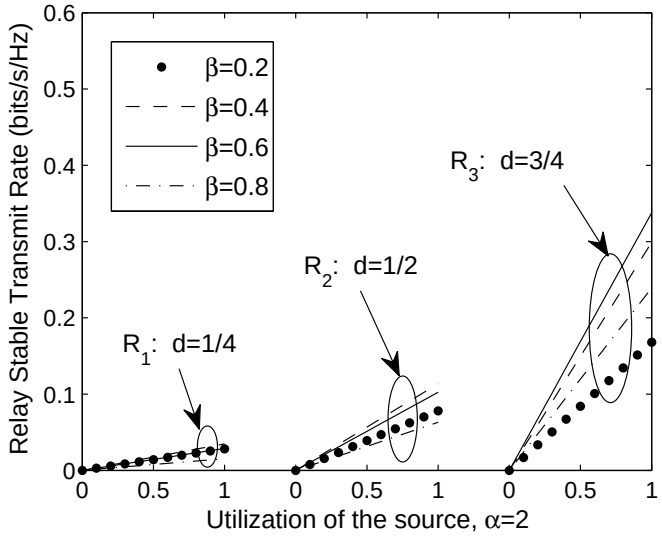

FIGURE 4.12: The relay's stable throughput in the simulation scenario of Fig 4.7 relying on the WW cooperative MAC protocol of Fig 4.2 in conjunction with the parameters of Table 4.3, when the sources factor of greediness is equal to 2.0 ($\alpha = 2.0$).

of $\mu_{\mathcal{S},coop}$ is decreased, as α is increased, which is evidenced by Fig 4.8.

By contrast, the SN's stable transmit rate is increased, when $\mathcal{S}$ becomes greedier due to the SN's increased transmit rate requirement. However, the probability of the successful transmission attempts, which can satisfy the source's transmit requirements, namely the source's stable throughput of $(\mu_{\mathcal{S},coop} + \mu_{\mathcal{S},non}^{R_{coop}})$ is decreased, when α is increased as shown in Fig 4.8. Furthermore, the reduction of the stable throughput of $(\mu_{\mathcal{S},coop}+\mu_{\mathcal{S},non}^{R_{coop}})$ becomes more obvious in Fig 4.8 when α is increased. Hence, the SN's stable transmit rate saturates for $\alpha > 1.8$ as seen in Fig 4.11.

Compared to the non-CSLS 2 scheme, where $\mathcal{S}$ exploits the same power control scheme, the stable transmit rate of $\mathcal{S}$ achieved by our CSLS remains high even for a high RN factor of greediness, such as $\beta = 0.8$ as shown in Fig 4.11. Hence, cooperation is indeed capable of improving the source's stable transmit rate.

4.4.3.2 Stable Transmit Rate of RN

Fig 4.12 and Fig 4.13 show the relay's stable transmit rate versus the 'utilization' of $\mathcal{S}$, where 'utilization' is defined as the average proportion of time that $\mathcal{S}$ is busy [132]. As mentioned in Section 4.4.2.2, the 'untilization' of $\mathcal{S}$ may be expressed as $\frac{\lambda_{\mathcal{S}}}{\mu_{\mathcal{S}}^{max}}$, according to Littles theorem [133, 198]. As seen in Fig 4.12 and Fig 4.13, the relay's stable transmit rate is increased, when $\mathcal{S}$ becomes busier. Based on our above discussions, this is plausible in the context of both Fig 4.9 and Fig 4.10, since the RNs benefit from more transmission

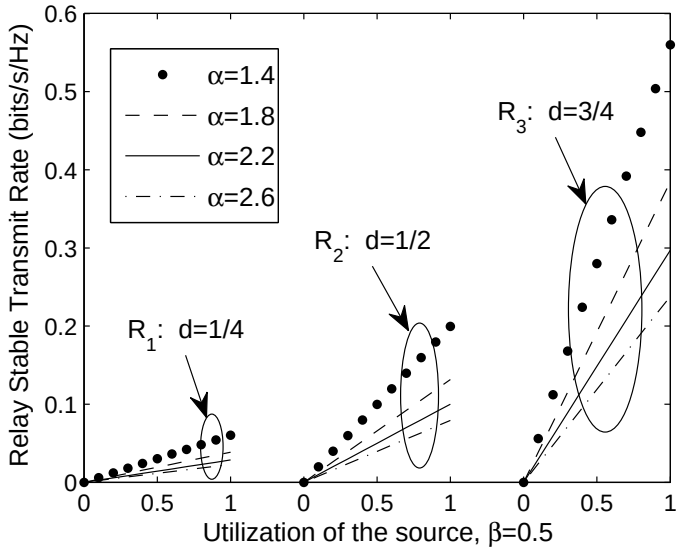

FIGURE 4.13: The relay's stable transmit rate in the simulation scenario of Fig 4.7 relying on the WW cooperative MAC protocol of Fig 4.2 in conjunction with the parameters of Table 4.3, when the relay's factor of greediness is equal to 0.5 ($\beta = 0.5$).

opportunities, when $\mathcal{S}$ has more data to transmit in a cooperative spectrum leasing system.

Similar to Fig 4.9 and Fig 4.10, both Fig 4.12 and Fig 4.13 indicate that the RN at '$d = 3/4$' - which is close to $\mathcal{D}$ - achieves the highest stable transmit rate, while the RN at '$d = 1/4$' - which is close to the $\mathcal{S}$ - has the lowest stable transmit rate. As above discussions in Section 4.4.2.2, since the RN at '$d = 3/4$' is close to $\mathcal{D}$, it has the highest pathloss reduction and the lowest outage probability for the RD link. Hence, the RN at '$d = 3/4$' may promise the lowest transmit power of $P_{\mathcal{R}_i}$ required for forwarding the superposition-coded data. Therefore, under the constraint of P_{max}, the RN at '$d = 3/4$' has the highest probability to be selected as the best RN, although it suffers from the highest outage probability for the SD link, as shown in Fig 4.9 and Fig 4.10. Hence, the RN positioned at '$d = 3/4$' achieves the highest stable transmit rate, as shown both in Fig 4.12 and Fig 4.13.

Furthermore, observe in Fig 4.12 that the relay's stable transmit rate is increased for $\beta \leq 0.6$, whilst it has the opposite tendency for $\beta > 0.6$. By contrast, it was demonstrated in Fig 4.9 that the RN's stable throughput was gradually decreased, as β increased. This is because when the RN becomes greedier, it is capable of conveying the superposition-coded data at a considerably higher rate due to its increased transmit rate requirement of $\beta C^{max}_{\mathcal{R}_i,\mathcal{D}}$, despite the fact that its transmission probability portrayed in Fig 4.9 is reduced for $\beta \leq 0.6$. However, the performance-erosion effect of the reduced cooperative probability observed in Fig 4.9 becomes more obvious for $\beta > 0.6$. Hence, as seen in Fig 4.12, the relay's stable transmit rate is reduced for $\beta > 0.6$. Therefore, the RN is capable of achieving its highest stable transmit rate by striking a tradeoff between its transmit rate and transmission probability,

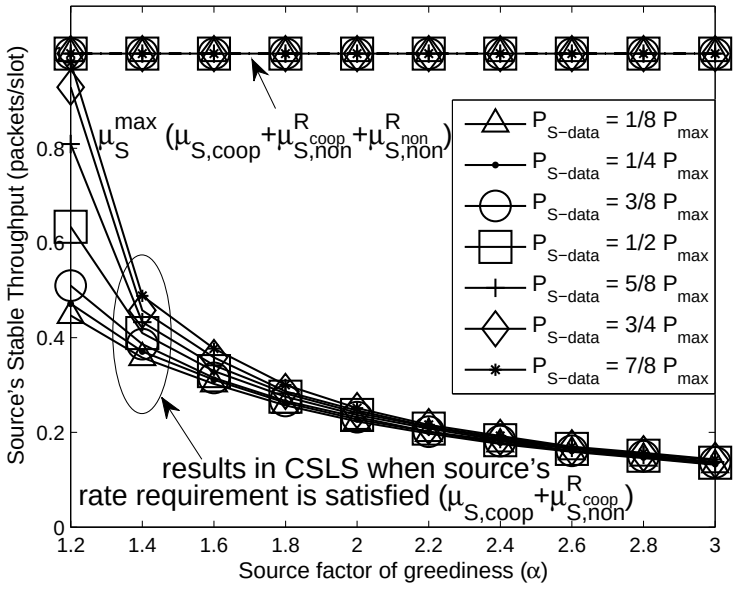

FIGURE 4.14: The source's stable throughput valuated from Eq (4.3), Eq (4.4), Eq (4.9) and Eq (4.18) in the simulation scenario of Fig 4.7 relying on the WW cooperative MAC protocol of Fig 4.2 in conjunction with the parameters of Table 4.3 for different powers of $P_{\mathcal{S}-data}$, when the relay's factor of greediness is equal to 0.5 ($\beta = 0.5$).

when its factor of greediness is about 0.6, as seen in Fig 4.12. Finally, observe in Fig 4.13 that when $\mathcal{S}$ becomes greedier, the relay's stable transmit rate is reduced because the increased transmit power of $P_{\mathcal{R}_i}$ decrease the probability of the event that RN $\mathcal{R}_i$ is granted the transmission opportunities under the constraint of P_{max} as seen in Fig 4.10. Observe in Eq (4.5) that the outage probability of the SR link may be increased, when $\mathcal{S}$ becomes greedier.

4.4.4 Effect of Power $P_{\mathcal{S}-data}$

In the above discussions, the transmit power of $P_{\mathcal{S}-data}$ is equal to $\frac{1}{2}P_{max}$. Fig 4.14 and Fig 4.15 show our comparison of both the source's and relay's stable throughput achieved by the scenarios relying on different powers of $P_{\mathcal{S}-data}$, when $\beta = 0.5$ is used. As observed in Fig 4.14, the maximum stable throughput of $\mathcal{S}$ is one packet per slot for the different values of power $P_{\mathcal{S}-data}$, provided that $\mathcal{S}$ has at least one packet in its buffer at the beginning of the slot. It can also be seen in Fig 4.14 that the SN's stable throughput of $(\mu_{\mathcal{S},coop} + \mu_{\mathcal{S},non}^{R_{coop}})$ is increased, when $\mathcal{S}$ broadcasts its data at a higher transmit power of $P_{\mathcal{S}-data}$, given α and β. When the transmit power of $P_{\mathcal{S}-data}$ is increased, the minimum SNR which has to be guaranteed by the cooperative transmission or the retransmission from $\mathcal{S}$ is reduced. Hence, more RNs may contend for cooperative transmission opportunities, because the transmit power of $P_{\mathcal{R}_i}^{\mathcal{R}}$ required for achieving the source's target transmit rate is reduced. Therefore we observe both in Fig 4.14 and Fig 4.15 that both the sources stable throughput achieved

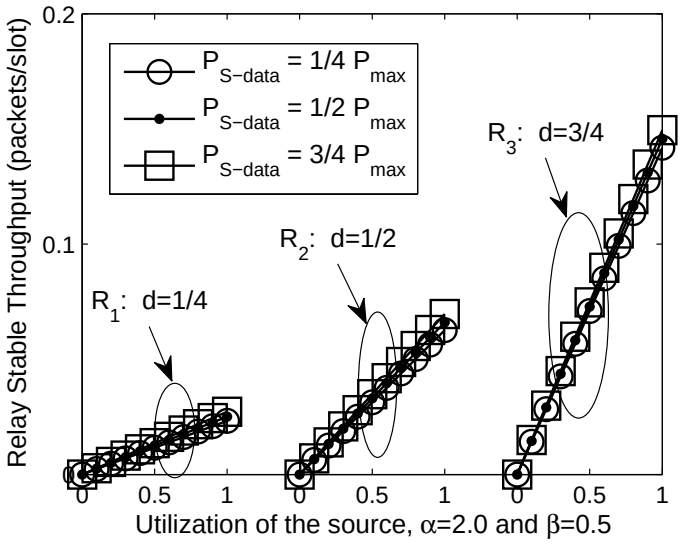

FIGURE 4.15: The relay's stable throughput evaluated from Eq (4.22), Eq (4.28) and Eq (4.36) in the simulation scenario of Fig 4.7 relying on the WW cooperative MAC protocol of Fig 4.2 in conjunction with the parameters of Table 4.3 for different powers of $P_{\mathcal{S}-data}$, when the source's factor of greediness is $\alpha = 2$ and the relay's factor of greediness $\beta = 0.5$.

by the cooperative transmission and the relays stable throughput, namely $\mu_{\mathcal{S},coop}$ and $\mu_{\mathcal{R}_i}$ are increased, when the transmit power of $P_{\mathcal{S}-data}$ is increased.

As seen in Table 4.2, if no RN is capable of providing cooperative transmission assistance for $\mathcal{S}$, a lower retransmit power of $P_{\mathcal{S},\mathcal{D}}^{(II)}$ is required for a successful retransmission from $\mathcal{S}$ in the second subslot, when a higher power of $P_{\mathcal{S}-data}$ is exploited for broadcasting the source's data in the first subslot. Hence, the probability of successful cooperative retransmission from $\mu_{\mathcal{S}}$ is increased, as $P_{\mathcal{S}-data}$ is increased. This phenomenon improves the source's stable throughput of $\mu_{\mathcal{S},non}^{R_{coop}}$ as evidenced in Fig 4.14. Hence, given α and β, the SN's stable throughput of $(\mu_{\mathcal{S},coop} + \mu_{\mathcal{S},non}^{R_{coop}})$ is increased in Fig 4.14, as the power of $P_{\mathcal{S}-data}$ becomes higher due to the increased probability of both successful cooperative transmission and successful cooperative retransmission from $\mathcal{S}$.

As seen in Fig 4.14, the source's stable throughput of $(\mu_{\mathcal{S},coop} + \mu_{\mathcal{S},non}^{R_{coop}})$ is decreased for all values of $P_{\mathcal{S}-data}$, when $\mathcal{S}$ becomes greedier. However, the difference between the results characterizing the scenarios exploiting different values of $P_{\mathcal{S}-data}$ is reduced in Fig 4.14, as α is increased. For example, the source's stable throughput of $(\mu_{\mathcal{S},coop} + \mu_{\mathcal{S},non}^{R_{coop}})$ approaches 1 in Fig 4.14, when we have $P_{\mathcal{S}-data} = \frac{7}{8}P_{max}$ and $\alpha = 1.2$ as well as $\beta = 0.5$, which implies that almost all the data transmission are capable of achieving source's target transmit rate, either with the aid of the cooperative transmissions from the best RN or with the aid of the cooperative retransmissions from $\mathcal{S}$. However, less than 50% of the data may be delivered at the source's target rate for $P_{\mathcal{S}-data} = \frac{1}{8}P_{max}$ and the same value of α and β, namely for $\alpha = 1.2$ and $\beta = 0.5$, as shown in Fig 4.14. Hence, there is a discrepancy between the

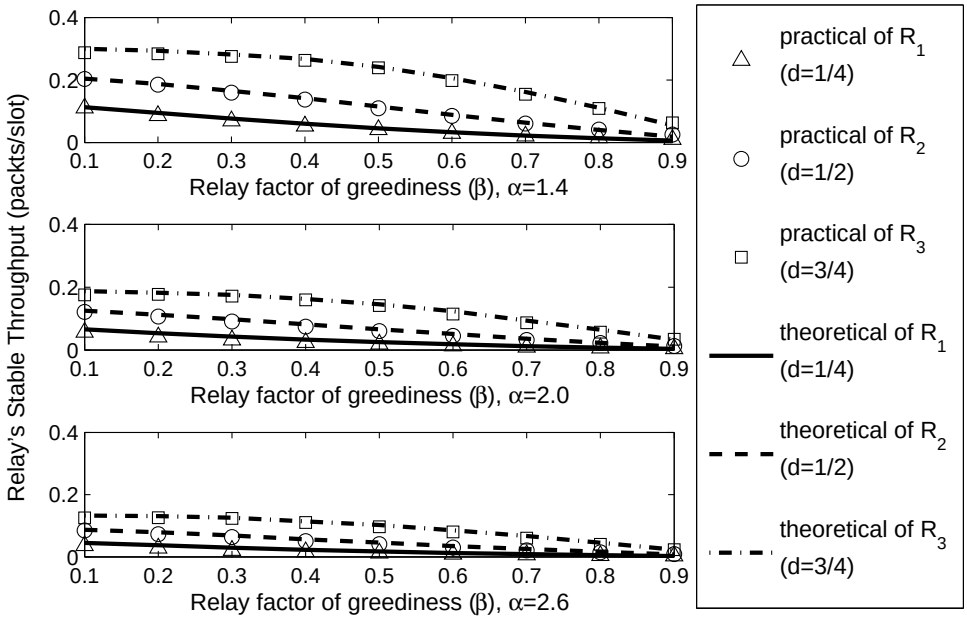

FIGURE 4.16: Comparison of the relay's practical stable throughput and theoretical stable throughput evaluated from Eq (4.22), Eq (4.28) and Eq (4.36) in the simulation scenario of Fig 4.7 relying on the WW cooperative MAC protocol of Fig 4.2 in conjunction with the parameters of Table 4.3, when the untilization of the source is 1.

curves characterizing the scenarios associated with $P_{\mathcal{S}-data} = \frac{1}{8}P_{max}$ and $P_{\mathcal{S}-data} = \frac{7}{8}P_{max}$ for $\alpha = 1.2$ in Fig 4.14. However, as seen in Fig 4.14 for $\alpha > 2.2$, the source's stable throughput of $(\mu_{\mathcal{S},coop} + \mu_{\mathcal{S},non}^{R_{coop}})$ remains near-constant in the scenarios exploiting different values of $P_{\mathcal{S}-data}$. As discussed above, in the context of Fig 4.8 the probability of successful cooperative transmissions relies on having a low outage probability for the SR link and on being able to afford the transmit power required for forwarding the superposition-coded data under the constraint of the maximum power P_{max}. As seen in Fig 4.14 for a high value of α, both the outage probability of the SR link and the probability that the total power $P_{\mathcal{R}_i}$ required for successful cooperative transmission exceeds the constraint of P_{max} become so high that the improvement attained by a higher power of $P_{\mathcal{S}-data}$ becomes negligible. Furthermore, observe in Fig 4.8 that since the probability of the successful cooperative retransmission from $\mathcal{S}$ in the second subslot is dramatically decreased as α is increased, $\mathcal{S}$ fails to satisfy its transmit rate requirement. Therefore we have $\mu_{\mathcal{S},non}^{R_{coop}} = 0$ for $\alpha > 2.0$. Hence, the throughput improvement achieved in Fig 4.14 by the higher power of $P_{\mathcal{S}-data}$ is reduced, when $\alpha > 2.0$.

4.4.5 Confidence Level of the Analysis

For the sake of evaluating the confidence level of our analysis provided in Section 4.3, Fig 4.16 and Fig 4.17 compare the theoretical stable transmit rate of both the RNs and $\mathcal{S}$

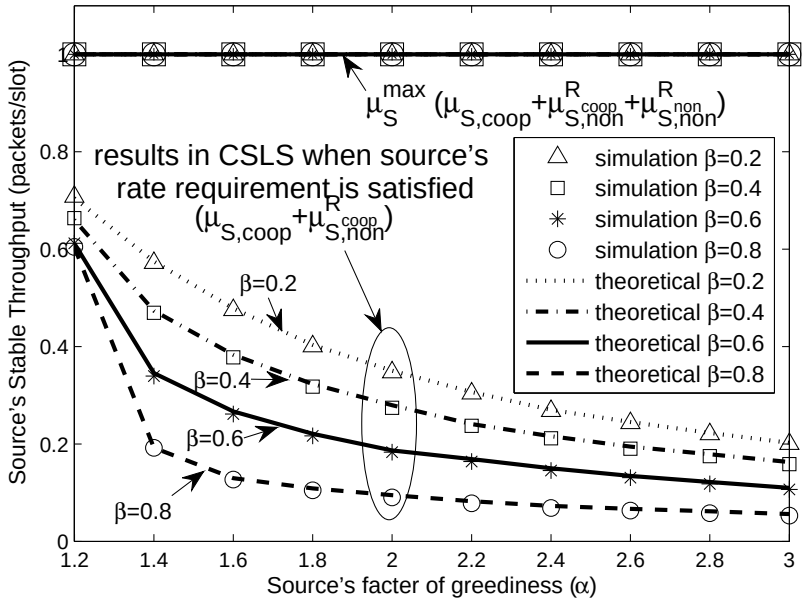

FIGURE 4.17: Comparison of the source's practical stable throughput and of its theoretical stable throughput evaluated from Eq (4.3), Eq (4.4), Eq (4.9) and Eq (4.18) in the simulation scenario of Fig 4.7 relying on the WW cooperative MAC protocol of Fig 4.2 in conjunction with the parameters of Table 4.3, when the untilization of the source is 1.

of in the CSLS of Section 4.3 for the corresponding simulation results obtained with the aid of Omnet++ [199]. As seen in Fig 4.16, the relay's theoretical throughput of Eq (4.36) and the practical results almost overlap each other. Furthermore, as shown in Fig 4.17, the difference between the source's theoretical stable throughput of Eq (4.3), Eq (4.4), Eq (4.9), Eq (4.18) and the simulation results is small. Hence, our theoretical stability analysis may be deemed reliable.

4.5 Chapter Summary

In this chapter, we analyzed the stability of a cooperative spectrum leasing system, which supports a single licensed transmission pair and exploits our distributed WW cooperative protocol of Section 4.2.3. In Section 4.2 we commence our discourse by describing the network's construction and the physical layer model of our cooperative spectrum leasing system. Section 4.2 also briefly introduced our distributed WW cooperative cooperative protocol of Section 3.3. The proposed distributed WW cooperative protocols were designed for striking a tradeoff between the achievable rate improvement and energy efficiency of the source, which is a licensed user. The source also granted transmission opportunities for the unlicensed users. The particular unlicensed user, who acts as the best RN jointly encodes the SN's and its own data by using superposition coding according to the transmit rate requirements of $\mathcal{S}$ and itself. The superposition-coded data is then forwarded to the

DN $\mathcal{D}$ as detailed in Section 4.2.3. Then $\mathcal{D}$ employs successive interference cancellation for decoding the superimposed source-relay data received from the relay and retrieves the source data by appropriately combining the direct and the relayed components.

Based on the queueing model of our cooperative spectrum leasing system shown in Fig 4.5 and detailed in Section 4.3.1, the stable throughput of both the $\mathcal{S}$ and the RN was derived in Section 4.3 according to the proposed distributed WW cooperative protocol of Section 4.2.3. The departure rate at the SN may be characterized by the sum of Eq (4.4), Eq (4.9) and Eq (4.18), where Eq (4.4) expressed the departure rate $\mu_{\mathcal{S},coop}$ achieved at $\mathcal{S}$ with the aid of cooperation, while Eq (4.9) described the departure rate $\mu_{\mathcal{S},non}^{R_{coop}}$ at $\mathcal{S}$, which was achieved by non-cooperative transmission at its target transmit rate. Furthermore, Eq (4.18) characterized the departure rate $\mu_{\mathcal{S},non}^{R_{non}}$ achieved at $\mathcal{S}$ by the non-cooperative transmission when the SN's transmit rate requirement cannot be satisfied in isolation under the constraint of the maximum transmit power. The unlicensed RNs were assumed to have two queues, namely queue $Q_{\mathcal{SR}_i}$ for storing the SN's and queue $Q_{\mathcal{R}_i}$ for storing the RN's data packets, as shown in Fig 4.5. The departure rate of the queue $Q_{\mathcal{SR}_i}$ is equal to the corresponding arrival rate, as formulated in Eq (4.35), which is determined by the probability of the SN being busy and the probability that RN $\mathcal{R}_i$ is selected as the best RN. Since superposition coding is used for jointly encoding the SN's and RN's data, the queue $Q_{\mathcal{R}_i}$ has the same departure rate as queue $Q_{\mathcal{SR}_i}$, as formulated by Eq (4.36).

The curves recorded in Fig 4.8-Fig 4.10 for the stable throughput as well as in Fig 4.11-Fig 4.13 for the stable transmit rate explicitly characterize the behaviour of both the SN and the RN. Compared to the benchmark systems, the cooperative spectrum leasing system exploiting the proposed distributed WW cooperative MAC protocol is capable of improving the stable throughput and the stable transmit rate for both the licensed SN and the unlicensed RN, as shown in Fig 4.8-Fig 4.13. When considering the constraint imposed on the maximum transmit power and the effects of pathloss, the RN at '$d = 3/4$' - which is close to $\mathcal{D}$ - achieves the highest stable throughput in Fig 4.9 and Fig 4.10, which is an explicit benefit of having the highest probability that it is selected as the best RN to provide cooperation for $\mathcal{S}$. Hence, it is capable of achieving the highest stable transmit rate. By contrast, the RN at '$d = 1/4$' - which is close to $\mathcal{S}$ - achieves the lowest stable throughput and lowest stable transmit rate in Fig 4.9, Fig 4.10, Fig 4.12 and Fig 4.13. Additionally, in Fig 4.14 and Fig 4.15 we estimated the effect of the transmit power of $P_{\mathcal{S}-data}$. It may be seen in Fig 4.14 that if $\mathcal{S}$ broadcasts its data at a higher transmit power of $P_{\mathcal{S}-data}$, the SN's stable throughput achieved by both the successful cooperative transmission and the successful retransmission - where the latter is capable of guaranteeing the SNs target transmit rate - is improved. This is an explicit benefit of its increased cooperation probability. However, this performance improvement becomes less obvious in Fig 4.15 for higher SN's greedy factors

α at the SN. Finally, in Fig 4.16 and Fig 4.17 we compare the stable throughput of both $\mathcal{S}$ and of the RNs evaluated from Eq (4.3) and Eq (4.36) to the corresponding simulation results obtained with the aid of Omnet++ for the sake of quantifying the confidence level of our analysis provided in Section 4.3.

Based on the above discussions, the single transmission pair based CSLS employing our distributed WW cooperative MAC protocol is deemed to be capable of providing considerable improvements in terms of both the stable throughput and of the stable rate for both the licensed SN and for the greedy unlicensed RN. This was achieved with the aid of our cooperative spectrum leasing scheme and joint superposition coding of both the sources and relays data at the RN as well as by combining the SD and RD signals at the DN. Our analysis was also confirmed by our simulation results.

In next chapter, we will design cooperative MAC protocol for supporting the reciprocal selection between the SNs and RNs in a cooperative system hosting multiple licensed transmission pairs and multiple unlicensed transmission pairs. Furthermore, the stability analysis of this multi-cooperative-pair system will also be presented in next chapter.

Chapter 5

Distributed 'Win-Win' Reciprocal-Selection-Based Cooperative Medium Access Scheme

5.1 Introduction

As mentioned in Chapter 3 and Chapter 4, Cognitive Radio (CR) techniques [200, 201] were proposed for efficiently exploiting the scarce spectral resources by enabling the unlicensed secondary users (SU) to access the spectrum originally licensed to the primary users (PU). The existing cognitive radio techniques may be classified into two categories, namely the common model[1] [181] and the spectrum leasing model[2] [52, 182], as detailed in Chapter 3 and Chapter 4. In contrast to the common model, the spectrum leasing scheme encourages the PUs to lease their spectral resources, whilst facilitating unhindered access for the SUs to the licensed spectrum.

The benefits of CR techniques may be further improved by combining it with the cooperative communications techniques [4, 194, 202], where the relay node (RN) forwards the source's data for the sake of improving the throughput, reducing the energy consumption

[1] According to the common model, the licensed PUs are capable of accessing the spectrum any time and are oblivious of the presence of unlicensed SUs. The SUs have to identify the the spectrum holes for the sake of conveying their data, provided that they do not substantially interfere with the transmissions of licensed users.

[2] Under the spectrum leasing model, the licensed PUs are aware of the presence of unlicensed SUs and intend to lease part of their spectral resources to these unlicensed users in exchange for appropriate 'remuneration'.

as well as extending the coverage area for the source, as discussed in Chapter 1. Numerous contributions have been developed based on the cooperative CR concept [36, 189, 203–211]. However, most of these existing contributions assumed that the relays agree to altruistically forward the data of the source node [36, 203–205, 207–211]. This unconditional altruistic behaviour is unrealistic to expect from the mobile stations (MS).

Bearing in mind the greedy behaviour of the mobile RNs, meritorious solutions were proposed in [41, 52, 162, 212] based on cooperative spectrum leasing, where the licensed PU intends to lease part of its spectral resources to the unlicensed SU in exchange for cooperative transmission assistance. The SU also has an incentive to forward data for the PU in exchange for a transmission opportunity for its own tele-traffic. Based on game theory, Wang *et al.* [212] designed a pricing-based cooperative spectrum leasing framework for a network supporting a single PU and multiple SUs. Furthermore, Jayaweera *et al.* [162] proposed auction-based dynamic spectrum leasing architectures, where the SUs calculate their bids for contending for a transmission opportunity within the licensed spectrum, while the PU leases its spectral resources to the SU in exchange for cooperative transmission assistance for the sake of saving energy. The author of [41] aimed for maximizing the transmission reliability for both the source's and the relay's data by designing an auction-based cooperative scheme. A 'win-win' cooperative MAC was developed in Chapter 3 [52] in order to improve the system's achievable rate and for reducing its energy consumption as well as for simultaneously satisfying the transmit rate requirements of both the PU and the SU.

However again, the above contributions [41, 52, 162, 212] focused on the *contention between the SUs* in the scenario of having a single PU and multiple SUs. As a further advance, considering the scenario of having multiple PUs and a single SU, Elkourdi *et al.* [80] designed a meritorious framework for the sake of making a decision on the *contention between the multiple PUs*. However, the reciprocal selection[3] between the PUs and SUs was not considered in the above contributions [41, 162, 212], neither has it been discussed in Chapter 3 or Chapter 4. Based on game theory, Li *et al.* [213] designed a coalitional game for cooperative spectrum leasing systems associated with multiple PUs and multiple SUs. Furthermore, Shamaiah *et al.* [214] and Bayat *et al.* [89] developed meritorious algorithms for finding the optimal matching between the PUs and SUs in order to maximize the utility of both the PUs and of the SUs. However, the authors of [89, 213, 214] aimed for maximizing either the *achievable transmit rate of PUs* [89, 213] or the *system's total transmit rate* [214]. Furthermore, the *global channel state information* of all SUs has to be available at each PU for selecting the best SU and vice versa [89, 213, 214].

[3]In this thesis, the "reciprocal selection" scheme is referred to as a selection scheme which allows the PU to select the winner of the contention between the SUs as its best cooperative partner and simultaneously allows the SU to select a best cooperative partner from multiple PUs which contend for the cooperative transmission assistance provided by this SU. Hence, in this thesis, the "reciprocal selection" scheme is designed by taking into accounting both the SU selection and PU selection.

Against this backcloth, we developed the following new contributions in this chapter.

1. We first formulate **a 'win-win' (WW) reciprocal-selection-based framework (WWRSF) for the sake of striking an attractive tradeoff between the *achievable rate improvement* and the *transmit power* required by a cooperative spectrum leasing system (CSLS) supporting *multiple* PUs and SUs.** More explicitly, each PU selects an appropriate SU as its best RN for minimizing its transmit power and for simultaneously improving its transmit rate. Furthermore, the SU intends to provide cooperative assistance for its best PU in order to minimize its transmit power and to simultaneously convey its own tele-traffic by using the licensed spectrum, whilst maintaining its target transmit rate.

2. **A distributed 'win-win' *reciprocal-selection-based* medium access scheme (DWWRS-MAS) is developed for *distributively* producing the best cooperative pairs** based on the system's objective functions formulated by the proposed WWRSF.

3. Considering the bursty nature of the PU's traffic, **we analyse the *queueing stability of the CSLS exploiting the proposed DWWRS-MAS* according to queueing theory**. As discussed in Chapter 4, most of the existing contributions [76,143,193,194, 215] related to the analysis of queueing stability were developed for cognitive networks relying on the common model. The queueing stability of the CSLS supporting a single PU and exploiting our distributed WW cooperative MAC protocol was analysed in Chapter 4. However, to the best of our knowledge, the queueing stability of the CSLS hosting multiple PUs and multiple SUs has not been investigated in the open literature. Hence, based on the method of analysing queueing stability, which was detailed in Chapter 2 and Chapter 4, we analyze the queueing stability of the CSLS relying on the proposed DWWRS-MAS.

4. Based on the matching theory [216], we analyse the **algorithmic stability** of our DWWRS-MAS.

5. We compared the performance of the CSLS exploiting our DWWRS-MAS to those achieved by two centralized CSLSs and by the random CSLS relying on a random reciprocal selection scheme. Moreover, two non-cooperative systems are introduced as our benchmarkers for evaluating the performance of the proposed DWWRS-MAS.

This chapter is organised as follows. Our system model and the proposed WWRSF are introduced in Section 5.2, while our DWWRS-MAS is described in Section 5.3. Section 5.4 analyzes both the queueing stability and the algorithmic stability of the proposed DWWRS-

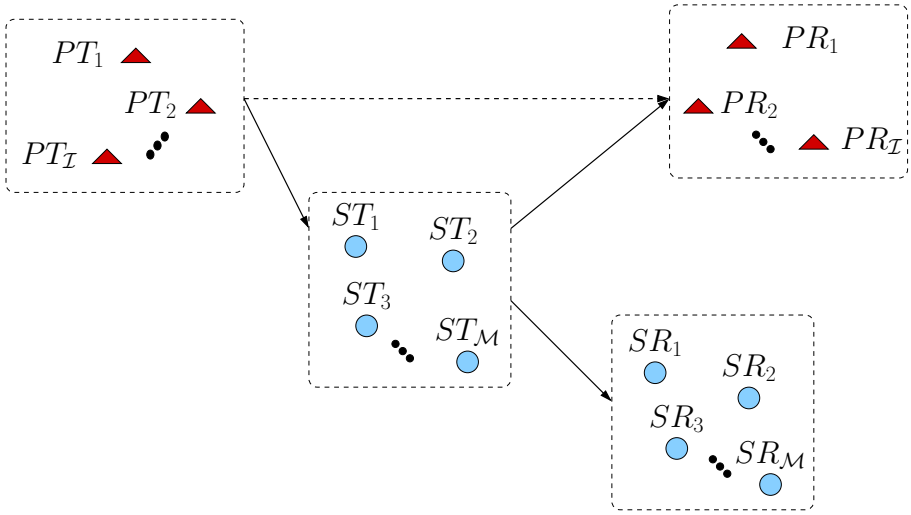

FIGURE 5.1: The system model.

MAS. In Section 5.5, the attainable performance of our scheme is quantified. Finally, we conclude in Section 5.6.

5.2 System Model

5.2.1 Network Construction and Assumptions

As seen in Fig 5.1, we consider a cooperative network having $\mathcal{I}$ primary transmission pairs (PTPs) in the set $\Theta_{PTP}(PT, PR) = \{\Theta_{PTP_i}(PT_i, PR_i)\}_{i=1}^{\mathcal{I}}$ and $\mathcal{M}$ secondary transmission pairs (STPs) in the set $\Theta_{STP}(ST, SR) = \{\Theta_{STP_m}(ST_m, SR_m)\}_{m=1}^{\mathcal{M}}$. [4] The variables PT_i and PR_i denote the PT and PR of the i-th primary transmission pair (PTP) Θ_{PTP_i}, while ST_m and SR_m are the ST and the SR, which constitute the m-th secondary transmission pair (STP) Θ_{STP_m}. Each PTP is granted access to a unique spectral band, while the $\mathcal{M}$ STPs are not licensees. Based on cooperative spectrum leasing strategies, PTP $\Theta_{PTP_i}(PT_i, PR_i)$ is encouraged to lease part of its spectral resources to a specific STP in exchange for cooperative transmission assistance, while each ST has an incentive to forward the PT's data for the sake of acquiring an opportunity to convey its own traffic within the licensed spectral band. Superposition coding (SPC) is invoked at the ST for jointly encoding the data of the PT and of itself. In order to eliminate the resultant interference at the corresponding PR and SR, Successive Interference Cancellation (SIC) is invoked at the receiver for separating the PT's and ST's data. Then the PR combines both the direct transmission and the relayed

[4] The cognitive network having multiple primary transmission pairs and multiple secondary transmission pairs was considered in [89, 213, 214]. A primary transmission pair is constituted by a primary transmitter (PT) and a primary receiver (PR), while a secondary transmitter (ST) and a secondary receiver (SRec) constitutes a secondary transmission pair.

transmission by using frame combining.

In order to simplify our investigations, we stipulate the following assumptions.

- *Channel Model*: all the channels involved are assumed to undergo quasi-static Rayleigh fading. Hence the complex-valued fading envelope remains constant during a transmission burst, while it is faded independently between the consecutive transmission bursts, where we define a transmission burst as a single transmission attempt. Furthermore, the duplex bi-directional channels between a pair of actively communicating nodes are assumed to be identical within a given transmission burst, while the channels of any of the remaining links are independent.

- *Wireless Environment*: we consider the effects of the free-space pathloss that is modelled by $\rho = 1/d^{\eta}$ [217], where d is the transmitter-to-receiver distance and η denotes the pathloss exponent, which is set to $\eta = 2$. The noise at all the receivers is assumed to be Additive White Gaussian Noise (AWGN) with zero mean and unit variance.

- *Power Constraint*: both PTs and STs are assumed to be limited by the same maximum transmit power P_{max}. The effects of different maximum transmit power constraints of the PT and ST are quantified in Section 5.5.6.

5.2.2 'Win-Win' Reciprocal-Selection-Based Framework

5.2.2.1 The Primary Transmitter's Objective Function

Rather than relying on monetary remuneration, each PT in our cooperative spectrum leasing system (CSLS) intends to lease part of its spectrum to a STP in exchange for cooperative transmission assistance for the sake of minimizing its transmit power as well as for improving its transmit rate. More explicitly, PTP Θ_{PTP_i} has a transmit rate requirement of $R^{req}_{PT_i} = \alpha C^{max}_{PT_i,PR_i}$ ($\alpha > 1$) which the ST should help achieve. In more detail, α is the ratio of the desired and affordable throughput termed as the PT's 'factor of greediness', while $C^{max}_{PT_i,PR_i}$ is the maximum achievable rate of the corresponding PT-to-PR (PP) link, which can be formulated as $C^{max}_{PT_i,PR_i} = \log_2(1 + \frac{\rho_{PT_i,PR_i}|h_{PT_i,PR_i}|^2 P_{max}}{P_N})$, where P_N is the power of the AWGN, while $|h_{PT_i,PR_i}|$ denotes the magnitude of the flat Rayleigh channel between PT_i and PR_i. Furthermore, ρ_{PT_i,PR_i} is the free-space pathloss between PT_i and PR_i. Based on the cooperative transmission assistance of ST_m, PT_i is capable of successfully conveying its data at a *reduced* transmit power of $P_p(i)$ and at an *increased* transmit rate of $R^{req}_{PT_i} = \alpha C^{max}_{PT_i,PR_i}$ ($\alpha > 1$). If PT_i cannot acquire any cooperative transmission assistance, it directly transmits its data to PR_i at a higher transmit power of $P^{nc}_{PT_i}$ and at the corresponding maximum

transmit rate of $R^{nc}_{PT_i}$. Hence, the Objective Function (OF) of the PT PT_i in our CSLS may be formulated as Eq (5.1)

$$OF_{PT_i} = \min\Big\{ \sum_{m=1}^{\mathcal{M}} \xi_{ps}(i,m) \cdot P_{PT}(i,m) \Big\}, \tag{5.1}$$

subject to

$$R_{PT_i}(i,m) = R^{req}_{PT_i}, \qquad \forall i \in \{1,\ldots,\mathcal{I}\},, \forall m \in \{1,\ldots,\mathcal{M}\}, \tag{5.2}$$

$$P_{PT}(i,m) \leq P_{max}, \qquad \forall i \in \{1,\ldots,\mathcal{I}\}, \forall m \in \{1,\ldots,\mathcal{M}\}, \tag{5.3}$$

$$\sum_{m=1}^{\mathcal{M}} \xi_{ps}(i,m) \leq 1, \qquad \forall i \in \{1,\ldots,\mathcal{I}\}, \tag{5.4}$$

$$\sum_{i=1}^{\mathcal{I}} \xi_{ps}(i,m) \leq 1, \qquad \forall m \in \{1,\ldots,\mathcal{M}\}, \tag{5.5}$$

$$\xi_{ps}(i,m) \in \{0,1\}, \qquad \forall i \in \{1,\ldots,\mathcal{I}\}, \forall m \in \{1,\ldots,\mathcal{M}\}. \tag{5.6}$$

We refer to $\mathcal{O}(PT_i, ST_m)$ as a cooperative pair, when ST_m is granted access to the spectrum, which was originally licensed to PT_i for providing cooperative transmission assistance for PT_i and for simultaneously conveying its own data within the licensed spectrum. In a cooperative pair $\mathcal{O}(PT_i, ST_m)$, ST_m is referred to the "cooperative partner" of PT_i, namely we have $M^*(i) = m$. The PT_i of the cooperative pair $\mathcal{O}(PT_i, ST_m)$ is also termed as the "cooperative partner" of ST_m, namely we have $I^*(m) = i$. Therefore, $\xi_{ps}(i,m)$ is equal to 1 when PT_i and ST_m constitute a cooperative pair $\mathcal{O}(PT_i, ST_m)$. Otherwise, $\xi_{ps}(i,m)$ is set to 0. Eq (5.2) and Eq (5.3) formulate the transmit rate requirement of PT_i and the maximum transmit power constraint, respectively. Eq (5.4) ensures that only a single ST provides cooperative transmission assistance for PT_i. Moreover, Eq (5.5) ensures that ST_m has only a single cooperative partner.

5.2.2.2 The Secondary Transmitter's Objective Function

Each ST has an incentive to forward data for its cooperative partner in exchange for accessing the SN's spectrum in order to convey its own traffic in the CSLS described in Section 5.2.1. Considering the greedy nature of ST, ST_m reserves a certain fraction of $R^{req}_{ST_m} = \beta C^{max}_{ST_m,SR_m}$ $(0 < \beta < 1)$ of the ST-to-SR (SS) channel's capacity for conveying its own tele-traffic, where β is the ST's 'factor of greediness' and $C^{max}_{ST_m,SR_m}$ is given by: $C^{max}_{ST_m,SR_m} = \log_2(1 + \frac{\rho_{ST_m,SR_m}|h_{ST_m,SR_m}|^2 P_{max}}{P_N})$, while $|h_{ST_m,SR_m}|$ denotes the magnitude of the flat Rayleigh channel between ST_m as well as SR_m. Furthermore, ρ_{ST_m,SR_m} is the free-space pathloss between ST_m and SR_m. We refer to $P^S_{ST}(i,m)$ as the transmit power

necessitated for achieving the target rate of ST_m, when PT_i is its cooperative partner. Furthermore, ST_m has to consume extra transmit power $P^P_{ST}(i,m)$ for helping PT_i achieve its target transmit rate $\alpha C^{max}_{PT_i,PR_i}$. Considering the selfish nature of the STs, when multiple PTs intend to lease part of their spectral resource to the ST ST_m, ST_m may provide cooperative transmission assistance for the best PT, which requires the lowest transmit power $P_{ST}(i,m) = P^S_{ST}(i,m) + P^P_{ST}(i,m)$ for the sake of minimizing its total transmit power $P_{ST}(i,m)$. Hence, each ST ST_m carries out autonomous decisions concerning its own cooperative strategy by optimizing its own OF, which may be formulated as:

$$OF_{ST_m} = \min \sum_{i=1}^{\mathcal{I}} \{\xi_{ps}(i,m) \cdot P_{ST}(i,m)\}, \tag{5.7}$$

subject to

$$R_{ST_m}(i,m) = R^{req}_{ST_m}, \qquad \forall i \in \{1,\ldots,\mathcal{I}\}, \forall m \in \{1,\ldots,\mathcal{M}\}, \tag{5.8}$$

$$R_{PT_i}(i,m) = R^{req}_{PT_i}, \qquad \forall i \in \{1,\ldots,\mathcal{I}\}, \forall m \in \{1,\ldots,\mathcal{M}\}, \tag{5.9}$$

$$P_{ST}(i,m) \leq P_{max}, \qquad \forall i \in \{1,\ldots,\mathcal{I}\}, \forall m \in \{1,\ldots,\mathcal{M}\}, \tag{5.10}$$

$$\sum_{i=1}^{\mathcal{I}} \xi_{ps}(i,m) \leq 1, \qquad \forall m \in \{1,\ldots,\mathcal{M}\}, \tag{5.11}$$

$$\sum_{m=1}^{\mathcal{M}} \xi_{ps}(i,m) \leq 1, \qquad \forall i \in \{1,\ldots,\mathcal{I}\}, \tag{5.12}$$

$$\xi_{ps}(i,m) \in \{0,1\} \qquad \forall i \in \{1,\ldots,\mathcal{I}\}, \forall m \in \{1,\ldots,\mathcal{M}\}. \tag{5.13}$$

Eq (5.8) and Eq (5.10) formulate the transmit rate requirement of ST_m and the maximum transmit power constraint at ST. Eq (5.12) ensures that PT_i has only a single cooperative partner.

Based on the above discussion, extra energy is dissipated for relaying the data of the PTs, when the STs provide cooperative transmission assistance. Hence, another OF is designed for minimizing the total transmit power of the PTs' cooperative partner, which may be formulated as:

$$OF^{sys}_{ST} = \min \sum_{m=1}^{\mathcal{M}} \sum_{i=1}^{\mathcal{I}} \Big\{\xi_{ps}(i,m) \cdot P_{ST}(m)\Big\}, \tag{5.14}$$

subject to Eq (5.8)- Eq (5.13).

Based on the OFs formulated for our WWRSF, it is quite a challenge to mathematically solve these optimization problems. Hence, in the next section we designed a distributed WW reciprocal-selection-based medium access scheme (DWWRS-MAS) for forming the co-

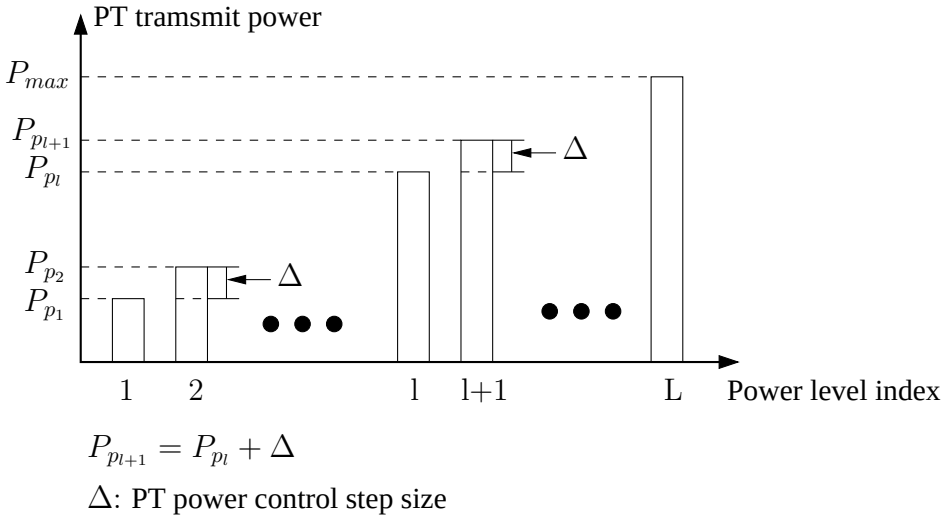

FIGURE 5.2: The transmit power level of the PTs in the network of Fig 5.1.

operative pairs based on the OFs formulated for our WWRSF.

5.3 Distributed WW Reciprocal-Selection-Based Medium Access Scheme

In this section, we introduce the proposed DWWRS-MAS designed for distributively selecting an appropriate cooperative partner for the PT PT_i in order to minimize its transmit power and for simultaneously achieving its target transmit rate, which is higher than that achieved by directly transmission, as formulated by the OF OF_{PT_i}. Furthermore, based on the OF_{ST_m}, the proposed DWWRS-MAS allows ST_m to select the best PT $PT_{I^*(m)}$ as its cooperative partner for the sake of minimizing its transmit power $P_{ST}(I^*(m), m)$ required for guaranteeing successful collaborative transmission. Moreover, a ST selection scheme is designed for distributively selecting the best ST for the sake of minimizing the total transmit power of the specific STs, which provide cooperative transmission assistance for the PTs, as given by the OF OF_{ST}^{sys}.

5.3.1 Discovery of Cooperative Partner

5.3.1.1 The Primary Transmitter's Behavior

In our DWWRS-MAS, the PTs scale their transmit power into several levels, namely we have $P_{p_l} \in \{P_{p_1}, \ldots, P_{max}\}$, as seen in Fig 5.2. Each power level may be given by $P_{p_{l+1}} = P_{p_l} + \Delta$, where Δ denotes the PT's power control step size, as shown in Fig 5.2. In order to minimize

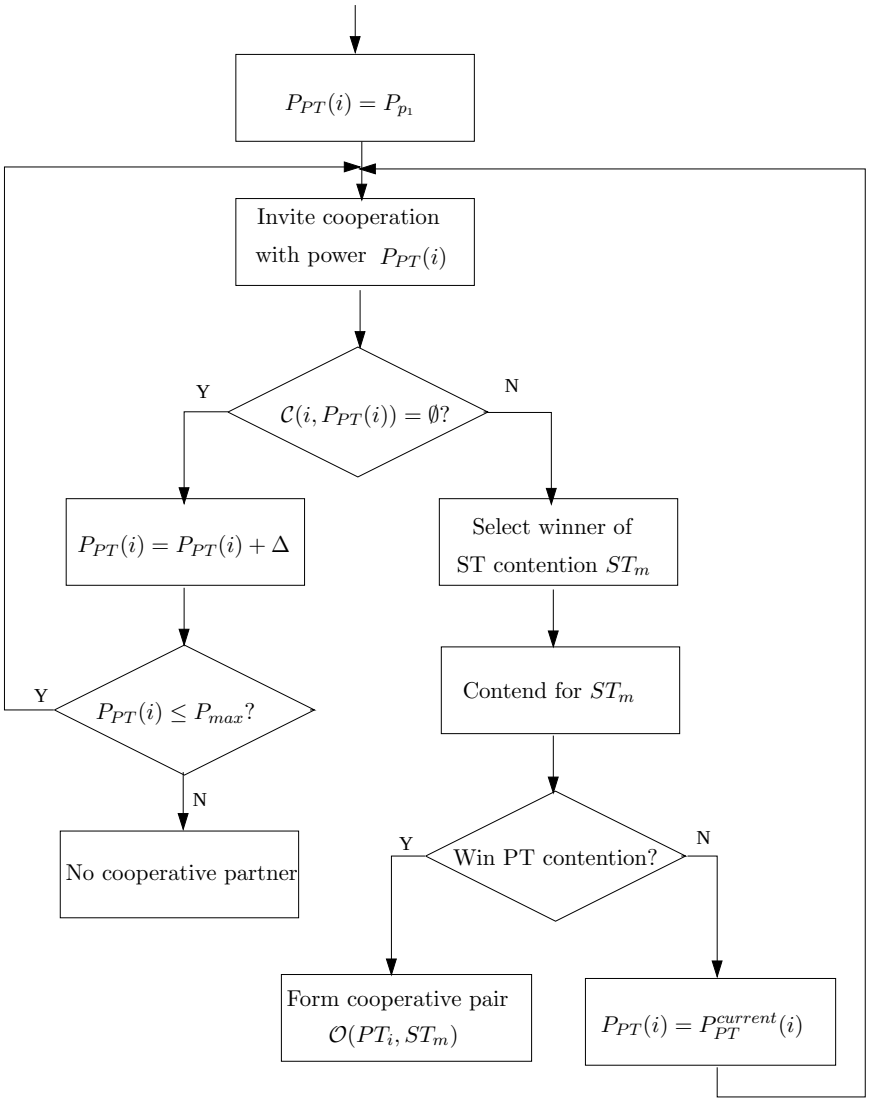

FIGURE 5.3: The flow chart of the operation of PT_i for forming a cooperative pair with an appropriate ST based on the power level of Fig 5.2 in the network of Fig 5.1.

the transmit power as formulated by OF_{PT} in Section 5.2.2, PT_i first broadcasts its target-QoS $\gamma_{ps}(i, P_{p_1})$, which has to be guaranteed by its cooperative partner, when PT_i consumes its *lowest* transmit power $P_{PT}(i) = P_{p_1}$ to convey its data, for the sake of discovering its candidate cooperative partners, which form a candidate set $\mathcal{C}_{PT}(i, P_{p_1})$. If we have $\mathcal{C}_{PT}(i, P_{p_1}) = \emptyset$, PT_i has to increase its transmit power to the next level of $P_{PT}(i) = P_{p_{l+1}}$ and calculate the corresponding target-QoS $\gamma_{ps}(i, P_{l+1})$. Then PT_i repeats the discovery procedure either until it finds an appropriate cooperative partner or until its transmit power achieves the maximum transmit power P_{max}, as seen in Fig 5.3 and Table 5.1. For example, as shown in Fig 5.4, we assume that the transmit power of PT_i is quantized into 3 levels. Hence, we have $P_{p_3} = P_{max}$. As seen in Fig 5.4, PT_i first discovers its cooperative partner with the lowest transmit power $P_{PT}(i) = P_{p_1}$. If PT_i fails to find a cooperative partner with P_{p_1}, namely we have $\mathcal{C}_{PT}(i, P_{p_1}) = \emptyset$, it repeats the discovery procedure by increasing its

TABLE 5.1: The PT behaviour for discovering and selecting cooperative partner based on the power level of Fig 5.2.

broadcast its target-QoS $\gamma_{ps}(i, P_{p_l})$ for discovering the set of $\mathcal{C}_{PT}(i, P_{p_1})$
wait for fixed duration of period of $(T_w + SlotTime)$ for collecting response
if receive response from potential cooperative partner
    contend for the cooperative assistance provided by the winner of ST contention $ST_{\hat{m}}$
else
    increase transmit power to next level $P_{PT}(i) = P_{p_{l+1}} = P_{p_l} + \Delta$
    if $P_{PT}(i) \leq P_{max}$
        calculate update target-QoS $\gamma_{ps}(i, P_{p_{l+1}})$
        repeat the operations in line 0 and broadcast $\gamma_{ps}(i, P_{p_{l+1}})$ instead of $\gamma_{ps}(i, P_{p_l})$
    else
        directly transmit its data ot PR_i.

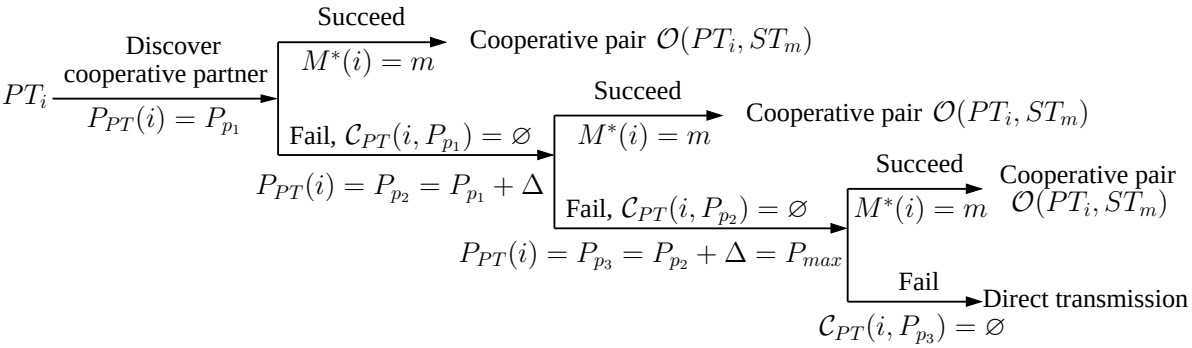

FIGURE 5.4: Illustration of the cooperative partner discovery process of PT_i based on the power level of Fig 5.2.

power to the second transmit power level. Hence namely we have $P_{PT}(i) = P_{p_2} = P_{p_1} + \Delta$, as seen in Fig 5.4. When the transmit power of PT_i is increased to the highest power level, namely $P_{p_3} = P_{max}$ in Fig 5.4, PT_i has to directly transmit its data without cooperative transmission assistance, provided that PT_i still fails to select its cooperative partner with the maximum transmit power P_{max}, as seen in Fig 5.4. However, if PT_i succeeds in finding a cooperative partner ST_m with a specific power, namely we have $M^*(i) = m$, it forms a cooperative pair $\mathcal{O}(PT_i, ST_m)$ with ST_m and curtails the discovery procedure, as seen in Fig 5.4.

According to the PT's target transmit rate of $\alpha C^{max}_{PT,PR}$, PT_i calculates the target-QoS $\gamma_{ps}(i, P_{p_l})$, which has to be guaranteed by its cooperative partner $ST_{M^*(i)}$, when PT_i transmits its data at the power of P_{p_l}. More explicitly, when the cooperative pair $\mathcal{O}(PT_i, ST_m)$ is appointed by our DWWRS-MAS, PT_i transmits its data to ST_m at the transmit power of $P_{PT}(i, m)$ and at its target transmit rate of $\alpha C^{max}_{PT,PR}$. Since α is higher than unity, the PR PR_i cannot correctly receive this data frame. However, PR_i will store this data frame and combines it with the duplicated data frame transmitted independently by the cooperative partner of PT_i, namely by ST_m, in order to achieve rate improvements. Therefore, the PT's aggregated rate achieved by using frame combining is given by $\alpha C^{max}_{PT_i,PR_i} =$

TABLE 5.2: The ST behaviour for discovering cooperative partner and contending for the transmission opportunity provided by the PTs in the network of Fig 5.1

```
0:  if receive cooperative invitation from PT_i
1:      calculate total power P_ST(i,m) required by successful collaborative transmission
2:      if P_ST(i,m) ≤ P_max
3:          if I*(m) > 0
4:              if P_ST(i,m) < P_ST(I*(m),m)
5:                  backoff for the duration of T_ST,bo(i,m)
6:                  send response to PT_i for contending for the transmission opportunity
7:              else
8:              ignore the invitation from PT_i
9:          else
10:             backoff for the duration of T_ST,bo(i,m)
11:             send response to PT_i for contending for the transmission opportunity
12:     else
13:         ignore the invitation from PT_i
```

$\log_2[1+\gamma^{(1)}_{PT_i,PR_i}(i,P_{p_l})+\gamma_{ps}(i,P_{p_l})], \alpha > 1$, where $\gamma^{(1)}_{PT_i,PR_i}(i,P_{p_l})$ denotes the receive Signal to Noise Ratio (SNR) at PR_i related to the erroneous direct transmission. Based on the assumptions stipulated in Section 5.2.1, the transmit rate requirement $\alpha C^{max}_{PT_i,PR_i}$ of PT_i remains constant, when PT_i selects its cooperative partner for conveying its current data. Hence, the target-QoS $\gamma_{ps}(i,P_{p_{l+1}})$ is lower than $\gamma_{ps}(i,P_{p_{p_l}})$, because PT_i increases its transmit power. This implies that more STs may intend to be the cooperative partner of PT_i, when PT_i updates its transmit power to the higher level of $P_{PT}(i) = P_{p_{l+1}}$, because a lower transmit power P_{ST} is required for satisfying the reduced PT's target-QoS $\gamma_{ps}(i,P_{p_{l+1}})$.

5.3.1.2 The Secondary Transmitter's Behaviour

After receiving the cooperative invitation from PT_i, ST_m first calculates the total transmit power $P_{ST}(i,m)$ required for satisfying the transmit rate of both PT_i and itself, as formulated by Eq (5.8) and Eq (5.9) of Section 5.2.2. If the power $P_{ST}(i,m)$ required for successful cooperative transmission does not exceed the maximum transmit power P_{max}, namely we have $P_{ST}(i,m) \leq P_{max}$, the PT_i becomes the potential cooperative partner of ST_m, as seen in Figure 5.5.

Based on above procedure, both the PTs and STs are aware of their candidate cooperative partner.

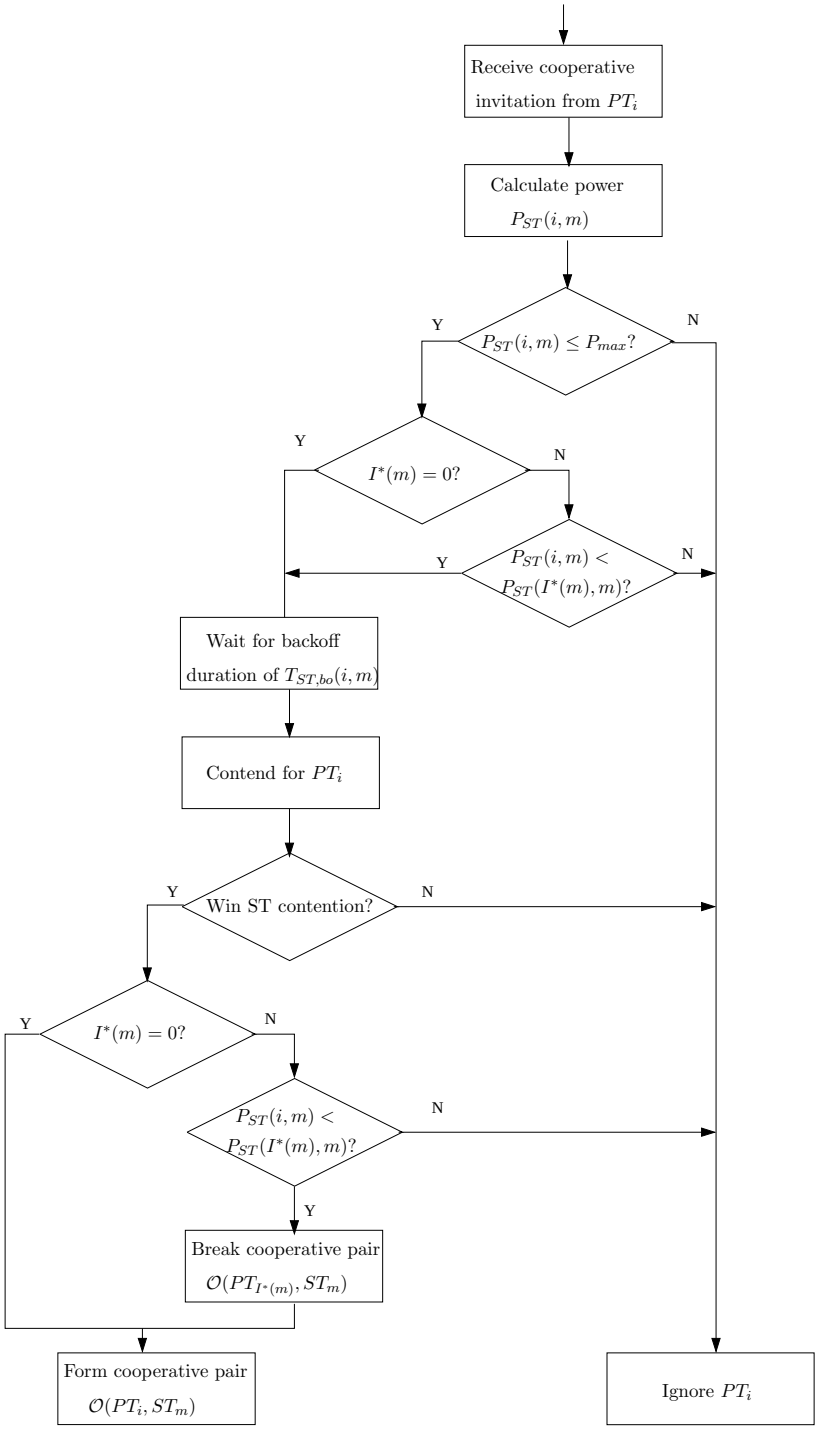

FIGURE 5.5: The flow chart of the operation of ST_m for forming a cooperative par with an appropriate PT in the network of Fig 5.1.

5.3.2 Selection of the Cooperative Partner

5.3.2.1 The Secondary Transmitter's Contention

When the STs are granted access to the licensed spectrum, extra transmit power has to be dedicated to the forwarding of PTs' data. Hence, a ST selection scheme is designed for minimizing the total transmit power consumed by the PTs' cooperative partners, as formulated by OF_{ST}^{sys} in Section 5.2.2. As shown in Fig 5.5 and Table 5.2, before contending for the transmission opportunity provided by PT_i, ST_m has to wait for a backoff duration of $T_{ST,bo}(i,m)$, which is defined as $T_{ST,bo}(i,m) = \varphi_{ST}(i,m) \cdot T_w$, where $T_w = CWmin \cdot aSlotTime$ is the contention window length, while $CWmin$ is the minimum contention window (CW) duration specified in the IEEE 802.11 standards [106]. The coefficient $\varphi_{ST}(i,m)$ is defined as $\varphi_{ST}(i,m) = P_{ST}(i,m)/P_{max}$. Hence, the specific ST, which promises the lowest transmit power P_{ST} may first transmit its response message, as a benefit of its shortest backoff time.

After broadcasting the cooperative invitation, PT_i has to wait for a fixed period of $(T_w + aSlotTime)$ in order to collect the responses of the candidate cooperative partners. Since the value of $P_{ST}(i,m)$ promised by ST_m is always lower than P_{max}, the back-off time allocated to ST_m will not exceed the PT's fixed waiting duration of $(T_w + aSlotTime)$. Hence, all the candidate cooperative partners of PT_i may issue their responses for contenting the transmit opportunity before PT_i stops waiting for the responses. Based on above discussion, PT_i may receive more than one response messages from multiple STs. However, PT_i intends to become the cooperative partner of the specific ST $ST_{\hat{m}}$ associated with the first response that was correctly received without considering any of the responses arriving later and without comparing the specific transmit power promised by the individual candidate cooperative pairs STs. This implies that the specific ST, which promises the lowest transmit power P_{ST} wins the STs' contention according to the proposed ST selection scheme. Bearing in mind the OF OF_{ST}^{sys} formulated by Eq (5.14) of Section 5.2.2,our ST selection scheme is designed for the sake of minimizing the transmit power of the PTs' cooperative partners by selecting the particular ST promising the lowest transmit power P_{ST}. Furthermore, the winner $ST_{\hat{m}}$ is selected in a distributed manner both without a centralized controller and without any information exchange between the candidate RNs.

Based on the outcome of the ST's contention, PT_i informs the winner $ST_{\hat{m}}$ that it intends to lease the transmission opportunity to $ST_{\hat{m}}$ and contends for the cooperative transmission assistance provided by $ST_{\hat{m}}$, as seen in Fig 5.3.

5.3.2.2 The Primary Transmitter's Contention

Based on the OF OF_{ST_m} formulated by Eq (5.7) of Section 5.2.2, each ST intends to select an appropriate PT for the sake of minimizing its transmit power required for successful cooperative transmission. Hence, if multiple PTs contend for the cooperative transmission assistance provided by ST_m, ST_m in our DWWRS-MAS forms a cooperative pair with the specific PT $PT_{\hat{i}}$, which requires the lowest power $P_{ST}(\hat{i}, m)$, when ST_m does not have a cooperative partner, as seen in Fig 5.5. Furthermore, when ST_m already has a cooperative partner PT_j, namely we have $I^*(m) = j$ and $M^*(j) = m$, ST_m may contend for the transmission opportunity leased by another $PT_{\hat{i}}$ and may form a new cooperative $\mathcal{O}(PT_{\hat{i}}, ST_m)$, provided that we have $P_{ST}(\hat{i}, m) < P_{ST}(j, m)$ and ST_m wins the ST contention for the cooperation with $PT_{\hat{i}}$, as observed in Fig 5.5 and Table 5.2.

As formulated by Eq (5.11) of Section 5.2.2, one of the contentions for the OF_{ST_m} is that each ST only has a single cooperative partner. Hence, ST_m has to break its current cooperative pair $\mathcal{O}(PT_j, ST_m)$, if it intends to form a new cooperative pair $\mathcal{O}(PT_{\hat{i}}, ST_m)$. If the cooperative pair $\mathcal{O}(PT_j, ST_m)$ is divorced, PT_j will find another cooperative partner, which is capable of successfully satisfying the target-QoS $\gamma_{ps}[j, P_{PT}(j, m)]$ that was guaranteed by the previous cooperative partner of PT_j, namely by ST_m, for the sake of acquiring cooperative transmission assistance without increasing the transmit power of PT_j. If no STs intend to become the cooperative partner of PT_j for guaranteeing the target-QoS $\gamma_{ps}(j, P_{p_l})$, PT_j increases its transmit power to the next power level according to $P_{PT}(i) = P_{p_{l+1}} = P_{p_l} + \Delta$ and repeats the above procedures, as shown in Table 5.3. For example, PT_j and ST_m form a cooperative pair $\mathcal{O}(PT_j, ST_m)$ when PT_j exploits its lowest transmit power, namely we have $P_{PT}(j, m) = P_{p_1}$. If the cooperative pair $\mathcal{O}(PT_j, ST_m)$ is divorced, PT_j has to discover other potential cooperative partners by using the current power P_{p_1}, rather than increasing its power to the second power level P_{p_2}, for the sake of acquiring cooperative transmission assistance without increasing its transmit power. However, if PT_j cannot form a cooperative pair with power P_{p_1}, it increases its transmit power to the second power level of $P_{p_2} = P_{p_1} + \Delta$ and repeats the discovery procedure of Fig 5.3 and Table 5.1 for seeking an appropriate cooperative partner for the sake of minimizing its transmit power and for achieving its target transmit rate.

5.4 Stability Analysis

Let us now consider the bursty nature of the transmissions from the PTs and STs. Section 5.4.1 analyses the queueing stability of the proposed DWWRS-MAS relying on queueing theory [103]. Based on matching theory [216], the algorithmic stability of our DWWRS-MAS

TABLE 5.3: The PT behaviour when its current cooperative pair is divorced in the network of Fig 5.1

0:	**if** ST_m breaks the cooperative pair with PT_j
1:	PT_j invites cooperation with power $P_{PT}(j,m)$
2:	**if** PT_j receive reply from new candidate cooperative partners
3:	PT_j repeat the option in line 3 in Table 5.1
4:	**else**
5:	PT_j increase its transmit power to $P_{PT}(j) = P_{PT}(j,m) + \Delta$
6:	**if** $P_{PT}(j) \leq P_{max}$
7:	PT_j calculate the corresponding target-QoS
8:	PT_j repeat cooperative partner discovery procedure in line 0 in Table 5.1 with the update target-QoS
9:	**else**
10:	PT_j directly transmits its data to PR_j.

is discussed in Section 5.4.2.

5.4.1 Queueing Stability of DWWRS-MAS

Before analysing the queueing stability of the CSLS relying on the proposed DWWRS-MAS, we describe the corresponding queueing model.

5.4.1.1 Queueing Model

Based on our DWWRS-MAS, we consider a cooperative queueing system, where each PT has a single queue for storing its data, while each ST is equipped with two queues, namely one for storing the data from its cooperative partner and one for its own data, as shown in Fig 5.6. In order to simplify our system stability analysis, we made the following assumptions:

- We consider a simple cooperative spectrum leasing system having two PTPs and multiple STPs.
- We assume that all the nodes have infinite-capacity buffers for storing their incoming packets.
- Each PT's data packet is transmitted within a specific time-slot (TS). Each PT transmits one data frame in each TS, which is assumed to be long enough for implementing the proposed DWWRS-MAS and for transmitting the data. Furthermore, we assume a network-wide synchronisation.
- The packet arrival processes at each node are assumed to be independent and stationary with a mean of λ_{PT_i} packets per slot for PT_i and λ_{ST_m} packets per slot for ST_m.

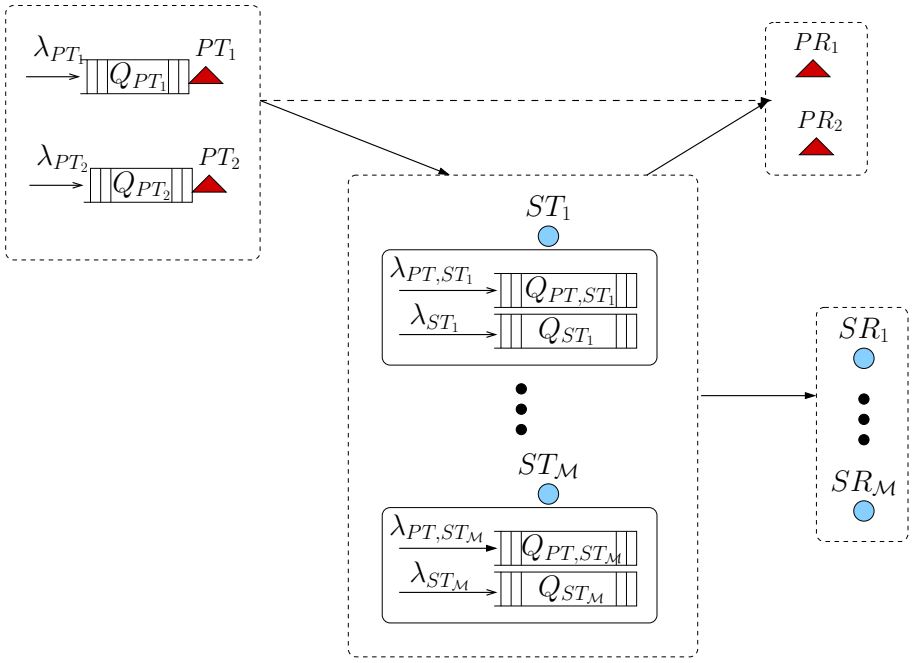

FIGURE 5.6: The queueing model of a cooperative spectrum leasing system, which supports two PTPs and multiple STPs as well as relies on the proposed DWWRS-MAS illustrated by Fig 5.3 and Fig 5.5.

- we assume perfect channel estimation for all nodes concerning their own channels, but no knowledge of the remaining links is assumed.

For source nodes generating bursty tele-traffic, the stability of a communication network is one of its fundamental performance measures. A network may be considered to be stable for a certain arrival rate vector, provided that all of its queues are stable, which implies that the length of all the queues remains finite, as discussed in Section 2.4.2. According to Loynes' theorem [134] introduced in Section 2.4, if the arrival and departure processes of a queueing system are stationary, the i_{th} queue is stable, when the average arrival rate λ_i is lower than the average departure rate μ_i ($\lambda_i < \mu_i$). Based on our assumptions, the stability of the queues may be verified with the aid of Loynes' theorem [134].

5.4.1.2 Stability of the Primary Transmitter's Queue

Based on the proposed DWWRS-MAS detailed in Section 5.3, the PT's data may be successfully delivered to the destination with the aid of cooperative transmission from its cooperative partner or may be directly transmitted from the PT to the destination, as seen in Fig 5.3. Hence, the maximum departure rate at the PT PT_i is formulated as:

$$\mu_{PT_i}^{max} = \mu_{PT_i}^{coop} + \mu_{PT_i}^{noncoop}. \tag{5.15}$$

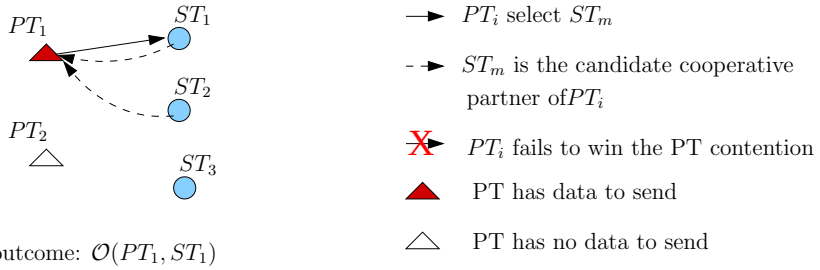

outcome: $\mathcal{O}(PT_1, ST_1)$

(a) Scenario 1 where P_2 is inactive and PT_1 has candidatet cooperative partner

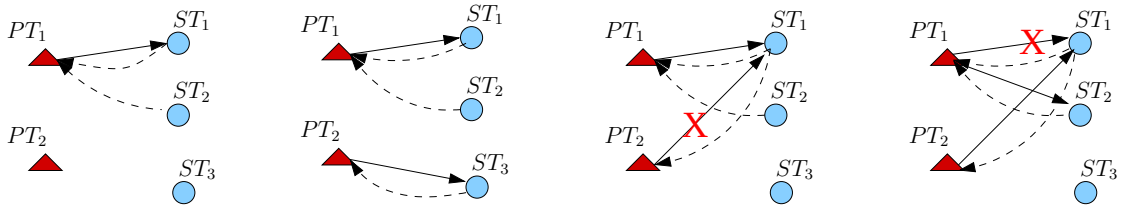

outcome: $\mathcal{O}(PT_1, ST_1)$ (b1) Scenario 2.1

coutcome: $\mathcal{O}(PT_1, ST_1)$ (b2) Scenario 2.2

outcome: $\mathcal{O}(PT_1, ST_1)$ (b3) Scenario 2.3

outcome: $\mathcal{O}(PT_1, ST_2)$ (b4) Scenario 2.4

(b) Scenario 2 where P_2 is active and PT_1 has multiple candidate cooperative partners

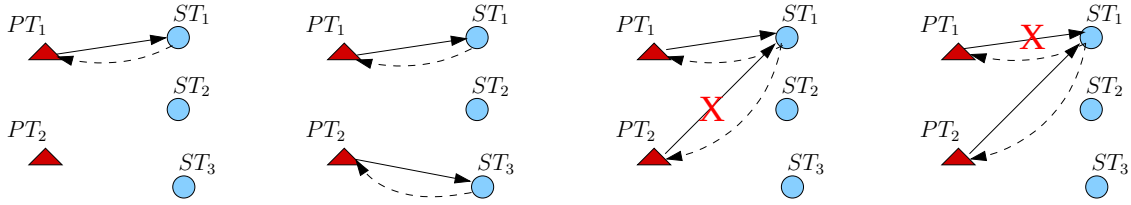

outcome: $\mathcal{O}(PT_1, ST_1)$ (c1) Scenario 3.1

coutcome: $\mathcal{O}(PT_1, ST_1)$ (c2) Scenario 3.2

outcome: $\mathcal{O}(PT_1, ST_1)$ (c3) Scenario 3.3

outcome: $M^*(1) = 0$ (c4) Scenario 3.4

(c) Scenario 3 where P_2 is active and PT_1 has only a single candidate cooperative partner

FIGURE 5.7: Examples of Scenario 1 and Scenario 2 as well as Scenario 3 discussed in Section 5.4.1.2 based on the network topology of Fig 5.6 relying on the proposed DWWRS-MAS illustrated by Fig 5.3 and Fig 5.5.

Let us now consider each term in detail.

Departure Rate of $\mu_{PT_i}^{coop}$***:*** According to the proposed DWWRS-MAS, PT_i may successfully select ST_m as its cooperative partner in one of the following scenarios:

- Scenario 1: we assume that only PT_i has data to send in the current time slot and its candidate cooperative partner set is not empty, i.e. we have $\mathcal{C}_{PT}(i) \nsubseteq \emptyset$. Then PT_i is capable of acquiring cooperative transmission assistance according to the proposed DWWRS-MAS illustrated by Fig 5.3 and Fig 5.5. For example, as seen in Fig 5.7(a), when PT_1 has candidate cooperative partners, namely we have $\mathcal{C}_{PT}(i) = \{ST_1, ST_2\}$ in Fig 5.7(a), based on our DWWRS-MAS illustrated in Fig 5.3 and Fig 5.5, PT_1 becomes capable of acquiring cooperative transmission assistance from the winner of

ST, say ST_1 in Fig 5.7(a) without contending with PT_2, because only PT_2 has no data to send in the current time slot.

- Scenario 2: let us consider the network shown in Fig 5.6, when *multiple* STs contend for the transmission opportunity granted by PT_i and the other PT also has data to send in the current time slot. Then at least one ST, say ST_m is capable of forming a cooperative pair of $\mathcal{O}(PT_i, ST_m)$ with PT_i, regardless whether both PT_i and the other PT contends for the same candidate cooperative partners or not, based on the proposed DWWRS-MAS illustrated by Fig 5.3 and Fig 5.5. More explicitly, as exemplified by the behaviour of PT_1 in Fig 5.7(b1), PT_1 is capable of acquiring cooperative assistance from the winner of the ST contention, say ST_1 without contending with PT_2 when no STs is capable of becoming the candidate cooperative partner of PT_2, according to our DWWRS-MAS illustrated by Fig 5.3 and Fig 5.5. Furthermore, when PT_1 and PT_2 have a different best cooperative partner, namely ST_1 is the winner of STs' competition for the transmission opportunity granted by PT_1 and ST_3 is the best cooperative partner of PT_2, as seen in Fig 5.7(b2), PT_1 is capable of forming a cooperative pair of $\mathcal{O}(PT_1, ST_1)$ with ST_1, which is achieved without contending with PT_2, as seen in Fig 5.3 and Fig 5.5. Moreover, when PT_1 and PT_2 has the same winner of the STs' competition, say ST_1 as exemplified by Fig 5.7(b3) and Fig 5.7(b4), PT_1 may form a cooperative pair of $\mathcal{O}(PT_1, ST_1)$ with ST_1 if it wins the PTs' competition as shown in Fig 5.7(b3). Alternatively, it may form a cooperative pair of $\mathcal{O}(PT_1, ST_2)$ with another candidate cooperative partner ST_2 if it fails to win the PTs' competition, as seen in Fig 5.7(b4), as dictated by our DWWRS-MAS illustrated in Fig 5.3 and Fig 5.5 as well as in Table 5.3. Hence, based on the above discussions, PT_1 is capable of acquiring cooperative assistance in all the scenarios, where *multiple* STs intend to become the cooperative partner of PT_1, provided that PT_2 also has data to send in the current time slot, as observed in Fig 5.7(b1)-Fig 5.7(b4).

- Scenario 3: let us assume that ST_m is the *only* candidate cooperative partner of PT_i and that another PT say PT_j also has data to send in the current time slot. Then, depending on the number of candidate cooperative partners of the other PT, namely of PT_j, ST_m may agree to become the cooperative partner of PT_i if any of the following events occur:

  - Scenario 3.1: If the candidate cooperative partner set of PT_j is empty, i.e. we have $\mathcal{C}_{PT}(j) = \emptyset$, no PT contends with PT_i for acquiring cooperative transmission assistance from ST_m, when the network has two PTPs. Hence, according to our DWWRS-MAS illustrated in Fig 5.3 and Fig 5.5, PT_i and ST_m constitute a cooperative pair $\mathcal{O}(PT_i, ST_m)$, when PT_i has only a single candidate cooperative partner and PT_j has no candidate cooperative partner, as exemplified by the

behaviour of PT_1 characterized in Fig 5.7(c1).

- Scenario 3.2: When both PT_i and PT_j have candidate cooperative partners, namely we have $\mathcal{C}_{PT}(i) = \{ST_m\}$ and $\mathcal{C}_{PT}(j) \neq \emptyset$, then ST_m will cooperatively forward data for PT_i in this scenario, if PT_i and PT_j gain cooperative assistance from different STs, according to our DWWRS-MAS illustrated in Fig 5.3 and Fig 5.5. For example, we assume that ST_1 is the winner of STs' competition for a transmission opportunity provided by PT_1, while ST_3 is the winner of STs' competition for a transmission opportunity PT_2, as seen in Fig 5.7(c2). Since PT_1 and PT_2 have a different best cooperative partner, namely ST_1 and ST_3, respectively, as seen in Fig 5.7(c2), PT_2 will not contend with PT_1 for acquiring cooperative transmission assistance from ST_1. Hence, based on the behaviour of both the PTs and STs specified by our DWWRS-MAS of Fig 5.3 and Fig 5.5, PT_1 is capable of acquiring cooperative transmission assistance from ST_1, when PT_1 has only a single candidate cooperative partner ST_1 and PT_2 has a different best cooperative partner, as seen in Fig 5.7(c2).
- Scenario 3.3: If we have $\mathcal{C}_{PT}(i) = \{ST_m\}$ and $ST_m \in \mathcal{C}_{PT}(j)$, PT_i and PT_j may contend for the one and only cooperative partner ST_m when ST_m is the winner of STs' competition for a cooperative opportunity as regards to both PT_i and PT_j. In this scenario, PT_i may become the cooperative partner of ST_m, if ST_m prefers to provide cooperative transmission assistance for PT_i, namely the required power is lower, as formulated in $P_{ST}(i,m) < P_{ST}(j,m)$, based on our DWWRS-MAS illustrated in Fig 5.3 and Fig 5.5 of Section 5.3.2. For example, as seen in Fig 5.7(c3), PT_1 and PT_2 contend for acquiring cooperative transmission assistance from ST_1, because ST_1 is the winner of STs' competition for a cooperative opportunity as regards to both PT_1 and PT_2. However, according to our DWWRS-MAS illustrated in Fig 5.3 and Fig 5.5, PT_1 of Fig 5.7(c3) wins the PTs' competition due to its lower transmit power requirement of $P_{ST}(1,1)$, namely because we have $P_{ST}(1,1) < P_{ST}(2,1)$. Hence, PT_1 forms a cooperative pair of $\mathcal{O}(PT_1, ST_1)$ with its one and only candidate cooperative partner ST_1, as seen in Fig 5.7(c3).

Furthermore, Fig 5.7(c4) shows Scenario 3.4, where PT_1 has only a single candidate cooperative partner ST_1, which is the common winner of STs' competition for a cooperative opportunity as regards to both PT_1 and PT_2. As discussed above, PT_1 and PT_2 has to contend for the cooperative transmission assistance provided by ST_1 based on our DWWRD-MASS, as seen in Fig 5.3 and Fig 5.5. Unfortunately, PT_1 of Fig 5.7(c4) fails to win this PTs' competition, because PT_2 required a lower transmit power, as formulated in $P_{ST}(1,1) > P_{ST}(2,1)$. Since PT_1 cannot form a cooperative pair with its one and only candidate cooperative partner ST_1, based on the PT's be-

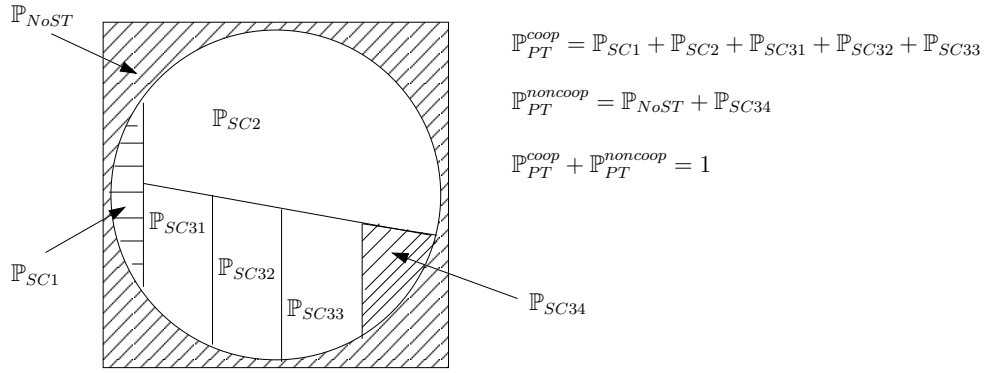

$\mathbb{P}_{SC1}$: probability of Scenario 1 $\mathbb{P}_{SC2}$: probability of Scenario 2

$\mathbb{P}_{SC31}$: probability of Scenario 3.1 $\mathbb{P}_{SC32}$: probability of Scenario 3.2

$\mathbb{P}_{SC33}$: probability of Scenario 3.3 $\mathbb{P}_{SC34}$: probability of Scenario 3.4

$\mathbb{P}_{NoST}$: probability that PT has no candidate cooperative partner

FIGURE 5.8: The relationship of the probability the scenarios exemplified by Fig 5.7 based on the network topology of Fig 5.1 relying on the proposed DWWRS-MAS illustrated by Fig 5.3 and Fig 5.5.

haviour in our DWWRS-MAS illustrated in Fig 5.3 and Table 5.3, PT_1 has to directly transmit its data to the destination. Hence we have $M^*(1) = 0$, as seen in Fig 5.7(c4). Based on the above discussions, when PT_i has only a single candidate cooperative partner and another PT - say PT_j - also has data to send in the current time slot, PT_i is capable of acquiring cooperative transmission assistance both in Scenario 3.1 and in Scenario 3.2 as well as in Scenario 3.3, as seen in Fig 5.7(c1)-Fig 5.7(c3).

Fig 5.8 shows the relationship of the probabilities of all the scenarios exemplified by Fig 5.7. As observed in Fig 5.8, the probability of the event that PT_i is capable of acquiring cooperative transmission assistance is given by the sum of the probabilities of Scenario 1 where only PT_i has data to send in the current time slot and $\mathcal{C}_{PT}(i) \neq \emptyset$, plus the probability of Scenario 2, where PT_i has *multiple* candidate cooperative partners and PT_j also has data to send, as well as of Scenario 3.1-Scenario 3.3 where PT_i has only a *single* candidate cooperative partners and PT_j also has data to send. Based on the above discussions, the average cooperative departure rate at PT_i may be written as:

$$\begin{aligned}\mu_{PT_i}^{coop} = & \underbrace{\mathbb{P}\{Q_{PT_j} = 0|_{i\neq j}\}}_{Q_{PT_j} \text{ is empty}} \cdot \underbrace{\mathbb{E}\Big\{\mathbb{P}\{\widetilde{M}(i) > 0\}\Big\}}_{\mathcal{C}_{PT}(i) \neq \emptyset} \\ & + \underbrace{\mathbb{P}\{Q_{PT_j} \neq 0|_{i\neq j}\}}_{PT_j \text{ has data to send}} \cdot \underbrace{\mathbb{E}\Big\{\mathbb{P}\{T_{PT_i}^{coop}|\widetilde{M}(i) > 1\} + \mathbb{P}\{T_{PT_i}^{coop}|\widetilde{M}(i) = 1\}\Big\}}_{PT_i \text{ has cooperative partner when } PT_j \text{ is also active}},\end{aligned} \tag{5.16}$$

where $\widetilde{M}(i)$ denotes the size of the candidate cooperative partner set $\mathcal{C}_{PT}(i)$ of PT_i, while

$\mathbb{P}\{T_{PT_i}^{coop}|\widetilde{M}(i) > 1\}$ denotes the probability that PT_i is capable of acquiring cooperative transmission assistance, when it has *multiple* candidate cooperative partners. The expression $\mathbb{P}\{T_{PT_i}^{coop}|\widetilde{M}(i) = 1\}$ denotes the probability of the event that the data of PT_i is delivered with the aid of cooperative transmission, when PT_i has *only one* candidate cooperative partner. Furthermore, $\mathbb{P}\{Q_{PT_j} \neq 0\}$ indicates that PT_j has data to send at the beginning of the current time slot. According to Little's theorem of Section 2.4 [198], the probability that the SN's queue is not empty is given by

$$\mathbb{P}\{Q_{PT_j} \neq 0\} = \lambda_{PT_j}/\mu_{PT_j}^{max}. \tag{5.17}$$

Furthermore, $\mathbb{P}\{Q_{PT_j} = 0\}$ indicates that PT_j does not have data to send at the beginning of the current time slot, which may also be expressed as $\mathbb{P}\{Q_{PT_j} = 0\} = 1 - \mathbb{P}\{Q_{PT_j} \neq 0\}$. Moreover, $\mathbb{P}\{\widetilde{M}(i) > 0\}$ represents the probability that PT_i does have candidate cooperative partners, which is formulated as:

$$\mathbb{P}\{\widetilde{M}(i) > 0\} = 1 - \mathbb{P}\{\widetilde{M}(i) = 0\} = 1 - \prod_{m=1}^{\mathcal{M}} \left\{ \prod_{P_x=P_{p_1}}^{P_{max}} \left(\overline{\mathbb{P}\{V_{SU}(i,m,P_x)\}} \right) \right\}, \tag{5.18}$$

where $\mathbb{P}\{V_{SU}(i,m,P_x)\}$ denotes the probability of the event that the ST_m is capable of providing cooperative transmission for PT_i, when PT_i will transmit its data to ST_m at P_x, which is given by:

$$\mathbb{P}\{V_{SU}(i,m,P_x,)\} = \mathbb{P}_{suc,PTS}(i,m,P_x) \cdot \mathbb{P}_{suc,SPR}(i,m,P_x), \tag{5.19}$$

where $\mathbb{P}_{suc,PTS}(i,m,P_x)$ denotes the probability of successful transmission from PT_i to ST_m, when PT_i relies on the transmit power level P_x, while $\mathbb{P}_{suc,SPR}(i,m,P_x)$ represents the probability of successful cooperative transmission from ST_m to PR_i, when PT_i transmits data to ST_m at P_x. Let us now derive the probability of $\mathbb{P}\{T_{PT_i}^{coop}|\widetilde{M}(i) > 1\}$ and $\mathbb{P}\{T_{PT_i}^{coop}|\widetilde{M}(i) = 1\}$.

Probability of $\mathbb{P}\{T_{PT_i}^{coop}|\widetilde{M}(i) > 1\}$ Based on the above discussions, PT_i is capable of finding an appropriate cooperative partner with the aid of the proposed DWWRS-MAS in Scenario 2 as seen in Fig 5.7(b), where PT_i has multiple candidate cooperative partners and all the PTs have data to send at the beginning of the current time slot. Hence, the probability of $\mathbb{P}\{T_{PT_i}^{coop}|\widetilde{M}(i) > 1\}$ may be formulated as:

$$\begin{aligned}\mathbb{P}\{T_{PT_i}^{coop}|\widetilde{M}(i) > 1\} =& \mathbb{P}\{\widetilde{M}(i,r) > 1\} \\ =& \sum_{m=1}^{\mathcal{M}} \sum_{P_x=P_{p_1}}^{P_{max}} \left(\mathbb{P}\{Z_{SU}(i,m,P_x)\} \cdot \sum_{P_y=P_x}^{P_{max}} \sum_{q=1}^{\mathcal{M}-1} \mathbb{P}\{B_{SU}^{(q)}(i,m,P_y)\} \right),\end{aligned} \tag{5.20}$$

where $\mathbb{P}\{Z_{SU}(i,m,P_x)\}$ denotes the probability of the events that ST_m is capable of successfully forwarding data for PT_i, when PT_i exploits the x-th transmit power level P_x, but ST_m cannot be the candidate cooperative partner of PT_i when PT_i relies on the power of P_{x-1}. Hence, the probability of $\mathbb{P}\{Z_{SU}(i,m,P_x)\}$ is given by:

$$\mathbb{P}\{Z_{SU}(i,m,P_x)\} = \begin{cases} \mathbb{P}\{V_{SU}(i,m,P_{p_1})\} & P_x = P_{p_1} \quad (5.21) \\ \mathbb{P}\{V_{SU}(i,m,P_x)|\overline{V_{SU}(i,m,P_{x-1})}\} & P_x > P_{p_1} \quad , \quad (5.22) \end{cases}$$

where $\overline{V_{SU}(i,m,P_{x-1})}$ models the event that ST_m cannot be the candidate cooperative partner of PT_i, when PT_i uses the transmit power of P_{x-1}, because the cooperative invitation of PT_i may not be correctly received by ST_m or because ST_m cannot afford the transmit power required for satisfying the transmit rate requirement of both PT_i and ST_m under the maximum transmit power constraint. Furthermore, $\mathbb{P}\{B_{SU}^{(q)}(i,m,P_y)\}$ denotes the probability of the event that PT_i has q candidate cooperative partners apart from ST_m, when PT_i exploits the y-th transmit power level P_y, but we have $\mathcal{C}_{PT}(i,P_{y-1}) = \{ST_m\}$. Hence, the probability $\mathbb{P}\{B_{SU}^{(q)}(i,m,P_y)\}$ may be written as:

$$\mathbb{P}\{B_{SU}^{(q)}(i,m,P_y)\} = \prod_{n\in\boldsymbol{E}(q)} \mathbb{P}\{Z_{SU}(i,n,P_y)\} \cdot \prod_{k\in\boldsymbol{G}} \overline{\mathbb{P}\{V_{SU}(i,k,P_y)\}}, \quad (5.23)$$

subject to $\boldsymbol{E} \cap \boldsymbol{G} = \emptyset$ and $\boldsymbol{E} \cup \boldsymbol{G} \cup m = \mathcal{M}$, where $\boldsymbol{E}$ denotes the set of the specific STs which may be the candidate cooperative partners of PT_i without considering the other PTs, while $\boldsymbol{G}$ denotes the complementary set of $\boldsymbol{E}$, apart from ST_m. The size of set $\boldsymbol{E}$ and $\boldsymbol{G}$ are q and $(\mathcal{M}-1-q)$ respectively. Furthermore, $\overline{\mathbb{P}\{V_{SU}(i,k,P_y)\}}$ in Eq (5.23) denotes the probability that ST_k cannot be the candidate cooperative partner of PT_i, when PT_i has a transmit power of P_y, which is equal to $1-\mathbb{P}\{V_{SU}(i,k,P_y)\}$.

Probability of $\mathbb{P}\{T_{PT_i}^{coop}|\widetilde{M}(i)=1\}$ According to the above discussions, as seen in Fig 5.7(c1)-Fig 5.7(c3), the probability that PT_i has a cooperative partner, when only a single ST intends to be its candidate cooperative partner is the sum of the probability of Scenario 3.1 and Scenario 3.2 as well as Scenario 3.3, which may be formulated as:

$$\begin{aligned} \mathbb{P}\{T_{PT_i}^{coop}|\widetilde{M}(i)=1\} = & \underbrace{\mathbb{P}\{I^*(\widehat{M}(i))=i|\widetilde{M}(i)=1,\widetilde{M}(j)=0\}}_{\text{Scenario 3.1: only } PT_i \text{ has candidate cooperative partner}} \\ & + \underbrace{\mathbb{P}\{I^*(\widehat{M}(i))=i|\widetilde{M}(i)=1,\widetilde{M}(j)>0,\widehat{M}(i)\neq\widehat{M}(j),i\neq j\}}_{\text{Scenario 3.2: } PT_i \text{ and } PT_j \text{ have different the winner of STs' competition}} \\ & + \underbrace{\mathbb{P}\{I^*(\widehat{M}(i))=i|\widetilde{M}(i)=1,\widetilde{M}(j)>0,\widehat{M}(i)=\widehat{M}(j),i\neq j\}}_{\text{Scenario 3.3: } PT_i \text{ wins the PTs' competition}} \quad (5.24) \end{aligned}$$

where $\widehat{M}(i)$ denotes the index of the specific ST, which won the ST's contention for the transmission opportunities provided by PT_i.

► The probability of $\mathbb{P}\{I^*(\widehat{M}(i)) = i|\widetilde{M}(i) = 1, \widetilde{M}(j) = 0\}$: Considering Scenario 3.1 exemplified by Fig 5.7(c1), PT_i and its one and only candidate cooperative ST partner constitute a cooperative pair without any PTs' contention, because no STs are capable of becoming the candidate partner of PT_j. Hence, the probability $\mathbb{P}\{I^*(\widehat{M}(i)) = i|\widetilde{M}(i) = 1, \widetilde{M}(j) = 0\}$ may be formulated as:

$$\mathbb{P}\{I^*(\widehat{M}(i)) = i|\widetilde{M}(i) = 1, \widetilde{M}(j) = 0\} = \mathbb{P}\{\widetilde{M}(i) = 1\} \cdot \mathbb{P}\{\widetilde{M}(j) = 0\}, \tag{5.25}$$

where $\mathbb{P}\{\widetilde{M}(j) = 0\}$ denotes the probability that no STs are capable of becoming the candidate cooperative partner of PT_j either due to the outage of the specific link from PT_j to ST (PTS) or because the required transmit power $P_{ST}(j, m)$ exceeds the maximum transmit power P_{max}. The probability $\mathbb{P}\{\widetilde{M}(j) = 0\}$ may be described by Eq (5.18). Furthermore, $\mathbb{P}\{\widetilde{M}(i) = 1\}$ denotes the probability of the event that PT_i has only a single candidate cooperative partner, which may correctly receive the data of PT_i and may also satisfy the transmit rate requirement of both PT_i and itself. Hence, the probability $\mathbb{P}\{\widetilde{M}(i) = 1\}$ may be expressed as:

$$\mathbb{P}\{\widetilde{M}(i) = 1\} = \sum_{m=1}^{\mathcal{M}} \sum_{P_x=P_1}^{P_{max}} \left\{ \mathbb{P}\{Z_{SU}(i, m, P_x)\} \cdot \prod_{n\in\mathcal{M}, n\neq m} \left(\overline{\mathbb{P}\{V_{SU}(i, n, P_x)\}} \right) \right\}. \tag{5.26}$$

► The probability of $\mathbb{P}\{I^*(\widehat{M}(i)) = i|\widetilde{M}(i) = 1, \widetilde{M}(j) > 0, \widehat{M}(i) \neq \widehat{M}(j), i \neq j\}$ When PT_i and PT_j have different ST winner as the outcome of the ST's contention, the specific winner $ST_{\widehat{M}(i)}$ which contended for the transmission opportunities provided by PT_i may not be the candidate cooperative partner of PT_j, namely we have $ST_{\widehat{M}(i)} \notin \mathcal{C}_{PT}(j)$. If $ST_{\widehat{M}(i)} \in \mathcal{C}_{PT}(j)$ is satisfied, then $ST_{\widehat{M}(i)}$ cannot win the contention for the specific transmission opportunities provided by PT_j. Hence, the probability $\mathbb{P}\{I^*(\widehat{M}(i)) = i|\widetilde{M}(i) = 1, \widetilde{M}(j) > 0, \widehat{M}(i) \neq \widehat{M}(j), i \neq j\}$ may be written as:

$$\begin{aligned}
&\mathbb{P}\{I^*(\widehat{M}(i)) = i|\widetilde{M}(i) = 1, \widetilde{M}(j) > 0, \widehat{M}(i) \neq \widehat{M}(j), i \neq j\} \\
&= \sum_{m=1}^{\mathcal{M}} \left\{ \underbrace{\mathbb{P}\{\widetilde{M}(i, m) = 1\}}_{\mathcal{C}_{PT}(i) = ST_m} \cdot \sum_{P_x=P_{p_1}}^{P_{max}} \left[\underbrace{\mathbb{P}\{\Psi_{SU}(j, m, P_x)\}}_{ST_m \notin \mathcal{C}_{PT}(j, P_x)} + \underbrace{\mathbb{P}\{W_{SU}(j, m, P_x)\}}_{m \neq \widehat{M}(j, P_x)} \right] \right\},
\end{aligned} \tag{5.27}$$

where $\mathbb{P}\{\widetilde{M}(i, m) = 1\}$ denotes the probability that ST_m is the only candidate cooperative

partner of PT_i, which may be expressed as:

$$\mathbb{P}\{\widetilde{M}(i,m)=1\}=\sum_{P_y=P_1}^{P_{max}}\left\{\mathbb{P}\{Z_{SU}(i,m,P_y)\}\cdot\prod_{n\in\mathcal{M},n\neq m}\left(\overline{\mathbb{P}\{V_{SU}(i,n,P_y)\}}\right)\right\}. \tag{5.28}$$

Based on the above discussions, the probability $\mathbb{P}\{Z_{SU}(i,m,P_y)\}$ was formulated in Eq (5.21) and Eq (5.22). Furthermore, let us introduce the variable $\Psi_{SU}(j,m,P_x)$ representing the event that ST_m cannot be the cooperative partner of PT_j, when PT_j has a candidate cooperative partner transmitting at the x-th power level P_x, therefore we have $\mathcal{C}_{PT}(j,P_x)\neq\emptyset$. Hence, the probability of $\mathbb{P}\{\Psi_{SU}(j,m,P_x)\}$ may be formulated as:

$$\mathbb{P}\{\Psi_{SU}(j,m,P_x)\}=\overline{\mathbb{P}\{V_{SU}(j,m,P_x)\}}\cdot\sum_{q=1}^{\mathcal{M}-1}\left(\mathbb{P}\{B_{SU}^{(q)}(j,m,P_x)\}\right), \tag{5.29}$$

where the probability of $\mathbb{P}\{B_{SU}^{(q)}(j,m,P_x)\}$ in Eq (5.29) was formulated in Eq (5.23), while $W_{SU}(j,m,P_x)$ in Eq (5.27) represents the event that ST_m does not win the contention, when we have $ST_m\in\mathcal{C}_{PT}(j,P_x)$. Hence, the probability of $\mathbb{P}\{W_{SU}(j,m,P_x)\}$ may be written as:

$$\begin{aligned}\mathbb{P}\{W_{SU}(j,m,P_x)\}=&Z_{SU}(j,m,P_x)\cdot\sum_{q=1}^{\mathcal{M}-1}\left(B_{SU}^{(q)}(j,m,P_x)\right)\\&\cdot\mathbb{P}\{m\neq\arg\min_{g}P_{ST}(j,g,P_x)|_{g\in(\boldsymbol{E}\cup m)}\},\end{aligned} \tag{5.30}$$

where $P_{ST}(j,g,P_x)$ denotes the transmit power promised by ST_g required for satisfying the transmit rate requirement of both PT_j and itself. According the ST selection scheme proposed in Section 5.3.2, the specific ST, which promises to require the lowest transmit power may win the contention.

► The probability of $\mathbb{P}\{I^*(\widehat{M}(i))=i|\widetilde{M}(i)=1,\widetilde{M}(j)>0,\widehat{M}(i)=\widehat{M}(j),i\neq j\}$: According to Eq (5.24), PT_i may acquire cooperative transmission assistance, when PT_i wins the competition with PT_j for the cooperative transmission assistance from the same ST, as exemplified by the Scenario 3.3 of in Fig 5.7(c3). More explicitly, when PT_j also has one and only cooperative ST candidate, namely we have $\widehat{M}(j)=1$, both PT_i and PT_j contend for acquiring access to this particular ST by increasing their transmit power level, whilst still satisfying the maximum transmit power constraint. However, when we have $\widehat{M}(j)>1$, PT_j may select other STs as its cooperative partner, if PT_i wins the competition. Hence, the probability of $\mathbb{P}\{I^*(\widehat{M}(i))=i|\widetilde{M}(i)=1,\widetilde{M}(j)>0,\widehat{M}(i)=\widehat{M}(j),i\neq j\}$ may be formulated

as:

$$\begin{aligned}
&\mathbb{P}\{I^*(\widehat{M}(i))=i|\widetilde{M}(i)=1,\widetilde{M}(j)>0,\widehat{M}(i)=\widehat{M}(j),i\neq j\}\\
&=\underbrace{\mathbb{P}\{I^*(\widehat{M})=i|\widetilde{M}(i)=1,\widetilde{M}(j)=1,\widehat{M}(i)=\widehat{M}(j),i\neq j\}}_{\mathcal{C}_{PT}(i)=\mathcal{C}_{PT}(j)=\{ST_m\},PT_i \text{ is winner},M^*(j)=0}\\
&+\underbrace{\mathbb{P}\{I^*(\widehat{M})=i|\widetilde{M}(i)=1,\widetilde{M}(j)>1,\widehat{M}(i)=\widehat{M}(j),i\neq j\}}_{\mathcal{C}_{PT}(i)=\{ST_m\},m=\widehat{M}(j),PT_i \text{ is winner, } M^*(j)=n\neq m}
\end{aligned} \tag{5.31}$$

▷ *The probability of* $\mathbb{P}\{I^*(\widehat{M}(i))=i|\widetilde{M}(i)=1,\widetilde{M}(j)=1,\widehat{M}(i)=\widehat{M}(j),i\neq j\}$*:* When both PT_i and PT_j have only one candidate cooperative partner, they have to increase their transmit power to win the cooperative opportunity provided by ST_m, if ST_m is the common candidate cooperative partner of both PT_i and PT_j. Hence, PT_i may become the cooperative partner of ST_m, provided that a lower transmit power is required when ST_m and PT_i form a cooperative pair, namely when we require the lowest power according to $P_{ST}(i,m,P_{max})<P_{ST}(j,m,P_{max})$. Therefore, the probability of $\mathbb{P}\{I^*(\widehat{M}(i))=i|\widetilde{M}(i)=1,\widetilde{M}(j)=1,\widehat{M}(i)=\widehat{M}(j),i\neq j\}$ may be characterized as:

$$\begin{aligned}
&\mathbb{P}\{I^*(\widehat{M}(i))=i|\widetilde{M}(i)=1,\widetilde{M}(j)=1,\widehat{M}(i)=\widehat{M}(j),i\neq j\}\\
&=\sum_{m=1}^{\mathcal{M}}\Big(\mathbb{P}\{\widetilde{M}(i,m)=1\}\cdot\mathbb{P}\{\widetilde{M}(j,m)=1\}\cdot\mathbb{P}\{P_{ST}(i,m,P_{max})<P_{ST}(j,m,P_{max})\}\Big).
\end{aligned} \tag{5.32}$$

▷ *The probability of* $\mathbb{P}\{I^*(\widehat{M}(i))=i|\widetilde{M}(i)=1,\widetilde{M}(j)>1,\widehat{M}(i)=\widehat{M}(j),i\neq j\}$*:* If ST_m is the common best candidate cooperative partner of PT_i and PT_j, ST_m intends to select the specific PT $PT_{\hat{i}}$, which requires a lower power $P_{ST}(\hat{i},m)$ for providing successful cooperative assistance. Hence, PT_i has to increase its transmission power $P_{PT}(i,m)$ for the sake of contending for the cooperative transmission assistance of ST_m, because ST_m is the only candidate cooperative partner. However, since PT_j has more than one candidate RNs, namely we have $\widetilde{M}(j)>1$, it may invite other candidate cooperative partners associated with the same PT power $P_{PT}(j,m)$, if ST_m selects another PT. Hence, the probability of $\mathbb{P}\{I^*(\widehat{M}(i))=i|\widetilde{M}(i)=1,\widetilde{M}(j)>1,\widehat{M}(i)=\widehat{M}(j),i\neq j\}$ may be formulated as:

$$\begin{aligned}
&\mathbb{P}\{I^*(\widehat{M}(i))=i|\widetilde{M}(i)=1,\widetilde{M}(j)>1,\widehat{M}(i)=\widehat{M}(j),i\neq j\}\\
&=\sum_{m=1}^{\mathcal{M}}\sum_{P_x=P_{p_1}}^{P_{max}}\Bigg\{\mathbb{P}\{Z_{SU}(i,m,P_x)\}\cdot B_{SU}^{(0)}(i,m,P_x)\cdot\sum_{P_y=P_{p_1}}^{P_{max}}\Bigg[\mathbb{P}\{Z_{SU}(j,m,P_y)\}\\
&\cdot\sum_{P_z=P_y}^{P_{max}}\sum_{q=1}^{\mathcal{M}-1}\Big(\mathbb{P}\{B_{SU}^{(q)}(j,m,P_z)\}\cdot\mathbb{P}\{U_{SU}(j,m,P_z)\}\Big)\Bigg]\Bigg\},
\end{aligned} \tag{5.33}$$

where $\mathbb{P}\{U_{SU}(j,m,P_z)\}$ is given by:

$$\mathbb{P}\{U_{SU}(j,m,P_z)\} = \begin{cases} F_{U1} & P_z = P_y \quad (5.34) \\ F_{U1} + F_{U2} & P_z > P_y \quad (5.35) \end{cases}$$

and where we have:

$$F_{U1} = \mathbb{P}\{m = \arg\min_{g} P_{ST}(j,g,P_z)|_{g\in(\boldsymbol{E}\cup m)}\} \cdot \mathbb{P}\{P_{ST}(i,m,P_x,r) < P_{ST}(j,m,P_z)\} \quad (5.36)$$

$$F_{U2} = \mathbb{P}\{m \neq \arg\min_{g} P_{ST}(j,g,P_z)|_{g\in(\boldsymbol{E}\cup m)}\} \cdot \mathbb{P}\{P_{ST}(i,m,P_x,r) < P_{ST}(j,m,P_{z-1})\}. \quad (5.37)$$

If PT_j cannot win the contention at the $(z-1)$-th power level P_{z-1} and we have $\mathcal{C}_{PT}(j,P_{z-1}) = \{ST_m\}$, PT_j has to increase its transmit power to next higher lever $P_z = P_{z-1} + \Delta$ for discovering new candidate cooperative partners, as seen in Table 5.2 and Fig 5.3. When we have $\widetilde{M}(j,P_z) > 1$, PT_j may find a new winner of the ST's contention at a transmit power of P_z and may hence stop contending for the cooperative transmission assistance from ST_m as seen in Table 5.2 and Fig 5.3. Hence, F_{U2} denotes the probability of the event that PT_j selects the new winner of the ST's contention.

Based on our analysis above, we can now calculate the departure rate $\mu_{PT_i}^{coop}$ at PT_i, which relies on cooperation, as formulated by Eq (5.16).

Departure Rate of $\mu_{PT_i}^{noncoop}$***:*** According to the proposed DWWRS-MAS in Section 5.3, PT_i may not be capable of acquiring cooperative transmission assistance in one of the following scenarios:

- When *no* ST contends for the transmission opportunity granted by PT_i even at the highest power level of PT_i, namely we have $P_{PT}(i) = P_{max}$, PT_i has to directly transmit its data to the destination without cooperative transmission, as seen in Fig 5.3 and Table 5.1.
- When both PT_i and PT_j have data to send at the beginning of current time slot and we have $\mathcal{C}_{PT}(i) = \{ST_m\}$, then ST_m may select the other PT, namely PT_j as its cooperative partner, if we have $ST_m \in \mathcal{C}_{PT}(j)$ and $P_{ST}(j,m) < P_{ST}(i,m)$, as exemplified by the Scenario 3.4 of Fig 5.7(c4). More explicitly, PT_1 and PT_2 of Fig 5.7(c4) contend for acquiring cooperative transmission assistance from ST_1. However, PT_2 is the winner of the PTs' contention. Since the only candidate cooperative partner of PT_1, namely ST_1 selects PT_2 as its cooperative partner as shown in Fig 5.7(c4), PT_1 has to directly transmit its data to the destination, namely we have $M^*(1) = 0$.

Based on the above discussions, the probability that PT_i cannot acquire cooperative trans-

mission assistance is equal to the sum of the probability that PT_i has no candidate cooperative partner under the maximum transmit power constraint and the probability of Scenario 3.4 of Fig 5.7(c4), where PT_i has only a single candidate cooperative partner and fails to win the PTs' contention, as shown in Fig 5.8. Hence, the average non-cooperative departure rate at PT_i may be written as:

$$\mu_{PT_i}^{noncoop} = \mathbb{P}\{\widetilde{M}(i) = 0\} + \underbrace{\mathbb{P}\{Q_{PT_j} \neq 0|_{i\neq j}\} \cdot \mathbb{P}\{T_{PT_i}^{noncoop}|\widetilde{M}(i) = 1\}}_{\text{Scenario 3.4 of Fig 5.7(c4)}}, \tag{5.38}$$

Where the probability of $\mathbb{P}\{\widetilde{M}(i) = 0\}$ is given by Eq (5.18). According to the behaviour of PT_i shown in Fig 5.3 and Table 5.3, when it has only one candidate cooperative partner, namely ST_m, the probability of $\mathbb{P}\{T_{PT_i}^{noncoop}|\widetilde{M}(i) = 1\}$ in Eq (5.38) may be characterized as:

$$\begin{aligned}
&\mathbb{P}\{T_{PT_i}^{noncoop}|\widetilde{M}(i) = 1\} \\
&= \underbrace{\mathbb{P}\{I^*(\widehat{M}(i)) = j|\widetilde{M}(i) = 1, \widetilde{M}(j) = 1, \widehat{M}(i) = \widehat{M}(j), i \neq j\}}_{\mathcal{C}_{PT}(i) = \{ST_m\},\ \widetilde{M}(j) = 1,\ \text{but } ST_m \text{ selects } PT_j} \\
&+ \underbrace{\mathbb{P}\{I^*(\widehat{M}(i)) = j|\widetilde{M}(i) = 1, \widetilde{M}(j) > 1, \widehat{M}(i) = \widehat{M}(j), i \neq j\}}_{\mathcal{C}_{PT}(i) = \{ST_m\},\ \widetilde{M}(j) > 1,\ \text{but } ST_m \text{ selects } PT_j}.
\end{aligned} \tag{5.39}$$

Let us first derive the probability of $\mathbb{P}\{I^*(\widehat{M}(i)) = j|\widetilde{M}(i) = 1, \widetilde{M}(j) = 1, \widehat{M}(i) = \widehat{M}(j), i \neq j\}$.

► *The probability of* $\mathbb{P}\{I^*(\widehat{M}(i)) = j|\widetilde{M}(i) = 1, \widetilde{M}(j) = 1, \widehat{M}(i) = \widehat{M}(j), i \neq j\}$*:* When we have $\mathcal{C}_{PT}(i) = \mathcal{C}_{PT}(j) = \{ST_m\}$, both PT_i and PT_j have to increase their transmit power to win the cooperative opportunity provided by ST_m until their transmit power reaches the maximum power of P_{max}, as seen in Fig 5.3 and Table 5.1. Hence, PT_i cannot be the winner of PT's contention, if we have $P_{ST}(i, m, P_{max}) > P_{ST}(j, m, P_{max})$. Therefore, the probability of $\mathbb{P}\{I^*(\widehat{M}(i)) = j|\widetilde{M}(i) = 1, \widetilde{M}(j) = 1, \widehat{M}(i) = \widehat{M}(j), i \neq j\}$ may be characterized as:

$$\begin{aligned}
&\mathbb{P}\{I^*(\widehat{M}(i)) = j|\widetilde{M}(i) = 1, \widetilde{M}(j) = 1, \widehat{M}(i) = \widehat{M}(j), i \neq j\} \\
&= \sum_{m=1}^{\mathcal{M}} \Big(\mathbb{P}\{\widetilde{M}(i, m) = 1\} \cdot \mathbb{P}\{\widetilde{M}(j, m) = 1\} \cdot \mathbb{P}\{P_{ST}(i, m, P_{max}) > P_{ST}(j, m, P_{max})\}\Big).
\end{aligned} \tag{5.40}$$

► *The probability of* $\mathbb{P}\{I^*(\widehat{M}(i)) = j|\widetilde{M}(i) = 1, \widetilde{M}(j) > 1, \widehat{M}(i) = \widehat{M}(j), i \neq j\}$*:* According to the proposed DWWRS-MAS in Section 5.3, if multiple PTs intend to become the cooperative partner of ST_m, the losers of the contention have to increased their transmit power P_{PT} for continued contention for the cooperative transmission opportunity, when they have *only one* candidate cooperative partner, as seen in Fig 5.3 and Table 5.1. Al-

ternatively, they have to select other candidate cooperative partners without opting for a higher power level, when they have *more than one* candidate cooperative partners, as dictated by the PTs' behaviour shown in Fig 5.3 and Table 5.1. Hence, the probability of $\mathbb{P}\{I^*(\widehat{M}(i)) = j|\widetilde{M}(i) = 1, \widetilde{M}(j) > 1, \widehat{M}(i) = \widehat{M}(j), i \neq j\}$ may be formulated as:

$$\begin{aligned}
&\mathbb{P}\{I^*(\widehat{M}(i)) = j|\widetilde{M}(i) = 1, \widetilde{M}(j) > 1, \widehat{M}(i) = \widehat{M}(j), i \neq j\} \\
&= \sum_{m=1}^{\mathcal{M}} \sum_{P_x=P_{p1}}^{P_{max}} \Bigg\{ \mathbb{P}\{Z_{SU}(i,m,P_x)\} \cdot \mathbb{P}\{B_{SU}^{(0)}(i,m,P_x)\} \cdot \sum_{P_y=P_{p1}}^{P_{max}} \Bigg[\mathbb{P}\{Z_{SU}(j,m,P_y)\} \\
&\cdot \sum_{P_z=P_y}^{P_{max}} \sum_{q=1}^{\mathcal{M}-1} \Big(\mathbb{P}\{B_{SU}^{(q)}(j,m,P_z)\} \cdot \mathbb{P}\{\Phi_{SU}(j,m,P_z)\} \Big) \Bigg] \Bigg\}, \qquad (5.41)
\end{aligned}$$

where $\mathbb{P}\{\Phi_{SU}(j,m,P_z)\}$ may be expressed as:

$$\mathbb{P}\{\Phi_{SU}(j,m,P_z)\} = \begin{cases} F_{\Phi 1} & P_z = P_y \qquad (5.42) \\ F_{\Phi 1} + F_{\Phi 2} & P_z > P_y, \qquad (5.43) \end{cases}$$

and where we have:

$$F_{\Phi 1} = \mathbb{P}\{m = \arg\min_g P_{ST}(j,g,P_z)|_{g\in(\boldsymbol{E}\cup m)}\} \cdot \mathbb{P}\{P_{ST}(i,m,P_x) > P_{ST}(j,m,P_z)\} \qquad (5.44)$$

$$F_{\Phi 2} = \mathbb{P}\{m \neq \arg\min_g P_{ST}(j,g,P_z)|_{g\in(\boldsymbol{E}\cup m)}\} \cdot \mathbb{P}\{P_{ST}(i,m,P_x) > P_{ST}(j,m,P_{z-1})\}, \qquad (5.45)$$

with $F_{\Phi 1}$ denoting the event that PT_j and ST_m constitute a cooperative pair $\mathcal{O}(PT_j, ST_m)$, when we have $\widetilde{M}(j,P_z) > 1$ and ST_m is the best candidate cooperative partner of both PT_i and of PT_j, provided that they intend to transmit their data at power P_z. Furthermore, PT_j may encounter a new winner of the STs' contention, when it opts for a higher transmit power level P_z. However, if PT_j wins the PTs' contention with a power of P_{z-1}, our DWWRS-MAS will still form the cooperative pair $\mathcal{O}(PT_j, ST_m)$ for the sake of conserving the transmit power for PT_j. In Eq (5.45) $F_{\Phi 2}$ denotes the event that PT_j and ST_m constitute a cooperative pair $\mathcal{O}(PT_j, ST_m)$, when PT_j wins the PTs' contention with a power of P_{z-1} and it may encounter a new winner of the STs' contention when it opts for a higher transmit power level P_z. Based on the above discussions, the departure rate at PT_i achieved by the non-cooperative transmission is given by Eq (5.38), which relies on Eq (5.39).

According to Eq (5.15), the total departure rate at PT_i in our system is characterized by the sum the cooperative departure rate of Eq (5.16) and that of its non-cooperative counterpart in Eq (5.38). This summation is necessary, because the PT's data may be successfully delivered to the destination with the aid of cooperative transmission from its cooperative partner or may be directly transmitted from the PT to the destination, as illustrated by Fig 5.3 in Section 5.3. Hence, the queue of PT_i is stable, as long as we satisfy $\lambda_{PT_i} < \mu_{PT_i}^{max}$.

5.4.1.3 Stability of the Secondary Source Node's Queue

Stability of Q_{PT,ST_m}***:*** In order to support cooperative transmissions, the ST ST_m is assumed to rely on the pair of queues Q_{ST_m} and Q_{PT,ST_m} for buffering both its own data and the PT's data, respectively, as shown in Fig 5.6. Based on our DWWRS-MAS proposed in Section 5.3, ST_m stores the PTs' data in Q_{PT,ST_m}, if the following two conditions are satisfied: (1) at least one PT has data to send at the beginning of the current time slot; (2) ST_m has a cooperative partner, namely we have $I^*(m) \neq 0$. Hence, the arrival rate of the PT's data at ST_m achieved in the scenario of having two PTPs as shown in Fig 5.6 may be written as:

$$\lambda_{PT,ST_m} = \underbrace{\sum_{i=1}^{2}\Big(\mathbb{P}\{Q_{PT_i} \neq 0\} \cdot \mathbb{P}\{Q_{PT_j} = 0|_{i\neq j}\} \cdot \mathbb{P}\{T^{(1)}_{ST_m}(i)\}\Big)}_{\text{only one PT has data to send}} + \underbrace{\prod_{i=1}^{2}\mathbb{P}\{Q_{PT_i} \neq 0\} \cdot \mathbb{P}\{T^{(2)}_{ST_m}\}}_{\text{both PTs have data to send}} \tag{5.46}$$

Based on the above discussion, the probability of $\mathbb{P}\{Q_{PT_i} \neq 0\}$ is given by $\lambda_{PT_i}/\mu^{max}_{PT_i}$ according to Little's theorem of Section 2.4 [198]. Furthermore, $\mathbb{P}\{T^{(1)}_{ST_m}(i)\}$ represents the probability that ST_m and PT_i form a cooperative partner, when only PT_i has data to send at the beginning of the current time slot, as exemplified by Scenario 1 of Fig 5.7(a), which may be formulated as:

$$\mathbb{P}\{T^{(1)}_{ST_m}(i)\} = \mathbb{P}\{M^*(i) = m|\widetilde{M}(i) = 1\} + \mathbb{P}\{M^*(i) = m|\widetilde{M}(i) > 1\}, \tag{5.47}$$

where $\mathbb{P}\{M^*(i) = m|\widetilde{M}(i) = 1\}$ denotes the probability that ST_m and PT_i constitute a cooperative pair when we have $\mathcal{C}_{PT}(i) = \{ST_m\}$ and only PT_i has data to send, which may be written as:

$$\mathbb{P}\{M^*(i) = m|\widetilde{M}(i) = 1\} = \sum_{P_x=P_1}^{P_{max}}\Big\{\mathbb{P}\{Z_{SU}(i,m,P_x)\} \cdot B^{(0)}_{SU}(i,m,P_x)\Big\}. \tag{5.48}$$

Furthermore, the expression of $\mathbb{P}\{M^*(i) = m|\widetilde{M}(i) > 1\}$ in Eq (5.47) represents the probability that PT_i forms a cooperative pair with ST_m, which is the winner of the STs' competition, when only PT_i has data to send and multiple STs become the candidate cooperative partners of PT_i, namely when we have $\widetilde{M}(i) > 1$. According to our DWWRS-MAS proposed in Section 5.3, $\mathbb{P}\{M^*(i) = m|\widetilde{M}(i) > 1$ may be expressed as:

$$\mathbb{P}\{M^*(i) = m|\widetilde{M}(i) > 1\} = \sum_{P_x=P_{p_1}}^{P_{max}}\Big\{\mathbb{P}\{Z_{SU}(i,m,P_x)\} \cdot \mathbb{P}\{\Lambda_{SU}(i,m,P_x)\}\Big\}, \tag{5.49}$$

where $\mathbb{P}\{\Lambda_{SU}(i,m,P_x)\}$ may be written as:

$$\mathbb{P}\{\Lambda_{SU}(i,m,P_x)\} = \sum_{q=1}^{\mathcal{M}-1} \Big(\mathbb{P}\{B_{SU}^{(q)}(i,m,P_x)\} \cdot \mathbb{P}\{m = \arg\min_{g} P_{ST}(i,g,P_x)|_{g\in(\boldsymbol{E}\cup m)}\}\Big). \tag{5.50}$$

Let us now introduce the notation $\mathbb{P}\{T_{ST_m}^{(2)}\}$, which denotes the probability that ST_m is capable of acquiring a cooperative transmission opportunity leased by its cooperative partner, when both PT_1 and PT_2 have data to send at the beginning of the current time slot. Hence, the probability of $\mathbb{P}\{T_{ST_m}^{(2)}\}$ may be formulated as:

$$\mathbb{P}\{T_{ST_m}^{(2)}\} = \mathbb{P}\{T_{ST_m}|M_1^* = m\} + \mathbb{P}\{T_{ST_m}|M_2^* = m\}, \tag{5.51}$$

where $\mathbb{P}\{T_{ST_m}|M_1^* = m\}$ denotes the probability of the event that ST_m wins over a cooperative partner by promising the lowest transmit power of P_{ST}, as exemplified by the ST_1 of Scenario 2 in Fig 5.7(b) and of Scenario 3 in Fig 5.7(c). Furthermore, $\mathbb{P}\{T_{ST_m}|M_2^* = m\}$ denotes the probability of the specific event that ST_m is selected by its cooperative partner $PT_{I^*(m)}$, when $PT_{I^*(m)}$ fails to win the PTs' competition for acquiring a cooperative transmission assistance from the winner of the STs' competition, say from ST_n as exemplified by ST_2 in Scenario 2.4 of Fig 5.7(b4). More explicitly, as seen in Fig 5.7(b4), PT_1 and PT_2 contend for a cooperative transmission assistance provided by ST_1, which is the common winner of the STs' competition for a transmission opportunity leased by PT_1 and PT_2. However, ST_1 in Fig 5.7(b4) selects PT_2 as its cooperative partner for the sake of reducing its power. Hence, PT_1 forms a cooperative pair with ST_2 which also is capable of providing cooperative transmission assistance for PT_1 even without requiring an increased transmit power of PT_1, as seen in Fig 5.7(b4). Let us first elaborate on the probability of $\mathbb{P}\{T_{ST_m}|M_1^* = m\}$.

The probability of $\mathbb{P}\{T_{ST_m}|M_1^* = m\}$: According to the proposed DWWRS-MAS, ST_m is capable of acquiring a transmission opportunity, if it is the one and only candidate cooperative partner of any PT, as exemplified by ST_1 in Fig 5.7(c) or if it is the winner of the STs' contention, as exemplified by ST_1 in Fig 5.7(b) and Fig 5.7(b3), regardless whether multiple PTs contend for cooperative transmission assistance from ST_m or not. Hence, the probability of $\mathbb{P}\{T_{ST_m}|M_1^* = m\}$ may be formulated as:

$$\mathbb{P}\{T_{ST_m}|M_1^* = m\} = 1 - \prod_{i=1}^{2} \Big(\overline{\mathbb{P}\{T_{ST_m}(PT_i)|M_1^* = m\}}\Big), \tag{5.52}$$

where $\overline{\mathbb{P}\{T_{ST_m}(PT_i)|M_1^*=m\}}$ is given by $1-\mathbb{P}\{T_{ST_m}(PT_i)|M_1^*=m\}$. The probability $\mathbb{P}\{T_{ST_m}(PT_i)|M_1^*=m\}$ denotes the sum of the probabilities of two events. The first event is one, when ST_m is the only candidate cooperative partner of PT_i, i.e. when we have $\widetilde{M}(i)=1$. The second event when ST_m is the winner of the STs' contention, i.e. when we have $\widetilde{M}(i)>1$. Hence, we arrive at:

$$\mathbb{P}\{T_{ST_m}(PT_i)|M_1^*=m\}=\sum_{P_x=P_{p_1}}^{P_{max}}\Big\{\mathbb{P}\{Z_{SU}(i,m,P_x)\}\cdot\Big(\mathbb{P}\{B_{SU}^{(0)}(i,m,P_x)\}+\mathbb{P}\{\Lambda_{SU}(i,m,P_x)\}\Big)\Big\}, \tag{5.53}$$

where $\mathbb{P}\{\Lambda_{SU}(i,m,P_x)\}$ is given by Eq (5.50), while $Z_{SU}(i,m,P_x)$ is expressed by Eq (5.21) and Eq (5.22). Moreover, $\mathbb{P}\{B_{SU}^{(q)}(i,m,P_x)\}$ is formulated by Eq (5.23).

The probability of $\mathbb{P}\{T_{ST_m}|M_2^*=m\}$: When a PT, such as PT_i contends with other PTs for the cooperative transmission assistance of say ST ST_n, PT_i cannot win the competition, if it requires higher power, i.e. we have $P_{ST}(i,n,P_x)>P_{ST}(j,n,P_y)$. Then PT_i invites other STs to become its cooperative partner at the same PT transmit power of P_y, as seen in Table 5.3. Hence, the ST ST_m, which promised the second lowest ST transmit power is capable of winning a transmission opportunity provided by the PT PT_i, as exemplified by ST_2 in Fig 5.7(b4). Therefore, the probability of $\mathbb{P}\{T_{ST_m}|M_2^*=m\}$ may be characterized as:

$$\begin{aligned}&\mathbb{P}\{T_{ST_m}|M_2^*=m\}\\&=\sum_{i=1}^{2}\sum_{n\in\mathcal{M},n\neq m}\sum_{P_x=P_{p_1}}^{P_{max}}\Big\{\mathbb{P}\{\Gamma_{SU}(j,n,P_x)\}\cdot\sum_{P_y=P_{p_1}}^{P_{max}}\Big[\mathbb{P}\{Z_{SU}(i,n,P_y)\}\\&\cdot\sum_{P_z=P_y}^{P_{max}}\sum_{q=1}^{\mathcal{M}-1}\left(\mathbb{P}\{A_{SU}^{(q)}(i,n,P_z)\}\cdot\mathbb{P}\{\Omega_{SU}(i,m,P_z)\}\right)\Big]\Big\}.\end{aligned} \tag{5.54}$$

When PT_j only has a single candidate partner say ST_n, namely we have $\widetilde{M}(j)=1$, ST_n will become the cooperative partner of PT_j without contending with other STs, provided that PT_j requires a low power according to $P_{ST}(j,n)<P_{ST}(i,n)$. Furthermore, PT_j and ST_n may form a cooperative pair, if ST_n is the winner of the STs' contention and it requires a low power, as indicated by $P_{ST}(j,n)<P_{ST}(i,n)$, when $\widetilde{M}(j)>1$. Hence the probability of $\mathbb{P}\{\Gamma_{SU}(j,n,P_x)\}$ in Eq (5.54) may be formulated as:

$$\mathbb{P}\{\Gamma_{SU}(j,n,P_x)\}=\mathbb{P}\{\Gamma_{SU}(j,n,P_x)|\widetilde{M}(j)=1\}+\mathbb{P}\{\Gamma_{SU}(j,n,P_x)|\widetilde{M}(j)>1\}, \tag{5.55}$$

where we have

$$\mathbb{P}\{\Gamma_{SU}(j,n,P_x)|\widetilde{M}(j)=1\}=\mathbb{P}\{Z_{SU}(j,n,P_x)\}\cdot\mathbb{P}\{B_{SU}^{(0)}(j,n,P_x)\} \tag{5.56}$$

$$\mathbb{P}\{\Gamma_{SU}(j,n,P_x)|\widetilde{M}(j)>1\}=\mathbb{P}\{Z_{SU}(j,n,P_x)\}\cdot\mathbb{P}\{\Lambda_{SU}(j,n,P_x)\}. \tag{5.57}$$

Still referring to Eq (5.54) $\mathbb{P}\{A_{SU}^{(q)}(i,n,P_z)\}$ denotes the probability that PT_i has q candidate cooperative partners apart from ST_n and $ST_m \in \mathcal{C}_{PT}(i)$. Hence, the probability $\mathbb{P}\{A_{SU}^{(q)}(i,n,P_z)\}$ in Eq (5.54) may be formulated as:

$$\mathbb{P}\{A_{SU}^{(q)}(i,n,P_z)\}=\prod_{k\in\mathcal{K}}\mathbb{P}\{Z_{SU}(i,k,P_z)\}\cdot\prod_{w\in\mathcal{W}}\overline{\mathbb{P}\{V_{SU}(i,w,P_z)\}}, \tag{5.58}$$

subject to $m\in\mathcal{K}$, $\mathcal{K}\cap\mathcal{W}=\emptyset$ and $\mathcal{K}\cup\mathcal{W}\cup n=\mathcal{M}$, where $\mathcal{K}$ denotes the set of the q candidate cooperative partners of PT_i apart from ST_n, while $\mathcal{W}$ is the set of STs, which cannot become the candidate cooperative partner either due to the outage of the PTS link or because the transmit power necessitated for satisfying the transmit rate requirements of both PT_i and itself exceed the maximum affordable transmit power. The size of the set $\mathcal{K}$ and $\mathcal{W}$ is given by q and $(\mathcal{M}-1-q)$, respectively.

Furthermore, the probability $\mathbb{P}\{\Omega_{SU}(i,m,P_z)\}$ in Eq (5.54) is formulated as:

$$\mathbb{P}\{\Omega_{SU}(i,m,P_z)\}=\begin{cases}F_{\Omega_1} & P_z=P_y \quad (5.59)\\ F_{\Omega_1}+F_{\Omega_2} & P_z>P_y, \quad (5.60)\end{cases}$$

where we have:

$$\begin{aligned}F_{\Omega_1}=&\mathbb{P}\{n=\arg\min_g P_{ST}(i,g,P_z)|_{g\in(\mathcal{K}\cup n)}\}\cdot\mathbb{P}\{m=\arg\min_l P_{ST}(i,l,P_z)|_{l\in\mathcal{K}}\}\\&\cdot\mathbb{P}\{P_{ST}(j,n,P_x)<P_{SU}(i,n,P_z)\} \quad (5.61)\\ F_{\Omega_2}=&\mathbb{P}\{m=\arg\min_g P_{ST}(i,g,P_z)|_{g\in(\mathcal{K}\cup n)}\}\cdot\mathbb{P}\{P_{ST}(j,n,P_x)<P_{SU}(i,n,P_{z-1})\}. \quad (5.62)\end{aligned}$$

When ST_m and PT_i constitute a cooperative pair, ST_m provides a data output for both the relaying queue Q_{PT,ST_m} and for the data queue Q_{ST_m} by exploiting superposition coding. In order to decouple the interaction between these two queues, we assume that if the ST's data queue Q_{ST_m} is empty, but Q_{PT,ST_m} has packets in its buffer, then the ST ST_m will superimpose the PT's data on a "dummy" packet. According to the proposed DWWRS-MAS, ST_m may be granted a transmission opportunity for conveying data in the queue Q_{PT,ST_m} and Q_{ST_m}, provided that both of the following two conditions are satisfied:

1. At least one PT has data to send at the beginning of the current time slot;
2. The ST ST_m becomes the cooperative partner of an active PT.

Therefore, the departure rate of the relaying queue Q_{PT,ST_m} may be expressed as:

$$\mu_{PT,ST_m} = \sum_{i=1}^{2} \Big(\mathbb{P}\{Q_{PT_i} \neq 0\} \cdot \mathbb{P}\{Q_{PT_j} = 0|_{i \neq j}\} \cdot \mathbb{P}\{T_{ST_m}^{(1)}(i)\} \Big) + \prod_{i=1}^{2} \mathbb{P}\{Q_{PT_i} \neq 0\} \cdot \mathbb{P}\{T_{ST_m}^{(2)}\}. \tag{5.63}$$

By composing the arrival rate of the PT's data at ST_m, according to Eq (5.46) and the departure rate of the relaying queue Q_{PT,ST_m} in Eq (5.63), we have:

$$\lambda_{PT,ST_m} = \mu_{PT,ST_m}. \tag{5.64}$$

The fundamental goal of the proposed DWWRS-MAS also transpires from Eq (5.64), namely that each arriving data transmission request will always be satisfied immediately in the relaying queue Q_{PT,ST_m}. Hence, the relaying queue Q_{PT,ST_m} always remains empty.

Stability of Q_{ST_m}***:*** Based on the proposed DWWRS-MAS, the ST ST_m jointly encodes a packet of its own data in the data queue Q_{ST_m} and a packet of the PT's data in the relaying queue Q_{PT,ST_m} by superposition coding, provided that ST_m constitutes a cooperative pair with one of the PTs. Hence, the queues Q_{PT,ST_m} and Q_{ST_m} have the same average departure rate, namely we have:

$$\begin{aligned} \mu_{ST_m} = \mu_{PT,ST_m} = & \sum_{i=1}^{2} \Big(\mathbb{P}\{Q_{PT_i} \neq 0\} \cdot \mathbb{P}\{Q_{PT_j} = 0|_{i \neq j}\} \cdot \mathbb{P}\{T_{ST_m}^{(1)}(i)\} \Big) \\ & + \prod_{i=1}^{2} \mathbb{P}\{Q_{PT_i} \neq 0\} \cdot \mathbb{P}\{T_{ST_m}^{(2)}\}. \end{aligned} \tag{5.65}$$

Based on the above analysis, the stability of the relay's data queue requires $\lambda_{ST_m} < \mu_{ST_m}$.

5.4.2 Algorithmic Stability of the Proposed DWWRS-MAS

A common and realistic assumption in a cooperative cognitive network is that both the PT and the ST focus their efforts on optimizing their own OF when they contend with other PTs or STs. Hence, based on the matching theory [216], this section analyzes the algorithmic stability of the proposed DWWRS-MAS by bearing in mind the selfish behaviour of both the PTs and the STs. Before analyzing the algorithmic stability of our DWWRS-MAS, let us first introduce the definition of a 'blocking pair' and of 'stable matching'.

When considering a stable marriage problem [216, 218], which seeks stable matching of K men and V women, a marriage matching X is blocked by the married couple (a, b), if man a and woman b prefer to get married with each other over their current partner $X(a)$ and $X(b)$ in matching X, where we have $X(a) \neq b$ and $X(b) \neq a$. The married couple (a, b) is

hence referred to as a 'blocking pair'. Hence, a 'stable matching' is defined as a matching without being prevented by 'blocking pair' [216,218]. An example of the problem is provided in Table 5.4. The number $(10, 7)$ in the cross-over point of man 1 and woman 1 indicates that the preference factor of man 1 is 10 for marrying woman 1, while the preference factor of women 1 is 7 for marrying man 1. This definition implies that man 1 prefers women 1 over women 2, man 2 prefers woman 2 over woman 1, woman 1 prefers man 1 over man 2 and woman 2 prefers man 2 over man 1, as shown in Table 5.4. Hence, the stable marriage problem of Table 5.4 is formulated as $X_{stable} = \{(1, 1), (2, 2)\}$,as seen in Fig 5.9(a). Furthermore, the matching $X_{unstable} = \{(1, 2), (2, 1)\}$ formed on the basis of the marriage problem of Table 5.4 is un-stable, because man 2 prefers woman 2 over woman 1 and woman 2 prefers man 2 over man 1, as shown in Fig 5.9(b). Hence, the matching $X_{unstable}$ is blocked by the blocking pair $(2, 2)$ in Fig 5.9(b).

TABLE 5.4: Example of Stable Marriage matching

	Woman 1	Woman 2
Man 1	(10,7)	(7,7)
Man 2	(5,10)	(10,10)

Based on the above discussions, we refer to a pair (PT_i, ST_m) as a blocking pair, if both PT_i and ST_m are capable of reducing their transmit power by acting as a cooperative pair $\mathcal{O}(PT_i, ST_m)$ by breaking their current cooperative pair $\mathcal{O}(PT_i, ST_{M^*(i)})$ and $\mathcal{O}(PT_{I^*(m)}, ST_m)$, where we have $M^*(i) \neq m$ and $I^*(m) \neq i$. The set of cooperative pairs, which is constructed according to our DWWRS-MAS is referred to here as a cooperative matching $X_{DWWRS-MAS}$. Hence, a cooperative matching $X_{DWWRS-MAS}$ is stable, when no blocking pair exists in $X_{DWWRS-MAS}$. Based on the above definitions, we have the following proposition.

Proposition 5.1: The proposed DWWRS-MAS of Section 5.3 produces a stable cooperative matching.

Proof: Assuming that the cooperative matching $X_{DWWRS-MAS}$ produced by our DWWRS-MAS is blocked by a blocking pair (PT_i, ST_m), we have:

$$P_{PT}(i, m) < P_{PT}[i, M^*(i)], \tag{5.66}$$

$$P_{ST}(i, m) < P_{ST}[I^*(m), m], \tag{5.67}$$

where $ST_{M^*(i)}$ and $PT_{I^*(m)}$ are the current cooperative partners of PT_i and ST_m in the cooperative matching $X_{DWWRS-MAS}$, respectively. Based on our DWWRS-MAS proposed in Section 5.3, PT_i first discovers its cooperative partner with the aid of lowest transmit power $P_{PT}(i) = P_{p_1}$. If PT_i fails to find a cooperative partner at the power of P_{p_1}, it

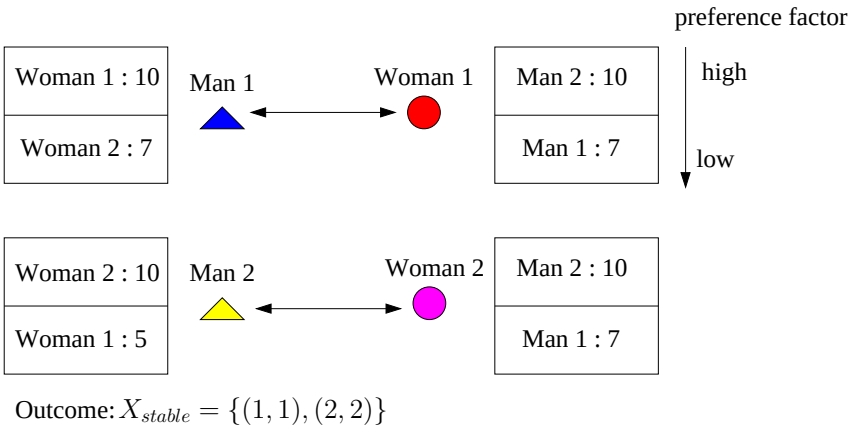

(a) Stable Maching

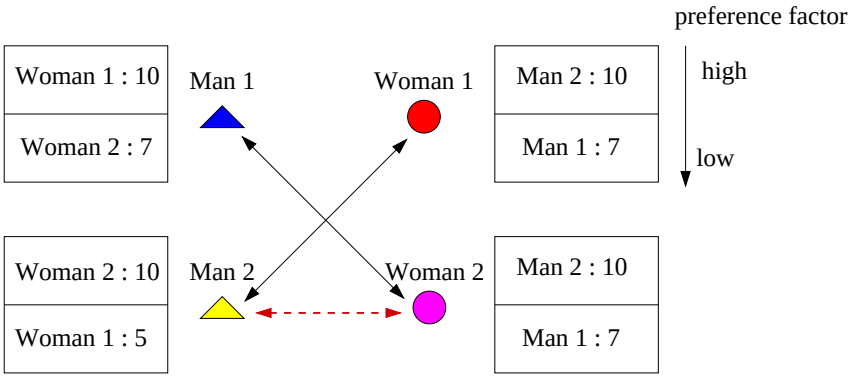

(b) Unstable Maching

FIGURE 5.9: Example of both stable and unstable marriage matching based on Table 5.4.

repeats the discovery procedure by increasing its power to the next higher power level, as seen in Fig 5.4 and Fig 5.3 as well as Table 5.1. Hence, Eq (5.66) implies that PT_i first selects ST_m as its cooperative partner at he lower power of $P_{PT}(i,m)$, but ST_m intends to provide cooperative transmission assistance for another PT for the sake of minimizing its transmit power. Hence PT_i has to increase its power to $P_{PT}[i, M^*(i)]$ in order to form a cooperative pair $\mathcal{O}(PT_i, ST_{M^*(i)})$ based on cooperative matching $X_{DWWRS-MAS}$, as designed by our DWWRS-MAS of Section 5.3. However, this contradicts the assumption formulated in Eq (5.67), which implies that ST_m prefers to form a cooperative pair for minimizing its transmit power. Hence, the cooperative matching $X_{DWWRS-MAS}$ produced by our DWWRS-MAS is stable.

Proposition 5.1 illustrates that the specific PT and ST, which constitute a cooperative pair according to our DWWRS-MAS cannot simultaneously reduce their transmit power, if they select another ST or PT as their cooperative partner.

Based on Proposition 5.1, we can derive the following proposition.

Proposition 5.2: The specific PT in the cooperative pair produced by our DWWRS-MAS is capable of conserving either the same power or in fact more power than in any other cooperative pair produced by any other stable matching algorithm having the same OFs, whilst relying on the same system configuration as our DWWRS-MAS.

Proof: Let us assume that the transmit power of PT_i is lower in the cooperative pair $\mathcal{O}_{other}(PT_i, ST_n)$ produced by another stable matching algorithm than that consumed by the cooperative pair $\mathcal{O}_{DWWRS-MAS}(PT_i, ST_m)$ produced by the proposed DWWRS-MAS, which is formulated as:

$$P_{PT}^{other}(i,n) < P_{PT}^{DWWRS-MAS}(i,m). \tag{5.68}$$

Since the other stable matching algorithm and our DWWRS-MAS has the same system configuration, the PTs in both systems have the same lowest power, which is the lowest power level. More explicitly we have $P_{p1}^{DWWRS-MAS} = P_{p1}^{other}$ and the same PT power control step size Δ. According to our DWWRS-MAS proposed in Section 5.3, PT_i has to increase its transmit power in order to seek a cooperative partner, when it cannot find a cooperative partner at a lower transmit power, as seen in Fig 5.4 and Fig 5.3 as well as in Table 5.1. Hence, Eq (5.68) implies that PT_i cannot form a cooperative partner with any STs, including ST_n by using the power of $P_{PT}^{other}(i,n)$ in our DWWRS-MAS. Therefore, PT_i has to increase its power to $P_{PT}^{DWWRS-MAS}(i,m)$ and then select ST_m as its cooperative partner. According to our DWWRS-MAS, ST_n cannot be the cooperative partner of PT_i in the following two scenarios:

- In the first scenario, ST_n cannot afford the transmit power $P_{ST}^{other}(i,n)$ required for satisfying the transmit rate requirement of both PT_i and ST_n under the maximum transmit power constraint. However, this phenomenon contradicts to the assumption that PT_i and ST_n constitute a cooperative pair $\mathcal{O}_{other}(PT_i, ST_n)$ in the system relying on another stable matching algorithm rather than on DWWRS-MAS. Based on the same system configuration and the same transmit power of $P_{ST}^{other}(i,n)$, ST_n is capable of successfully conveying data for both PT_i and itself in our DWWRS-MAS if it is acting as the cooperative partner of PT_i in the system relying on another stable matching algorithm. Hence, the assumption formulated by Eq (5.68) is false in this scenario.
- In the second scenario, according to our DWWRS-MAS, if ST_n is capable of satisfying the transmit requirements of both PT_i and itself, ST_n may opt out of becoming the cooperative partner of PT_i, when the transmit power of PT_i equals $P_{PT}^{other}(i,n)$,

because ST_n can save some transmit power with the aid of its current cooperative partner PT_v. Therefore, the matching X_{other} produced by another stable matching algorithm is blocked by the pair (PT_v, ST_n) within the same system configuration, which contradicts to the assumption that the matching X_{other} produced by another matching algorithm is stable, hence conforming Proposition 5.2.

Considering an unstable matching produced by any other algorithm, let us now formulate the following proposition relying on Proposition 5.1.

Proposition 5.3: As least one pair of PT and ST, which form a cooperative pair produced by our DWWRS-MAS is capable of acquiring more benefits in terms of the transmit power and the transmit rate than the pair of users forming a cooperative pair of an unstable matching produced by any other algorithm having the same OFs and the system configuration as our DWWRS-MAS.

Proof: Let us first assume that PTs and STs are capable of consuming a lower transmit power by forming a cooperative pair in an unstable matching produced by any other algorithm than the cooperative pair of the stable matching produced by our DWWRS-MAS. Bearing in mind the specific number of matched pairs in both the unstable matching and in the stable matching produced by our DWWRS-MAS, let us now continue by proving the Proposition 5.3 by considering the following three scenarios:

1. *The PTs and STs having a cooperative partner in our DWWRS-MAS also have a cooperative partner in the unstable matching produced by another algorithm.* Let us now assume that PT_i and ST_n form a cooperative pair $\mathcal{O}_{unstable}(PT_i, ST_n)$ in the unstable matching produced by another algorithm, whilst $\mathcal{O}_{DWWRS-MAS}(PT_i, ST_m)$ and $\mathcal{O}_{DWWRS-MAS}(PT_v, ST_n)$ are two cooperative pairs in the stable matching produced by our DWWRS-MAS. Assuming that both the PTs and STs are capable of conserving more power by forming a cooperative pair in an unstable matching produced by any other algorithm than in our DWWRS-MAS, we have:

$$P_{PT}^{unstable}(i,n) < P_{PT}^{DWWRS-MAS}(i,m), \tag{5.69}$$

$$P_{ST}^{unstable}(i,n) < P_{ST}^{DWWRS-MAS}(v,n). \tag{5.70}$$

Eq (5.69) formulates the assumption that PT_i is capable of reducing its transmit power by forming a cooperative pair $\mathcal{O}_{unstable}(PT_i, ST_n)$ with ST_n in the unstable matching produced by another algorithm, rather than forming a cooperative pair $\mathcal{O}_{DWWRS-MAS}(PT_i, ST_m)$ with ST_m in the stable matching produced by our DWWRS-MAS. Furthermore, Eq (5.70) describes the assumption that ST_n is capable of saving

more power, if it selects PT_i as its cooperative partner relying on any other algorithm, which produces unstable matching, rather than selecting PT_v according to our DWWRS-MAS. Based on the definition of a 'blocking pair' stipulated in Section 5.4.2 [216, 218], the matching produced by our DWWRS-MAS is blocked by the pair (PT_i, ST_n), as formulated in Eq (5.69) and Eq (5.70). However, this phenomenon contradicts to the conclusion of Proposition 5.1, namely that our DWWRS-MAS generates a stable matching. Hence, the PTs and STs are capable of saving more power in our DWWRS-MAS than under any other algorithm producing an unstable matching, when the other algorithms have the same number of matched PTs and STs, as our DWWRS-MAS.

2. *More PTs and STs have a cooperative partner in our DWWRS-MAS than under the unstable matching produced by another algorithm.* Since the PTs are capable of saving some of their transmit power and improving their transmit rate, when they have cooperative partners forwarding data for them, the PTs which are not matched in the unstable matching, but have a cooperative partner in our DWWRS-MAS may consume a higher transmit power and achieve lower transmit rate in the unstable matching produced by another algorithm. Furthermore, the STs which are not matched in the unstable matching produced by another algorithm, but have a cooperative partner in our DWWRS-MAS cannot win a transmit opportunity for their own traffic and hence their achievable transmit rate is zero in the unstable matching produced by another algorithm. However, these STs are capable of conveying their data within the licensed spectrum at their target transmit rate in our DWWRS-MAS, because their cooperative partners in our DWWRS-MAS will lease part of their licensed spectral resources to them in this scenario currently being considered.

3. *Less PTs and STs have a cooperative partner in our DWWRS-MAS than in the unstable matching produced by another algorithm.* In this scenario at least one of the PTs which do not have a cooperative partner in our DWWRS-MAS is matched in the unstable matching generated by another algorithm. We refer to PT_i as the PT, which is matched in unstable matching rather than in our stable matching. Since the PTs are capable of saving some of their transmit power, when they have cooperative partners forwarding data for them, PT_i has to consume more transmit power in our DWWRS-MAS due to the absence of a cooperative partner, namely we have $P_{PT}^{unstable}(i,m) < P_{PT}^{DWWRS-MAS}(i,0)$. Hence, PT_i intends to form a cooperative pair with ST_m in our DWWRS-MAS for the sake of reducing its transmit power and for improving its transmit rate. Furthermore, we refer to ST_m as the ST, which is matched in unstable matching, rather than in our stable matching. Hence, the transmit rate of ST_m achieved by our DWWRS-MAS is zero, because ST_m cannot acquire

a transmission opportunity from its cooperative partner. However, ST_m is capable of transmitting its data at its target transmit rate by forwarding data for its cooperative partner PT_i under the unstable matching generated by another algorithm. Hence, ST_m also intends to form a cooperative pair with PT_i in our DWWRS-MAS. Based on the definition of 'blocking pair' as exemplified by Table 5.4 and Fig 5.9, the cooperative pair $\mathcal{O}^{unstable}(PT_i, ST_m)$ forms a blocking pair of the matching produced by our DWWRS-MAS, which contradicts to Proposition 5.1. Moreover, if ST_m has a cooperative partner under the stable matching generated by our DWWRS-MAS as well as under the unstable matching generated by another algorithm, namely when we have $\mathcal{O}^{DWWRS-MAS}(PT_j, ST_m)$ and $\mathcal{O}^{unstable}(PT_i, ST_m)$, then PT_i cannot be matched in our stable matching. This is because ST_m selects PT_j as its cooperative partner for reducing its transmit power. Since our DWWRS-MAS is capable of generating stable matching, the cooperative pair $\mathcal{O}^{DWWRS-MAS}(PT_j, ST_m)$ forms a 'blocking pair' of the unstable matching generated by another algorithm. Therefore, at least one pair of PT and ST gleans more benefit both in terms of their transmit power and transmit rate in our DWWRS-MAS than in the context of other algorithms, which generate unstable matching.

5.5 Simulation Results

5.5.1 Simulation Configuration

In order to evaluate the achievable performance of the proposed scheme, we consider two specific scenarios for investigating both the achievable rate and transmit power, as well as for analyzing both the effects of a user's greedy factor and the system's stability.

- In the first scenario, both the primary transmitters and primary receivers are randomly located on the opposite sides of the entire network area as seen in Fig 5.10. Each of the secondary transmission pairs (ST,SR) are randomly distributed in this scenario across the entire network's area. The primary network has two PTPs, while the number of secondary transmission pairs ranges from $\mathcal{M} = 5$ to $\mathcal{M} = 11$ nodes for the sake of evaluating the influence of the network's size on the system's performance. The transmit rate requirements of the PT and ST are equal to $\alpha C^{max}_{PT,PR}$ and $\beta C^{max}_{ST,SR}$ respectively, where α is the PT's factor of greediness while β is the ST's greedy factor. In order to investigate the performance of the scenario having more PTPs, the number of PTPs will be increased to $\mathcal{I} = 5$ and $\mathcal{I} = 8$ in Section 5.5.7.

- In order to evaluate the system's stability, we considered a symmetric scenario having

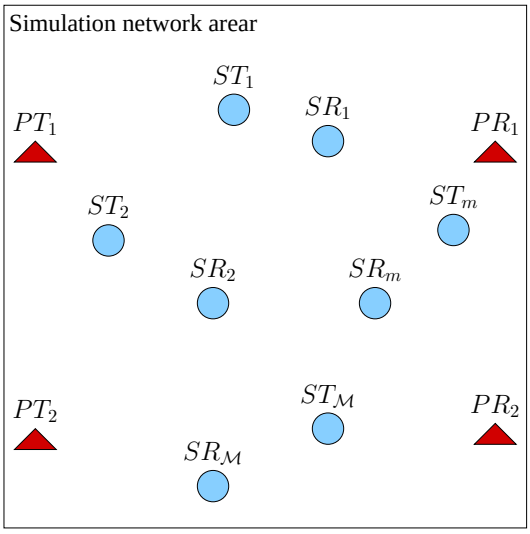

FIGURE 5.10: The network topology of the first simulation scenario having two PTPs and $\mathcal{M}$ STPs relying on the proposed DWWRS-MAS of Fig 5.3 and Fig 5.5.

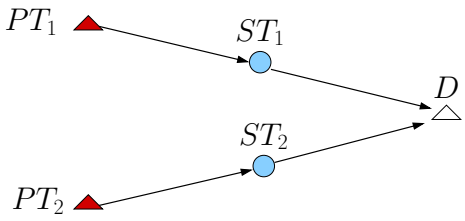

FIGURE 5.11: The symmetric network considered for evaluating the stable throughput of PT and ST relying on the the proposed DWWRS-MAS of Fig 5.3 and Fig 5.5 and on the queueing model of Fig 5.6.

two PTs and two STs as well as a common destination D[5], where all the nodes have fixed positions, as shown in Fig 5.11. More explicitly, the distance from each PT to the destination is the same, while one of the two STs is allocated in the middle of the link between PT_1 and D. Another ST is in the middle of the link between PT_2 and D.

Two centralized cooperative systems (CCS) are considered as the cooperative benchmarkers of our scheme.

- In the first centralized cooperative system (CCS-1), the centralized controller relies on an optimal algorithm for minimizing the total transmit power of all the *PTs and STs*, whilst exploiting the CSI knowledge of all the links. Hence, the objective function of

[5]This scenario is a special instance of the network model considered in Section 5.2.1. A viable scenario would be for example to consider a network conveying a large amount of data as the primary network, which is combined with an access network conveying for example sensory data as the secondary network. Both two access networks can have the same "hub" for linking up with the core network.

PT \ ST (P_{PT}, P_{ST})	ST_1	ST_2	ST_3
PT_1	(p_1, p_4)	(p_1, p_5)	(p_2, p_1)
PT_2	(p_3, p_5)	(p_3, p_{10})	(p_4, p_7)

Power $p_1 < p_2 < p_3 \cdots < p_{10}$
$(p_5 + p_5) < (p_4 + P_{10})$
P_{PT}^{all} : total power of all PTs
P_{ST}^{all} : total power of all STs

Outcome:

CCS−1: Controller $\xrightarrow{\min(P_{PT}^{all} + P_{ST}^{all})}$ $p_2 + p_1 + p_3 + p_5 \xrightarrow{\arg\min}$ $\{\mathcal{O}(PT_1, ST_3), \mathcal{O}(PT_2, ST_1)\}$

CCS−2: Controller $\xrightarrow{\min P_{PT}^{all}}$ $p_1 + p_3 \xrightarrow{\min P_{ST}^{all}}$ $p_5 + p_5 \xrightarrow{\arg\min}$ $\{\mathcal{O}(PT_1, ST_2), \mathcal{O}(PT_2, ST_1)\}$

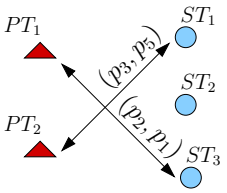

Outcome of CCS−1

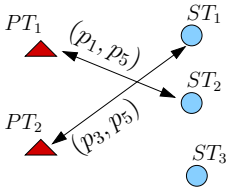

Outcome of CCS−2

FIGURE 5.12: Example of cooperative pairs formed in CCS-1 formulated by Eq (5.71) and in CCS-2 which are formulated by Eq (5.81) and Eq (5.89).

the centralized controller in CCS-1 may be characterized as:

$$\mathcal{O}^*(M^*_{CCS1}, I^*_{CCS1}) = \arg \min_{\mathcal{O}(i,m)} \sum_{i=1}^{\mathcal{I}} \sum_{m=0}^{\mathcal{M}} \Big\{ \xi_{ps}(i,m) \cdot P_{total}(i,m) \Big\}. \tag{5.71}$$

subject to

$$R_{PT_i}(i,m) = R^{req}_{PT}, \qquad \forall i \in \{1,\ldots,\mathcal{I}\}, \forall m \in \{1,\ldots,\mathcal{M}\} \tag{5.72}$$

$$R_{ST_m}(i,m) = R^{req}_{ST}, \qquad \forall i \in \{1,\ldots,\mathcal{I}\}, \forall m \in \{1,\ldots,\mathcal{M}\} \tag{5.73}$$

$$P_{PT}(i,m) \leq P_{max}, \qquad \forall i \in \{1,\ldots,\mathcal{I}\}, \forall m \in \{1,\ldots,\mathcal{M}\} \tag{5.74}$$

$$P_{ST}(i,m) \leq P_{max}, \qquad \forall i \in \{1,\ldots,\mathcal{I}\}, \forall m \in \{1,\ldots,\mathcal{M}\} \tag{5.75}$$

$$\sum_{m=0}^{\mathcal{M}} \xi_{ps}(i,m) = 1, \qquad \forall i \in \{1,\ldots,\mathcal{I}\} \tag{5.76}$$

$$\sum_{i=1}^{\mathcal{I}} \xi_{ps}(i,m) \leq 1, \qquad \forall m \in \{1,\ldots,\mathcal{M}\} \tag{5.77}$$

$$\xi_{ps}(i,m) \in \{0,1\}, \qquad \forall i \in \{1,\ldots,\mathcal{I}\}, \forall m \in \{0,\ldots,\mathcal{M}\}, \tag{5.78}$$

where $\xi_{ps}(i,m)$ is equal to 1 when PT_i and ST_m form a cooperative pair $\mathcal{O}(PT_i, ST_m)$. Otherwise, $\xi_{ps}(i,m)$ is set to 0. Furthermore, Eq (5.72) and Eq (5.73) formulate the transmit rate requirement of PT_i and ST_m, respectively. Eq (5.74) and Eq (5.75)

characterize the maximum transmit power constraint. Moreover, $m = 0$ models the event that PT_i directly transmits its data to PR_i, because it cannot acquire any cooperative transmission assistance. Hence, Eq (5.76) ensures that only a single ST provides cooperative transmission assistance for PT_i or PT_i directly transmits its data, when no ST is willing to act as its cooperative partner. Eq (5.77) ensures that ST_m has only a single cooperative partner. $P_{total}(i,m)$ denotes the total transmit power of PT_i and ST_m if they inform a cooperative pair $\mathcal{O}(PT_i, ST_m)$, which may be formulated as:

$$P_{totalmax}(i,m) = \begin{cases} P_{PT}(i,m) + P_{ST}(i,m) & m > 0 \quad (5.79) \\ P_{PT}^{nc} & m = 0 \quad , \quad (5.80) \end{cases}$$

where $P_{PT_i}^{nc}$ represents the non-cooperative transmit power of PT_i. According to Eq (5.71), the centralized controller in CCS-1 forms a set of cooperative pairs for the sake of minimizing the total transmit power of all the PTs and STs. An example of CCS-1 is provided in Fig 5.12. We assume that the network hosts two PTPs and three STPs. The transmit power dissipation of PT and ST, when they form a cooperative pair is given by the table in Fig 5.12. The combination of (p_1, p_4) in the cross-over point of PT_1 and ST_1 indicates that when PT_1 and ST_1 form a cooperative pair, the power dissipation of PT_1 is p_1, while ST_1 has to dissipate a power of p_4 for satisfying the transmit rate requirement of both PT_1 and itself. We assume that the power associated with a smaller index is lower than the one with a higher index, namely we have $p_1 < p_2 < \cdots < p_{10}$. As seen in Fig 5.12, when PT_1 forms a cooperative pair $\mathcal{O}(PT_1, ST_3)$ with ST_3 and PT_2 forms a cooperative pair $\mathcal{O}(PT_2, ST_1)$ with ST_1, the PTs and STs dissipate the lowest total transmit power, namely $(p_2 + p_1 + p_3 + p_5)$. Hence, according to the objective function of CCS-1 formulated by Eq (5.71)-Eq (5.78), the cooperative pair set of $\{\mathcal{O}(PT_1, ST_3), \mathcal{O}(PT_2, ST_1)\}$ is formed for the sake of minimizing the total transmit power of all the PTs and STs, as seen in Fig 5.12.

- Considering the priority of PTs, the centralized controller forms the optimal cooperative pair for the sake of minimizing the total transmit power of all the *PTs* in the second centralized cooperative system (CCS-2) based on the global CSI knowledge of all the links. When multiple cooperative pairs are capable of promising the same lowest transmit power of all PTs, the centralized controller in CCS-2 selects the specific ST, which can minimize the total transmit power of the STs. Hence, the best cooperative pairs in CCS-2 may be produced in the following two steps:

  1. Firstly, the centralized controller finds a set of optimal cooperative pairs $\mathcal{V} = \{\widehat{\mathcal{O}}(M_{CCS2}^*(i), I_{CCS2}^*(m)\}, \forall i \in \mathcal{I}, \forall m \in \mathcal{M}$ which are capable of minimizing the total transmission power of all the PTs. Hence, the first objective function of

CCS-2 may be formulated as:

$$\widehat{\mathcal{O}}(M^*_{CCS2}, I^*_{CCS2}) = \arg \min_{\{\mathcal{O}(i,m)\}} \sum_{i=1}^{\mathcal{I}} \sum_{m=0}^{\mathcal{M}} \Big\{ \xi_{ps}(i,m) \cdot P_{PT}(i,m) \Big\} \tag{5.81}$$

subject to

$$R_{PT_i}(i,m) = R^{req}_{PT}, \qquad \forall i \in \{1,\ldots,\mathcal{I}\}, \forall m \in \{1,\ldots,\mathcal{M}\} \tag{5.82}$$

$$R_{ST_m}(i,m) = R^{req}_{ST}, \qquad \forall i \in \{1,\ldots,\mathcal{I}\}, \forall m \in \{1,\ldots,\mathcal{M}\} \tag{5.83}$$

$$P_{PT}(i,m) \leq P_{max}, \qquad \forall i \in \{1,\ldots,\mathcal{I}\}, \forall m \in \{1,\ldots,\mathcal{M}\} \tag{5.84}$$

$$P_{ST}(i,m) \leq P_{max}, \qquad \forall i \in \{1,\ldots,\mathcal{I}\}, \forall m \in \{1,\ldots,\mathcal{M}\} \tag{5.85}$$

$$\sum_{m=0}^{\mathcal{M}} \xi_{ps}(i,m) = 1, \qquad \forall i \in \{1,\ldots,\mathcal{I}\} \tag{5.86}$$

$$\sum_{i=1}^{\mathcal{I}} \xi_{ps}(i,m) \leq 1, \qquad \forall m \in \{1,\ldots,\mathcal{M}\} \tag{5.87}$$

$$\xi_{ps}(i,m) \in \{0,1\}, \qquad \forall i \in \{1,\ldots,\mathcal{I}\}, \forall m \in \{0,\ldots,\mathcal{M}\}, \tag{5.88}$$

where $\xi_{ps}(i,m)$ is equal to 1, when PT_i and ST_m form a cooperative pair $\mathcal{O}(PT_i, ST_m)$. Otherwise, $\xi_{ps}(i,m)$ is set to 0. Furthermore, Eq (5.82) and Eq (5.83) formulate the transmit rate requirement of PT_i and ST_m in CCS-2, respectively. Eq (5.84) and Eq (5.85) characterize the maximum transmit power constraint. Moreover, Eq (5.86) ensures that only a single ST provides cooperative transmission assistance for PT_i or PT_i directly transmits its data, when no ST is willing to act as its cooperative partner. Eq (5.87) ensures that ST_m has only a single cooperative partner. Based on the first objective function of CCS-2 formulated by Eq (5.81)-Eq (5.88), a set $\mathcal{V}$ of cooperative pairs is formed for minimizing the total transmit power of all PTs.

2. Given the set $\mathcal{V}$ of cooperative pairs formed by minmizing the total transmit power of all PTs, the centralized controller in CCS-2 produces the best cooperative pair $\mathcal{O}^*(M^*_{CCS2}, I^*_{CCS2})$, which is capable of minimizing the total transmit power of all the cooperative partners of the PTs. Hence, the second objective function namely that of CCS-2 may be formulated as:

$$\mathcal{O}^*(M^*_{CCS2}, I^*_{CCS2}) = \arg \min_{\{\mathcal{O}(i,m)\}} \sum_{\mathcal{O}(i,m) \in \mathcal{V}} \Big\{ \xi_{ps}(i,m) \cdot P_{ST}(i,m) \Big\}. \tag{5.89}$$

subject to

$$\sum_{i\in\mathcal{V}} \xi_{ps}(i,m) \leq 1, \qquad \forall m \in \mathcal{V} \tag{5.90}$$

$$\sum_{m\in\mathcal{V}} \xi_{ps}(i,m) \leq 1, \qquad \forall i \in \mathcal{V} \tag{5.91}$$

$$\xi_{ps}(i,m) \in \{0,1\}, \qquad \forall i \in \mathcal{V}, \qquad \forall m \in \mathcal{V}, \tag{5.92}$$

where Eq (5.90) ensures that each PT in the set of $\mathcal{V}$ has only a single cooperative partner, which is also in the set of $\mathcal{V}$. Furthermore, Eq (5.91) ensures that each ST in the set of $\mathcal{V}$ provides cooperative transmission assistance for only a single PT in the same cooperative pair set $\mathcal{V}$. As exemplified in Fig 5.12, when the power dissipation of PT_1 and PT_2 is equal to p_1 and p_3 respectively, the minimum total transmit power is dissipated by all PTs. Hence, as seen in Fig 5.12, the total transmit power of all PTs can be minimized either when PT_1 forms cooperative pair with ST_2 and PT_2 forms cooperative pair with ST_1, namely when we have $\{\mathcal{O}(PT_1, ST_2), \mathcal{O}(PT_2, ST_1)\}$ or when PT_1 forms cooperative pair with ST_1 and PT_2 forms a cooperative pair with ST_2, namely we have $\{\mathcal{O}(PT_1, ST_1), \mathcal{O}(PT_2, ST_2)\}$. Hence, based on the example seen in Fig 5.12, the cooperative pair set $\mathcal{V}$ generated for minimizing the transmit power of all PTs is equal to $\mathcal{V} = \{[\mathcal{O}(PT_1, ST_2), \mathcal{O}(PT_2, ST_1)], [\mathcal{O}(PT_1, ST_1), \mathcal{O}(PT_2, ST_2)]\}$. Assuming that $(p_5{+}p_5) < (p_4{+}p_{10})$, the STs in the set of $\{\mathcal{O}(PT_1, ST_2), \mathcal{O}(PT_2, ST_1)\}$ dissipate a lower power of $(p_5 + p_5)$ than in the set $\{\mathcal{O}(PT_1, ST_1), \mathcal{O}(PT_2, ST_2)\}$. Hence, according to the second objective function of CCS-2 formulated by Eq 5.89-Eq (5.92), the centralized controller of CCS-2 forms the best cooperative pair set of $\{\mathcal{O}(PT_1, ST_2), \mathcal{O}(PT_2, ST_1)\}$ for the sake of minimizing the power dissipation of the cooperative partners of the PTs in the cooperative pair set $\mathcal{V}$.

Based on the OF formulated by Eq (5.71)-Eq (5.78), the centralized controller in CCS-1 selects the best cooperative pair set for the sake of minimizing the total transmit power of all the PTs and STs without considering the priority of PTs, as exemplified in Fig 5.12. However, in CCS-2 the centralized controller assumes that the PTs have a higher priority than the STs and produces the best cooperative pair set for the sake of minimizing the total transmit power of all the PTs, as formulated by Eq (5.81) and as seen in Fig 5.12. When multiple cooperative pair sets are capable of promising the same lowest total transmit power to be dissipated by the cooperative partner of the PTs, the specific cooperative pair set, which promises the lowest total transmit power of all the STs is selected as the best cooperative pair set, as formulated by Eq (5.89) and as exemplified in Fig 5.12.

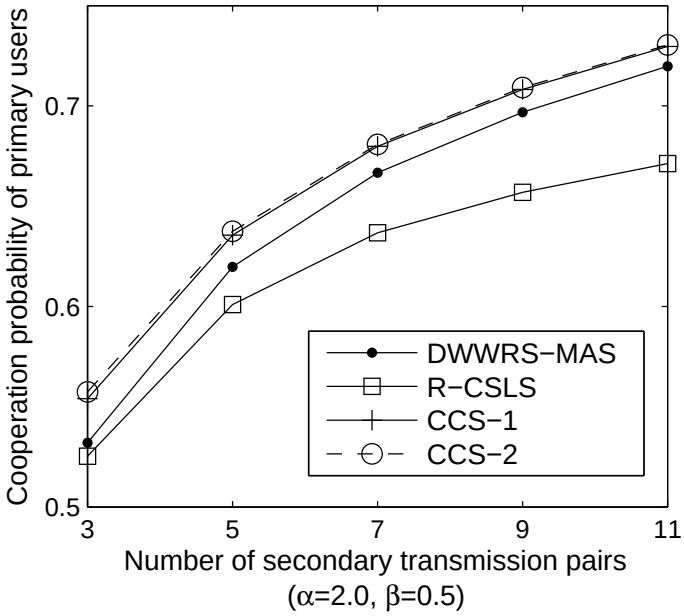

FIGURE 5.13: Cooperation probability of the PTs versus the number of secondary users for $\mathcal{I} = 2$, $\alpha = 2.0$ and $\beta = 0.5$ in the simulation scenario of Fig 5.10 relying on the proposed DWWRS-MAS of Fig 5.3 and Fig 5.5. The results are contrasted to those of the benchmark systems introduced in Section 5.5.1.

Additionally, we also introduce a random cooperative spectrum leasing system (R-CSLS), where a PT randomly selects a ST as its cooperative partner, if both the PT's and ST's transmit rate requirement can be satisfied by forming this cooperative pair.

In order to evaluate the benefits of our scheme, two non-cooperative systems (NCS) are introduced as the benchmarkers for our comparisons. We compare the system's achievable total transmit rate (TTR) constituted by the sum of all the PTs' and STs' transmit rate to that of the first non-cooperative system (nCS-1), which dissipates the same total transmission power as our cooperative spectrum leasing system (CSLS). Additionally, we compare the total transmission power to that of the second non-cooperative system (nCS-2), which is capable of achieving the same TTR as our CSLS. Since the PT's data is transmitted twice, namely once by itself and additionally by its cooperative partner in our CSLS, provided that the cooperative transmission is successful, two direct transmission phases are exploited in both nCS-1 and nCS-2. Additionally, all the assumptions mentioned in Section 5.2.1 are exploited by both nCS-1 and nCS-2.

5.5.2 Cooperation Probability

Fig 5.13 compares the successful cooperation probability of the PTs achieved by our DWWRS-MAS, and by the R-CSLS as well as by the CCS-1 and CCS-2 versus different-size secondary networks for $\mathcal{I} = 2$, $\alpha = 2.0$ and $\beta = 0.5$. Given the size of the secondary network, our

DWWRS-MAS is capable of providing a higher cooperation probability for the PTs and more transmission opportunities for the secondary transmission pairs than the R-CSLS, which again relies on a random relay selection scheme, as seen in Fig 5.13. By contrast, the cooperation probability achieved by the random matching algorithm is lower than that achieved by both the centralized systems CCS-1 and CCS-2, as seen in Fig 5.13. Based on the global CSI knowledge, the centralized controller of both CCS-1 and CCS-2 is capable of finding the optimal cooperative pairs for the sake optimizing the corresponding OFs, albeit this is achieved at the cost of a considerable computational complexity. Furthermore, the selfish nature of the STs is not considered in CCS-1 and CCS-2, as exemplified in Fig 5.12. According to the OFs of both CCS-1 and CCS-2, the cooperative pair set of $\{\mathcal{O}(PT_1, ST_2), \mathcal{O}(PT_2, ST_1)\}$ is formed in Fig 5.12. However, as observed in Fig 5.12, ST_1 is capable of reducing its transmit power if it forms a cooperative pair with PT_1, rather than with PT_2. Hence, ST_1 in the example of Fig 5.12 may contend for the transmission opportunity provided by PT_1 due to the selfish nature of STs, which is not considered either in both CCS-1 or in CCS-2. However, our DWWRS-MAS is designed by taking into account the selfish nature of STs, which hence may result in reducing the cooperation probability of PTs in our DWWRS-MAS, when a ST is invited by multiple PTs to form cooperative pairs. For example, PT_i has two candidate cooperative partners, namely ST_m and ST_n, while ST_m is the only candidate cooperative partner of PT_j. When both PT_i and PT_j invites ST_m to be its cooperative partner, ST_m selects PT_i to become its cooperative partner, provided that this way a lower transmit power is required for forwarding the data of PT_i. Hence, only a single cooperative pair $\mathcal{O}(PT_i, ST_m)$ is generated in our DWWRS-MAS. However, ST_m may become the cooperative partner of PT_j in both CCS-1 and CCS-2 for the sake of minimizing the system's transmit power and the PTs' transmit power, respectively. Therefore, there are two cooperative pairs in these two centralized systems, namely $\mathcal{O}(PT_i, ST_n)$ and $\mathcal{O}(PT_j, ST_m)$.

Observe in Fig 5.13 that the cooperation probability achieved in all the cooperative system considered in this section is increased, when more STPs intends to access the licensed spectrum, because the probability of the event that the STs are capable of successfully forwarding the superposition-coded data is increased, as the secondary network becomes larger. As seen in Fig 5.13, the cooperation probability curve of our DWWRS-MAS gradually approaches those of the centralized systems CCS-1 and CCS-2, when network has more STPs. As discussed above, the selfish nature of STs may reduce the cooperation probability of PTs according to the proposed DWWRS-MAS. Hence, a small discrepancy of about 0.01 persists between the PTs' cooperation probability achieved by our DWWRS-MAS for $\mathcal{M} = 11$ and those achieved by CCS-1 and CCS-2, as seen in Fig 5.13. When the secondary network size is increased, both the PTs and STs may have more candidate cooperative partners. Hence, the probability that multiple PTs contend for a single ST may be reduced and the loser

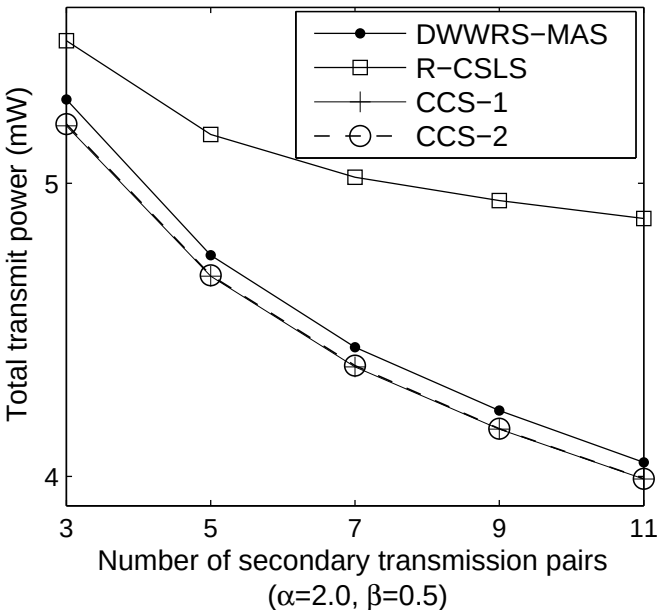

FIGURE 5.14: The system's total transmit power versus the number of secondary users for $\mathcal{I} = 2$, $\alpha = 2.0$ and $\beta = 0.5$ in the network of Fig 5.10, while achieving the cooperation probability of Fig 5.13 when relying on the proposed DWWRS-MAS of Fig 5.3 and Fig 5.5. This results are contrasted to those of the benchmark systems introduced in Section 5.5.1.

of the contention has a higher probability of forming a cooperative pair with other STs in the larger network. This phenomenon reduces the gap between the cooperation probability achieved by the proposed DWWRS-MAS and those achieved by both CCS-1 and CCS-2. Compared to the cooperation probability achieved by R-CSLS, the advantage of the proposed DWWRS-MAS becomes more evident, as the number of STPs is increased due to the increased number of candidate cooperative partners of both the PTs and STs, as seen in Fig 5.13.

5.5.3 Transmit Power Consumption

Let us commence by first evaluating the system's total transmit power (STTP) for the cooperative systems considered in this section, namely that of the proposed DWWRS-MAS, CCS-1, CCS-2 as well as R-CSLS for $\mathcal{I} = 2$, $\alpha = 2.0$ and $\beta = 0.5$. The STTP is given by the sum of the transmit power of all the PTs and STs, which were granted transmission opportunities. This is formulated as:

$$\underbrace{\frac{1}{N_{all}} \cdot \sum_{x=1}^{N_{all}} \Big[\sum_{i=1}^{\mathcal{I}} P_{PT}^{x}(i) \Big]}_{\text{Part I: total transmit power of all PTs}} + \underbrace{\frac{1}{N_{all}} \cdot \sum_{x=1}^{N_{all}} \Big[\sum_{m=1}^{\mathcal{M}} P_{ST}^{x}(m) \Big]}_{\text{Part II: total transmit power of all STs}} \tag{5.93}$$

where N_{all} denotes the total number of instances of our DWWRS-MAS in the Monte Carlo simulation. Moreover, $P_{PT}^{x}(i)$ represents the transmit power consumed by PT_i, whilst relying on either the cooperative transmission or the direct transmission of its data to PR_i during the x-th instance of the Monte Carlo simulation. Furthermore, $P_{ST}^{x}(m)$ denotes the transmit power dissipated by ST_m, when successfully conveying the superposition-coded data during the x-th instance of the Monte Carlo simulation. If ST_m fails to win a transmission opportunity during the x-th instance of the Monte Carlo simulation, the $P_{ST}^{x}(m)$ is equal to zero. Hence, the term in part I of Eq (5.93) formulates the average total transmit power of all the PTs dissipated, when transmitting their data with or without the aid of cooperative transmission. Furthermore, the term in part II of Eq (5.93) formulates the average total transmit power of all the STs dissipated, while conveying the superposition-coded data. The STTP is calculated in terms of Eq (5.93), which formulates the sum of the transmit power of all the PTs and STs.

Observe in Fig 5.14 that our DWWRS-MAS is capable of saving considerably more STTP than R-CSLS. This is not unexpected, because the proposed DWWR-SMAS was designed for the sake of minimizing the transmit power of both PTs and STs as well as that of the secondary network. By contrast, the cooperative pairs are randomly formed in R-CSLS without considering the transmit power dissipation of the STs. Based on the global CSI information knowledge, the centralized controller selects the optimal cooperative pairs for the sake of minimizing the system's total transmit power in CCS-1, as characterized in Eq (5.71). Hence, the users of CCS-1 consume the lowest transmit power, as seen in Fig 5.14. Since both the PTs and STs are assumed to have the same maximum transmit power constraint, CCS-2 dissipates a similar STTP to CCS-1, as shown in Fig 5.14. The effect of using different maximum transmit power constraints for the PTs and STs will be evaluated in Section 5.5.6. It is worth noting that the STTP curve of our DWWRS-MAS which selects the cooperative pairs in a *distributed* fashion, i.e. without a central controller, approaches that of the *centralized* system considered in this section, as shown in Fig 5.14. However, the STTP dissipated by in our DWWRS-MAS cannot become as low as that consumed in CCS-1 due to the selfish nature of both the PTs and STs, as discussed in the context of Fig 5.13 of Section 5.5.2.

When the network has a high number of secondary transmission pairs, the probability of beneficial cooperative pairs, which are capable of approaching the global optimum of the system's OFs is increased. Furthermore, based on the above discussions, it becomes plausible that the cooperation probability of the PTs is also increased as the secondary network becomes larger, as seen in Fig 5.13. Hence, the STTP consumed both by our DWWRS-MAS and by the benchmark systems is reduced, when more STs intend to access the primary network.

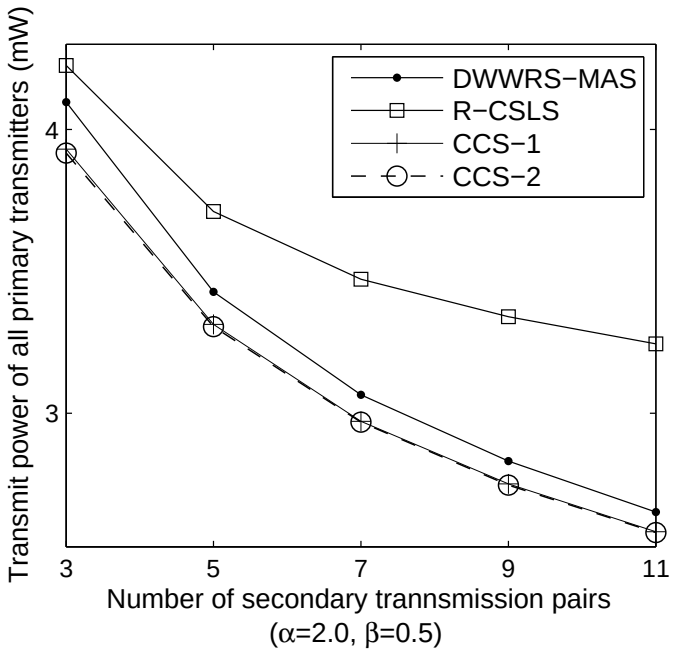

FIGURE 5.15: The transmit power of all PTs versus the number of secondary users for $\mathcal{I} = 2$, $\alpha = 2.0$ and $\beta = 0.5$ in the network of Fig 5.10, while achieving the cooperation probability of Fig 5.13 and dissipating the total transmit power of all PTs and STs as quantified in Fig 5.14 when relying on the proposed DWWRS-MAS of Fig 5.3 and Fig 5.5. This results are contrasted to those of the benchmark systems introduced in Section 5.5.1.

Fig 5.15 shows our comparison between the total transmit power of all PTs (TPP) consumed in the proposed DWWRS-MAS versus that dissipated by the benchmark systems namely CCS-1, CCS-2 and R-CSLS for $\mathcal{I} = 2$, $\alpha = 2.0$ and $\beta = 0.5$. In this context the TPP is formulated as:

$$\frac{1}{N_{all}} \cdot \sum_{x=1}^{N_{all}} \Big[\sum_{i=1}^{\mathcal{I}} P_{PT}^{x}(i) \Big] \tag{5.94}$$

where N_{all} denotes the total number of instances of our DWWRS-MAS in the Monte Carlo simulation. Furthermore, $P_{PT}^{x}(i)$ represents the transmit power consumed by PT_i, whilst relying on either the cooperative transmission or on the direct transmission of its data to PR_i during the x-th instance of the Monte Carlo simulation. It can be seen that Eq (5.94) represents Part I of Eq (5.93). Hence, Eq (5.94) formulates the total transmit power dissipated by all the PTs, when transmitting their data with the aid of cooperative transmission or when directly transmitting their data to the corresponding PRs.

Considering the higher priority of PTs, the centralized controller produces the optimal cooperative pairs in CCS-2 for the sake of first minimizing the transmit power of the PTs. Hence, the PTs in CCS-2 consume the lowest transmit power, as shown in Fig 5.15. By contrast, the highest TPP is consumed in R-CSLS, where the cooperative pairs are randomly formed, as seen in Fig 5.15. Compared to the TPP of R-CSLS, our DWWRS-MAS is

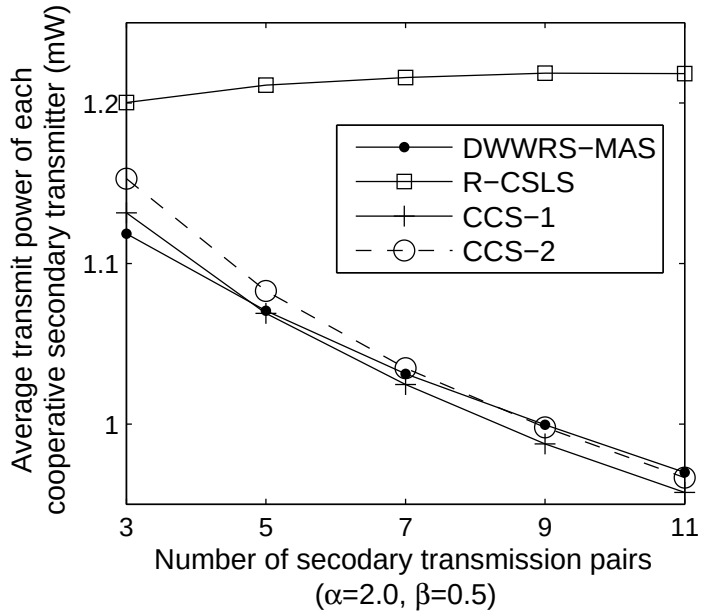

FIGURE 5.16: The average transmit power of each matched ST versus the number of STPs for $\mathcal{I} = 2$, $\alpha = 2.0$ and $\beta = 0.5$ in the network of Fig 5.10 required for achieving the cooperation probability of Fig 5.13 and dissipating the total transmit power of all PTs and STs as quantified in Fig 5.14. The transmit power of all PTs is characterized in Fig 5.15 when relying on the proposed DWWRS-MAS of Fig 5.3 and Fig 5.5. The results are contrasted to those of the benchmark systems introduced in Section 5.5.1.

capable of saving valuable TPP, which may become as high as 90% of that saved in CCS-2 for $\mathcal{M} = 11$, as seen in Fig 5.15. Based on the above discussions, it becomes plausible that the selfish nature of the STs and the lack of global information reduces the cooperation probability, whilst increasing the TPP of the proposed DWWRS-MAS, as shown in Fig 5.13 and Fig 5.15, respectively. When the secondary network becomes larger, the increased probability of meritorious cooperation pairs combined with a higher cooperation probability reduces the TPP in all the cooperative systems considered in this section, namely in the proposed DWWRS-MAS as well as in the CCS-1, CCS-2 and R-CSLS, as seen in Fig 5.15. This phenomenon widens the gap between the curves of our DWWRS-MAS as well as the R-CSLS, whilst reducing the discrepancy between our DWWRS-MAS and CCS-2, as seen in Fig 5.15.

Fig 5.16 compare the average transmit power of each cooperative ST (ATPES) operating under by our DWWRS-MAS as well as under the benchmark systems. Here the ATPES is given by:

$$\frac{1}{N_{ST,all}^{coop}} \cdot \sum_{y=1}^{N_{ST}^{coop}} P_{ST}^{y}, \tag{5.95}$$

where $N_{ST,all}^{coop}$ denotes the total number of transmission opportunities granted to all the STs,

namely we have $N_{ST,all}^{coop} = \sum_{m=1}^{\mathcal{M}} N_{ST}^{coop}(m)$. The variable $N_{ST}^{coop}(m)$ represents the number of transmission opportunities granted to ST_m. Furthermore, P_{ST}^{y} denotes the transmit power dissipated by the ST, when conveying the superposition-coded data during the y-th transmission opportunity granted to all the STs. Based on the above discussions, Eq (5.95) formulates the average transmit power dissipated by each ST, when successfully conveying the superposition-coded data.

Observe in Fig 5.16 that the lowest ATPES is consumed in CCS-1. This is indeed expected, because the transmit power of the ST is reduced as the PT increases its transmit power, the centralized controller in CCS-1 may be able to select the optimal cooperative pair, which requires a lower ST power and a higher PT power than their counterparts both in CCS-2 and in our DWWRS-MAS for the sake of minimizing the system's total transmit power, as exemplified by Fig 5.12 where the controller in CCS-1 forms the cooperative pair $\mathcal{O}(PT_1, ST_3)$, which dissipates higher PT transmit power p_2 and a lower ST transmit power p_1 than the other pairs. Hence, CCS-1 requires the lowest ATPES for minimizing the STTP, which is achieved at the cost of increasing the TPP, as seen in Fig 5.14, Fig 5.15 and Fig 5.16. However, the PTPs have a higher priority than the STPs in a cognitive network. Considering the priority of PTPs, the CCS-2 are capable of improving the cooperation probability, whilst simultaneously reducing the transmit power of the PTs, albeit this is achieved at the cost of the ATPES, as seen in Fig 5.13, Fig 5.15 and Fig 5.16. It is worth noting that the ATPES of our DWWRS-MAS is lower than that consumed in CCS-2 for $\mathcal{M} < 11$ and even lower than that consumed in CCS-1 when $\mathcal{M} = 3$, as shown in Fig 5.16. This phenomenon is due to the selfish nature of STs, which is not considered in CCS-1 and CCS-2. For example, PT_i has two candidate cooperative partners, namely ST_m and ST_n, while ST_m is the only candidate cooperative partner of PT_j. When both PT_i and PT_j invites ST_m to be its cooperative partner, ST_m selects PT_i to become its cooperative partner, provided that this way a lower transmit power is required for forwarding the data of PT_i. Hence, only a single cooperative pair $\mathcal{O}(PT_i, ST_m)$ is generated in our DWWRS-MAS. However, ST_m may become the cooperative partner of PT_j in CCS-1 and CCS-2 for the sake of minimizing the system's transmit power and the PTs' transmit power, respectively. This phenomenon reduces both the cooperation probability and the average transmit power dissipated by each ST, which was granted transmission opportunities in our DWWRS-MAS, as seen in Fig 5.13 and Fig 5.16. Observe in Fig 5.16 that the ATPES consumed in R-CSLS is higher than that of the other cooperative systems, because the cooperative pairs are randomly selected without considering the transmit power of the ST.

When more STPs intend to access the primary network, the ATPES consumed in our DWWRS-MAS and CCS-1 as well as in CCS-2 is reduced, which is shown in Fig 5.16. This observation is plausible due to the increased probability of forming meritorious cooperative

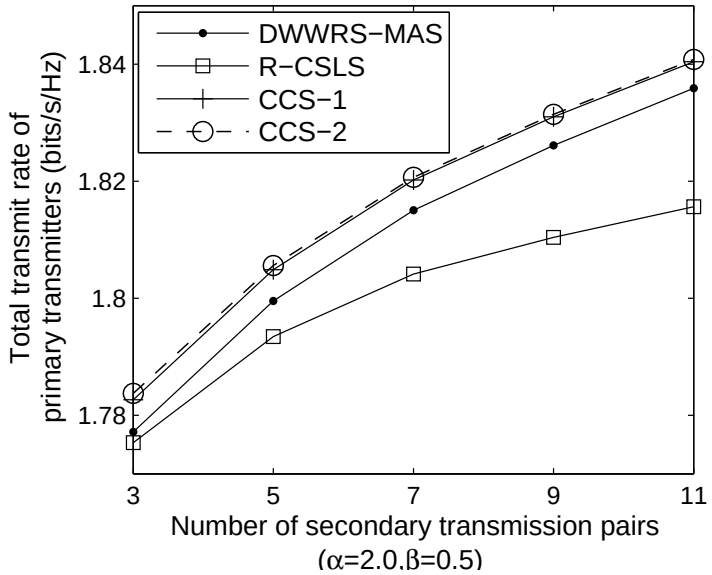

FIGURE 5.17: The achievable transmit rate of all PTs versus the number of secondary users for $\alpha = 2.0$ and $\beta = 0.5$ in the network of Fig 5.10 while achieving the cooperation probability of Fig 5.13 relying on the proposed DWWRS-MAS of Fig 5.3 and Fig 5.5. The results are contrasted to those of the benchmark systems introduced in Section 5.5.1.

pairs, where both the PT and ST dissipate a very low transmit power. However, the probability that a PT selects an undesirable ST, which consumes higher transmit power as its cooperative partner is also increased in R-CSLS, when the secondary network has more STPs. Hence, the ATPES consumed in R-CSLS is increased, as the secondary network becomes larger, as seen in Fig 5.16.

5.5.4 Achievable Transmit Rate

According to the OFs of our DWWRS-MAS, the transmit rate requirement of both the PT PT_i and of the ST ST_m has to be satisfied, if PT_i and ST_m constitute a cooperative pair. Hence, we evaluate the transmit rate of the PTs and STs. Fig 5.17 shows the total transmit rate of the PTs (TTRP) achieved by the proposed DWWRS-MAS and by the benchmark systems, when the network has two PTRs and the greedy factor of the PT and ST are $\alpha = 2.0$ and $\beta = 0.5$, respectively. The TTRP is formulated as

$$\frac{1}{N_{all}} \cdot \sum_{x=1}^{N_{all}} \Big[\sum_{i=1}^{\mathcal{I}} R_{PT}^{x}(i) \Big], \tag{5.96}$$

where N_{all} denotes the total number of instances of our DWWRS-MAS in the Monte Carlo simulation. Furthermore, $R_{PT}^{x}(i)$ denotes the transmit rate achieved by either the cooperative transmission or the direct transmission of its data to PR_i during the x-th instance of the Monte Carlo simulation. Observe in Fig 5.17 that the highest TTRP is achieved

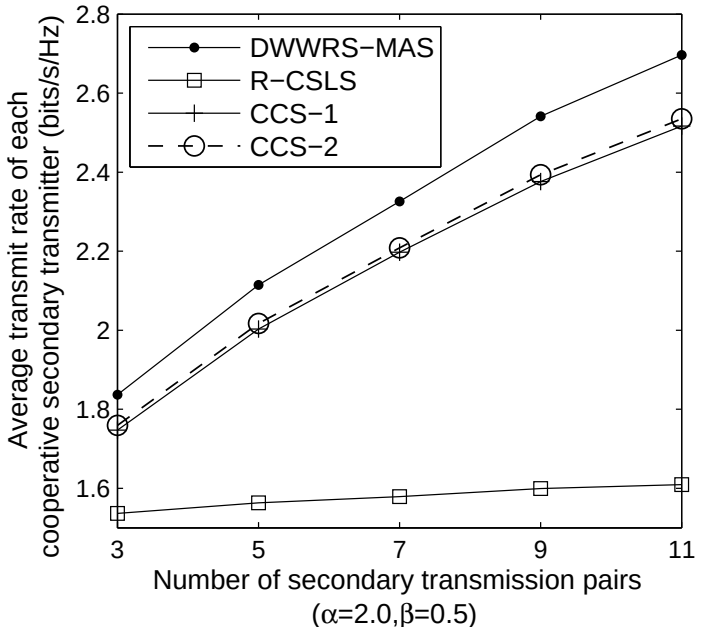

FIGURE 5.18: The average transmit rate of each cooperative ST versus the number of secondary users for $\alpha = 2.0$ and $\beta = 0.5$ in the network of Fig 5.10 having the cooperation probability of Fig 5.13, while relying on the proposed DWWRS-MAS of Fig 5.3 and Fig 5.5. The results are contrasted to those of the benchmark systems introduced in Section 5.5.1.

by CCS-2 relying on the highest cooperation probability, as seen in Fig 5.13. As discussed above, the PTs are capable of reducing their transmit power, whilst simultaneously achieving their target rate of $\alpha C^{max}_{PT,PR}$ with the aid of cooperative transmissions. Hence, the TTRP may be maximized in CCS-2, when the optimal cooperative pairs are formed for the sake of minimizing transmit power of the PTs. Compared to the TTRP achieved in the R-CSLS, our DWWRS-MAS provides a benefited improvement, which is more than 77% of the improvement promised by CCS-2 for $\mathcal{M} = 11$, as seen in Fig 5.17. When the secondary network becomes larger, an increased TTRP can be provided by all the systems considered due to the increased probability of cooperative transmission, which is capable of achieving the target transmit rate of the PTs.

Fig 5.18 illustrates our comparison of the average transmit rate of each cooperative STs (ATRES) achieved by the proposed DWWRS-MAS and by the benchmark systems for $\mathcal{I} = 2$, $\alpha = 2.0$ and $\beta = 0.5$. The ATRES is characterized as

$$\frac{1}{N^{coop}_{ST,all}} \cdot \sum_{y=1}^{N^{coop}_{ST}} R^{y}_{ST}, \tag{5.97}$$

where $N^{coop}_{ST,all}$ denotes the total number of transmission opportunities granted to the all the STs, namely when we have $N^{coop}_{ST,all} = \sum_{m=1}^{\mathcal{M}} N^{coop}_{ST}(m)$. The variable $N^{coop}_{ST}(m)$ represents the number of transmission opportunities granted to ST_m. Furthermore, R^{y}_{ST} denotes the

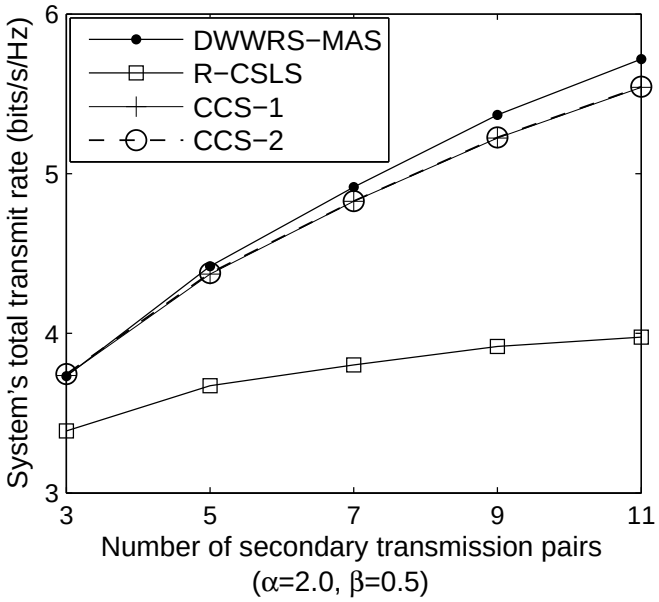

FIGURE 5.19: Total transmit rate versus the number of secondary users for $\alpha = 2.0$ and $\beta = 0.5$ in the network of Fig 5.10 having the cooperation probability of Fig 5.13 and achieving the transmit rate of all PTs as characterized in Fig 5.17 and the average transmit rate of each cooperative ST of Fig 5.18 relying on the proposed DWWRS-MAS of Fig 5.3 and Fig 5.5. The results are contrasted to those of the benchmark systems introduced in Section 5.5.1.

transmit rate of the ST achieved when the y-th transmission opportunity is granted to ST. Based on the above discussions, the ATRES given by Eq (5.97) is the average achievable transmit rate of each ST.

Compared to CCS-1 and CCS-2, our DWWRS-MAS is capable of achieving the highest ATRES, as shown in Fig 5.18. According to the proposed DWWRS-MAS, the specific ST which promises a lower transmit power required for successfully conveying the superposition-coded data may benefit from a better channel for the link between the ST to SR and hence this specific ST may achieve a higher transmit rate. Therefore, our DWWRS-MAS is capable of achieving a higher ATRES than CCS-2 as shown in Fig 5.18. Furthermore, the PT PT_i which fails to contend for matching with the ST ST_m has to increase its transmit power for the sake of searching for a new candidate cooperative partner, when PT_i does not have other candidate cooperative partners at the current transmit power level, as seen in Fig 5.3 and Table 5.1 as well as Table 5.3. Then a better ST, such as ST_n which can promise a lower transmit power than ST_m may become the new candidate cooperative partner of PT_i at a higher PT transmit power level. This phenomenon is also beneficial for improving the ATRES in our DWWRS-MAS. Observe in Fig 5.18 that compared to R-CSLS, our DWWRS-MAS is capable of significantly improving the ATRES. When more STPs intend to access the licensed spectrum, the ATRES achieved in our DWWRS-MAS and by our benchmark systems are increased, as evidenced by Fig 5.18. As mentioned above, the probability that

TABLE 5.5: Performance comparison between our cooperative system and the non-cooperative systems nCS-1 and nCS-2.

Number of STs	System'S Transmit Rate Ratio $(\mathbb{E}\{R_{nCS-1}\}/\mathbb{E}\{R_{DWWRS-MAS}\})$	System'S Transmit Power Ratio $(\mathbb{E}\{P_{nCS-2}\}/\mathbb{E}\{P_{DWWRS-MAS}\})$
3	0.6084	1.7831
5	0.5459	2.3310
7	0.5070	2.9103
9	0.4730	3.6655
11	0.4504	4.4024

a beneficial ST is selected as the cooperative partner is increased in a larger network. This phenomenon is capable of improving the ATPES.

Based on the above discussions, our DWWRS-MAS is capable of achieving a higher total transmit rate (TTR) than both CCS-1 and CCS-2, as seen in Fig 5.19. This is due to the higher ATRES, which is shown in Fig 5.18. The TTR is defined as the sum of the achievable transmit rate of all the PTs and of all the STs. Hence, the TTR may be expressed as

$$\underbrace{\frac{1}{N_{all}} \cdot \sum_{x=1}^{N_{all}} \Big[\sum_{i=1}^{\mathcal{I}} R_{PT}^{x}(i) \Big]}_{\text{part I: total rate of all PTs}} + \underbrace{\frac{1}{N_{all}} \cdot \sum_{x=1}^{N_{all}} \Big[\sum_{m=1}^{\mathcal{M}} R_{ST}^{x}(m) \Big]}_{\text{part II: total rate of all STs}}. \tag{5.98}$$

As mentioned above, N_{all} denotes the total number of instances of our DWWRS-MAS in the Monte Carlo simulation. Moreover, $R_{PT}^{x}(i)$ denotes the transmit rate achieved by either the cooperative transmission or the direct transmission of its data to PR_i during the x-th instance of the Monte Carlo simulation. Furthermore, $R_{ST}^{x}(m)$ represents the achievable transmit rate of the ST, when the ST ST_m is granted a transmit opportunity during the x-th instance of the Monte Carlo simulation. If ST_m cannot win a transmission opportunity during the x-th instance of the Monte Carlo simulation, $R_{ST}^{x}(m)$ is equal to zero. Compared to R-CSLS, a considerable rate-improvement is provided by our DWWRS-MAS, as observed in Fig 5.19. As mentioned above, having an increased probability of a beneficial ST is capable of improving the TTRP and ATPES. Hence, the TTR achieved in our DWWRS-MAS and by the benchmark systems is also significantly improved in Fig 5.19, when the secondary network became larger.

5.5.5 Comparison with non-cooperative system

In this section, we introduce two non-cooperative systems, namely nCS-1 and nCS-2 as the benchmark systems for further characterizing both the transmit power and transmit rate of our DWWRS-MAS. As described in Section 5.5.1, nCS-1 consumes the same STTP as our DWWRS-MAS, while nCS-2 is capable of achieving the same TTR as the proposed

DWWRS-MAS. Table 5.5 lists the system's transmit rate ratio (STRaR) and system's transmit power ratio (STPowR) for $\mathcal{I} = 2$, $\alpha = 2.0$ and $\beta = 0.5$, where STRaR is formulated as $\mathbb{E}\{R_{nCS-1}\}/\mathbb{E}\{R_{DWWRS-MAS})\}$, with R_{nCS-1} and $R_{DWWRS-MAS}$ denoting the achievable TTR of nCS-1 and of our DWWRS-MAS, respectively. Furthermore STPowR is given by $(\mathbb{E}\{P_{nCS-2}\}/\mathbb{E}\{P_{DWWRS-MAS})\}$, where P_{nCS-2} denotes the STTP dissipated by nCS-2 and $P_{DWWR-SMAS}$ is the STTP consumed in the proposed DWWRS-MAS. Observe in Table 5.5 that nCS-1 is capable of achieving 60% of the TTR achieved by our DWWRS-MAS in the scenario of supporting $\mathcal{M} = 3$ STPs, where our DWWRS-MAS consumes the most STTP. Based on the same STTP, we observe in Table 5.5 that the TTR achieved by nCS-1 is less than half of that achieved by our DWWRS-MAS, when the number of STPs is more than $\mathcal{M} = 7$. When aiming for achieving the same TTR, nCS-2 has to dissipate more than twice the STTP of our DWWRS-MAS, when the secondary network has more than $\mathcal{M} = 3$ STPs. Based on the above discussions, our DWWRS-MAS is capable of considerably saving STTP and simultaneously significantly improving the TTR, compared to the non-cooperative systems.

5.5.6 The Effect of the Maximum Transmit Power Constraint

In Section 5.5.2, 5.5.3 and 5.5.4 we assumed that both the PT and ST have the same maximum transmit power constraint. By contrast, in this section, the PT and ST are assumed to have a different maximum transmit power constraint, namely P_{max}^{PT} and P_{max}^{ST}. The effect of different maximum transmit power constraints is evaluated according to the cooperation probability, transmit power consumption as well as the achievable transmit rate.

Cooperation Probability

Fig 5.20 shows the cooperation probability of the PT achieved by our DWWRS-MAS, CCS-1, CCS-2 and R-CSLS under different maximum transmit power constraints imposed on both the PT and the ST, when we have $\mathcal{I} = 2$, $\alpha = 2.0$ and $\beta = 0.5$. When P_{max}^{PT} is increased based on the scenario, where the PT and ST have the same maximum transmit power constraint, a reduced number of STs can satisfy the increased transmit rate requirements $\alpha C_{PT,PR}^{max}$ of the PT, whilst simultaneously achieving their own target transmit rate of $\beta C_{ST,SR}^{max}$ under a severe power constraint of P_{max}^{ST}. Hence, more than half of the PTs' data is directly conveyed to the corresponding PR in the scenario of $P_{max}^{PT} > P_{max}^{ST}$, as seen in Fig 5.20. However, more STs are capable of affording the transmit power required for satisfying the transmit rate requirements of both the PT and itself, when the ST's maximum transmit power constraint is increased based on the scenario, where $P_{max}^{PT} = P_{max}^{ST}$. Hence, observe in Fig 5.20 that the cooperation probability is significantly increased in the scenario of $P_{max}^{PT} < P_{max}^{ST}$. When

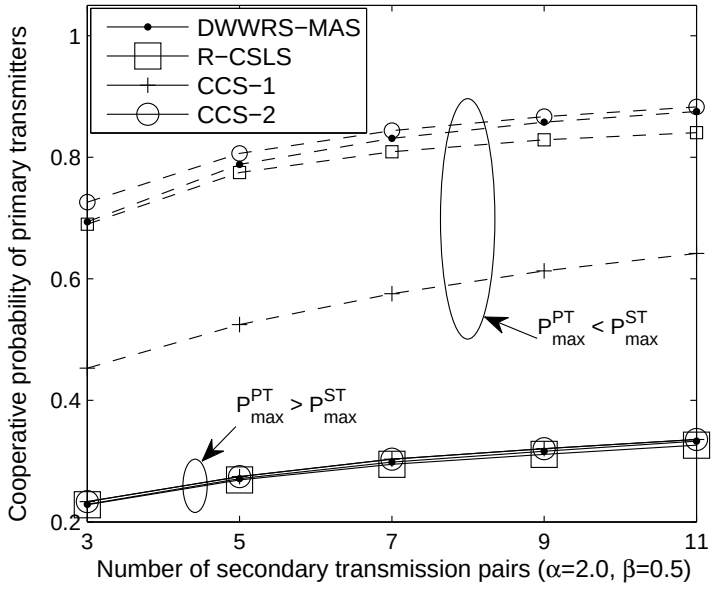

FIGURE 5.20: Cooperation probability of PTs versus the number of secondary users for $\mathcal{I} = 2$, $\alpha = 2.0$ and $\beta = 0.5$ when the PTs and STs have different maximum transmit power constraints in the network of Fig 5.10 relying on the proposed DWWRS-MAS of Fig 5.3 and Fig 5.5. The results are contrasted to those of the benchmark systems introduced in Section 5.5.1.

aiming for minimizing the STTP, the centralized controller may allow some of the PTs to directly transmit their data without any cooperative transmission assistance, when the total transmit power of the PT and its cooperative partner is higher than the PT's transmit power required for successfully directly convey its data, i.e. directly, without cooperation. Hence, observe in Fig 5.20 that CCS-1 achieves the lowest cooperation probability in the scenario of $P_{max}^{PT} < P_{max}^{ST}$. However, the centralized controller in CCS-2 intends to maximize the cooperation probability of the PTs for the sake of minimizing the TPP. Hence, CCS-2 always achieves the highest cooperation probability in Fig 5.20, regardless whether P_{max}^{PT} is higher than P_{max}^{ST} or not. It is worth noting that the cooperation probability achieved by our DWWRS-MAS gradually approaches that attained in CCS-2, when the secondary network became larger, which was an exlicit benefit of having an increased probability of beneficial STs as evidenced in Fig 5.20.

Transmit Power Consumption

Fig 5.21 shows the STTP consumed in our DWWRS-MAS and in the other cooperative systems, namely in CCS-1, CCS-2 and R-CSLS under different maximum transmit power constraints of the PT and ST for $\mathcal{I} = 2$, $\alpha = 2.0$ and $\beta = 0.5$. Compared to the performance of our DWWRS-MAS associated with $P_{max}^{PT} < P_{max}^{ST}$, a higher STTP is consumed by our DWWRS-MAS in the scenario of $P_{max}^{PT} > P_{max}^{ST}$, as seen in Fig 5.21, because more than

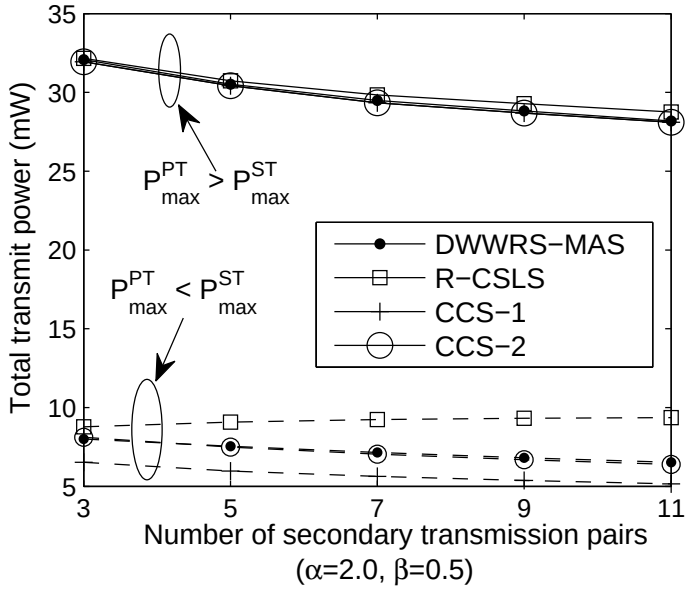

FIGURE 5.21: The system's total transmit power versus the number of secondary users for $\mathcal{I} = 2$, $\alpha = 2.0$ and $\beta = 0.5$ when the PTs and STs have different maximum transmit power constraints in the network of Fig 5.10 while using the cooperation probability of Fig 5.20 relying on the proposed DWWRS-MAS of Fig 5.3 and Fig 5.5. The results are contrasted to those of the benchmark systems introduced in Section 5.5.1.

70% of the PT's data is directly transmitted to the corresponding PR, when the PT has higher maximum transmit power P_{max}^{PT}, i.e. a more relaxed constraint, as shown in Fig 5.20. The lower cooperation probability in the scenario of $P_{max}^{PT} > P_{max}^{ST}$ also limits the STTP of CCS-1 and CCS-2. Hence, there is no evident difference between the STTP of these two centralized cooperative systems, when the PT has a higher maximum transmit power P_{max}^{PT}, as shown in Fig 5.21. However, observe in Fig 5.21 that CCS-1 and CCS-2 exhibit a different performance, when the ST has a higher maximum transmit power due to the increased cooperation probability seen in Fig 5.20. Considering the scenario of $P_{max}^{PT} < P_{max}^{ST}$, CCS-2 dissipates a higher STTP than CCS-1, because CCS-2 is designed for minimizing the TPP by taking into account the higher priority of the PT, instead of minimizing the STTP, which is the OF of CCS-1. Since the higher priority of the PT is also considered in our DWWRS-MAS, observe in Fig 5.21 that the STTP consumed by the proposed DWWRS-MAS is higher than that in CCS-1. Furthermore, the STTP consumed by our DWWRS-MAS is close to that of CCS-2 in Fig 5.21. When the secondary network becomes larger, the STTP of our DWWRS-MAS is reduced due to the increased probability of matching with beneficial STs, regardless whether P_{max}^{PT} is higher than P_{max}^{ST} or not, which is explicitly see in Fig 5.21.

Compared to the scenario of $P_{max}^{PT} > P_{max}^{ST}$, considerable TPP may be conserved, when P_{max}^{PT} is lower than P_{max}^{ST} due to the higher cooperation probability, as seen in Fig 5.22 and Fig 5.20. Based on the OF of CCS-2 formulated by Eq (5.89), the PTs consume the lowest TTP in CCS-2, as seen in Fig 5.22. When we have $P_{max}^{PT} > P_{max}^{ST}$, less ST can afford the

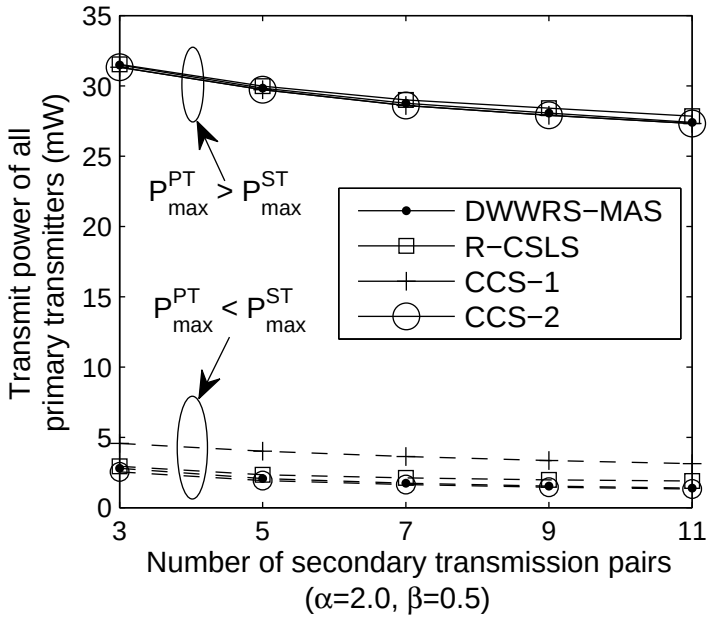

FIGURE 5.22: The transmit power of all PTs versus the number of secondary users for $\mathcal{I} = 2$, $\alpha = 2.0$ and $\beta = 0.5$ when the PTs and STs have different maximum transmit power constraints in the network of Fig 5.10 while using the cooperation probability of Fig 5.20 relying on the proposed DWWRS-MAS of Fig 5.3 and Fig 5.5. The results are contrasted to those of the benchmark systems introduced in Section 5.5.1.

transmit power required for satisfying the transmit rate requirement of both the PT and itself under the constraint of a lower maximum transmit power P_{max}^{ST}. Hence, CCS-2 and CCS-1 as well as our DWWRS-MAS consume a similar TTP in Fig 5.22, because most of the PT's data is directly transmitted to the PR, when $P_{max}^{PT} > P_{max}^{ST}$. However, as portrayed in Fig 5.22 the advantage of CCS-2 becomes more evident in Fig 5.22 for $P_{max}^{PT} < P_{max}^{ST}$, because the probability that ST is capable of affording the transmit power required for successfully transmitting the superposition-coded data is increased, when STs have a higher maximum transmit power, i.e. they are less constrained. It is worth noting that the TTP of our DWWRS-MAS is almost as low as that of CCS-2, as shown in Fig 5.22.

Fig 5.23 illustrates the ATPES of the proposed DWWRS-MAS, CCS-1, CCS-2 and R-CSLS for $\mathcal{I} = 2$, $\alpha = 2.0$ and $\beta = 0.5$. Observe in Fig 5.23 that a higher ATPES is dissipated for $P_{max}^{PT} < P_{max}^{ST}$, because the ST is capable of transmitting the superposition-coded data at a higher transmit power, which becomes affordable under the more relaxed maximum transmit power constraint P_{max}^{ST}. Compared to the scenario of $P_{max}^{PT} > P_{max}^{ST}$, the difference between the ATPES of our DWWRS-MAS and CCS-1 as well as CCS-2 becomes more evident for $P_{max}^{PT} < P_{max}^{ST}$ due to the increased cooperation probability and as a benefit of the higher maximum transmit power P_{max}^{ST} of the ST, as shown in Fig 5.23. Based on the above discussion, less STs can afford the transmit power required for achieving the increased target transmit rate of the PT, whilst satisfying its own transmit rate requirement at a constraint power P_{max}^{ST}, when we have $P_{max}^{PT} > P_{max}^{ST}$. Hence, most of the PTs' data

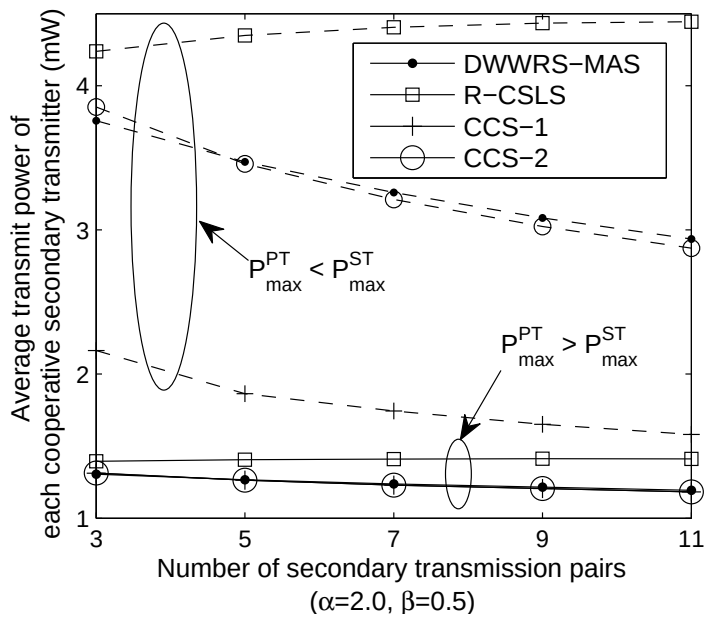

FIGURE 5.23: The average transmit power of each matched ST versus the number of secondary users for $\mathcal{I} = 2$, $\alpha = 2.0$ and $\beta = 0.5$ when the PTs and STs have different maximum transmit power constraints in the network of Fig 5.10 while using the cooperation probability of Fig 5.20 relying on the proposed DWWRS-MAS of Fig 5.3 and Fig 5.5. The results are contrasted to those of the benchmark systems introduced in Section 5.5.1.

is directly delivered to the PRs, when we have $P_{max}^{PT} > P_{max}^{ST}$. Observe in Fig 5.23 that this phenomenon reduced the gap between the curves of the cooperative systems considered in this section. For $P_{max}^{PT} < P_{max}^{ST}$, the increased probability of finding beneficial STs and the increased P_{max}^{ST} result in having more candidate cooperative pairs for the controller in CCS-1 and CCS-2. When aiming for minimizing the STTP, the centralized controller in CCS-1 has to minimize the ATPES, when we have $P_{max}^{PT} < P_{max}^{ST}$, as shown in Fig 5.23. Upon considering the priority of the PTs, CCS-2 aims for minimizing the TPP at the cost of a higher ATPES.

Achievable Transmit Rate

Fig 5.24, Fig 5.25 and Fig 5.26 evaluate the effect of the maximum transmit power of both PT and ST on the TTRP, ATRES as well as TTR respectively, when $\mathcal{I} = 2$, $\alpha = 2.0$ and $\beta = 0.5$. As seen in Fig 5.24, a lower TTRP is achieved when $P_{max}^{PT} < P_{max}^{ST}$ due to the lower transmit rate requirement $\alpha C_{PT,PR}^{max}$ of the PT. By contrast, a higher ATRES and TTR is achieved for $P_{max}^{PT} < P_{max}^{ST}$ due to the higher transmit rate requirement $\beta C_{ST,SR}^{max}$ of the ST and owing to the increased cooperation probability, as shown in Fig 5.26 and Fig 5.25. Furthermore, the particular ST, which promises to require a reduce transmit power for successfully conveying the superposition-coded data may benefit from a better channel for the link between the ST and SR. This phenomenon may also improve the ATRES. For

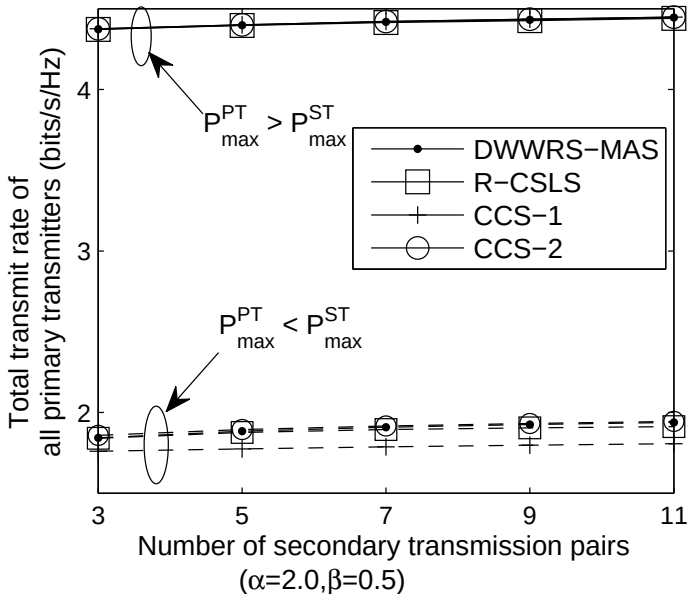

FIGURE 5.24: The achievable transmit rate of all PTs versus the number of secondary users for $\alpha = 2.0$ and $\beta = 0.5$ when the PTs and STs have different maximum transmit power constraints in the network of Fig 5.10 using the cooperation probability of Fig 5.20 relying on the proposed DWWRS-MAS of Fig 5.3 and Fig 5.5. The results are contrasted to those of the benchmark systems introduced in Section 5.5.1.

example, CCS-1 achieved the highest ATRES for $P_{max}^{PT} < P_{max}^{ST}$ as seen in Fig 5.25, while the lowest ATPES is dissipated in CCS-1, as seen in Fig 5.23. Observe in Fig 5.26 that an increased TTR is achieved, when we have $P_{max}^{PT} > P_{max}^{ST}$ for $\mathcal{M} < 5$ due to the associated higher TTRP. By contrast, a higher TTR is achieved for $P_{max}^{PT} < P_{max}^{ST}$, when relying on the higher ATRES, as seen in Fig 5.26.

5.5.7 Effect of Number of PTPs

Assuming that the PTs and STs have the same maximum transmit power constraints, in this section we evaluate the performance of the proposed DWWRS-MAS, when the primary network has more than two PTPs.

Cooperation Probability

Fig 5.27 shows the comparison of the average cooperation probability of each PT and of each ST, when the primary network has $\mathcal{I} = 2$ PTPs, $\mathcal{I} = 5$ PTPs and $\mathcal{I} = 8$ PTPs. Given the size of the secondary network, observe in Fig 5.27 that more PTs might fail to find a cooperative partner as the number of PTPs is increased, because the contention between the PTs becomes more intense. Furthermore, the probability of the PTs, which fail to find candidate cooperative partners is increased, when the primary network becomes larger.

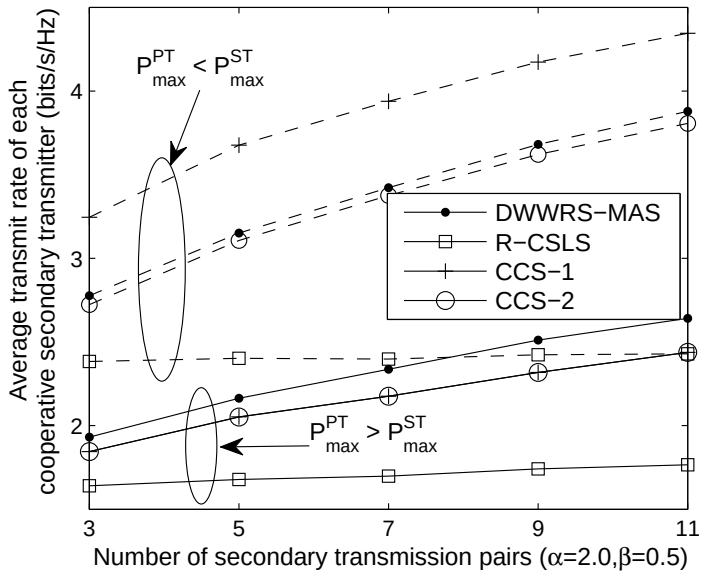

FIGURE 5.25: The average transmit rate of each matched ST versus the number of secondary users for $\alpha = 2.0$ and $\beta = 0.5$ when the PTs and STs have different maximum transmit power constraints in the network of Fig 5.10 using the cooperation probability of Fig 5.20 and relying on the proposed DWWRS-MAS of Fig 5.3 and Fig 5.5. The results are contrasted to those of the benchmark systems introduced in Section 5.5.1.

Hence, the cooperation probability of the PTs is reduced from 52% to 34% for $\mathcal{M} = 3$, when the number of PTPs is increased from $\mathcal{I} = 2$ to $\mathcal{I} = 8$, as seen in Fig 5.27. By contrast, the cooperation probability of the STs is increased, when the primary network becomes larger as shown in Fig 5.27, because the STs benefit from more opportunities of accessing the licensed spectrum, as the primary network has more PTPs. When the secondary network becomes larger, the cooperation probability of the PTs is increased, since they benefit from having an increased probability of finding meritorious STs, as seen in Fig 5.27. By contrast, the cooperation probability of the STs is reduced, as the number of STPs is increased due to the more intense competition between the STs and owing to the increased probability of having deficient STs which cannot become the cooperative partner of the PT or cannot even become a candidate cooperative partner.

Transmit Power Consumption

Fig 5.28, Fig 5.29, Fig 5.30 characterize the performance of the TPP, STTP and the total transmit power of all the STs (TTPS) respectively, when the primary network has different number of PTPs for $\alpha = 2.0$ and $\beta = 0.5$. Here the TTPS is formulated as $\frac{1}{N_{all}} \cdot \sum_{x=1}^{N_{all}} \left[\sum_{m=1}^{\mathcal{M}} P_{ST}^{x}(m) \right]$, where N_{all} denotes the total number of instances of our DWWRS-MAS in the Monte Carlo simulation. Furthermore, $P_{ST}^{x}(m)$ denotes the transmit power dissipated by ST_m, when successfully conveying the superposition-coded data

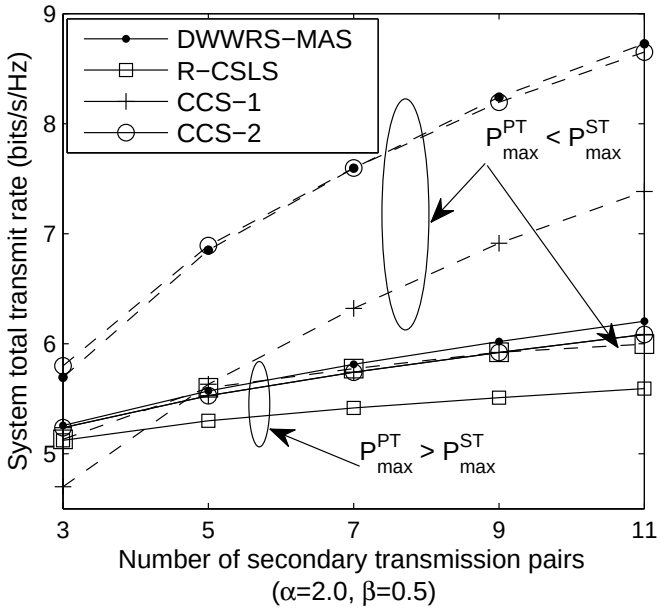

FIGURE 5.26: The system's total transmit rate versus the number of secondary user for $\alpha = 2.0$ and $\beta = 0.5$ when the PTs and STs have different maximum transmit power constraints in the network of Fig 5.10 using the cooperation probability of Fig 5.20 and achieving the total transmit rate of all PTs quantified in Fig 5.24 and the average transmit rate of each matched ST characterized in Fig 5.25 relying on the proposed DWWRS-MAS of Fig 5.3 and Fig 5.5. The results are contrasted to those of the benchmark systems introduced in Section 5.5.1.

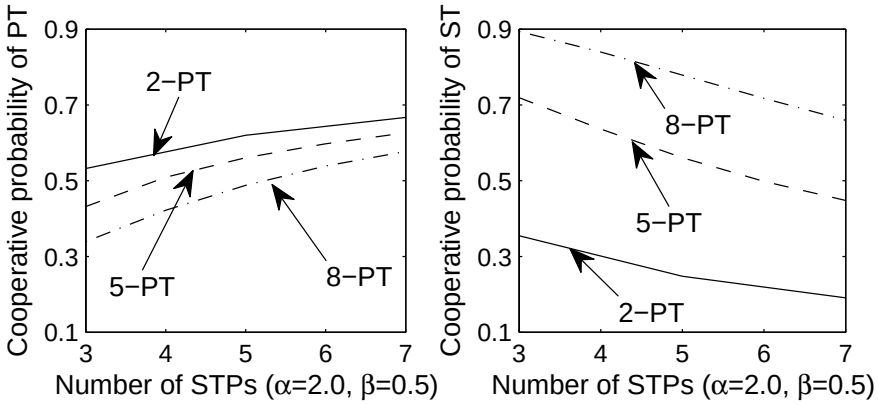

FIGURE 5.27: Average cooperation probability of each PT and of each ST versus the number of secondary users for $\alpha = 2.0$ and $\beta = 0.5$ versus the number of PTs relying on the proposed DWWRS-MAS of Fig 5.3 and Fig 5.5.

during the x-th instance of the Monte Carlo simulation. If ST_m cannot win a transmission opportunity during the x-th instance of the Monte Carlo simulation, the power $P^x_{ST}(m)$ is equal to zero. As observed in Fig 5.28 and Fig 5.29, the highest TTP and STTP are dissipated, when the primary network has $\mathcal{I} = 8$ PTPs. As seen in Fig 5.28 and Fig 5.29, both the TTP and STTP are reduced as the size of the primary network is increased, because more PTs invert their transmit power into transmitting their data with the aid of cooperative transmissions or into directly conveying their data to the corresponding PR.

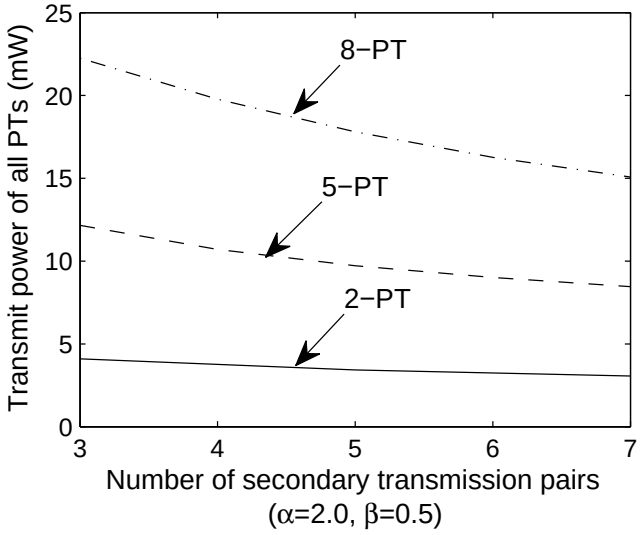

FIGURE 5.28: The total transmit power of all PTs versus the number of secondary users for $\alpha = 2.0$ and $\beta = 0.5$ parameterized with the number of PTs and using the average cooperation probability of Fig 5.27 relying on the proposed DWWRS-MAS of Fig 5.3 and Fig 5.5.

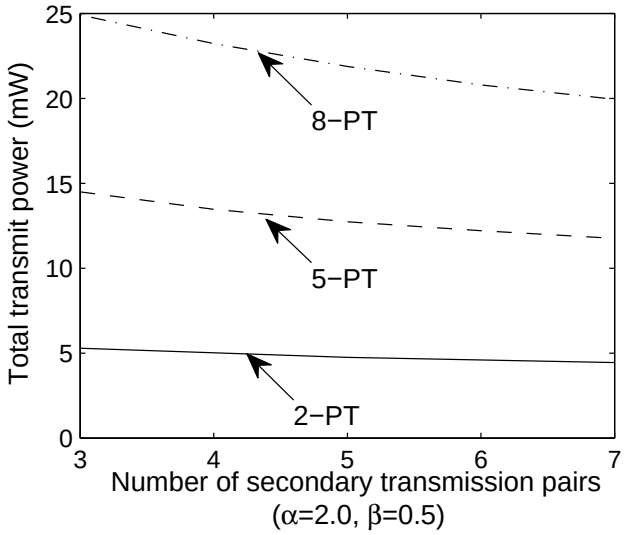

FIGURE 5.29: The system's total transmit power versus the number of secondary users for $\alpha = 2.0$ and $\beta = 0.5$ associated with different number of PTs using the average cooperation probability of Fig 5.27 and dissipating the total transmit power of all PTs as quantified in Fig 5.28 as well as consuming the total transmit power of all the STs as quantified in Fig 5.30 relying on the proposed DWWRS-MAS of Fig 5.3 and Fig 5.5.

As seen in Fig 5.30, the TTPS is also increased, when the primary network becomes larger, because the STs may be granted more opportunities for transmitting their data within the licensed spectrum in the larger primary network. As discussed above, the TTPS is increased as the secondary network becomes larger due to the increased cooperation probability of the PTs in Fig 5.27. However, observe in Fig 5.30 that TTPS is increased in the network supporting $\mathcal{I} = 8$ PTPs more rapidly than that in the network having $\mathcal{I} = 2$ PTPs. Up on

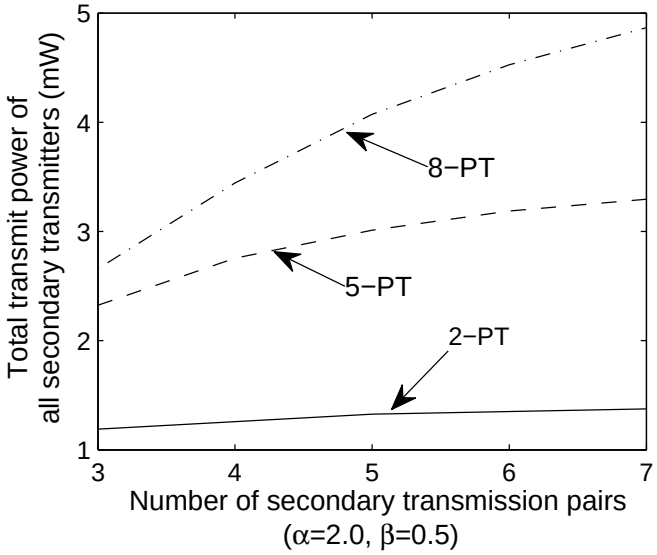

FIGURE 5.30: The transmit power of matched STs versus the number of secondary users for $\alpha = 2.0$ and $\beta = 0.5$ associated with different number of PTs using the average cooperation probability of Fig 5.27 and dissipating the total transmit power of all the PTs and STs as quantified in Fig 5.29 as well as consuming the total transmit power of all PTs of Fig 5.28 relying on the proposed DWWRS-MAS of Fig 5.3 and Fig 5.5.

considering a cognitive network, where the number of STPs varies from $\mathcal{M} = 3$ to $\mathcal{M} = 7$, the number of PTs is always lower than that of the STs, when the primary network has $\mathcal{I} = 2$ PTPs. When both of the two PTs have cooperative partners, only two of the STs are granted transmission opportunities even in the largest secondary network associated with $\mathcal{M} = 7$. Hence, as shown in Fig 5.30 the TTPS is slightly increased in the network having $\mathcal{I} = 2$ PTPs when the number of STPs is increased from $\mathcal{M} = 3$ to $\mathcal{M} = 7$. Bearing in mind the above-mentioned cognitive network, where the number of STPs varies from $\mathcal{M} = 3$ to $\mathcal{M} = 7$, the number of PTPs is always higher than that of the STPs, when the primary network has $\mathcal{I} = 8$ PTPs. Hence, some of the PTs might still fail to find cooperative partners even in the best scenario where all the STs have a cooperative partner. Hence, as evidenced by Fig 5.30 more STs may become cooperative partners in the cognitive network having $\mathcal{I} = 8$ PTPs, when the number of STPs is increased. This phenomenon noticeably increases the TTPS consumed in the network having more PTPs than STPs.

Achievable Transmit Rate

Fig 5.31 and Fig 5.32, evaluate the effect of different number of PTPs on the TTR and total transmit rate of all cooperative STs (TTRS) respectively, when we have $\alpha = 2.0$ and $\beta = 0.5$. The TTRS is formulated as $\frac{1}{N_{all}} \cdot \sum_{x=1}^{N_{all}} \left[\sum_{m=1}^{\mathcal{M}} R_{ST}^{x}(m) \right]$, where N_{all} denotes the total number of instances of our DWWRS-MAS in the Monte Carlo simulation. Furthermore, $R_{ST}^{x}(m)$ denotes the achievable transmit rate of the ST, when the ST ST_m is granted a

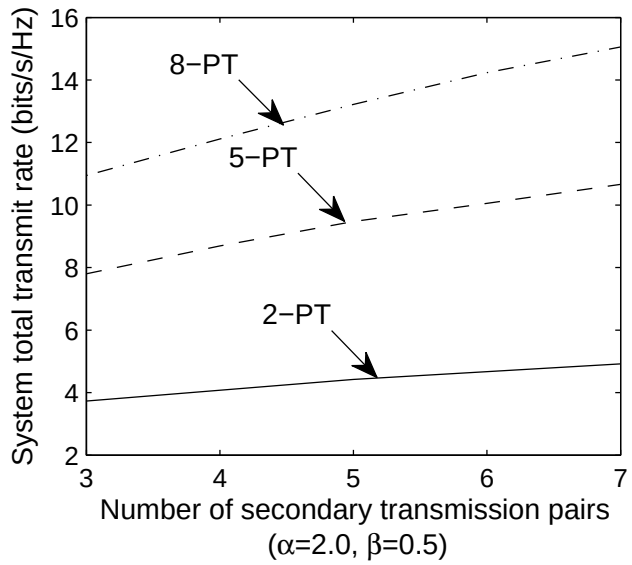

FIGURE 5.31: The system's total transmit rate versus the number of secondary users for $\alpha = 2.0$ and $\beta = 0.5$ associated with different number of PTs using the average cooperation probability of Fig 5.27 relying on the proposed DWWRS-MAS of Fig 5.3 and Fig 5.5.

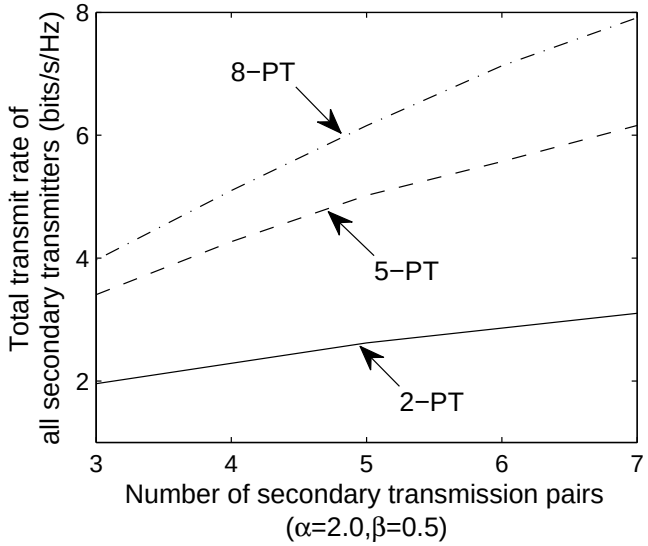

FIGURE 5.32: The achievable transmit rate of all STs versus the number of secondary users for $\alpha = 2.0$ and $\beta = 0.5$ associated with different number of PTs using the average cooperation probability of Fig 5.27 and achieving the total transmit rate of all the PTs and STs as quantified in Fig 5.31 relying on the proposed DWWRS-MAS of Fig 5.3 and Fig 5.5.

transmit opportunity during the x-th instance of the Monte Carlo simulation. If ST_m cannot win a transmission opportunity during the x-th instance of the Monte Carlo simulation, $R^x_{ST}(m)$ is equal to zero. Observe in Fig 5.31 that TTR is increased, when the primary network becomes larger due to the increased number of cooperative transmissions. More explicitly, when more PTs intend to lease part of their spectrum in exchange for cooperative transmission assistance, the cooperation probability of the ST is increased, as shown in Fig 5.27. This phenomenon improves the TTRS in the larger primary network. Hence, the

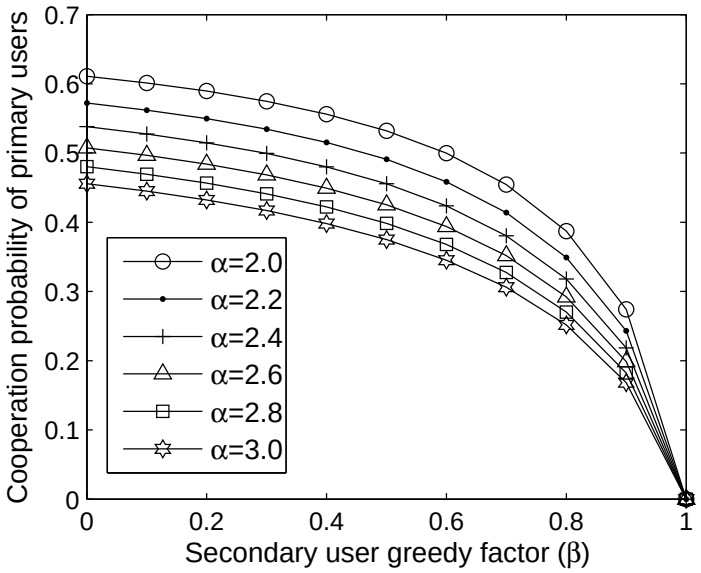

FIGURE 5.33: Cooperation probability of the PT versus the STs' greedy factor parameterized by the PTs' greedy factor α in a network hosting two PTPs and three STPs relying the the proposed DWWRS-MAS of Fig 5.3 and Fig 5.5.

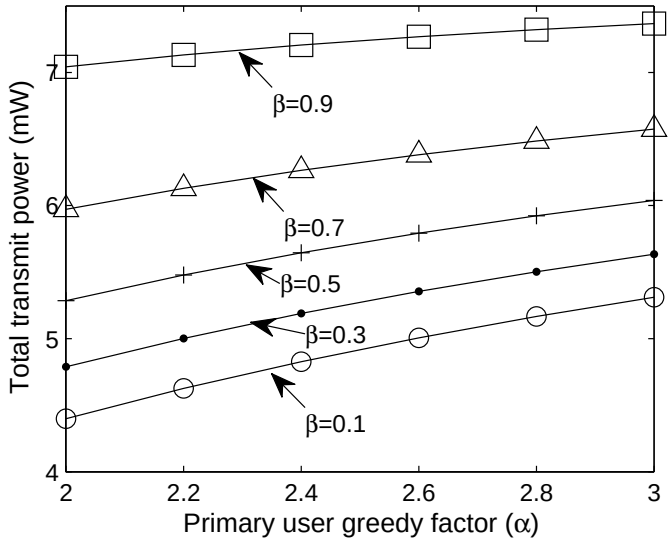

FIGURE 5.34: The total transmit power of users versus the PTs' greedy factor α parameterized by the STs' greedy factor β in a network hosting two PTPs and three STPs as well as using the cooperation probability of the PT quantified in Fig 5.33 relying on the the proposed DWWRS-MAS of Fig 5.3 and Fig 5.5.

highest TTRS is achieved, when the network supporting $\mathcal{I} = 8$ PTPs, as seen in Fig 5.32.

5.5.8 Effect of the Users' Greedy Factor

Fig 5.33, Fig 5.34 and Fig 5.35 characterize the effect of different greedy factors of both the PT and ST on the cooperation probability of PT, STTP and TTR in our DWWRS-MAS

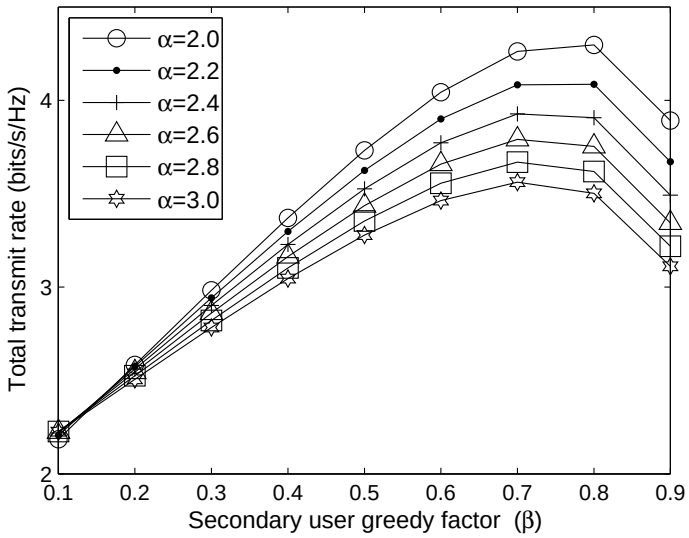

FIGURE 5.35: The system's total transmit rate versus the STs' greedy factor β parameterized by the PTs' greedy factor α in a network hosting two PTPs and three STPs as well as using the cooperation probability of the PT quantified in Fig 5.33 relying the the proposed DWWRS-MAS of Fig 5.3 and Fig 5.5.

respectively, when the network has two PTPs and three STPs. Observe in Fig 5.33 that the cooperation probability of the PT is reduced, when either the PT or the ST becomes greedier. When the PT's greedy factor α is increased, less STs are capable of affording the increased transmit power required for satisfying the higher transmit rate requirement of the PT. This phenomenon reduces the cooperation probability of the PTs and simultaneously increases the transmit power of the specific STs, which are the cooperative partners of the PTs. Hence, a higher STTP is dissipated as PTs' greedy factor α is increased, which is explicitly seen in Fig 5.34. Although the PTs' transmit rate requirement of $\alpha C_{PT,PR}^{max}$ is increased, when the PTs become greedier, less PTs are capable of achieving the increased target transmit rate due to the reduced cooperation probability. Hence, the TTR is reduced, when α is increased, as evidenced by Fig 5.35

Given the greediness of the PTs, the STs have to dissipated an increased transmit power for achieving their higher target transmit rate, when the STs becomes greedier. Hence, the cooperation probability is reduced and STTP is increased, when the ST's greedy factor β is increased, as seen in Fig 5.33 and Fig 5.34, because less STs are capable of affording the increased transmit power required for satisfying their higher transmit rate requirement under the maximum transmit power constraint. Observe in Fig 5.35 that the TTR is increased, when the STs become greedier for $\beta \leq 0.8$, because the achievable transmit rate $\beta C_{ST,SR}^{max}$ of the STs is increased as β becomes higher. However, the increased transmit rate of ST still fails to compensate for the detrimental effect of the reduced cooperation probability observed in Fig 5.35 for $\beta > 0.8$. Hence, the TTR is reduced, when the greedy factor of the ST exceeds $\beta = 0.8$, as seen in Fig 5.35.

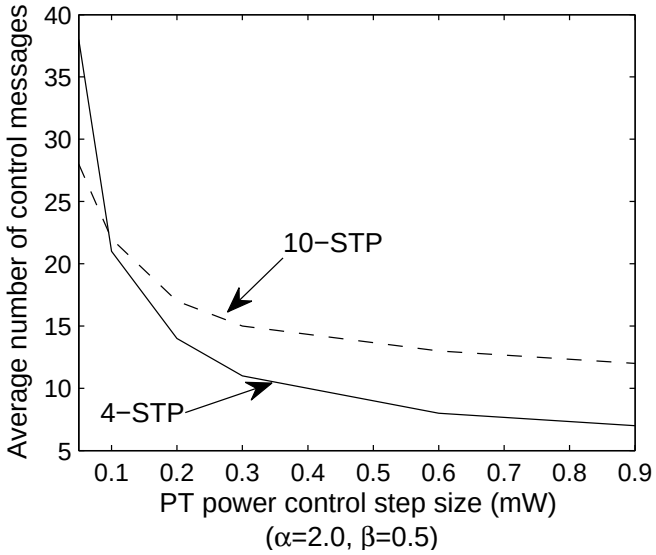

FIGURE 5.36: Number of control messages exchanged during the selection of the cooperative pairs in the network of Fig 5.10 relying on the proposed DWWRS-MAS of Fig 5.3 and Fig 5.5 versus the PTs' transmit power control step size Δ of Fig 5.2 for $\alpha = 2.0$ and $\beta = 0.5$.

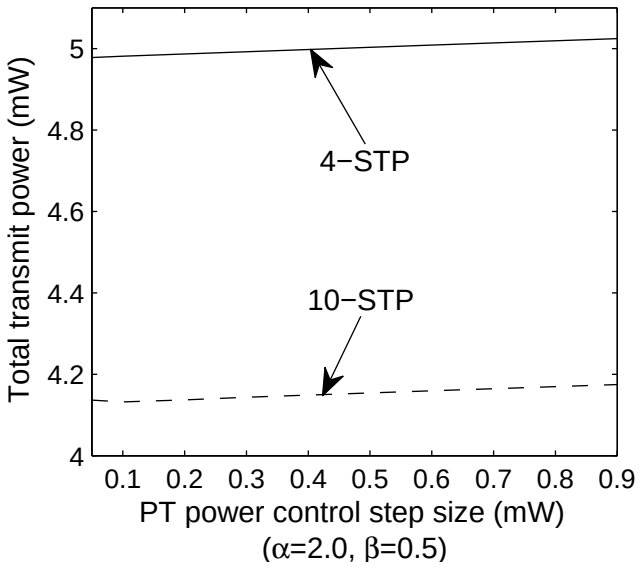

FIGURE 5.37: The system's total transmit power in the network of Fig 5.10 relying on the proposed DWWRS-MAS of Fig 5.3 and Fig 5.5 versus the PTs' transmit power control step size Δ of Fig 5.2 for $\alpha = 2.0$ and $\beta = 0.5$.

5.5.9 Effect of the PT Power Control Step Size

Based on the network having two PTPs, where the transmit power of both the PTs and STs is constrained by the same upper bound P_{max}, in this section we evaluate the effect of different transmit power control steps size Δ of the PTs on the performance of our DWWRS-MAS for $\alpha = 2.0$ and $\beta = 0.5$. To this effect, Fig 5.36 portrays the number of control messages required between the PTs and STs for selecting their cooperative partners

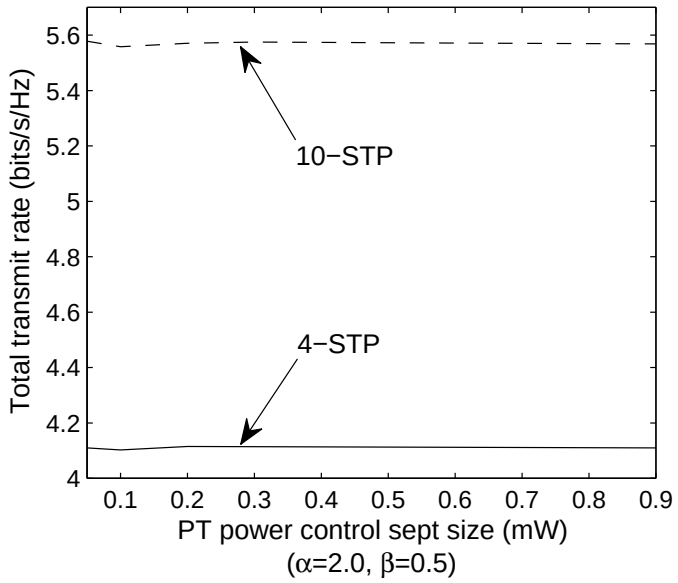

FIGURE 5.38: The system's total transmit rate in the network of Fig 5.10 relying on the proposed DWWRS-MAS of Fig 5.3 and Fig 5.5 versus the PTs' transmit power control step size Δ of Fig 5.2 for $\alpha = 2.0$ and $\beta = 0.5$.

in our DWWRS-MAS as a function of the PT transmit power control step size Δ. Observe in Fig 5.36 that the number of control messages is significantly reduced, as the step size Δ of the PTs' transmit power is increased in the range of $\Delta < 0.2$. For $\Delta > 0.2$, the number of control messages is slightly reduced, as Δ is increased, as seen in Fig 5.36. According to the proposed DWWRS-MAS, the PT increases its transmit power step by step, when it cannot find a cooperative partner at the current power level as seen in Fig 5.4 and Table 5.1. Hence, the PTs have more legitimate transmit power levels for a smaller Δ. However, observe in Fig 5.36 that having a reduced step size Δ significantly increased the number of control messages exchanged before the PTs succeed in selecting an appropriate cooperative partner, when the PTs have a small step size Δ, such as $\Delta = 0.05$. Observe in Fig 5.2, the PTs have less legitimate transmit power levels for a larger Δ. Hence, observe in Fig 5.36 that the average number of control messages exchanged between the PTs and STs is reduced from $\mathcal{N}_{control} = 11$ to $\mathcal{N}_{control} = 7$ for $\mathcal{M} = 4$ and from $\mathcal{N}_{control} = 15$ to $\mathcal{N}_{control} = 13$ for $\mathcal{M} = 10$, when Δ is increased from $\Delta = 0.3$ to $\Delta = 0.9$. When the secondary network becomes larger, the PTs benefit from having more candidate cooperative partners due to the increased probability of finding meritorious STs. Hence, more control messages are sent by the candidate partners of the PTs for the sake of contending for transmission opportunities in the network having more STPs, as shown in Fig 5.36.

As discussed above, the probability that the PTs find their cooperative partners, when they have a high transmit power level is increased upon increasing the PTs' transmit power control step size Δ. Hence, a higher STTP is dissipated for a larger Δ, as seen in Fig 5.37. According to the proposed DWWRS-MAS, provided that ST_m could still become a candi-

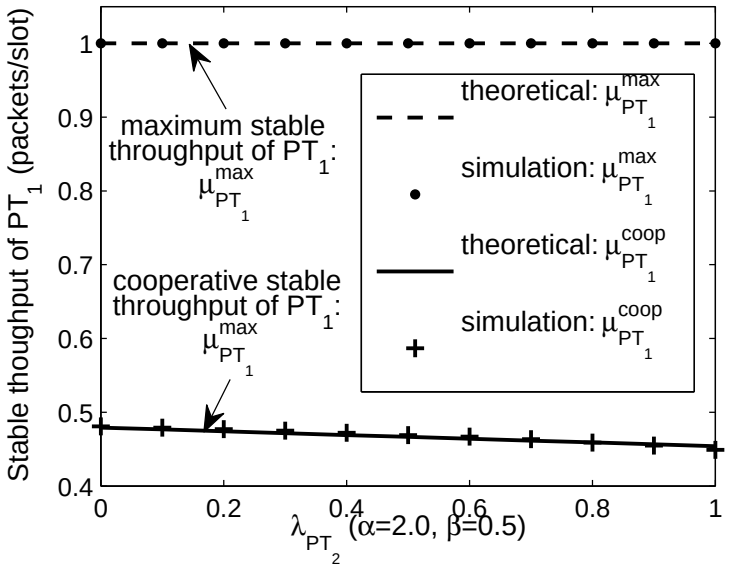

FIGURE 5.39: The stable throughput of PT_1 formulated by Eq (5.15) versus the arrival rate of λ_{PT_2} for $\alpha = 2.0$ and $\beta = 0.5$ for the network of Fig 5.11 relying on the proposed DWWRS-MAS of Fig 5.3 and Fig 5.5 and on the queueing model of Fig 5.6.

date cooperative partner of PT_i, when PT_i relies on a reduced lower transmit power level, naturally ST_m still remains a legitimate candidate cooperative partner of PT_i at an increased transmit power level of PT_i. This is plausible, because the ST's transmit power required for successfully conveying the superposition-coded data is reduced, when the transmit power of PT is increased in our DWWRS-MAS. Hence, increasing Δ does not affect the cooperation probability of PT, when the PT's transmit power reaches its highest power level, namely P_{max}. Therefore, the TTR remains near-constant as Δ is increased, which is explicitly observed in Fig 5.38.

Based on the above discussions, there is a tradoff between the average number of control messages and the STTP. According to Fig 5.36 and Fig 5.37, $\Delta = 0.3$ constitutes an appropriate transmit power control step size, which is capable of ensuring an acceptable amount of control message without an excessive degradation of STTP.

5.5.10 Stable throughput

As mentioned in Section 5.5.1, in this section we will consider as a small network supporting two PTs and two STs as well as a common destination D, when evaluating the stable throughput of both the PTs and STs, as seen in Fig 5.11. The distance from each PT to D is the same, while ST_1 is allocated in the middle of the link between PT_1 and D. Finally ST_2 is in the middle of the link between PT_2 and D, as seen in Fig 5.11.

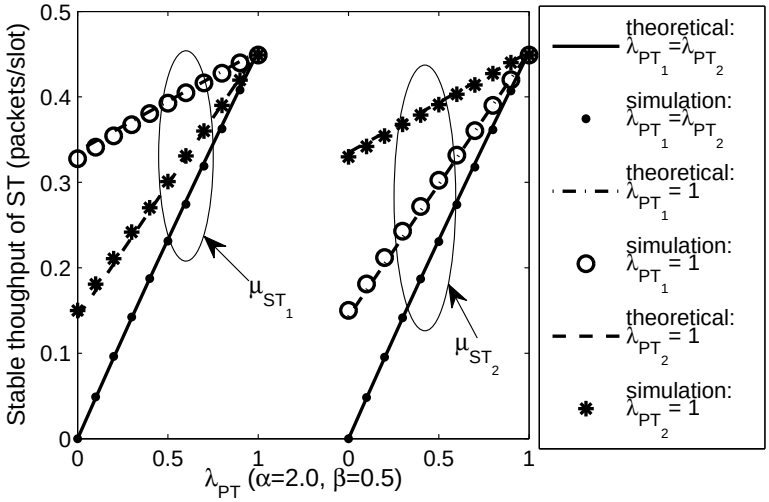

FIGURE 5.40: The stable throughput of the ST formulated by Eq (5.65) versus the arrival rate of λ_{PT_2} and λ_{PT_2} for $\alpha = 2.0$ and $\beta = 0.5$ for the network of Fig 5.11 relying on the proposed DWWRS-MAS of Fig 5.3 and Fig 5.5 and on the queueing model of Fig 5.6.

According to the proposed DWWRS-MAS, the PTs' data may be delivered with the aid of cooperative transmission assistance from the STs, when the PTs and STs form cooperative pairs. If no ST can be the cooperative partner of a PT, this PT directly transmits its data to D. Hence, the maximum stable throughput of PT_1 formulated by Eq (5.15) is one packet per slot as shown in Fig 5.39. However, an increased transmit rate is achieved by the PTs with the aid of cooperative transmission assistance. Hence, the stable throughput of PT_1 achieved by the cooperative transmission $\mu_{PT_1}^{coop}$ is also shown in Fig 5.39. When the average arrival rate λ_{PT_2} is increased, the competition between PT_1 and PT_2 becomes more intense. Hence, $\mu_{PT_1}^{coop}$ is reduced, when PT_2 has more data to send, as seen in Fig 5.39.

Fig 5.40 shows the stable throughput of ST_1 and ST_2 in packets/slot achieved in three different scenarios for $\alpha = 2.0$ and $\beta = 0.5$, where PT_1 and PT_2 have the same average arrival rate, namely $\lambda_{PT_1} = \lambda_{PT_2}$ in Scenario 1. In Scenario 2, PT_1 always has data to send, namely we have $\lambda_{PT_1} = 1$, while λ_{PT_2} is increased from 0 to 1. By contrast, PT_2 always has data to send, while λ_{PT_1} varies from 0 to 1. Observe in Fig 5.40 that the stable throughput of both ST_1 and ST_2 is increased, as the arrival rate of the PTs becomes higher. As a benefit of our cooperative spectrum leasing system, the STs may be granted a transmission opportunity only when at least one PT has data to send, as mentioned in Section 5.4.1.3. This phenomenon implies that the STs may be granted more frequent transmission opportunities, when the PTs have more packets to send. Hence, the STs' stable throughput are increased, as either λ_{PT_1} or λ_{PT_2} is increased.

As shown in Fig 5.40, ST_1 and ST_2 achieve a similar stable throughput for $\lambda_{PT_1} = \lambda_{PT_2}$ due to their symmetric locations, as seen in Fig 5.11. However, when we have $\lambda_{PT_1} = 1$ and

$\lambda_{PT_2} < 1$, μ_{ST_1} is higher than μ_{ST_2}, as shown in Fig 5.40. Based on the symmetric network topology of Fig 5.11 considered in this section, ST_1 is closer to PT_1 than ST_2, which implies that the pathloss reduction of the link between PT_1 and ST_1 is higher than that of the link between PT_1 and ST_2, which implies that the ST_1 has a higher probability to become the cooperative partner of PT_1, provided that PT_1 has data to send in the current time slot. However, the probability that ST_1 and PT_2 form a cooperative pair $\mathbb{O}(PT_2, ST_1)$ is lower than the probability of $\mathbb{O}(PT_2, ST_2)$ when PT_2 has data to send in the current time slot, which is a consequence of having a higher distance between PT_2 and ST_1. Hence, ST_1 is capable of achieving a higher stable throughput for $\lambda_{PT_1} = 1$ and $\lambda_{PT_2} < 1$, as seen in Fig 5.40. However, when PT_2 provides more transmit opportunities for the STs due to the higher average arrival rate λ_{PT_2}, ST_2 becomes capable of achieving a higher stable throughput, as observed in Fig 5.40. More explicitly, we have $\mu_{ST_1} < \mu_{ST_2}$, as shown in Fig 5.40, because ST_2 is granted more transmission opportunities by PT_2, when PT_1 does not send data. Observe in both Fig 5.39 and Fig 5.40 that the theoretical curve and the practical results almost overlap each other. Hence, our stability analysis of Section 5.4.1 may be deemed accurate.

5.6 Chapter Summary

In this chapter, we first formulated a WWRSF for a CSLS hosting multiple PTPs and multiple STPs, as described in Section 5.2.1. Based on our WWRSF of in Section 5.2.2, the PTs lease part of their spectral resource to STs in exchange for cooperative transmission assistance for the sake of minimizing their transmit power and simultaneously for achieving their target transmit rate which is higher than the maximum rate achieved by conventional direct transmission. The STs, which provide cooperative transmission assistance for their cooperative partners are capable of accessing the licensed spectrum originally granted to their cooperative partner for conveying their data. However, these STs have to dissipate extra transmit power for conveying the PTs' data. Hence, the other OFs aim for minimizing the total transmit power of the cooperative partners of the PTs. Furthermore, considering the selfish nature of the ST, each ST selects the best PT as its cooperative partner for the sake of minimizing its transmit power, when multiple PTs contend for acquiring cooperative transmission assistance from this ST.

In Section 5.3, our DWWRS-MAS was developed for the sake of distributively selecting cooperative pairs based on the proposed WWRSF. In order to select the best cooperative pairs, we designed a distributed reciprocal selection scheme, which allows the PTs to select their best cooperative partner - best ST - which require the lowest PT transmit power, as seen in Fig 5.3 and Table 5.1. Acting as RNs, each ST intends to select its best cooperative

partner - best PT - which requires the lowest ST transmit power, when the ST has multiple candidate cooperative partners, as seen in Fig 5.5 and Table 5.2. Furthermore, the specific ST, which promises to require the lowest transmit power may win the contention for the transmit opportunity granted by the PT relying on the proposed ST selection scheme of Section 5.3, which was conceived for the sake of minimizing the total transmit power of the cooperative partners of the PTs.

The stable throughput of each PT based on the proposed DWWRS-MAS was derived in Section 5.4.1.1. Based on the queueing model of Fig 5.6, the average departure rate at the PT PT_i is expressed by Eq (5.15), which is constituted by the sum of the average departure rate $\mu_{PT_i}^{coop}$ achieved by the cooperative transmission plus the average departure rate $\mu_{PT_i}^{noncoop}$ achieved by the direct transmission without any cooperative transmission assistance. Furthermore, Section 5.4.1.3 analyzes the stable throughput of each ST in the queueing system modelled in Section 5.4.1.1, as seen in Fig 5.6. The ST ST_m is assumed to rely on the pair of queues Q_{ST_m} and Q_{PT,ST_m}, where the former was provided for buffering its own data, while the latter for the PT's data. The average departure rate of the queues Q_{ST_m} is equal to the corresponding average arrival rate, which is limited by the probability that the PTs' queue is not empty and by the probability that its has a cooperative partner, as encapsulated in Eq (5.46). Both the queues Q_{ST_m} and Q_{PT,ST_m} have the same average departure rate as formulated by Eq (5.65), which is a constraint imposed by superposition coding. The algorithmic stability of the proposed DWWRS-MAS was analysed in Section 5.4.2 based on the matching theory. According to the definition of stable match as exemplified by Table 5.4 Fig 5.9, the proposed DWWRS-MAS is capable of producing stable cooperative pairs. Moreover, at least one cooperative pair formed by the proposed DWWRS-MAS is capable of acquiring more benefit in terms of the transmit power and transmit rate than the cooperative pairs produced by either other non-stable matching algorithms or other stable matching algorithms.

A pair of centralized cooperative spectrum leasing systems were also introduced in Section 5.5 for the sake of benchmarking the performance of the proposed DWWRS-MAS. As exemplified in Fig 5.12, the centralized controller of CCS-1 selects the appropriate cooperative pairs for the sake of minimizing the system's total transmit power, as formulated by Eq (5.71), while the CCS-2 is designed for first minimizing the transmit power of the PTs, and then minimizing the total transmit power of the STs, when multiple STs require the same transmit power of the PTs, as portrayed by Eq (5.81) and Eq (5.89). Furthermore, the R-CSLS of the Section 5.5.1 where PTs randomly select their cooperative partner was also introduced as a benchmarker. Based on the discussions of Section 5.5.2, Section 5.5.3 and Section 5.5.4, the proposed DWWRS-MAS is capable of significantly improving both the cooperation probability and the achievable transmit rate as well as reducing the transmit

power compared to R-CSLS, as seen in Fig 5.13-Fig 5.19. As a further benefit, the proposed DWWRS-MAS is capable of achieving a performance comparable to those achieved by either CCS-1 or CCS-2, as observed in Fig 5.13-Fig 5.19. Compared to the non-cooperative system achieving the same system total transmit rate, considerable total transmit power reductions may be attained by our DWWRS-MAS, as seen in Table 5.5. Moreover, compared to the non-cooperative system, which consumes the same total transmit power as our DWWRS-MAS, the proposed DWWRS-MAS is capable of significantly improving the system's total transmit rate, as shown in Table 5.5.

We assume that the transmit power of both the PTs and STs is constrained by the same upper bound P_{max} in Section 5.5.2, Section 5.5.3 and Section 5.5.4. Assuming that the PTs and STs have different transmit power constraints, Section 5.5.6 evaluated the cooperation probability, transmit power dissipation and the achievable transmit rate of PTs and STs. Compared to the scenario of $P_{max}^{PT} > P_{max}^{ST}$, a higher cooperation probability is achieved for $P_{max}^{PT} < P_{max}^{ST}$, as seen in Fig 5.20, because more STs are capable of affording the transmit power required for conveying the superposition-coded data under the more relaxed maximum transmit power constraint of P_{max}^{ST}. Furthermore, a beneficial STTP reduction is achieved as well as the TTR is significantly improved, when we have $P_{max}^{PT} < P_{max}^{ST}$, as an advantage of the higher cooperation probability, as seen in Fig 5.20, Fig 5.21 and Fig 5.24. Hence, a higher transmit rate may be achieved by dissipating a moderate transmit power, if the transmit power constraints of both PTs and STs are carefully selected.

Section 5.5.7 quantifies the performance of the proposed DWWRS-MAS, when the number of PTPs varies from $\mathcal{I} = 2$ to $\mathcal{I} = 8$. Given the size of secondary network, more transmit opportunities are provided by the PTs in exchange for the cooperative transmission assistance, when the primary network becomes larger. Hence, the TTR is improved at the cost of dissipating a higher STTP, when the number of PTPs is increased, as seen in Fig 5.31 and Fig 5.29. The effect of the greedy factor of both the PT and ST as well as that of the PT's transmit power control step size was discussed in Section 5.5.8 and Section 5.5.9.

Given the bursty nature of the PTs' transmissions, in Section 5.5.10 we also had to investigate the stable throughput of each PT and each ST in a small network of Fig 5.11, which relied on the proposed DWWRS-MAS. As shown in Fig 5.39, the stable throughput of the PT achieved by cooperative transmission is impacted by the activity of the other PTs. When PT_2 has more data to send, the competition between PTs becomes more intense. Hence, it was shown in Fig 5.39 that the stable throughput $\mu_{PT_1}^{coop}$ was reduced, as λ_{PT_2} became higher. The stable throughput at the ST was increased, when more PTs became active, as seen in Fig 5.40. This phenomenon characterizes the innate feature of spectrum leasing schemes, namely that the STs may be granted a transmission opportunity only, when at least one PT has data to send. Finally, our analysis of the queueing stability was also confirmed by our

simulation results as seen in Fig 5.39 and Fig 5.40.

In the next chapter we will conclude by a summary of our research and discuss ideas set aside for future research.

Chapter 6

Conclusions and Future Work

In this chapter, we draw conclusions for each chapter and provide the suggestions for the further investigation.

6.1 Conclusions

In this thesis, we have developed a variety of cooperative medium access control (MAC) schemes for different cooperative spectrum leasing systems for the sake of improving the system's transmit rate and for reducing its energy consumption as well as for granting transmission opportunities for the unlicensed RNs. Furthermore, we have investigated various cooperative spectrum leasing systems exploiting the proposed MAC schemes by mathematically analysing the system's stability. In comparison to the benchmark systems, the proposed cooperative MAC schemes are capable of significantly improving the system's transmit rate, whilst reducing its energy dissipation. Below we first summarise our main findings obtained in each of the chapters.

6.1.1 Chapter 1

In this chapter, we discussed the motivation of the research documented in this thesis and presented an overview of various existing cooperative MAC protocols. As discussed in Section 1.1, our research was motivated by aiming for designing appropriate cooperative MAC schemes for enhancing the benefits of cooperative transmissions. In Section 1.2, we investigated a range of existing contributions on the subject of cooperative MAC protocols in terms of their fundamental design. According to the specific objective function (OF) used for system-optimization, the family of existing cooperative MAC protocols may be classified

TABLE 6.1: Summary of the cooperative MAC strategies proposed in Chapter 3 and Chapter 5 based on the discussion of existing cooperative MAC schemes in Chapter 1.

Chapter Number	Chapter 3	Chapter 5
Proposed Scheme	Distributed WW Cooperative MAC	DWWRS-MAS
Research Objective	multiple-objective (rate and power)	multiple-objective (rate and power)
Network Model	single licensed SN and multiple unlicensed users	multiple PTs and multiple STs
Selection Scheme	single RN selection	reciprocal selection
Outcome	$\mathcal{R}_{\hat{i}}$ is selected as best RN	Cooperative pair set $\{\mathcal{O}(PT_i, ST_m)\}$ is formed
Cooperative Activation	proactive relay selection	proactive relay selection

into single-objective protocols and multi-objective protocols. Section 1.2.1 briefly touched upon the research goals considered in existing single-objective protocols, such as the optimization of the system throughput, as well as its energy efficiency and transmission delay. The combination of these individual research objectives may become the design motivation of multi-objectives protocols, whose OF may have several variables, which was hence the design motivation of the cooperative MAC strategies of Chapter 3 and Chapter 5, as shown in Table 6.1. As discussed in Section 1.2.2, the cooperative MAC protocols may rely on the following regimes: the two-hop single-relay-aided network of Fig 1.2; the single-hop single-relay-aided network of Fig 1.3 which was exploited in Chapter 3; the multiple-source single-relay-aided networks of Fig 1.4; the two-hop multiple-relay-aided network of Fig 1.5; the multiple-hop multiple-relay-aided networks of Fig 1.6; the multiple-source multiple-relay networks of Fig 1.7, which was considered in Chapter 5. In Section 1.2.3, we investigated the cooperation activation principles routinely exploited in existing cooperative MAC protocols, which may be classified into three categories: proactive relay selection which was exploited both in Chapter 3 and Chapter 5 again, as shown in Table 6.1, as well as reactive relay selection and hybrid relay selection schemes. Furthermore, the best relay node (RN) set was selected by the existing cooperative MAC protocols either relying on the assumption of having global information of all the candidate RNs or on the local information of each candidate RN, as detailed in Section 1.2.4. Then the signalling procedure design of existing cooperative MAC protocols was discussed in Section 1.2.5. In order to support the coexistence of cooperative communication systems and conventional non-cooperative systems, most existing cooperative MAC protocols were developed based on the conventional MAC protocols, such as the Institute of Electrical and Electronics Engineers (IEEE) 802.11 standards, the IEEE 802.16 standards and the family of hybrid Automatic Repeat reQuest (ARQ) schemes. Finally, we detailed the outline of the thesis in Fig 1.10 and highlighted our novel contributions in Section 1.3. Let us now elaborate on these contributions a little further.

6.1.2 Chapter 2

In this chapter, fundamental techniques of this thesis were introduced. The MAC protocol was developed based on the layered network architecture. In order to investigate the class of conventional wireless MAC protocols, Section 2.2 introduced the layered network protocol architecture of Fig 2.1. Based on this layered network architecture, in Section 2.3 we commenced by detailing the functions of the MAC layer of Fig 2.3d and those of the existing conventional wireless medium access schemes, as shown in Fig 2.4 and Fig 2.5. Then, the conventional MAC protocols specified in the IEEE 802.11 standards were introduced in Section 2.3.2. Since the cooperative MAC scheme proposed in Chapter 3 are developed based on the DCF scheme specified by the IEEE 802.11 standards, Section 2.3.2 elaborated on the handshaking procedure of the DCF scheme and on the formats of both the data frame and of the control messages introduced by the DCF scheme, as seen in Fig 2.6-Fig 2.12.

Furthermore, Fig 2.15 of Section 2.4 presented the description of the queue, which stores the packets waiting for the service provided by the MAC layer where the methods used for analysing the stability of queueing systems were also discussed. In Section 2.4.1, we introduced the description of queueing systems and the most important theorems. Generally speaking, a queue may be described by four parameters: the average arrival rate of the packets, their average departure rate, the number of servers and the size of the buffer, as seen in Fig 2.15. Then, Little's theorem, which was exploited in Chapter 4 and Chapter 5 was presented by Eq (2.3)-Eq (2.6) in Section 2.4.1, which is an important theorem routinely used for deriving the probability that a queue is empty, when the system reaches its steady state. Moreover, Section 2.4.2 described the stability of a queue, where a queue was deemed to be stable, if the queue length remained finite, as the time tended to infinity, which was formulated in Definition 2.1. When all the queues in the queueing system are stable, this system is also stable [103]. According to the definition of a stable queueing system, the non-Markovian analysis method was discussed in Section 2.4.2, which was exploited in Chapter 4 and Chapter 5 for analysing the stability of the proposed cooperative communication systems. The first step of the non-Markovian analysis method is to derive the average arrival rate and the average departure rate of each queue in the system. Then, the stability region and stable throughput were derived according to the stability conditions specified by Loynes' theorem [134], as detailed in Section 2.4.2.2.

6.1.3 Chapter 3

Based on the discussion of existing cooperative MAC protocols in Chapter 1 and on the introduction of conventional wireless MAC protocols in Chapter 2, in Section 3.2 we first formulated a 'win-win' (WW) cooperative framework (WWCF) for striking a tradeoff be-

tween the achievable system rate improvement and energy dissipation reduction as well as for granting transmission opportunities for the unlicensed RNs. More explicitly, the source node (SN) of the proposed WWCF intends to lease part of its spectrum to the unlicensed RNs in exchange for cooperatively supporting the source's transmission for the sake of reducing the SN's target transmit power and for improving the SN's transmit rate. Furthermore, the unlicensed RNs have an incentive to provide cooperative transmission assistance for the licensed SNs in our WWCF for the sake of accessing the SN's spectrum to convey their own traffic.

With the goal of practically implementing the proposed WWCF, a distributed WW cooperative MAC protocol was developed in Section 3.3 by designing the specific signalling procedure of Fig 3.2 and a convenient transmission format for both the data frame and for the control messages, as seen in Fig 3.3. Based on the Request-To-Send (RTS) / Clear-To-Send (CTS) signalling of the legacy IEEE 802.11 protocol shown in Fig 2.9, the SN first issues an RTS message to the destination node (DN) for reserving the channel and for announcing its transmission intention, as seen in Fig 3.2. After receiving the CTS message from the DN, $\mathcal{S}$ broadcasts its data at its increased target transmit rate and at a reduced target transmit power, as seen in Fig 3.2 and Fig 3.5. During the relay selection phase of Fig 3.2, the specific RNs, which perfectly detected the SN's data and simultaneously are capable of affording the transmit power required for satisfying the transmit rate requirement of both the SN and of their own become candidate RNs, as shown in Fig 3.4 and Table 3.1. According to the proposed backoff algorithm formulated in Eq (4.2) of Section 3.3.2, the specific RN which promises to require the lowest transmit power may be selected as the best RN for the sake of minimizing the system transmit energy dissipation. The best RN will then jointly encode both the SN's message and its own data with the aid of superposition coding (SPC) and will forward the superposition-coded data frame to the DN. Finally, the DN employs Successive Interference Cancellation (SIC) for decoding the superposition-coded source-relay data received from the relay and subsequently retrieves the source data by appropriately combining the direct and the relayed cooperative transmission.

Section 3.4 evaluates the achievable performance of the proposed distributed WW cooperative MAC protocol by introducing two non-cooperative systems and a Ran-CSLS as the benchmarker used in our comparisons. When compared to the Ran-CSLS, where the best RN is randomly selected, the distributed WW cooperative MAC protocol proposed in Section 3.3 is capable of achieving a higher total transmit rate, despite dissipating a lower total transmit power without increasing the complexity of the interaction between the SN and RNs, as seen in Fig 3.7 and Fig 3.8. Furthermore, compared to the non-cooperative systems, the performance results of this chapter seen in Fig 3.9-Fig 3.12 demonstrate that both substantial rate improvements and considerable energy savings are achieved by the proposed

distributed WW cooperative MAC protocol at the cost of introducing the moderate overhead quantified in Fig 3.13. Moreover, the erroneous transmission of control messages in the cooperative spectrum leasing system implementing the proposed distributed WW cooperative MAC protocol dissipates an increased energy owing to retransmitting both the data frame and the erroneous control messages. Furthermore, the throughput may be reduced owing to the retransmissions, when all the control messages are prone to corruption, as characterized in Fig 3.16 and Fig 3.17. However, as discussed in Section 3.4.6, these detrimental effects are significantly reduced, when only the RTS message may be corrupted again, as seen in Fig 3.16 and Fig 3.17. This event may occur more often than the event of all control messages being corrupted, because the RTS and CTS messages are capable of protecting all other control messages by disallowing the adjacent nodes' transmissions, as discussed in Chapter 2 [174].

6.1.4 Chapter 4

Based on the queueing theory and the non-Markovian stability analysis method discussed in Section 2.4, in this chapter, we analysed the stability of the cooperative spectrum leasing system of Chapter 3 exploiting the proposed distributed WW cooperative MAC protocol. According to the system model outlined in Section 4.2, we constructed the queueing model shown in Fig 4.5 and presented our assumptions stipulated for the sake of simplifying the analysis of Section 4.3. Based on the non-Markovian analysis method detailed in Section 2.4.2.2, Section 4.3 derived the stable throughput of the queue at both the SN and the RNs, which is limited by the proposed distributed WW cooperative MAC protocol.

According to the proposed distributed WW cooperative MAC protocol, the departure rate at the SN of our system is characterised by the sum of Eq (4.4), Eq (4.9) and Eq (4.18), where Eq (4.4) expressed the departure rate $\mu_{\mathcal{S},coop}$ achieved at $\mathcal{S}$ with the aid of cooperation. Furthermore, Eq (4.9) described the departure rate $\mu_{\mathcal{S},non}^{R_{coop}}$ at $\mathcal{S}$, which was achieved by non-cooperative transmission at its target transmit rate. Moreover, Eq (4.18) characterised the departure rate $\mu_{\mathcal{S},non}^{R_{non}}$ achieved at $\mathcal{S}$ by the non-cooperative transmission, when the SN's transmit rate requirement cannot be satisfied in isolation under the constraint of the maximum transmit power. The unlicensed RNs were assumed to have two queues, namely queue $Q_{\mathcal{SR}_i}$ for storing the SN's and queue $Q_{\mathcal{R}_i}$ for storing its own data packets, as shown in Fig 4.5. The departure rate of queue $Q_{\mathcal{SR}_i}$ is equal to the corresponding arrival rate, which is determined by the busy probability of SN and the probability that RN $\mathcal{R}_i$ is selected as the best RN, as formulated by Eq (4.35). Since superposition coding is used for jointly encoding the SN's and RN's data, the queue $Q_{\mathcal{R}_i}$ has the same departure rate as queue $Q_{\mathcal{SR}_i}$, as indicated by Eq (4.36).

Compared to the benchmark systems, the cooperative spectrum leasing system exploiting the proposed distributed WW cooperative MAC protocol is capable of providing an increased stable throughput for both the licensed SN and the unlicensed RN, as seen in Fig 4.8-Fig 4.10. Furthermore, both Fig 4.9 and Fig 4.10 characterised the cooperative spectrum leasing system, indicating that the relay's stable throughput is increased when the licensed SN becomes busier, because the unlicensed RNs may be granted more transmission opportunities. Moreover, the RN's stable throughput of Fig 4.9 is reduced, when the RN becomes greedier, which inevitable results in a reduced cooperative probability. However, the RN's increased greedy factor is capable of improving its achievable transmit rate owing to its increased target transmit rate. Hence, the RN is capable of achieving its highest stable transmit rate by striking a tradeoff between its transmit rate and transmission probability, which is achieved with the aid of using the most appropriate greedy factor, say $\beta = 0.6$ as seen in Fig 4.12. Furthermore, the SN's stable throughput achieved by a successful transmission, which can satisfy the source's rate requirement is increased, when the SN broadcasts its data at a higher transmit power of $P_{\mathcal{S}-data}$, because more RNs may contend for cooperative transmission opportunities, as seen in Fig 4.14. However, this stable throughput improvement is achieved at the cost of an increased transmit power dissipation of the SN. Hence, an algorithm may be designed in our future work for calculating the most appropriate transmit power of $P_{\mathcal{S}-data}$ in order to strike a tradeoff between the SN's stable throughput and its transmit power dissipation. Finally, our analysis was also confirmed by our simulation results, as seen in Fig 4.17 and Fig 4.16.

6.1.5 Chapter 5

Again, in Chapter 3, we proposed a distributed WW cooperative MAC protocol for a cooperative spectrum leasing system supporting a single licensed SN and multiple unlicensed RNs, as seen in Table 6.1 and Fig 3.1. Upon considering the cooperative spectrum leasing system hosting multiple licensed primary transmission pairs and multiple unlicensed secondary transmission pairs as shown in Fig 5.1, we formulated a WW reciprocal-selection-based framework (WWRSF) in Section 5.2.2 for the sake of striking an attractive tradeoff between the achievable transmit rate and the transmit power dissipated. Based on the proposed WWRSF, each primary transmitter (PT) intends to lease its spectral resources to an appropriate secondary transmitter (ST) in exchange for cooperative transmission assistance for the sake of minimizing its transmit power, whilst simultaneously satisfying its transmit rate requirement. Furthermore, the ST intends to provide cooperative assistance for its best PT in order to minimize its transmit power and simultaneously to access the licensed spectrum for conveying its own traffic at its target transmit rate.

Based on the OFs of the proposed WWRSF, a distributed WW reciprocal-selection-based

medium access scheme (DWWRS-MAS) was designed for forming suboptimal but still beneficial cooperative pairs relying on the reciprocal selection strategy of Section 5.3 between the PTs and STs. The proposed DWWRS-MAS allowed the PT to seek meritorious cooperative partner by gradually increasing its transmit power for the sake of minimizing its transmit power dissipation and for simultaneously satisfying its transmit rate requirement, as seen in Fig 5.3, Fig 5.4 and Table 5.1. In order to minimize the transmit power dissipation, the ST exploiting the proposed DWWRS-MAS intends to provide cooperative transmission assistance for the specific PT, which requires the lowest relaying transmit power, when the ST has multiple candidate cooperative partners, as seen in Fig 5.5 and Table 5.2.

In Section 5.4, the analysis of both the queueing stability and of the algorithmic stability of the cooperative spectrum leasing system exploiting our DWWRS-MAS of Section 5.3 was presented. Based on the queueing model of Fig 5.6 and the PTs' behaviour specified by the proposed DWWRS-MAS shown in Fig 5.5, the average departure rate at the PT PT_i is equal to the sum of the average departure rate $\mu_{PT_i}^{coop}$ achieved by the cooperative transmission and the average departure rate $\mu_{PT_i}^{noncoop}$ of the direct transmission operating without any cooperative transmission assistance, as shown in Eq (5.15). The ST ST_m is assumed to rely on the pair of queues Q_{ST_m} and Q_{PT,ST_m} dedicated to buffer both its own data and the PT's data, respectively, as shown in Fig 5.6. The average departure rate of the queues Q_{ST_m} and Q_{PT,ST_m} are expressed by Eq (5.63) and Eq (5.65). The analysis of the algorithmic stability provided in Section 5.4.2 indicated that the proposed DWWRS-MAS is capable of forming stable cooperative pairs. Moreover, at least one cooperative pair produced by the proposed DWWRS-MAS is capable of acquiring more benefit in terms of the transmit power and transmit rate than the cooperative pairs formed by either other non-stable matching algorithms or by other stable matching algorithms.

Our performance results seen in Fig 5.13-Fig 5.19 demonstrated that the performance of the cooperative spectrum leasing system (CSLS) exploiting the proposed DWWRS-MAS is comparable to those of the pair of optimal centralized systems, which form the optimal cooperative pairs with the aid of the global Channel Sate Information (CSI) knowledge assumed and without considering the selfish nature of STs. Furthermore, the CSLS exploiting the proposed DWWRS-MAS outperforms the random cooperative spectrum leasing system (R-CSLS) where the PTs randomly select their cooperative partner, i.e. without giving any cognizance to the transmit power dissipation, as seen in Fig 5.13-Fig 5.19. Compared to the non-cooperative systems, the proposed DWWRS-MAS is capable of significantly improving the system's total transmit rate (TTR), despite considerably reducing the system's total transmit power (STTP), as shown in Table 5.5. Moreover, when either the PTs or the STs become greedier, an increased STTP is dissipated due to the reduced cooperative probability, as shown in Fig 5.33 and Fig 5.34. However, the TTR characterized in Fig 5.35 is

first increased when the STs become greedier and then it is reduced for $\beta > 0.8$, because the increased transmit rate of the ST still fails to compensate for the detrimental effect of the reduced cooperation probability for higher β values. Hence, the STs are capable of achieving the highest transmit rate by using an appropriate greedy factor of say $\beta = 0.8$, as shown in Fig 5.35. According to the proposed DWWRS-MAS, the PT increases its transmit power step by step, when it fails to find a cooperative partner at the current power level, as seen in Fig 5.4 and Table 5.1. When a smaller power control step size is used by the PTs, the STTP is reduced at a cost of increasing the average number of control messages, as observed in Fig 5.36 and Fig 5.37. Furthermore, as evidenced by Fig 5.37 an increased STTP is dissipated for a larger power control step size Δ, albeit less control messages are exchanged between the PTs and STs, as seen in Fig 5.36. Hence, using an appropriate transmit power control step size of $\Delta = 0.3$ is capable of ensuring an acceptable amount of control message without an excessive degradation of STTP, as evidenced by Fig 5.36 and Fig 5.37. Considering the CSLS hosting multiple PTs and exploiting our DWWRS-MAS, the stable throughput of a PT achieved by cooperative transmission is impacted by the activity of the other PTs. For instance, a reduced stable throughput is achieved by a PT, when other PTs have more data to send, because the competition between PTs becomes more vigorous, as shown in Fig 5.39. The stable throughput of STs seen in Fig 5.40 characterizes an innate feature of spectrum leasing schemes, namely that the STs may only be granted a transmission opportunity when at least one PT has data to send. Finally, our analysis of the queueing stability was also confirmed by our simulation results seen in Fig 5.39 and Fig 5.40.

6.2 Suggestions for Future Work

In this thesis, we developed cooperative MAC strategies for supporting the cooperative transmission in spectrum leasing systems hosting either a single licensed SN or multiple licensed SNs and for balancing the tradeoff between the achievable *transmit rate* and *energy consumption*. However, there are further design issues that may be taken into account, when designing MAC strategies for cooperative communication systems, such as fairness, transmission reliability, spectrum utilization efficiency and so on. In this section, several suggestions are provided for our future work.

6.2.1 Fairness

In the cooperative spectrum leasing systems considered in this thesis, the unlicensed RN is capable of accessing the licensed spectrum for conveying its own traffic by providing

cooperative transmission assistance to the licensed SN. However, the RNs which are located in "good" positions may win significantly more transmission opportunities than the RNs in less beneficial position [202, 219]. Hence, when the privileged RN located in beneficial positions are granted excessive transmission opportunities may increase the queue length of the RNs roaming in less privileged positions, which imposes a detrimental effect on the system's stability. Furthermore, activating RNs in unfavourable positions reduces the system's overall performance. Hence, a trade-off has to be struck between RN fairness and the achievable system performance.

One of the possible solutions is to introduce the concept of "credit rewards" [220, 221]. If the RN $\mathcal{R}_i$ is in a beneficial position, but it does not have data to send, it may provide cooperative transmission assistance for the SN in order to collect either calling credits in form of monetary rewards or relaying credits for its future transmission opportunities. The spectrum leased by the licensed SN for the cooperation provided by $\mathcal{R}_i$ may be allocated to the other RNs foaming in less privileged locations, which presently have data to send. When multiple RNs intend to access the spectrum leased by the SN for conveying their data, the access priority of RNs may be determined by their accumulated credit or by the system's state or, alternatively, by the quality of service (QoS). For example, the specific RN which collects the highest amount of credit may win the current transmission opportunity.

6.2.2 Transmission Reliability

As discussed in Section 1.2.3, a proactive relay selection scheme is capable of maximizing the benefits generated by cooperative transmission by selecting an appropriate RN, while a reactive relay selection scheme is capable of improving the transmission reliability relying on the cooperative transmission opportunities provided by the RN. In [84], a twin-relay-based cooperative MAC protocol was proposed by combining the proactive relay selection scheme of Section 1.2.3 and the reactive relay selection scheme of Section 1.2.3 for the sake of maximizing the system's throughput, whilst reducing its delay. The studies disseminated in [84] show that the hybrid relay selection scheme of Section 1.2.3 is capable of combining the advantages of both the proactive and of the reactive relay selection scheme. The resultant hybrid relay selection scheme constitutes an attractive solution for multiple-objective cooperative system optimization.

A cooperative ad hoc network was considered in [84], where the RN was assumed to altruistically forward data for the SN. Hence, the design of the cooperative MAC protocol relying on a *hybrid relay selection scheme* for improving the performance of *cooperative spectrum leasing*, whilst simultaneously enhancing the *transmission reliability* remains an open problem at the time of writing.

6.2.3 Spectrum Utilisation Efficiency

Based on the cooperative MAC schemes proposed in this thesis, the unlicensed RN is capable of accessing the licensed spectrum for conveying its traffic if and only if it provides cooperative transmission assistance for the active licensed SN. However, such a cooperative spectrum leasing scheme may reduce the spectrum utilisation efficiency, when the licensed SN remains silent most of the time, because the unlicensed RN fails to win transmission opportunities, if the licensed SNs do not have data in their buffers ready for transmission. In order to improve the spectrum utilisation efficiency, the licensed SN may allow the unlicensed RN to provide other remuneration in exchange for an opportunity to access the primary network, such as monetary rewards. Moreover, the unlicensed RN may combine different access schemes for accessing the licensed spectrum [222]. For example, the unlicensed RN may lease spatial resources, while simultaneously sensing the "spectrum holes" for increasing the transmission opportunities and for improving the spectrum utilisation efficiency.

6.2.4 Processing Energy Consumption

In this thesis, we mainly considered the energy required for conveying data from the SN to the DN when we designed the system's objective functions. However, sensing the channel's state during the idle phase and then processing the received signal also dissipates the energy at the terminals [223]. Switching to sleep mode potentially saves energy [224]. However, opting for the inappropriate sleep mode duration may decrease the probability of cooperative transmissions and may increase the system's total energy dissipation. Hence, the total energy consumption including both the processing energy consumption and transmission energy consumption may be considered in our future work.

6.2.5 Performance Analysis

Investigating new cooperative strategies requires a deep understanding of the cooperative behaviour of all the participants in the systems considered [225]. Based on the queueing theory in Section 2.4, we analysed the stability of cooperative communication systems exploiting the proposed cooperative MAC schemes. Furthermore, the algorithmic stability was also investigated in Section 5.4.2, whilst relying on the matching theory. Apart from queueing stability and algorithm stability, there are performance metrics worth analysing. Both the end-to-end delay and the throughput were used as important performance metrics in [194, 225–229]. Moreover, the average outage probability [69, 230] was analysed for the

sake of investigating the effects of the proposed cooperative strategies on the system's performance. We may further investigate the proposed cooperative MAC protocol by analysing its end-to-end delay and throughput in the future.

6.2.6 Cross-Layer Collaboration

Sophisticated cross-layer collaboration may be required for supporting cooperative transmissions in large networks. For example, cooperative MAC protocols relying on multiple relay selection schemes may rely on either distributed space-time coding [231] or beamforming [92, 232] for supporting the parallel transmissions of multiple RNs within the best RN set. Moreover, the cross-layer collaboration between MAC layer and network layer is beneficial for extending the coverage area of the cooperative regime [75]. The global information of the entire network may be made available at the MAC layer with the aid of network layer. Hence, the performance of the network relying on mobile RNs may be improved by combining a cooperative MAC protocol with a cooperative routing protocol. Furthermore, when considering the different QoS requirements of diverse applications, a cooperative MAC protocol may be required for identifying these applications and for supporting different services [233]. Hence, the service priority of the applications may be embedded into the data at the application layer. Based on the service priority, the cooperative MAC protocol may allow either the SN or the RN to convey its data by obeying the most appropriate order for the sake of satisfying the different QoS requirements of the diverse applications. Bearing in mind the advantages of cross-layer design, we may consider the collaboration of the physical layer, MAC layer and higher layers in the future.

Appendix A

Appendices

A.1 Proof of Proposition 1

Based on the idealized simplifying assumption of using perfect capacity-achieving coding, the achievable rate of the data transmitted from $\mathcal{R}_i$ to $\mathcal{D}$ may be formulated as:

$$R_{\mathcal{R}_i} = \log_2(1 + \frac{\rho_{\mathcal{R}_i,\mathcal{D}}|h_{\mathcal{R}_i,\mathcal{D}}|^2 P_{\mathcal{R}_i}}{P_N}). \tag{A.1}$$

Upon introducing the short-hand of $\Upsilon_{\mathcal{R}_i,\mathcal{D}} = \frac{\rho_{\mathcal{R}_i,\mathcal{D}}|h_{\mathcal{R}_i,\mathcal{D}}|^2}{P_N}$, we have $R_{\mathcal{R}_i} = \log_2(1 + \Upsilon_{\mathcal{R}_i,\mathcal{D}} P_{\mathcal{R}_i})$. Given the bandwith and the length of data frame, the transmit energy consumption of succesful data transmission from $\mathcal{R}_i$ to $\mathcal{D}$ may be characterized as:

$$E_{\mathcal{R}_i} = \mathcal{C} \cdot \frac{P_{\mathcal{R}_i}}{R_{\mathcal{R}_i}} = \mathcal{C} \cdot \frac{P_{\mathcal{R}_i}}{\log_2(1 + \Upsilon_{\mathcal{R}_i,\mathcal{D}} P_{\mathcal{R}_i})}. \tag{A.2}$$

where $\mathcal{C}$ is a constant, which is given by $\mathcal{C} = \frac{L}{Bw}$, while L denotes the length of the data frame. Hence, the first derivative of $E_{\mathcal{R}_i}$ with respect to $P_{\mathcal{R}_i}$ is given by:

$$\frac{dE_{\mathcal{R}_i}}{dP_{\mathcal{R}_i}} = \frac{\log_2(1 + \Upsilon_{\mathcal{R}_i,\mathcal{D}} P_{\mathcal{R}_i}) - \dfrac{\Upsilon_{\mathcal{R}_i,\mathcal{D}} P_{\mathcal{R}_i}}{(1 + \Upsilon_{\mathcal{R}_i,\mathcal{D}} P_{\mathcal{R}_i}) \cdot \ln 2}}{\Big\{ \log_2(1 + \Upsilon_{\mathcal{R}_i,\mathcal{D}} P_{\mathcal{R}_i}) \Big\}^2}. \tag{A.3}$$

Upon denoting $\mathcal{F}_{\mathcal{R}_i}(P_{\mathcal{R}_i}) = \log_2(1 + \Upsilon_{\mathcal{R}_i,\mathcal{D}} P_{\mathcal{R}_i}) - \dfrac{\Upsilon_{\mathcal{R}_i,\mathcal{D}} P_{\mathcal{R}_i}}{(1 + \Upsilon_{\mathcal{R}_i,\mathcal{D}} P_{\mathcal{R}_i}) \cdot \ln 2}$, the first derivative of $\mathcal{F}_{\mathcal{R}_i}$ with respect to $P_{\mathcal{R}_i}$ is given by:

$$\frac{d\mathcal{F}_{\mathcal{R}_i}}{dP_{\mathcal{R}_i}} = \frac{\Upsilon^2_{\mathcal{R}_i,\mathcal{D}} P_{\mathcal{R}_i}}{(1 + \Upsilon_{\mathcal{R}_i,\mathcal{D}} P_{\mathcal{R}_i})^2 \cdot \ln 2}. \tag{A.4}$$

According to Eq (A.4), we have $\frac{d\mathcal{F}_{\mathcal{R}_i}}{dP_{\mathcal{R}_i}} > 0$. Hence, $\mathcal{F}_{\mathcal{R}_i}(P_{\mathcal{R}_i})$ is a monotonically increasing function of $P_{\mathcal{R}_i}$ [234], while we have $\mathcal{F}_{\mathcal{R}_i}(0) = 0$. Therefore we have:

$$\mathcal{F}_{\mathcal{R}_i}(P_{\mathcal{R}_i}) > 0 \qquad \forall P_{\mathcal{R}_i} > 0 \tag{A.5}$$

$$\Rightarrow \frac{dE_{\mathcal{R}_i}}{dP_{\mathcal{R}_i}} > 0 \qquad \forall P_{\mathcal{R}_i} > 0. \tag{A.6}$$

Eq (A.6) concludes that the transmit energy consumption $E_{\mathcal{R}_i}$ of data transmission from $\mathcal{R}_i$ to $\mathcal{D}$ is an increasing function of the corresponding transmit power $P_{\mathcal{R}_i}$, when perfect capacity-achieving coding is assumed.

Appendix B

Appendices

Appendices

B.1 Proof of Proposition 1

Given the CSI and free-space pathloss gain of the SD link, i.e. $(h_{\mathcal{S},\mathcal{D}}, \rho_{\mathcal{S},\mathcal{D}})$ as well as the factors of greediness namely (α, β), the variable $\gamma^{\mathcal{S}}_{\mathcal{R}_i}(r)$ becomes a constant for all RNs. Furthermore, let $\phi = \gamma^{\mathcal{S}}_{\mathcal{R}_i}(r) + 1$, then $\phi \in (1, +\infty)$. Let $G_{\mathcal{R}_i} = \rho_{\mathcal{R}_i,\mathcal{D}}|h_{\mathcal{R}_i,\mathcal{D}}|^2$, then we have:

$$P_{\mathcal{R}_i}(G_{\mathcal{R}_i}) = \phi\frac{(1+\frac{G_{\mathcal{R}_i}P_{max}}{P_N})^{\beta}P_N}{G_{\mathcal{R}_i}} - \frac{P_N}{G_{\mathcal{R}_i}}. \tag{B.1}$$

Hence, the first derivative of $P_{\mathcal{R}_i}(G_{\mathcal{R}_i})$ with respect to $G_{\mathcal{R}_i}$ is given by:

$$\begin{aligned}\frac{dP_{\mathcal{R}_i}}{dG_{\mathcal{R}_i}} =& \frac{P_N}{G^2_{\mathcal{R}_i}} - \frac{\phi P_N}{G^2_{\mathcal{R}_i}}(1+\frac{G_{\mathcal{R}_i}P_{max}}{P_N})^{\beta} \\ &+ \frac{\phi P_{max}\beta}{G_{\mathcal{R}_i}}(1+\frac{G_{\mathcal{R}_i}P_{max}}{P_N})^{(\beta-1)}.\end{aligned} \tag{B.2}$$

If $\frac{dP_{\mathcal{R}_i}}{dG_{\mathcal{R}_i}}$ is less than zero, $P_{\mathcal{R}_i}(G_{\mathcal{R}_i})$ is a decreasing function of $\rho_{\mathcal{R}_i,\mathcal{D}}|h_{\mathcal{R}_i,\mathcal{D}}|^2$ for different RNs [234]. Hence, we assume:

$$\frac{dP_{\mathcal{R}_i}}{dG_{\mathcal{R}_i}} < 0 \qquad \Longrightarrow \qquad \phi(1+\varphi)^{(\beta-1)}(1+\varphi-\beta\varphi) > 1$$

where

$$\varphi = P_{max}\frac{G_{\mathcal{R}_i}}{P_N} \qquad \varphi \in (0, +\infty).$$

Hence, we have:

$$\ln\phi + (\beta-1)\ln(1+\varphi) + \ln(1+\varphi-\beta\varphi) > 0. \tag{B.3}$$

Since $\phi \in (1,+\infty)$, $\ln\phi$ is higher than zero. Therefore, $\frac{dP_{\mathcal{R}_i(t)}}{dG_{\mathcal{R}_i}}$ is less than zero, if we have $(\beta-1)\ln(1+\varphi)+\ln(1+\varphi-\beta\varphi)>0$. Let $\Psi = 1+\varphi(1-\beta)-(1+\varphi)^{(1-\beta)}$. Then the derivative of Ψ with respect to φ is formulated by:

$$\frac{d\Psi}{d\varphi} = (1-\beta)\left[1-(1+\varphi)^{(-\beta)}\right],$$

where

$$\beta \in (0,1) \qquad \varphi \in (0,+\infty).$$

Then the value of $1-(1+\varphi)^{(-\beta)}$ is higher than zero. Hence, we arrive at $\frac{d\Psi}{d\varphi} > 0$. Therefore, the function $\Psi(\varphi) = 1+\varphi(1-\beta)-(1+\varphi)^{(1-\beta)}$ is a incresing function [234]. When $\varphi = 0$, $\Psi(0)$ equals to 0. For $\varphi > 0$, we have:

$$\begin{aligned}\Psi(\varphi) > 0 \Rightarrow & 1+\varphi(1-\beta) > (1+\varphi)^{(1-\beta)} \\ \Rightarrow & (\beta-1)\ln(1+\varphi)+\ln(1+\varphi-\beta\varphi) > 0.\end{aligned} \tag{B.4}$$

According to Eq (B.4), we can obtain:

$$\begin{aligned}&\ln\phi + (\beta-1)\ln(1+\varphi)+\ln(1+\varphi-\beta\varphi) > 0 \\ \Rightarrow & \phi(1+\varphi)^{(\beta-1)}(1+\varphi-\beta\varphi) > 1 \\ \Rightarrow & \frac{dP_{\mathcal{R}_i}}{dG_{\mathcal{R}_i}} < 0.\end{aligned} \tag{B.5}$$

Eq (B.5) concludes that $P_{\mathcal{R}_i}(r)$ is a decreasing function of $\rho_{\mathcal{R}_i,\mathcal{D}}|h_{\mathcal{R}_i,\mathcal{D}}|^2$ for different RNs. For RN $\mathcal{R}_i$, the variable $\rho_{\mathcal{R}_i,\mathcal{D}}$ has a fixed value in our system. Hence, $P_{\mathcal{R}_i}(r)$ is a decreasing function of $|h_{\mathcal{R}_i,\mathcal{D}}|^2$ for RN $\mathcal{R}_i$.

B.2 Proof of Proposition 2

Let $G_{\mathcal{S}} = \rho_{\mathcal{S},\mathcal{D}}|h_{\mathcal{S},\mathcal{D}}|^2$. Then the SN's retransmission power of $P^{(II)}_{\mathcal{S},\mathcal{D}}(r)$ may be rewritten as:

$$P^{(II)}_{\mathcal{S},\mathcal{D}}(r) = \frac{1}{G_{\mathcal{S}}}(1+G_{\mathcal{S}}P_{max})^{\alpha} - \frac{1}{G_{\mathcal{S}}} - P_{\mathcal{S}-data}. \tag{B.6}$$

Based on Eq (B.6), the first derivative of $P^{(II)}_{\mathcal{S},\mathcal{D}}(r)$ with respect to $G_{\mathcal{S}}$ is formulated as:

$$\frac{dP^{(II)}_{\mathcal{S},\mathcal{D}}(r)}{dG_{\mathcal{S}}} = \frac{1+(1+G_{\mathcal{S}}P_{max})^{(\alpha-1)}\cdot[G_{\mathcal{S}}P_{max}(\alpha-1)-1]}{G^2_{\mathcal{S}}}, \tag{B.7}$$

subject to:

$$G_{\mathcal{S}} > 0 \qquad \alpha > 1 \qquad P_{max} > 0. \tag{B.8}$$

Based on Eq (B.8), we have:

$$\begin{aligned} &(1 + G_{\mathcal{S}} P_{max})^{(\alpha-1)} > 0 \\ &G_{\mathcal{S}} P_{max}(\alpha - 1) - 1 > -1 \\ \Rightarrow &\frac{dP_{\mathcal{S},\mathcal{D}}^{(II)}(r)}{dG_{\mathcal{S}}} > 0. \end{aligned} \tag{B.9}$$

Hence, $P_{\mathcal{S},\mathcal{D}}^{(II)}(r)$ is an increasing function of $\rho_{\mathcal{S},\mathcal{D}}|h_{\mathcal{S},\mathcal{D}}|^2$ [234]. Assuming that both $\mathcal{S}$ and $\mathcal{D}$ have fixed positions, $P_{\mathcal{S},\mathcal{D}}^{(II)}(r)$ is a increasing function of $|h_{\mathcal{S},\mathcal{D}}|^2$, when the AWGN has a zero mean and a unit variance.

B.3 Proof of Proposition 3

Proof of condition (i): When the RN $\mathcal{R}_i$ is selected as the best relay, it has to correctly receive the SN's data. Upon denoting the channel gain of the SD link by $H_{\mathcal{S},\mathcal{D}} = |h_{\mathcal{S},\mathcal{D}}|^2$, we have:

$$\alpha C_{\mathcal{S},\mathcal{D}}^{max} < C_{\mathcal{S},\mathcal{R}_i} \Longrightarrow (1 + \frac{\rho_{\mathcal{S},\mathcal{D}} H_{\mathcal{S},\mathcal{D}} P_{max}}{P_N})^{\alpha} < (1 + \frac{\rho_{\mathcal{S},\mathcal{R}_i} H_{\mathcal{S},\mathcal{R}_i} P_{\mathcal{S}-data}}{P_N}). \tag{B.10}$$

Upon introducing the shorthand of $\nu = \frac{\rho_{\mathcal{S},\mathcal{D}} P_{max}}{P_N}$ and $Y(x) = (1 + \nu x)^{\alpha}$ as well as $\Omega_{\mathcal{S}\mathcal{R}_i} = 1 + \frac{\rho_{\mathcal{S},\mathcal{R}_i} H_{\mathcal{S},\mathcal{R}_i} P_{\mathcal{S}-data}}{P_N}$, we arrive at the first condition in Eq (4.13).

Given α and ν, the first derivative of $Y(x)$ may be formulated as:

$$\frac{dY}{dx} = \alpha\nu(1 + \nu x)^{(\alpha-1)}. \tag{B.11}$$

Subject to the conditions of

$$\alpha > 1 \qquad \nu > 0 \qquad x > 0 \tag{B.12}$$

From Eq (B.12) we arrive at:

$$1 + \nu x > 1 \qquad \alpha - 1 > 0 \tag{B.13}$$

$$\Rightarrow \frac{dY}{dx} > 0. \tag{B.14}$$

Hence, $Y(x)$ is an monotonically increasing function of x for $x > 0$ and $\alpha > 1$ as well as $\nu > 0$.

Proof of condition (ii): If the RN $\mathcal{R}_i$ is selected as the best RN, it also has to be capable of affording the transmit power $P_{\mathcal{R}_i}(r)$ required for relaying the superposition-coded data under the constraint of having a maximum transmit power of P_{max}. Hence the second condition may be written

as:

$$P_{\mathcal{R}_i}(r) < P_{max}. \tag{B.15}$$

According to Eq (4.7),we have:

$$\gamma^{\mathcal{S}}_{\mathcal{R}_i}(r) < \Omega^{(1-\beta)}_{\mathcal{R}_i\mathcal{D}} - 1. \tag{B.16}$$

where $\gamma^{\mathcal{S}}_{\mathcal{R}_i}(r)$ and $\Omega_{\mathcal{R}_i\mathcal{D}}$ are given by:

$$\gamma^{\mathcal{S}}_{\mathcal{R}_i}(r) = 2^{\alpha C^{max}_{\mathcal{S},\mathcal{D}}} - \frac{\rho_{\mathcal{S},\mathcal{D}} H_{\mathcal{S},\mathcal{D}} P_{\mathcal{S}-data}}{P_N} - 1, \tag{B.17}$$

$$\Omega_{\mathcal{R}_i\mathcal{D}} = 1 + \frac{\rho_{\mathcal{R}_i\mathcal{D}} H_{\mathcal{R}_i\mathcal{D}} P_{max}}{P_N}. \tag{B.18}$$

Since we have $P_{\mathcal{S}-data} < P_{max}$, based on Eq (B.16) we arrive at:

$$2^{\alpha C^{max}_{\mathcal{S},\mathcal{D}}} - \nu H^{max}_{\mathcal{S},\mathcal{D}} < \Omega^{(1-\beta)}_{\mathcal{R}_i\mathcal{D}}, \tag{B.19}$$

$$\Rightarrow (1 + \nu H_{\mathcal{S},\mathcal{D}})^{\alpha} - \nu H_{\mathcal{S},\mathcal{D}} < \Omega^{(1-\beta)}_{\mathcal{R}_i\mathcal{D}}. \tag{B.20}$$

Up on introducing the shorthand $Z(x) = (1 + \nu x)^{\alpha} - \nu x$, we have:

$$Z(H_{\mathcal{S},\mathcal{D}}) < \Omega^{(1-\beta)}_{\mathcal{R}_i\mathcal{D}}, \tag{B.21}$$

where

$$\Omega_{\mathcal{R}_i\mathcal{D}} = 1 + \frac{\rho_{\mathcal{R}_i\mathcal{D}} H_{\mathcal{R}_i\mathcal{D}} P_{max}}{P_N}. \tag{B.22}$$

Based on Eq (B.21), the first derivative of $Z(x)$ may be expressed as:

$$\frac{dZ}{dx} = \nu\{\alpha(1 + \nu x)^{(\alpha-1)} - 1\}, \tag{B.23}$$

Subject to the conditions

$$\alpha > 1 \qquad \nu > 0 \qquad x > 0. \tag{B.24}$$

according to Eq (B.24), we arrive at:

$$(1 + \nu x)^{(\alpha-1)} - 1 > 0 \tag{B.25}$$

$$\Rightarrow \frac{dZ}{dx} > 0. \tag{B.26}$$

Hence, $Z(x)$ is a monotonically increasing function of x for $x > 0$ and $\alpha > 1$ as well as $\nu > 0$.

B.4 The Probability of $\mathbb{P}\{\rho_{\mathcal{R}_i,\mathcal{D}}|h_{\mathcal{R}_i,\mathcal{D}}|^2 > \rho_{\mathcal{R}_j,\mathcal{D}}|h_{\mathcal{R}_j,\mathcal{D}}|^2|_{j\neq i}\}$

Up on introducing the notation of $H_i = |h_{\mathcal{R}_i,\mathcal{D}}|^2$ and $H_j = |h_{\mathcal{R}_j,\mathcal{D}}|^2$, we arrive at:

$$\begin{aligned}
&\mathbb{P}\{\rho_{\mathcal{R}_i,\mathcal{D}}|h_{\mathcal{R}_i,\mathcal{D}}|^2 > \rho_{\mathcal{R}_j,\mathcal{D}}|h_{\mathcal{R}_j,\mathcal{D}}|^2|_{j\neq i}\} \\
&= \mathbb{P}\{H_i > \frac{\rho_{\mathcal{R}_j,\mathcal{D}}}{\rho_{\mathcal{R}_i,\mathcal{D}}} H_j\} \\
&= 1 - \int_0^\infty \mathbb{P}\{H_i < \chi_{j,i} H_j | H_j\} f_{H_j}(H_j) dH_j \\
&= 1 - \int_0^\infty F_{H_i}(\chi_{j,i} H_j) f_{H_j}(H_j) dH_j,
\end{aligned} \tag{B.27}$$

where $F_X(x)$ and $f_X(x)$ denote the cumulative distribution function (CDF) and the probability density function (PDF) of the random variable X, respectively, while $\chi_{j,i}$ represents the value of $\frac{\rho_{\mathcal{R}_j,\mathcal{D}}}{\rho_{\mathcal{R}_i,\mathcal{D}}}$. Based on our assumptions, the PDF of H_j is given by [235]:

$$f_{H_j}(H) = \exp(-H). \tag{B.28}$$

The CDF of H_i is formulated as [235]:

$$F_{H_i}(H) = 1 - \exp(-H). \tag{B.29}$$

Hence, the probability of $\mathbb{P}\{\rho_{\mathcal{R}_i,\mathcal{D}}|h_{\mathcal{R}_i,\mathcal{D}}|^2 > \rho_{\mathcal{R}_j,\mathcal{D}}|h_{\mathcal{R}_j,\mathcal{D}}|^2\}$ may be written as:

$$\begin{aligned}
&\mathbb{P}\{\rho_{\mathcal{R}_i,\mathcal{D}}|h_{\mathcal{R}_i,\mathcal{D}}|^2 > \rho_{\mathcal{R}_j,\mathcal{D}}|h_{\mathcal{R}_j,\mathcal{D}}|^2\} \\
&= 1 - \int_0^\infty [1 - \exp(-\chi_{j,i} H_j)] \exp(-H_j) dH_j \\
&= \frac{1}{\chi_{j,i} + 1} \\
&= \frac{\rho_{\mathcal{R}_i\mathcal{D}}}{\rho_{\mathcal{R}_i\mathcal{D}} + \rho_{\mathcal{R}_j\mathcal{D}}}.
\end{aligned} \tag{B.30}$$

B.5 The Probability of $\mathbb{P}\{\rho_{\mathcal{R}_i,\mathcal{D}}|h_{\mathcal{R}_i,\mathcal{D}}|^2 > \rho_{\mathcal{R}_j,\mathcal{D}}|h_{\mathcal{R}_j,\mathcal{D}}|^2 > \rho_{\mathcal{R}_k,\mathcal{D}}|h_{\mathcal{R}_k,\mathcal{D}}|^2|_{i\neq j\neq k}\}$

Let H_i and H_j denote $|h_{\mathcal{R}_i,\mathcal{D}}|^2$ and $|h_{\mathcal{R}_j,\mathcal{D}}|^2$, respectively, while H_k represents $|h_{\mathcal{R}_k,\mathcal{D}}|^2$. In order to simplify our discussions, I and J as well as K are employed to denote the RD link's pathloss of $\rho_{\mathcal{R}_i,\mathcal{D}}$ and $\rho_{\mathcal{R}_j,\mathcal{D}}$ as well as $\rho_{\mathcal{R}_k,\mathcal{D}}$. Hence, the probability of $\mathbb{P}\{\rho_{\mathcal{R}_i,\mathcal{D}}|h_{\mathcal{R}_i,\mathcal{D}}|^2 > \rho_{\mathcal{R}_j,\mathcal{D}}|h_{\mathcal{R}_j,\mathcal{D}}|^2 > \rho_{\mathcal{R}_k,\mathcal{D}}|h_{\mathcal{R}_k,\mathcal{D}}|^2|_{i\neq j\neq k}\}$ may be written as:

$$\begin{aligned}
&\mathbb{P}\{KH_k < JH_j < IH_i|_{i\neq j\neq k}\} \\
&= \int_0^\infty \int_0^{\frac{I}{J}H_i} \int_0^{\frac{J}{K}H_j} f_{H_k}(H_k) f_{H_j}(H_j) f_{H_i}(H_i) dH_k dH_j dH_i \\
&= \frac{I}{I+J} - \frac{IK}{IJ+JK+IK} \\
&= \frac{\rho_{\mathcal{R}_i,\mathcal{D}}}{\rho_{\mathcal{R}_i,\mathcal{D}} + \rho_{\mathcal{R}_j,\mathcal{D}}} - \frac{\rho_{\mathcal{R}_i,\mathcal{D}}\rho_{\mathcal{R}_k,\mathcal{D}}}{\rho_{\mathcal{R}_i,\mathcal{D}}\rho_{\mathcal{R}_j,\mathcal{D}} + \rho_{\mathcal{R}_j,\mathcal{D}}\rho_{\mathcal{R}_k,\mathcal{D}} + \rho_{\mathcal{R}_i,\mathcal{D}}\rho_{\mathcal{R}_k,\mathcal{D}}}.
\end{aligned} \tag{B.31}$$

According to in Appendix B.4, $f_X(x)$ denotes the CDF of the random variable X, which obeys $f_X(x) = \exp(-x)$.

Glossary

ACK	Acknowledgement.
AP	Access Point.
ARQ	Automatic Repeat reQuest.
ATPES	Average Transmit Power of Each Cooperative Secondary Transmitter.
ATRES	Average Transmit Rate of Each Cooperative Secondary Transmitter.
AWGN	Additive White Gaussian Noise.
BS	Base Station.
BSS	Basic Service Set.
BSSID	Basic Service Set ID.
BSSs	Basic Service Sets.
CA	Collision Avoidance.
CCS	Centralized Cooperative Systems.
CCS-1	First Centralized Cooperative System.
CCS-2	Second Centralized Cooperative System.
CDF	Cumulative Distribution Function.
CDMA	Code Division Multiple Access.
CF-End	Contention-Free-End.
CF-Poll	Contention-Free-Poll.
CFP	Contention Free Period.
CP	Contention Period.
CR	Cognitive Radio.
CRC	Cyclic Redundancy Check.
CSI	Channel Sate Information.
CSLS	Cooperative Spectrum Leasing System.

CSMA	Carrier Sense Multiple Access.
CTS	Clear-to-Send.
CW	Contention Window.
CWmax	Maximum Contention Window.
CWmin	Minimum Contention Window.
D	Duration.
DA	Destination Address.
DCF	Distributed Coordination Function.
DIFS	Distributed Coordination Function Interframe Space.
DN	Destination Node.
DS	Distribution System.
DSTC	Distributed Space-Time Coding.
DWWRS-MAS	Distributed 'Win-Win' Reciprocal-Selection-Based Medium Access Scheme.
EC	Energy Consumption.
ECR	Energy Consumption Ratio.
EIFS	Extended Interframe Space.
FC	Frame Control.
FCS	Frame Check Sequence.
FDMA	Frequency Division Multiple Access.
FTP	File Transfer Protocol.
HCF	Hybrid Coordination Function.
HTS	Helper Ready To Send.
HTTP	Hypertext Transfer Protocol.
I	ID.
IBSS	Independent Basic Service Set.
IEEE	Institute of Electrical and Electronics Engineers.
IP	Internet Protocol.
ISO	International Organization for Standardization.
LLC	Logical Link Control.
MAC	Medium Access Control.
MARCH	beaMforming and Automatic repeat request aided oppoRtunistic speCtrum scHeduling.

MIMO	Multiple-Input-Multiple-Output.
MS	Mobile Station.
MTU	Maximum Transmission Unit.
NACK	Negative-Acknowledgement.
NCS	Non-Cooperative Cystems.
NCS-1	Non-Cooperative System 1.
nCS-1	First non-Cooperative System.
NCS-2	Non-Cooperative System 2.
nCS-2	Second non-Cooperative System.
non-CSLS	non-Cooperative Spectrum Leasing System.
OF	Objective Function.
OSI	Open Systems Interconnection.
PC	Point Coordinator.
PCF	Point Coordination Function.
PDU	Protocol Data Unit.
PIFS	Point Coordination Function Interframe Space.
PP	PT-to-PR.
PR	Primary Receiver.
PS	Please-Send.
PT	Primary Transmitter.
PTP	Primary Transmission Pair.
PTPs	Primary Transmission Pairs.
PTS	PT-to-ST.
PU	Primary User.
PUs	Primary Users.
QC	Quality Control.
QoS	Quality of Service.
R-CSLS	Random Cooperative Spectrum Leasing System.
RA	Receiver Address.
Ran-CSLS	Random Cooperative Spectrum Leasing System.
RD	Relay-to-Destination.
RN	Relay Node.
RNs	Relay Nodes.
RR	Relay Requirement.

RRTS	Relay-Request-To-Send.
RTS	Request-to-Send.
SA	Source Address.
SC	Sequence Control.
SD	Source-to-Destination.
SIC	Successive Interference Cancellation.
SIFS	Short Interframe Space.
SMTP	Simple Mail Transfer Protocol.
SN	Source Node.
SNR	Signal-to-Noise-Ratio.
SPC	SuperPosition Coding.
SRec	Secondary Receiver.
SS	ST-to-SR.
ST	Secondary Transmitter.
STP	Secondary Transmission Pair.
STPowR	System Transmit Power Ratio.
STPs	Secondary Transmission Pairs.
STRaR	System Transmit Rate Ratio.
STTP	System's Total Transmit Power.
SU	Secondary User.
SUs	Secondary Users.
TA	Transmitter Address.
TCP	Transport Control Protocol.
TDMA	Time Division Multiple Access.
TDTP	Total Data Transmit Power.
TP	Transmit Power.
TPP	Transmit Power of All Primary Transmitters.
TR	Transmit Rate.
TS	Time-Slot.
TTPS	Total Transmit Power of All The Cooperative Secondary Transmitters.
TTR	Total Transmit Rate.
TTRP	Total Transmit Rate of Primary Transmitters.
TTRR	Total Transmit Rate Ratio.
TTRS	Total Transmit Rate of All Cooperative Secondary Transmitters.
UDP	User Datagram Protocol.

UN	Unlicensed Node.
WiMAX	Worldwide Interoperability for Microwave Access.
WLANs	Wireless Local Areas Networks.
WW	'Win-Win'.
WW-CSLS	'Win-Win' Cooperative Spectrum Leasing System.
WWCF	'Win-Win' Cooperative Framework.
WWRSF	'Win-Win' Reciprocal-Selection-Based Framework.

Bibliography

[1] D. Feng, C. Jiang, G. Lim, J. Cimini, G. Feng, and G. Li, "A Survey of Energy-Efficient Wireless Communications," *IEEE Communications Surveys and Tutorials*, vol. 15, pp. 167 – 178, First Quarter 2013.

[2] F. Gomez-Cuba, R. Asorey-Cacheda, and F. Gonzalez-Castano, "A Survey on Cooperative Diversity for Wireless Networks," *IEEE Communications Surveys and Tutorials*, vol. 14, pp. 822 – 835, Third Quarter 2012.

[3] L. Hanzo, O. Alamri, N. El-Hajjar, and N. Wu, *Near-Capacity Multi Functional MIMO Systems*. New York, USA: IEEE Press - John Wiley, 2009.

[4] L. Hanzo, Y. Akhtman, L. Wang, and M. Jiang, *MIMO-OFDM for LTE, WIFI and WIMAX: Coherent versus Non-Coherent and Cooperative Turbo-Transceivers*. New York, USA: IEEE Press - John Wiley, 2010.

[5] M. Tao and Y. Liu, "A Network Flow Approach to Throughput Maximization in Cooperative OFDMA Networks," *IEEE Transactions on Wireless Communications*, vol. 12, pp. 1138 – 1148, March 2013.

[6] S. Syue, C. Wang, T. Aguilar, V. Gauthier, and H. Afifi, "Cooperative Geographic Routing with Radio Coverage Extension for SER-Constrained Wireless Relay Networks," *IEEE Journal on Selected Areas in Communications*, vol. 30, pp. 271 – 279, February 2012.

[7] G. Lim and L. Cimini, "Energy-Efficient Cooperative Beamforming in Clustered Wireless Networks," *IEEE Transactions on Wireless Communications*, vol. 12, pp. 1376 – 1385, March 2013.

[8] T. Cover and A. Gamal, "Capacity Theorems for the Relay Channel," *IEEE Transactions on Information Theory*, vol. 25, pp. 572 – 584, September 1979.

[9] J. Zhang, L. Yang, and L. Hanzo, "Multi-User Performance of the Amplify-and-Forward Single-Relay Assisted SC-FDMA Uplink," in *Vehicular Technology Conference Fall (VTC 2009-Fall), 2009 IEEE 70th*, Alaska, USA, September 2009, pp. 1 – 5.

[10] M. Butt, R. Riaz, S. Ng, and L. Hanzo, "Distributed Self-Concatenated Coding for Cooperative Communication," *IEEE Transactions on Vehicular Technology*, vol. 59, pp. 3097 – 3104, July 2010.

[11] L. Kong, S. Ng, R. Maunder, and L. Hanzo, "Distributed Self-Concatenated Coding for Cooperative Communication," *IEEE Transactions on Vehicular Technology*, vol. 59, pp. 1511 – 1517, January 2010.

[12] M. Butt, S. Ng, and L. Hanzo, "Self-Concatenated Code Design and its Application in Power-Efcient Cooperative Communications," *IEEE Communications Surveys and Tutorials, IEEEXplore Early Access*, vol. 51, pp. 1 – 26, September 2011.

[13] R. Zhang and L. Hanzo, "Cooperative Downlink Multicell Preprocessing Relying on Reduced-Rate Back-Haul Data Exchange," *IEEE Transactions on Vehicular Technology*, vol. 60, pp. 539 – 545, February 2011.

[14] L. Wang and L. Hanzo, "Dispensing with Channel Estimation: Differentially Modulated Cooperative Wireless Communications," *IEEE Communications Surveys and Tutorials*, vol. 14, pp. 836 – 857, Third Quarter 2012.

[15] H. Nguyen, S. Ng, and L. Hanzo, "Irregular Convolution and Unity-Rate Coded Network-Coding for Cooperative Multi-User Communications," *IEEE Transactions on Wireless Communications*, vol. 12, pp. 1231 – 1243, March 2013.

[16] S. Sugiura, S. Ng, L. Kong, S. Chen, and L. Hanzo, "Quasi-Synchronous Cooperative Networks: A Practical Cooperative Transmission Protocol," *IEEE Vehicular Technology Magazine*, vol. 7, pp. 66 – 76, December 2012.

[17] A. Behboodi and P. Piantanida, "Cooperative Strategies for Simultaneous and Broadcast Relay Channels," *IEEE Transactions on information Theory*, vol. 59, pp. 1417 – 1443, March 2013.

[18] A. Sendonaris, E. Erkip, and B. Aazhang, "Increasing Uplink Capacity Via User Cooperation Diversity," *in Proceedings of IEEE International Symposium on Information Theory 1998 (ISIT 1998)*, p. 156, August 1998.

[19] C. Nie, P. Liu, T. Korakis, E. Erkip, and S. Panwar, "Cooperative Relaying in Next-Generation Mobile WiMAX Networks," *IEEE Transactions on Vehicular Technology*, vol. 62, pp. 1399 – 1405, March 2013.

[20] D. Nguyen and M. Krunz, "Price-Based Joint Beamforming and Spectrum Management in Multi-Antenna Cognitive Radio Networks," *IEEE Journal on Selected Areas in Communications*, vol. 30, pp. 2295 – 2305, December 2012.

[21] P. Liu, C. Nie, T. Korakis, E. Erkip, S. Panwar, F. Verde, and A. Scaglione, "STiCMAC: A MAC Protocol for Robust Space-Time Coding in Cooperative Wireless LANs," *IEEE Transactions on Wireless Communications*, vol. 11, pp. 1358 – 1369, April 2012.

[22] Y. Jin, G. Kesidis, and W. Ju, "A Channel Aware MAC Protocol in an ALOHA Network with Selfish Users," *IEEE Journal on Selected Areas in Communications*, vol. 30, pp. 128 – 137, January 2012.

[23] L. Li, F. Zhong, and D. Kaleshi, "CARLA: Combining Cooperative Relaying and Link Adaptation for IEEE 802.11 Wireless Networks," in *2012 IEEE 75th Vehicular Technology Conference (VTC Spring)*, Yokohama, Japan, May 2012, pp. 1 – 5.

[24] C. Oh and T. Lee, "Cooperative MAC Protocol Using Active Relays for Multi-Rate WLANs," *Journal of Communications and Networks*, vol. 13, pp. 463 – 471, October 2011.

[25] Y. Hong, C. Lin, and S. Wang, "Exploiting Cooperative Advantages in Slotted ALOHA Random Access Networks," *IEEE Transactions on Information Theory*, vol. 56, pp. 3828 – 3846, July 2010.

[26] P. Liu, C. Nie, E. Erkip, and S. Panwar, "Robust Cooperative Relaying in a Wireless LAN: Cross-Layer Design and Performance Analysis," in *Global Telecommunications Conference, 2009. GLOBECOM 2009. IEEE*, Hawaii, USA, CD ROM, September 2009, pp. 1–6.

[27] A. Crismani, F. Babich, and L. Hanzo, "Cross-Layer Solutions for Cooperative Medium Access Control Protocols," in *Vehicular Technology Conference (VTC 2010-Spring), 2010 IEEE 71st*, Taipei, Taiwan, CD ROM, May 2010, pp. 1–5.

[28] J. Zhang, Q. Zhang, and W. Jia, "VC-MAC: ACooperative MAC Protocol in Vehicular Networks," *IEEE Transactions on Vehicular Technology*, vol. 58, pp. 1561 – 1571, March 2009.

[29] W. Yang, J. Wu, L. Wang, and T. Lee, "A Cooperative Multi-Group Priority MAC Protocol for Multi-Packet Reception Channels," *IEEE Transactions on Wireless Communications*, vol. 8, pp. 5416 – 5421, November 2009.

[30] P. Liu, Z. Tao, S. Narayanan, T. Korakis, and S. Panwar, "CoopMAC: A Cooperative MAC for Wireless LANs," *IEEE Journal on Selected Areas in Communications*, vol. 25, pp. 340 – 354, February 2007.

[31] J. Laneman, D. Tse, and G. Wornell, "Cooperative Diversity In Wireless Networks: Efficient Protocols and Outage Behavior," *IEEE Transactions on Information Theory*, vol. 50, pp. 3062 – 3080, December 2004.

[32] T. Luo, M. Motani, and V. Srinivasan, "Energy-Efficient Strategies for Cooperative Multichannel MAC Protocols," *IEEE Transactions on Mobile Computing*, vol. 11, pp. 553 – 566, April 2012.

[33] G. Botter, J. Alonso-Zarate, L. Alonso, F. Granelli, and C. Verikoukis, "Extending The Lifetime of M2M Wireless Metworks Through Cooperation," in *2012 IEEE International Conference on Communications (ICC)*, Ottawa, Canada, June 2012, pp. 6003 – 6007.

[34] C. Khirallah, D. Vukobratovic, and J. Thompson, "Performance Analysis and Energy Efficiency of Random Network Coding in LTE-Advanced," *IEEE Transactions on Wireless Communications*, vol. 11, pp. 4275 – 4285, December 2012.

[35] H. Fang, X. Lin, and T. Lok, "Power Allocation for Multiuser Cooperative Communication Networks Under Relay-Selection Degree Bounds," *IEEE Transactions on Vehicular Technology*, vol. 61, pp. 2991 – 3001, September 2012.

[36] J. Feng, R. Zhong, S. Ng, and L. Hanzo, "Relay Selection for Energy-Efficient Cooperative Media Access Control," in *2011 IEEE Wireless Communications and Networking Conference (WCNC)*, Cancun, Mexico, March 2011, pp. 1–6.

[37] A. B. Nacef, S. Senouci, Y. Ghamri-Doudane, and A. Beylot, "A Cooperative Low Power Mac Protocol for Wireless Sensor Networks," in *2011 IEEE International Conference onvCommunications (ICC)*, Kyoto, Japan, June 2011, pp. 1 – 6.

[38] J. Alonso-Zarate, E. Stavrou, A. Stamou, P. Angelidis, L. Alonso, and C. Verikoukis, "Energy-Efficiency Evaluation of a Medium Access Control Protocol for Cooperative ARQ," in *2011 IEEE International Conference on Communications (ICC)*, Kyoto, Japan, June 2011, pp. 1 – 5.

[39] M. Gokturk and O. Gurbuzs, "Cooperation In Wireless Sensor Networks: Design and Performance Analysis of A MAC Protocol," in *IEEE International Conference on Communications, 2008. ICC '08.*, BeiJing, China, May 2008, pp. 4284 – 4289.

[40] S. Moh and C. Yu, "A Cooperative Diversity-Based Robust MAC Protocol in Wireless Ad Hoc Networks," *IEEE Transactions on Parallel and Distributed Systems*, vol. 22, pp. 353 – 363, March 2011.

[41] I. Stanojev, O. Simeone, U. Spagnolini, Y. Bar-Ness, and R. Pickholtz, "Cooperative ARQ Via Auction-Based Spectrum Leasing," *IEEE Transactions on Communications*, vol. 58, pp. 1843 – 1856, June 2010.

[42] T. Guo, R. Carrasco, and W. Woo, "Differentiated Cooperative Multiple Access for Multimedia Communications Over Fading Wireless Networks," *IET Communications*, vol. 3, pp. 1005 – 1015, June 2009.

[43] S. Kim, D. Kim, and Y. Suh, "Distributing Data Rate Using Cooperative Channel Assignment for Multi-Rate Wireless Mesh Networks," in *2010 IEEE Wireless Communications and Networking Conference (WCNC)*, Sydeny, Australia, April 2010, pp. 1 – 6.

[44] P. Kong, C. Mar, and C. Tham, "CoRex: A Simple MAC Layer Cooperative Retransmission Scheme for Wireless Networks," in *2010 IEEE Wireless Communications and Networking Conference (WCNC)*, Sydeny, Australia, April 2010, pp. 1 – 6.

[45] J. Liu, W. Chen, Z. Cao, and Y. Zhang, "Token-Based Opportunistic Scheduling Protocol for Cognitive Radios with Distributed Beamforming," *IET Communications*, vol. 6, pp. 945 – 954, May 2012.

[46] B. Lorenzo and S. Glisic, "Context-Aware Nanoscale Modeling of Multicast Multihop Cellular Networks," *IEEE/ACM Transactions on Networking*, vol. 21, pp. 359 – 372, April 2013.

[47] M. Peng, Y. Liu, D. Wei, W. Wang, and H. Chen, "Hierarchical Cooperative Relay Based Heterogeneous Networks," *IEEE Wireless Communications*, vol. 18, pp. 48 – 56, June 2011.

[48] S. Chu, X. Wang, and Y. Yang, "Exploiting Cooperative Relay for High Performance Communications in MIMO Ad Hoc Networks," *IEEE Transactions on Computers*, vol. 62, pp. 716 – 729, April 2013.

[49] M. Tao and R. Wang, "Linear Precoding for Multi-Pair Two-Way MIMO Relay Systems With Max-Min Fairness," *IEEE Transactions on Signal Processing*, vol. 60, pp. 5361 – 5370, October 2012.

[50] R. Vaze, "Throughput-Delay-Reliability Tradeoff with ARQ in Wireless Ad Hoc Networks," *IEEE Transactions on Wireless Communications*, vol. 10, pp. 2142 – 2149, July 2011.

[51] G. Shirazi, P. Kong, and C. Tham, "Optimal Cooperative Relaying Schemes in IR-UWB Networks," *IEEE Transactions on Mobile Computing*, vol. 9, pp. 969 – 981, July 2010.

[52] J. Feng, R. Zhang, and L. Hanzo, "A Spectrum Leasing Cooperative Medium Access Protocol and its Stability Analysis," *IEEE Transactions on Vehicular Technology*, vol. 61, pp. 3718 – 3730, October 2012.

[53] J. Liu, W. Wang, Z. Zheng, X. Zhang, C. Chen, and X.Shen, "Lifetime Extended Cooperative MAC Protocol for Wireless Lans," in *2012 IEEE Global Communications Conference (GLOBECOM)*, California, USA, December 2012, pp. 5476 – 5481.

[54] Y. Zhou, J. Liu, L. Zheng, C. Zhai, and H. Chen, "Link-Utility-Based Cooperative MAC Protocol for Wireless Multi-Hop Networks," *IEEE Transactions on Wireless Communications*, vol. 10, pp. 995 – 1005, March 2011.

[55] J. Feng, R. Zhong, and L. Hanzo, "Auction-Style Cooperative Medium Access Control," in *Vehicular Technology Conference (VTC), 2011 IEEE 74th*, San Francisco, USA, September 2011, pp. 1–5.

[56] N. Hu, Y. Yao, and Z. Yang, "Analysis of Cooperative TDMA in Rayleigh Fading Channels," *IEEE Transactions on Vehicular Technology*, vol. 62, pp. 1158 – 1168, March 2013.

[57] X. Wang and J. Li, "Network Coding Aware Cooperative MAC Protocol for Wireless Ad Hoc Networks," *IEEE Transactions on Parallel and Distributed System*, vol. PP, pp. 1 – 13, January 2013.

[58] S. Chu and X. Wang, "Opportunistic and Cooperative Spatial Multiplexing in MIMO Ad Hoc Networks," *IEEE/ACM Transactions on Networking*, vol. 18, pp. 1610 – 1623, October 2010.

[59] F. Verde, T. Korakis, E. Erkip, and A. Scaglione, "A Simple Recruitment Scheme of Multiple Nodes for Cooperative MAC," *IEEE Transactions on Communications*, vol. 58, pp. 2667 – 2682, September 2010.

[60] X. Wang, J. Li, and M. Guizani, "NCAC-MAC: Network Coding Aware Cooperative Medium Access Control for Wireless Networks," in *2012 IEEE Wireless Communications and Networking Conference (WCNC)*, Pairs, France, April 2012, pp. 1636 – 1641.

[61] B. Cao, G. Feng, Y. Li, and C. Wang, "Cooperative Media Access Control with Optimal Relay Selection in Error-prone Wireless Networks," *IEEE Transactions on Vehicular Technology*, vol. PP, pp. 1 – 12, December 2012.

[62] T. Zhou, H. Sharif, M. Hempel, P. Mahasukhon, W. Wang, and T. Ma, "A Novel Adaptive Distributed Cooperative Relaying MAC Protocol for Vehicular Networks," *IEEE Journal on Selected Areas in Communications*, vol. 29, pp. 72 – 82, January 2011.

[63] J. Cloud, L. Zeger, and M. Medard, "MAC Centered Cooperation Synergistic Design of Network Coding, Multi-Packet Reception, and Improved Fairness to Increase Network Throughput," *IEEE Journal on Selected Areas in Communications*, vol. 20, pp. 341 – 349, February 2012.

[64] H. Lu and W. Liao, "Cooperative Strategies in Wireless Relay Networks," *IEEE Journal on Selected Areas in Communications*, vol. 30, pp. 323 – 330, February 2012.

[65] R. Wang, Z. Wang, Z. Chen, and L. Zhang, "A 3G-802.11p Based OLT-TDMA Mechanism for Cooperative Safety in a Dense Traffic Scenario," in *2011 IEEE 73rd Vehicular Technology Conference (VTC Spring)*, Budapest, Hungary, May 2011, pp. 1 – 5.

[66] A. Sendonaris, E. Erkip, and B. Aazhang, "User Cooperative Diversity, Part I: System," *IEEE Transactions on Communications*, vol. 51, pp. 1927 –1938, November 2003.

[67] H. Liang and W. Zhuang, "Double-Loop Receiver-Initiated MAC for Cooperative Data Dissemination via Roadside WLANs," *IEEE Transactions on Communications*, vol. 60, pp. 2644 – 2656, August 2012.

[68] A. Argyriou, "Coordinating Interfering Transmissions in Cooperative Wireless LANs," *IEEE Transactions on Wireless Communications*, vol. 10, pp. 3804 – 3812, September 2011.

[69] K. Liu and H. Chen, "Performance Analysis of Threshold Relaying with Random Channel Access over Non-Identically Distributed Rayleigh-Fading Channels," *IEEE Journal on Selected Areas in Communications*, vol. 30, pp. 1703 – 1710, October 2012.

[70] H. Shen, H. Y. B. Sikdar, and S. Kalyanaraman, "A Distributed System for Cooperative MIMO Transmissions," in *IEEE Global Telecommunications Conference, 2008. IEEE GLOBECOM 2008*, New Orleans, USA, December 2008, pp. 1 – 5.

[71] H. Shan, H. Cheng, and W. Zhuang, "Cross-Layer Cooperative MAC Protocol in Distributed Wireless Networks," *IEEE Transactions on Wireless Communications*, vol. 10, pp. 2603 – 2615, August 2011.

[72] T. Guo and R. Carrasco, "CRBAR: Cooperative Relay-Based Auto Rate mac for Multirate Wireless Networks," *IEEE Transactions on Wireless Communications*, vol. 8, pp. 5938 – 5947, December 2009.

[73] T. Guo, R. Carrasco, and W. Woo, "Differentiated Cooperative Multiple Access for Multimedia Communications Over Fading Wireless Networks," *IET Communications*, vol. 10, pp. 1005 – 1015, June 2009.

[74] J. Alonso-Zarate, L. Alonso, and C. Verikoukis, "Performance Analysis of A Persistent Relay Carrier Sensing Multiple Access Protocol," *IEEE Transactions on Wireless Communications*, vol. 8, pp. 5827 – 583, December 2009.

[75] T. Aguilar, S. Syue, V. Gauthier, and H. Afifi, "CoopGeo: A Beaconless Geographic Cross-Layer Protocol for Cooperative Wireless Ad Hoc Networks," *IEEE Transactions on Wireless Communications*, vol. 10, pp. 2554 – 2565, August 2011.

[76] I. Krikidis, B. Rong, and A. Ephremides, "Network-Level Cooperation for a Multiple-Access Channel Via Dynamic Decode-and-Forward," *IEEE Transactions on Information Theory*, vol. 57, pp. 7759 – 7770, December 2011.

[77] I. Krikidis, N. Devroye, and J. Thompson, "Stability Analysis for Cognitive Radio with Multi-access Primary Transmission," *IEEE Transactions on Wireless Communications*, vol. 9, pp. 72 – 77, January 2010.

[78] A. Argyriou, "Cross-Layer and Cooperative Opportunistic Network Coding in Wireless Ad Hoc Networks," *IEEE Transactions on Vehicular Technology*, vol. 59, pp. 803 – 812, February 2010.

[79] A. Sharifi, F. Ashtiani, H. Keshavarz, and M. Nasiri-Kenari, "Impact of Cognition and Cooperation on MAC Layer Performance Metrics, Part I: Maximum Stable Throughput," *IEEE Transactions on Wireless Communications*, vol. 11, pp. 4252 – 4263, December 2012.

[80] T. Elkourdi and O. Simeone, "Spectrum Leasing via Cooperation With Multiple Primary Users," *IEEE Transactions on Vehicular Technology*, vol. 61, pp. 820 – 825, February 2012.

[81] J. Zheng and M. Ma, "QoS-Aware Cooperative Medium Access Control for MIMO Ad-Hoc Networks," *IEEE Communications Letters*, vol. 14, pp. 48 – 50, January 2010.

[82] J. Liu, W. Chen, Z. Cao, and Y. Zhang, "Cooperative Beamforming for Cognitive Radio Networks: A Cross-Layer Design," *IEEE Transactions on Communications*, vol. 60, pp. 1420 – 1431, May 2012.

[83] C. Nie, P. Liu, T. Korakis, E. Erkip, and S. Panwar, "CoopMAX: A Cooperative MAC with Randomized Distributed Space-Time Coding for an IEEE 802.16 Network," in *IEEE International Conference on Communications, 2009. ICC '09*, Dresden, Gemany, June 2009, pp. 1 – 6.

[84] M. Khalid, Y. Wang, I. Ra, and S. Ravi, "Two-Relay-Based Cooperative MAC Protocol for Wireless Ad hoc Networks," *IEEE Transactions on Vehicular Technology*, vol. 60, pp. 3361 – 3373, September 2011.

[85] A. Ozgur, R. Johari, D. Tse, and O. Leveque, "Information-Theoretic Operating Regimes of Large Wireless Networks," *IEEE Transactions on Information Theory*, vol. 56, pp. 427 – 437, January 2010.

[86] Y. Zhou, J. Liu, C. Zhai, and L. Zheng, "Two-Transmitter Two-Receiver Cooperative MAC Protocol: Cross-Layer Design and Performance Analysis," *IEEE Transactions on Vehicular Technology*, vol. 59, pp. 4116 – 4127, October 2010.

[87] A. Kailas, L. Thanayankizil, and M. Ingram, "A Simple Cooperative Transmission Protocol for Energy-Efficient Broadcasting Over Multi-hop Wireless Networks," *Journal of Communications and Networks*, vol. 10, pp. 213 – 220, October 2008.

[88] W. Liang, J. Feng, S. Ng, and L. Hanzo, "Pragmatic Distributed Algorithm for Spectral Access in Cooperative Cognitive Radio Networks," 2013, submitted to IEEE Transactions on Communications.

[89] S. Bayat, R. Louie, Y. Li, and B. Vucetic, "Cognitive Radio Relay Networks with Multiple Primary and Secondary Users: Distributed Stable Matching Algorithms for Spectrum Access," in *2011 IEEE International Conference on Communications (ICC)*, Kyoto, Japan, June 2011, pp. 1 – 6.

[90] Z. Zhou, S. Zhou, J. Cui, and S. Cui, "Energy-Efficient Cooperative Communication Based on Power Control and Selective Single-Relay in Wireless Sensor Networks," *IEEE Transactions on Communications*, vol. 7, pp. 1536–1276, August 2008.

[91] Y. Hua, Q. Zhang, and Z. Niu, "A Cooperative MAC Protocol with Virtual-Antenna Array Support in A Multi-AP WLAN System," *IEEE Transactions on Wireless Communications*, vol. 8, pp. 4806 – 4814, October 2009.

[92] J. Liu, W. Chen, Z. Cao, and Y. Zhang, "Cooperative Beamforming Aided Incremental Relaying in Cognitive Radios," in *Communications (ICC), 2011 IEEE International Conference on*, Paris, France, July 2011, pp. 1 – 5.

[93] J. An, S. Bae, and N. Kim, "A Cooperative ARQ Strategy with Adaptive Back-Off for Mobile Multimedia Communication Using Cognitive Relays," in *Vehicular Technology Conference (VTC Fall), 2011 IEEE*, San Francisco, USA, Jue 2011, pp. 1 – 5.

[94] Z. Yang, Y. Yao, X. Li, and D. Zheng, "A TDMA-Based MAC Protocol With Cooperative Diversity," *IEEE Communications Letters*, vol. 14, pp. 542 – 544, June 2010.

[95] M. Lu, P. Steenkiste, and T. Chen, "Robust Wireless Video Streaming Using Hybrid Spatial/Temporal Retransmission," *IEEE Journal on Selected Areas in Communications*, vol. 28, pp. 476 – 487, April 2010.

[96] S. Ivanov, D. Botvich, and S. Balasubramaniam, "Cooperative Wireless Sensor Environments Supporting Body Area Networks," *IEEE Transactions on Consumer Electronics*, vol. 58, pp. 284 – 292, May 2012.

[97] B. Han, J. Li, J. Su, and J. Cao, "Self-Supported Cooperative Networking for Emergency Services in Multi-Hop Wireless Networks," *IEEE Journal on Selected Areas in Communications*, vol. 30, pp. 450 – 457, February 2012.

[98] T. Elkourdi and O. Simeone, "Spectrum Leasing Via Cooperative Interference Forwarding," *IEEE Transactions on Vehicular Technology*, vol. 62, pp. 1367 – 1372, March 2013.

[99] F. Babich and A. Crismani, "Incremental and Complementary Coding Techniques for Cooperative Medium Access Control Protocols," in *2011 IEEE 73rd Vehicular Technology Conference (VTC Spring)*, Budapest, Hungary, May 2011, pp. 1 – 5.

[100] Q. Zhao and B. Sadler, "A Survey of Dynamic Spectrum Access," *IEEE Signal Processing Magazine*, vol. 24, pp. 79 –89, May 2007.

[101] K. Zhu, D. Niyato, P. Wang, and Z. Han, "Dynamic Spectrum Leasing and Service Selection in Spectrum Secondary Market of Cognitive Radio Networks," *IEEE Transactions on Wireless Communications*, vol. 11, pp. 1136 – 1145, March 2012.

[102] H. Lim, M. Song, and G. Im, "Cooperation-Based Dynamic Spectrum Leasing via Multi-Winner Auction of Multiple Bands," *IEEE Transactions on Communications*, vol. 61, pp. 1136 – 1145, April 2013.

[103] M. Zukerman, "Introduction to Queueing Theory and Stochastic Teletraffic Models," 2008, Downloadable at http://www.mendeley.com/catalog/introduction-queueing-theory-stochastic-teletraffic-models-1/.

[104] J. Feng, R. Zhang, L. Hanzo, and S. Ng, "Cooperative Medium Access Control Based on Spectrum Leasing," 2013, accepted by IEEE Transactions on Vehicular Technolog.

[105] J. Feng, W. Liang, S. Ng, and L. Hanzo, "A Reciprocal-Selection-Based Spectrum Leasing Cooperative Medium Access Control and its Stability Analysis," 2013, prepared to be submitted to IEEE Transactions on Vehicular Technology.

[106] "IEEE Standard for Information Technology – Telecommunications and Information Exchange Between Systems – Local and Metropolitan Area Networks-Specific Requirements – Part 11: Wireless LAN Medium Access Control (MAC) and Physical Layer (PHY) Specifications," 2007, Downloadable at http://standards.ieee.org/getieee802/802.11.html.

[107] W. Stallings, *Wireless Communications and Networks*. New Jersey, USA: Prentice-hall, Inc, 2005.

[108] "International Organization for Standardization. ISO/IEC 7498-1:1994 Information Technology – Open Systems Interconnection – Basic Reference Model: The Basic Model," 1994. [Online]. Available: http://www.iso.org/iso/catalogue_detail.htm?csnumber=20269

[109] W. Stevens, *TCP/IP Illustrated, Vol. 1: The Protocols*. Boston, USA: Addison-Wesley, 1994.

[110] "RFC2616: Hypertext Transfer Protocol HTTP/1.1," Network Working Group,, June, 1999, Downloadable at http://www.ietf.org/rfc/rfc2616.txt.

[111] "RFC959: File Transfer Protocol (FTP)," Network Working Group,, October,1985, Downloadable at http://www.ietf.org/rfc/rfc959.txt.

[112] "RFC5321: Simple Mail Transfer Protocol," Network Working Group,, October,2008, Downloadable at http://www.ietf.org/rfc/rfc5321.txt.

[113] "IEEE 802.3-2008 IEEE Standard for Information technology-Specific requirements - Part 3: Carrier Sense Multiple Access with Collision Detection (CSMA/CD) Access Method and Physical Layer Specifications," 2008, Downloadable at http://http://standards.ieee.org/about/get/802/802.3.html.

[114] " IEEE 802.5 Token Ring MIB," Network Working Group,, May,1991, Downloadable at http://www.ietf.org/rfc/rfc1231.txt.

[115] A. Goldsmith, *Wireless Communications*. Cambridge, UK: Cambridge University Press, 2005.

[116] L. Zhao, L. Guo, J. Zhang, and H. Zhang, "Game-Theoretic Medium Access Control Protocol for Wireless Sensor Networks," *IET Communications*, vol. 3, pp. 1274 – 1283, July 2009.

[117] K. Sohrabi, J. Gao, V. Ailawadhi, and G. Pottie, "Protocols for Selforganization of A Wireless Sensor Network," *IEEE Personal Communications*, vol. 7, pp. 16–27, October 2000.

[118] S. Kucera, L. Kucera, and B. Zha, "Efficient Distributed Algorithms for Dynamic Access to Shared Multiuser Channels in SINR-Constrained Wireless Networ," *IEEE Transactions on Mobile Computing*, vol. 11, pp. 2087 – 2097, December 2012.

[119] J. Park, P. Paweczak, and D. Cabric, "Performance of Joint Spectrum Sensing and MAC Algorithms for Multichannel Opportunistic Spectrum Access Ad Hoc Networks," *IEEE Transactions on Mobile Computing*, vol. 10, pp. 1011 – 1027, July 2011.

[120] K. Kim, K. Kwak, and B. Choi, "Performance Analysis of Opportunistic Spectrum Access Protocol for Multi-Channel Cognitive Radio Networks," *Journal of Communications and Networks*, vol. 15, pp. 77 – 86, February 2013.

[121] L. Kuo and T. Melodia, "Distributed Medium Access Control Strategies for MIMO Underwater Acoustic Networking," *IEEE Transactions on Wireless Communications*, vol. 10, pp. 2523 – 2533, August 2011.

[122] N. Abramson, "Development of the ALOHAnet," *IEEE Transactions on Information Theory*, vol. 31, pp. 119 – 123, March 1985.

[123] ——, "The ALOHA System-Another alternative for computer communications," *Proc. AFIPS-Fall Joint Comput. Conf.*, vol. 37, pp. 281 – 285, November 1970.

[124] X. Wang, A. Wong, and P. Ho, "Stochastic Medium Access for Cognitive Radio Ad Hoc Networks," *IEEE Journal on Selected Areas in Communications*, vol. 29, pp. 770 – 783, April 2011.

[125] L. Lei, J. Zhou, X. Chen, L. Qi, and S. Cai, "Modelling and Analysing Medium Access Delay for Differentiated Services in IEEE 802.11 Wireless Mesh Networks," *IET Networks*, vol. 1, pp. 91 – 99, June 2012.

[126] F. Hsu and H. Su, "Analysis of a Reservation-Based Random Access Network: Throughput Region and Power Consumption," *IEEE Transactions on Communications*, vol. 61, pp. 237 – 247, January 2013.

[127] W. Liao and C. Huang, "SF-MAC: A Spatially Fair MAC Protocol for Underwater Acoustic Sensor Networks," *IEEE Sensors Journal*, vol. 12, pp. 1686 – 1694, June 2012.

[128] L. Roberts, "Aloha Packet System With And Without Slots And Capture," *Computer Communications Review*, vol. 5, pp. 28 – 42, April 1975.

[129] "IEEE Standard for Information Technology – Telecommunications and Information Exchange Between Systems – Local and Metropolitan Area Networks-Specific Requirements – Part 11: Wireless LAN Medium Access Control (MAC) and Physical Layer (PHY) Specifications – amendment 5: Enhancement for higher throughput," 2009. [Online]. Available: http://standards.ieee.org/getieee802/802.11.html

[130] M. Schwartz, *Mobile Wireless Communications*. Cambridge, UK: Cambridge University Press, 2005.

[131] D. G. Kendall, "Stochastic Processes Occurring In The Theory of Queues and Their Analysis By The Method of The Imbedded Markov Chain," *The Annals of Mathematical Statistics*, vol. 24, pp. 338 – 354, September 1953.

[132] D. Gross, J. Shortle, J. Thompson, and C. Harris, *Fundamentals of Queueing Theory (4th Edition)*. New York, USA: IEEE Press - John Wiley, 2008.

[133] D. Bertsekas and R. Gallager, *Data Network*. Englewood Cliffs, NJ: Prentice-Hall, 1987.

[134] R. Loynes, "The Stability of A Queue With Non-Independent Inter-Arrival and Service Times," *Mathematical Proceedings of the Cambridge Philosophical Society*, vol. 58, pp. 497 – 520, July 1962.

[135] R. Rao and A. Ephremides, "On the Stability of Interacting Queues in a Multi-Access System," *IEEE Transactions on Information Theory*, vol. 34, pp. 918 – 930, September 1988.

[136] Y. Sagduyu and A. Ephremides, "On Broadcast Stability of Queue-Based Dynamic Network Coding Over Erasure Channels," *IEEE Transactions on Information Theory*, vol. 55, pp. 5463 – 5478, November 2009.

[137] I. Krikidis, "Stability Analysis for Bidirectional MABC-DF Relay Networks With Bursty Traffic," *IEEE Transactions on Vehicular Technology*, vol. 60, pp. 2844 – 2849, July 2011.

[138] A. Sadek, K. Liu, and A. Ephremides, "Cognitive Multiple Access Via Cooperation: Protocol Design and Performance Analysis," *IEEE Transactions on Information Theory*, vol. 53, pp. 3677 – 3696, October 2007.

[139] O. Simeone, Y. Bar-Ness, and U. Spagnolini, "Stable Throughput of Cognitive Radios With and Without Relaying Capability," *IEEE Transactions on Communications*, vol. 55, pp. 2351 – 2360, December 2007.

[140] N. Pappas, J. Jeongho, A. Ephremides, and A. Traganitis, "Optimal Utilization of A Cognitive Shared Channel With A Rechargeable Primary Source Node," *Journal of Communications and Networks*, vol. 14, pp. 162 – 168, April 2012.

[141] A. Sharifi, F. Ashtiani, H. Keshavarz, and M. Nasiri-Kenari, "Impact of Cognition and Cooperation on MAC Layer Performance Metrics, Part I: Maximum Stable Throughput," *IEEE Transactions on Wireless Communications*, vol. 11, pp. 4252 – 4263, December 2012.

[142] I. Krikidis, T. Charalambous, and J. Thompsonand, "Stability Analysis and Power Optimization for Energy Harvesting Cooperative Networks," *IEEE Signal Processing Letters*, vol. 19, pp. 20 – 23, January 2012.

[143] A. El-Sherif, A. Sadek, and K. Liu, "Opportunistic Multiple Access for Cognitive Radio Networks," *IEEE Journal on Selected Areas in Communications*, vol. 29, pp. 704 – 715, April 2011.

[144] P. Wong, D. Yin, and T. Lee, "Analysis of Non-Persistent CSMA Protocols with Exponential Backoff Scheduling," *IEEE Transactions on Communications*, vol. 59, pp. 2206 – 2214, August 2011.

[145] L. Pan and H. Wu, "Design and Analysis of Prioritized Medium Access Control Protocol for Backbone Routers in Wireless Mesh Networks," *Tsinghua Science and Technology*, vol. 17, pp. 537 – 552, October 2012.

[146] R. Urgaonkar and M. Neely, "Opportunistic Cooperation in Cognitive Femtocell Networks," *IEEE Journal on Selected Areas in Communications*, vol. 30, pp. 607 – 616, April 2012.

[147] X. Zhang and H. Su, "CREAM-MAC: Cognitive Radio-Enabled Multi-Channel MAC Protocol Over Dynamic Spectrum Access Networks," *IEEE Journal of Selected Topics in Signal Processing*, vol. 5, pp. 110 – 123, February 2011.

[148] L. Kleinrock, *Queueing Systems: Theory.* New York, USA: Wiley Interscience, 1975.

[149] J. W. Huang, Z. Han, M. Chiang, and H. V. Poor, "Auction-Based Resource Allocation for Cooperative Communications," *IEEE Journal on Selected Areas in Communications*, vol. 26, pp. 1226 – 1237, September 2008.

[150] G. Shirazi, P. Kong, and C. Tham, "Distributed Reinforcement Learning Frameworks for Cooperative Retransmission in Wireless Networks," *IEEE Transactions on Vehicular Technology*, vol. 59, pp. 4157 – 4162, October 2010.

[151] T. Luo, M. Motani, and V. Srinivasan, "Cooperative Asynchronous Multichannel MAC: Design, Analysis, and Implementation," *IEEE Transactions on Mobile Computing*, vol. 8, pp. 338 – 352, March 2009.

[152] T. Luo, V. Srinivasan, and M. Motani, "A Metric for DISH Networks: Analysis, Implications, and Applications," *IEEE Transactions on Mobile Computing*, vol. 9, pp. 376 – 389, March 2010.

[153] A. Tajer and X. Wang, "Beacon-Assisted Spectrum Access with Cooperative Cognitive Transmitter and Receiver," *IEEE Transactions on Mobile Computing*, vol. 9, pp. 112 – 126, January 2010.

[154] H. Shan, W. Zhuang, and Z. Wang, "Distributed Cooperative MAC for Multihop Wireless Networks," *IEEE Communications Magazine*, vol. 47, pp. 126 – 133, February 2009.

[155] S. Mehta and K. Kwak, "An Energy-Efficient MAC Protocol in Wireless Sensor Networks: A Game Theoretic Approach," *EURASIP Jounal on Wireless Communications and Networking*, vol. 2010, pp. 1 – 10, May 2010.

[156] K. Letaief and W. Zhang, "Cooperative Communications for Cognitive Radio Networks," *Proceedings of the IEEE*, vol. 97, pp. 878 – 893, May 2009.

[157] A. Sadek, Z. Han, and K. Liu, "Distributed Relay-Assignment Protocols for Coverage Expansion in Cooperative Wireless Networks," *IEEE Transactions on Mobile Computing*, vol. 9, pp. 505 – 515, April 2010.

[158] R. Madan, N. Mehta, A. Molisch, and J. Zhang, "Energy-Efficient Cooperative Relaying over Fading Channels with Simple Relay Selection," *IEEE Transactions on Communications*, vol. 7, pp. 3013 – 3025, August 2008.

[159] T. Luo, M. Motani, and V. Srinivasan, "Energy-Efficient Strategies for Cooperative Multi-Channel MAC Protocols," *IEEE Transactions on Mobile Computing*, vol. PP, pp. 1 – 13, April 2011.

[160] Y. Zhou, J. Liu, C. Zhai, and L. Zheng, "Two-Transmitter Two-Receiver Cooperative MAC Protocol: Cross-Layer Design and Performance Analysis," *IEEE Transactions on Vehicular Technology*, vol. 9, pp. 4116 – 4127, October 2010.

[161] A. Mukherjee and H. Kwon, "General Auction-Theoretic Strategies for Distributed Partner Selection in Cooperative Wireless Networks," *IEEE Transactions on Communications*, vol. 58, pp. 2903 – 2915, October 2010.

[162] S. Jayaweera, M. Bkassiny, and K. Avery, "Asymmetric Cooperative Communications Based Spectrum Leasing via Auctions in Cognitive Radio Networks," *IEEE Transactions on Wireless Communications*, vol. 10, pp. 2716 – 2724, August 2011.

[163] F. Pantisano, M. Bennis, W. Saad, and M. Debbah, "Spectrum Leasing as an Incentive Towards Uplink Macrocell and Femtocell Cooperation," *IEEE Journal on Selected Areas in Communications*, vol. 30, pp. 617 – 630, April 2012.

[164] Asaduzzaman, H. Y. Kong, and I. Koo, "Opportunistic Relaying Based Spectrum Leasing for Cognitive Radio Networks," *Journal of Communications and Networks*, vol. 13, pp. 50 – 55, February 2011.

[165] M. Hafeez and J. Elmirghani, "Analysis of Dynamic Spectrum Leasing for Coded Bi-Directional Communication," *IEEE Journal on Selected Areas in Communications*, vol. 30, pp. 1500 – 1512, September 2012.

[166] S. Cui, R. Madan, A. Goldsmith, and S. Lall, "Cross-Layer Energy and Delay Optimization in Small-Scale Sensor Networks," *IEEE Transactions on Wireless Communications*, vol. 6, pp. 3688 – 3699, October 2007.

[167] Z. Zhou, S. Zhou, S. Cui, and J. Cui, "Energy-Efficient Cooperative Communication in a Clustered Wireless Sensor Network," *IEEE Transactions on Vehicular Technology*, vol. 57, pp. 3618 – 3628, November 2008.

[168] S. Huang, H. Chen, Y. Zhang, and F. Zhao, "Energy-Efficient Cooperative Spectrum Sensing with Amplify-and-Forward Relaying," *IEEE Communications Letters*, vol. 16, pp. 450 – 453, April 2012.

[169] D. Chase, "Digital Signal Design Concepts for a Time-Varying Rician Channel," *IEEE Transactions on Communications*, vol. 24, pp. 164 –172, February 1976.

[170] I. Stanojev, O. Simeone, Y. Bar-ness, and C. You, "Performance of multi-relay collaborative hybrid-ARQ protocols over fading channels," *IEEE Communications Letters*, vol. 10, pp. 522 – 524, July 2006.

[171] T. Cover and J. Thomas, *Elements of Information Theory*. New Jersey, USA: WILEY-INTERSCIENCE, 2006.

[172] R. Zhang and L. Hanzo, "A Unified Treatment of Superposition Coding Aided Communications: Theory and Practice," *IEEE Communications Surveys and Tutorials*, vol. 13, pp. 503 – 520, Third Quarter 2011.

[173] L. Hanzo, M. Munster, B. Choi, and T. Keller, *OFDM and MC-CDMA for Broadcasting Multi-User Communications, WLANs and Broadcasting*. Chichester,England: IEEE Press - John Wiley, 2003.

[174] S. Wu, Y. Tseng, and J. Sheu, "Energy-Constrained Modulation Optimization," *IEEE Transactions on Wireless Communications*, vol. 5, pp. 2349 – 2360, September 2005.

[175] M. Butt, S. Ng, and L. Hanzo, "Self-Concatenated Code Design and its Application in Power-Efficient Cooperative Communications," *IEEE Communications Surveys and Tutorials*, vol. 14, pp. 858 – 883, Third Quarter 2012.

[176] A. El-Sherif and K. Liu, "Joint Design of Spectrum Sensing and Channel Access in Cognitive Radio Networks," *IEEE Transactions on Wireless Communications*, vol. 10, pp. 1743 – 1753, June 2011.

[177] W. Saad, H. Zhu, T. Basar, M. Debbah, and A. Hjorungnes, "Hedonic Coalition Formation for Distributed Task Allocation among Wireless Agents," *IEEE Transactions on Mobile Computing*, vol. 10, pp. 1327 – 1344, September 2011.

[178] "FCC Fules and Regulations," 2010. [Online]. Available: http://louise.hallikainen.org/FCC/FccRules/2010

[179] J. Kim and D. Kim, "Outage Probability and Achievable Diversity Order of Opportunistic Relaying in Cognitive Secondary Radio Networks," *IEEE Transactions on Communications*, vol. 60, pp. 2456 – 2466, September 2012.

[180] M. Pan, P. Liz, and Y. Fang, "Cooperative Communication Aware Link Scheduling for Cognitive Vehicular Networks," *IEEE Journal on Selected Areas in Communications*, vol. 30, pp. 760 – 768, May 2012.

[181] O. Simeone, I. Stanojev, S. Savazzi, and Y. Bar-Ness, "Spectrum Leasing to Cooperating Secondary Ad Hoc Networks," *IEEE Journal on Selected Areas in Communications*, vol. 26, pp. 203 – 213, January 2008.

[182] Q. Zhao and B. Sadler, "A Survey of Dynamic Spectrum Access," *IEEE Signal Processing Magazine*, vol. 24, pp. 79 – 89, May 2007.

[183] D. Li, Y. Xu, X. Wang, and M. Guizani, "Coalitional Game Theoretic Approach for Secondary Spectrum Access in Cooperative Cognitive Radio Networks," *IEEE Transactions on Wireless Communications*, vol. 10, pp. 844 – 856, March 2011.

[184] Y. Zou, Y. Yao, and B. Zheng, "A Cooperative Sensing Based Cognitive Relay Transmission Scheme Without a Dedicated Sensing Relay Channel in Cognitive Radio Networks," *IEEE Transactions on Signal Processing*, vol. 59, pp. 854 – 858, January 2011.

[185] T. Cui, F. Gao, and A. Nallanathan, "Optimization of Cooperative Spectrum Sensing in Cognitive Radio," *IEEE Transactions on Vehicular Technology*, vol. 60, pp. 1578 – 1589, May 2011.

[186] D. Tse and P. Viswanath, *Fundamentals of Wireless Communication*. Cambridge, U.K.: Mass: The MIT Press, 2005.

[187] K. Huang and R. Zhang, "Cooperative Feedback for Multiantenna Cognitive Radio Networks," *IEEE Transactions on Signal Processing*, vol. 59, pp. 747 – 758, February 2011.

[188] P. Chen and Q. Zhang, "Joint Temporal and Spatial Sensing Based Cooperative Cognitive Networks," *IEEE Communications Letters*, vol. 15, pp. 530 – 532, May 2011.

[189] W. Ao, S. Cheng, and K. Chen, "Connectivity of Multiple Cooperative Cognitive Radio Ad Hoc Networks," *IEEE Journal on Selected Areas in Communications*, vol. 30, pp. 263 – 270, February 2012.

[190] A. Zarrebini-Esfahani and M. Nakhai, "Secondary Spectrum Access And Cell-Edge Coverage in Cognitive Cellular Networks," *IET Communications*, vol. 6, pp. 845 – 851, May 2012.

[191] L. Li, X. Zhou, H. Xu, G. Li, D. Wang, and A. Soong, "Simplified Relay Selection and Power Allocation in Cooperative Cognitive Radio Systems," *IEEE Transactions on Wireless Communications*, vol. 10, pp. 33 – 36, January 2011.

[192] R. Wang, V. Lau, and H. Huang, "Opportunistic Buffered Decode-Wait-and-Forward (OB-DWF) Protocol for Mobile Wireless Relay Networks," *IEEE Transactions on Wireless Communications*, vol. 10, pp. 1224 – 1231, April 2011.

[193] J. Liu, W. Chen, Z. Cao, and Y. Zhang, "Delay Optimal Scheduling for Cognitive Radios with Cooperative Beamforming: A Structured Matrix-Geometric Method," *IEEE Transactions on Mobile Computing*, vol. 11, pp. 1412 – 1423, August 2012.

[194] X. Bao, P. Martins, T. Song, and L. Shen, "Stable Throughput and Delay Performance in Cognitive Cooperative Systems," *IET Communications*, vol. 5, pp. 190 – 198, January 2011.

[195] I. Krikidis, J. Laneman, J. Thompson, and S. Mclaughlin, "Protocol Design and Throughput Analysis for Multi-user Cognitive Cooperative Systems," *IEEE Transactions on Wireless Communications*, vol. 8, pp. 4740 – 4751, October 2009.

[196] L. Koralov and Y. Sinai, *Theory of Probability and Random Processes*. New York, USA: Springer-Verlag Berlin Heidelberg, 2007.

[197] G. Thomas, M. Weir, and J. Hass, *Thomas' Calculus: Early Transcendentals*. Boston, MA, USA: Addison-Wesley, 2009.

[198] D. Bertsekas and R. Gallager, *Data Networks*. Englewood Cliffs, NF: Prentice-Hall, 1987.

[199] A. Varga, "Omnet++ discrete event simulation system version 3.2 user manual," 2005.

[200] W. Ao and K. Chen, "Cognitive Radio-Enabled Network-Based Cooperation: From a Connectivity perspective," *IEEE Journal on Selected Areas in Communications*, vol. 30, pp. 1969 – 1982, November 2012.

[201] N. Qiang and C. Zarakovitis, "Nash Bargaining Game Theoretic Scheduling for Joint Channel and Power Allocation in Cognitive Radio Systems," *IEEE Journal on Selected Areas in Communications*, vol. 30, pp. 70 – 81, January 2012.

[202] Q. Ni and C. Zarakovitis, "Nash Bargaining Game Theoretic Scheduling for Joint Channel and Power Allocation in Cognitive Radio Systems," *IEEE Journal on Selected Areas in Communications*, vol. 30, pp. 70 – 81, Janruary 2012.

[203] Y. Zou, Y. Yao, and B. Zheng, "Diversity-Multiplexing Tradeoff in Selective Cooperation for Cognitive Radio," *IEEE Transactions on Communications*, vol. 60, pp. 2467 – 2481, September 2012.

[204] Y. Cao, T. Jiang, C. Wang, and L. Zhang, "CRAC: Cognitive Radio Assisted Cooperation for Downlink Transmissions in OFDMA-Based Cellular Networks," *IEEE Journal on Selected Areas in Communications*, vol. 30, pp. 1614 – 1622, October 2012.

[205] T. Luan, F. Gao, and X. Zhang, "Joint Resource Scheduling for Relay-Assisted Broadband Cognitive Radio Networks," *IEEE Transactions on Wireless Communications*, vol. 11, pp. 3090 – 3100, September 2012.

[206] W. Ao and K. Chen, "Cognitive Radio-Enabled Network-Based Cooperation: From a Connectivity Perspective," *IEEE Journal on Selected Areas in Communications*, vol. 30, pp. 1969 – 1982, November 2012.

[207] M. Xia and S. Aissa, "Cooperative AF Relaying in Spectrum-Sharing Systems: Outage Probability Analysis under Co-Channel Interferences and Relay Selection," *IEEE Transactions on Communications*, vol. 60, pp. 3252 – 3262, November 2012.

[208] T. Luan, F. Gao, X. Zhang, J. Li, and M. Lei, "Rate Maximization and Beamforming Design for Relay-Aided Multiuser Cognitive Networks," *IEEE Transactions on Vehicular Technology*, vol. 61, pp. 1940 – 1945, May 2012.

[209] M. Shaat and F. Bader, "Asymptotically Optimal Resource Allocation in OFDM-Based Cognitive Networks with Multiple Relays," *IEEE Transactions on Wireless Communications*, vol. 11, pp. 892 – 897, March 2012.

[210] A. El-Sherif, A. Sadek, and K. Liu, "Opportunistic Multiple Access for Cognitive Radio Networks," *IEEE Journal on Selected Areas in Communications*, vol. 29, pp. 704 – 715, April 2011.

[211] R. Wang, V. Lau, and Y. Cui, "Decentralized Fair Scheduling in Two-Hop Relay-Assisted Cognitive OFDMA Systems," *IEEE Journal of Selected Topics in Signal Processing*, vol. 5, pp. 171 – 181, February 2011.

[212] X. Wang, K. Ma, Q. Han, Z. Liu, and X. Guan, "Pricing-Based Spectrum Leasing in Cognitive Radio Networks," *IET Networks*, vol. 1, pp. 116 – 125, September 2012.

[213] D. Li, Y. Xu, X. Wang, and M. Guizani, "Coalitional Game Theoretic Approach for Secondary Spectrum Access in Cooperative Cognitive Radio Networks," *IEEE Transactions on Wireless Communications*, vol. 10, pp. 844 – 856, March 2011.

[214] M. Shamaiah, S. Lee, S. Vishwanath, and H. Vikalo, "Distributed Algorithms for Spectrum Access in Cognitive Radio Relay Networks," *IEEE Journal on Selected Areas in Communications*, vol. 30, pp. 1947 – 1957, November 2012.

[215] A. Sultan, A. El-Sherif, and K. Seddik, "Cognitive Multiple Access Using Soft Sensing and Secondary Channel State Information," in *2012 IEEE Wireless Communications and Networking Conference (WCNC)*, Paris, France, April 2012, pp. 803–808.

[216] D. Gusfield and R. Irving, *The Stable Marriage Problem: Structure and Algorithms*. Cambridge, U.K.: Cambridge Univ. Press, 1989.

[217] C. Dong, L. Yang, and L. Hanzo, "Performance Analysis of Multihop-Diversity-Aided Multihop Links," *IEEE Transactions on Vehicular Technology*, vol. 61, pp. 2504 – 2516, July 2012.

[218] D. Ho and S. Valaee, "Information Raining and Optimal Link-Layer Design for Mobile Hotspots," *IEEE Transactions on Mobile Computing*, vol. 4, pp. 271 – 284, June 2005.

[219] R. Xie, H. Ji, and P. Si, "Optimal joint transmission time and power allocation for heterogeneous cognitive radio networks," in *Communications (ICC), 2011 IEEE International Conference on*, Paris, France, July 2011, pp. 1 – 5.

[220] W. Liang, S. Ng, and L. Hanzo, "Adaptive Turbo Trellis Coded Modulation aided cooperative Cognitive Radio," in *2012 IEEE Wireless Communications and Networking Conference (WCNC)*, Paris, France, April 2012, pp. 2362 – 2366.

[221] ——, "Cooperative Communication Between Cognitive And Primary User," 2013, submitted to IET Communications.

[222] L. Duan, J. Huang, and B. Shou, "Investment and Pricing with Spectrum Uncertainty A Cognitive Operator's Perspective," *IEEE Transactions on Mobile Computing*, vol. 10, pp. 1590 – 1604, November 2011.

[223] W. Chien, C. Yang, and Y. Huang, "Energy-Saving Cooperative Spectrum Sensing Processor for Cognitive Radio System," *IEEE Transactions on Circuits and Systems I: Regular Papers*, vol. 58, pp. 711 – 723, April 2011.

[224] R. Deng, J. Chen, C. Yuen, P. Cheng, and Y. Sun, "Energy-Efficient Cooperative Spectrum Sensing by Optimal Scheduling in Sensor-Aided Cognitive Radio Networks," *IEEE Transactions on Vehicular Technology*, vol. 61, pp. 716 – 725, February 2012.

[225] N. Tadayon, H. Wang, and D. Kasilingam, "Analytical Modeling of Medium-Access Delay for Cooperative Wireless Networks Over Rayleigh Fading Channels," *IEEE Transactions on Vehicular Technology*, vol. 62, pp. 349 – 359, January 2013.

[226] J. Jang, S. Kim, and S. Wie, "Throughput and Delay Analysis of A Reliable Cooperative MAC Protocol in Ad Hoc Networks," *Journal of Communications and Networks*, vol. 14, pp. 524 – 532, October 2012.

[227] Q. Chen, J. Tang, D. Wong, X. Peng, and Y. Zhang, "Directional Cooperative MAC Protocol Design and Performance Analysis for IEEE 802.11ad WLANs," *IEEE Transactions on Vehicular Technology*, vol. PP, pp. 1 – 11, February 2013.

[228] S. Bharati and W. Zhuang, "Performance Analysis of Cooperative ADHOC MAC for Vehicular Networks," in *2012 IEEE Global Communications Conference (GLOBECOM)*, California, USA, Dec. 2012, pp. 5482 – 5487.

[229] Y. Bi, L. Cai, X. Shen, and H. Zhao, "Efficient and Reliable Broadcast in Intervehicle Communication Networks: A Cross-Layer Approach," *IEEE Transactions on Vehicular Technology*, vol. 59, pp. 2404 – 2417, June 2010.

[230] B. Maham, A. Behnad, and M. Debbah, "Analysis of Outage Probability and Throughput for Half-Duplex Hybrid-ARQ Relay Channels," *IEEE Transactions on Vehicular Technology*, vol. 61, pp. 3061 – 3070, September 2012.

[231] P. Liu, C. Nie, T. Korakis, E. Erkip, S. Panwar, F. Verde, and A. Scaglione, "STiCMAC: A MAC Protocol for Robust Space-Time Coding in Cooperative Wireless LANs," *IEEE Transactions on Wireless Communications*, vol. 11, pp. 1358 – 1369, April 2012.

[232] S. Safavi, M. Ardebilipour, and S. Salari, "Relay Beamforming in Cognitive Two-Way Networks with Imperfect Channel State Information," *IEEE Wireless Communications Letters*, vol. PP, pp. 1 – 4, February 2012.

[233] P. Lin, J. Jia, Q. Zhang, and M. Hamdi, "Dynamic Spectrum Sharing with Multiple Primary and Secondary Users," *IEEE Transactions on Vehicular Technology*, vol. 60, pp. 1756 – 1765, May 2011.

[234] S. Boyd and L. Vandenberghe, *Convex Optimization*. Cambridge, UK: Cambridge University Press, 2009.

[235] J. Proakis, *Digital Communications, 4th ed.* New York, USA: McGraw-Hill, 2001.

Author Index